The University Of Sheffield.

Conformational Studies of Poly(2-(dimethylamino ethyl methacrylate) (PDMAEMA) and Poly(acrylic acid) (PAA) using Fluorescence Spectroscopy.

By

Ameerah M. Theqah

A thesis submitted in part fulfilment of the condition of admittance to the degree of Doctor of Philosophy (Ph.D.) of the Department of Chemistry, University Of Sheffield, Sheffield, UK.

March, 2016

Declaration

This thesis is submitted to the University of Sheffield for the degree of Doctor of Philosophy, having not been submitted to any other University or Teaching Institution for obtaining any degree. I declare that all work presented in this thesis is my own work, excluding where acknowledged and referenced accordingly.

Ameerah Theqah

March 2016

Acknowledgements

I would like to thank my supervisors, Dr Linda Swanson, Dr Ahmed Iraqi and Dr Stephen Rimmer for their invaluable guidance and support throughout the PhD.

I would like to thank all of my colleagues on F-floor for contributing to a comfortable work environment. I would also like to thank Melanie Hannah and Heather Grievson for her much appreciated technical assistance.

The Saudi Ministry of Higher Education is gratefully acknowledged for providing support in the form of finance my PhD study.

Finally, I would like to thank my family (my mother, my brothers and my husband) and my neighbour for their continuing support.

Contents

Chapter 1 Introduction 1

1.1 Polyelectrolytes 2

1.1.1 Poly (dimethylamino) ethyl methacrylate (PDMAEMA) 3

1.1.2 Poly (acrylic acid) (PAA) 5

1.1.3 PDMAEMA and PAA applications 5

1.2 Fluorescence Studies of poly(2-(dimethylamino ethyl methacrylate) and of poly(acrylic acid) 6

1.3 Fluorescence Probes 8

1.4 Photophysics and Photochemical Processes 9

1.5 Principles of Luminescence 10

1.5.1 Fluorescence lifetime and the quantum yield 12

1.5.2 Fluorescence lifetime measurements 13

1.5.3 Fluorescence quenching phenomenon 14

1.5.4 Nonradiative energy transfer 14

1.5.5 Time-resolved anisotropy measurements (TRAMS) 16

1.6 Studies of the interactions of the surfactants with polyelectrolytes 19

1.7 Aims and objectives of the present work 22

1.8 General Objectives 22

1.9 Specific Objectives 22

Chapter 2 Experimental 23

2.1 Preparation and synthesis of materials for linear polymers 23

2.1.1 Solvents 23

2.1.2 General reagents 23

2.1.3 Polymerisation initiator and coupling agents 24

2.1.4 Fluorescent labels 24

2.1.5 Monomers 26
2.1.6 Synthesis unlabelled and fluorescently labelled Poly-2-(dimethylamino)ethyl methacrylate preparation 26
2.1.7 Synthesis unlabelled and fluorescently labelled Poly-acrylic acid 31
2.2 Characterisation Techniques 34
2.2.1 Nuclear magnetic spectroscopy (NMR) 34
2.2.2 Ultraviolet spectroscopy (UV) 34
2.2.3 Gel-permeation chromatography (GPC) 35
2.3 Calculations 35
2.3.1 Yield calculations 35
2.3.2 Fluorescent label content 35
2.4 Results of characterisation: 39
2.4.1 PDMAEMA- No label 39
2.4.2 PDMAEMA-ACE 39
2.4.3 PDMAEMA-ACE-AMMA 39
2.4.4 PAA-No label 40
2.4.5 PAA-ACE 40
2.4.6 PAA-ACE-AMMA 40
2.5 Fluorescence Measurements 41
2.5.1 Preparations of samples for photophysics studies 41
2.5.2 Fluorescence steady state measurements 41
2.5.3 Fluorescence lifetime and time resolved measurements 41
Chapter 3 Fluorescence investigations of the solution behaviour of pH responsive polymers 42
3.1 Conformational Behaviour of ACE-labelled PAA as a Function of pH 42

3.1.1 Fluorescence steady state spectra of ACE- labelled PAA as a function of pH..... 42

3.1.2 Fluorescence exited state lifetimes of ACE- labelled PAA as a function of pH..... 43

3.1.3 Fluorescence Time-resolved anisotropy measurements (TRAMS) of ACE labelled PAA as a function of pH 47

3.2 Conformational Behaviour of ACE-AMMA-PAA as a Function of pH 51

3.2.1 Fluorescence steady state spectra of ACE-AMMA-PAA as a function of pH..... 51

3.2.2 Fluorescence exited state lifetimes of ACE-AMMA-PAA as a function of pH..... 54

3.3 Conformational Behaviour of ACE-labelled PDMAEMA as a Function of pH ... 59

3.3.1 Fluorescence steady state spectra of ACE-labelled PDMAEMA as a function of pH..... 59

3.3.2 Fluorescence exited state lifetimes of ACE- labelled PDMAEMA as a function of pH..... 63

3.3.3 Fluorescence Time-resolved anisotropy measurements (TRAMS) of ACE-labelled PDMAEMA as a function of pH 66

3.4 Conformational Behaviour of ACE-AMMA labelled PDMAEMA as a Function of pH..... 69

3.4.1 Fluorescence steady state spectra of ACE-AMMA-PDMAEMA as a function of pH..... 70

3.4.2 Fluorescence exited state lifetimes of ACE-AMMA- PDMAEMA as a function of pH..... 72

Chapter 4 Fluorescence investigation of pH responsive polymers in the presence of various salts..... 76

4.1 Fluorescence investigation of poly (acrylic acid) PAA in the presence of various salts. 76

4.1.1 Fluorescence steady state spectra of ACE-AMMA labelled PAA in the presence of NaCl as a function of pH 77

4.1.2 Fluorescence excited state lifetimes of singly and doubly labelled PAA in the presence of NaCl as a function of pH 80

4.1.3 Fluorescence Time-Resolved Anisotropy Measurements (TRAMS) of ACE-PAA in the presence of NaCl as a function of pH 86

4.1.4 Fluorescence steady state spectra of ACE-AMMA labelled PAA in the presence of $CaCl_2$ as a function of pH 90

4.1.5 Fluorescence excited state lifetimes of singly and doubly labelled PAA in the presence of $CaCl_2$ as a function of pH 93

4.1.6 Fluorescence Time-Resolved Anisotropy Measurements (TRAMS) of ACE-PAA in the presence of $CaCl_2$ as a function of pH 97

4.1.7 Fluorescence steady state spectra of ACE-AMMA labelled PAA in the presence of NaBr as a function of pH 99

4.1.8 Fluorescence excited state lifetimes of singly and doubly labelled PAA in the presence of NaBr as a function of pH 104

4.1.9 Fluorescence time-resolved anisotropy measurements (TRAMS) of ACE-PAA in the presence of NaBr as a function of pH 109

4.1.10 Fluorescence steady state spectra of ACE-AMMA labelled PAA in the presence of $CaBr_2$ as a function of pH 112

4.1.11 Fluorescence excited state lifetimes of singly and doubly labelled PAA in the presence of $CaBr_2$ as a function of pH 116

4.1.12 Fluorescence time-resolved anisotropy measurements (TRAMS) of ACE-PAA in the presence of $CaBr_2$ as a function of pH 121

4.1.13 A comparative summary 125

4.2 Fluorescence investigation of Poly (dimethylamino) ethyl methacrylate (PDMEAMA) in the presence of various salts 133

4.2.1 Fluorescence steady state spectra of ACE- AMMA labelled PDMEAMA in the presence of NaCl as a function of pH 133

4.2.2 Fluorescence excited state lifetimes of singly and doubly labelled PDMAEMA in the presence of NaCl as a function of pH 136

4.2.3 Fluorescence time-resolved anisotropy measurements (TRAMS) of ACE-PDMAMA in the presence of NaCl as a function of pH 141

4.2.4 Fluorescence steady state spectra of ACE- AMMA labelled PDMEAMA in the presence of $CaCl_2$ as a function of pH 144

4.2.5 Fluorescence excited state lifetimes of singly and doubly labelled PDMAEMA in the presence of $CaCl_2$ as a function of pH. 147

4.2.6 Fluorescence time-resolved anisotropy measurements (TRAMS) of ACE-PDMAMA in the presence of $CaCl_2$as a function of pH 152

4.2.7 Fluorescence steady state spectra of ACE- AMMA labelled PDMEAMA in the presence of NaBr as a function of pH. 155

4.2.8 Fluorescence excited state lifetimes of singly and doubly labelled PDMAEMA in the presence of NaBr as a function of pH 158

4.2.9 Fluorescence time-resolved anisotropy measurements (TRAMS) of ACE-PDMAMA in the presence of NaBr as a function of pH 163

4.2.10 Fluorescence steady state spectra of ACE-AMMA labelled PDMEAMA in the presence of $CaBr_2$ as a function of pH 167

4.2.11 Fluorescence excited state lifetimes of singly and doubly labelled PDMAEMA in the presence of $CaBr_2$ as a function of pH 170

4.2.12 Fluorescence time-resolved anisotropy measurements (TRAMS) of ACE-PDMAMA in the presence of $CaBr_2$ as a function of pH 174

4.2.13 A comparative summary 178

Chapter 5 The use of fluorescence spectoscropy to study the molecular interactions between [poly(dimethylaminoethyl) methacrylate] and poly(acrylic acid) with oppositely charged surfactant micelles in aqueous solutions 186

5.1 Fluorescence investigation of poly(acrylic acid) in the presence of oppositely charged surfactant micelles (Hexadecyltrimethylammonium chloride)..... 187

5.1.1 Fluorescence steady state spectra of ACE- AMMA labelled PAA in the presence of Hexadecyltrimethylammonium chloride as a function of pH 187

5.1.2 Fluorescence excited state lifetimes of an aqueous solution of ACE-AMMA PAA in the presence of Hexadecyltrimethylammonium chloride as a function of pH..... 189

5.1.3 Fluorescence time-resolved anisotropy measurements (TRAMS) of ACE-PAA in the presence of Hexadecyltrimethylammonium chloride as a function of pH..... 191

5.2 Fluorescence investigation of poly(dimethylamino)ethyl methacrylate (PDMEAMA) in the presence of oppositely charged surfactant micelles (sodium hexadecyl sulphate). 195

5.2.1 Fluorescence steady state spectra of ACE-AMMA labelled PDMAEMA in the presence of sodium hexadecyl sulphate as a function of pH 195

5.2.2 Fluorescence excited state lifetimes of an aqueous solution of ACE AMMAPDMAEMA in the presence of sodium hexadecyl sulphate as a function of pH 196

5.2.3 Fluorescence time-resolved anisotropy measurements (TRAMS) of ACE-PDMAEMA in the presence of (Sodium hexadecyl sulphate) as a function of pH ... 199

Chapter 6 Conclusions 204

Chapter 7 Future work. 207

Chapter 8 References: 208

Abstract

This project aims to explore the aqueous solution dynamics of the poly(dimethyl aminoethyl methacrylate) (PDMAEMA) and poly(acrylic acid) (PAA) systems using fluorescence techniques. Both of these polymers were synthesised several times using free radical polymerisation techniques with two types of fluorophore labels included in synthesis. The resultant polymers were investigated using fluorescence techniques which include steady state fluorescence studies, fluorescence decay lifetimes and time resolved anisotropy measurements.

Initial solution dynamics of these polymer show that the PDMAEMA exhibits a coiled conformation at high pH values and adopts an expanded form at low pH values. PAA exhibits a partially coiled form at low pH values, but adopt a relatively expanded chain at a pH approximately more than their pKa. The study also shows that the pendant amine groups of the PDMAEMA polymer effect the fluorescence of the labels, and this is what is observed at high pH.

Addition of salts to PAA polymer promote coiling at low and high pH except salt of NaCl and $CaBr_2$. When they added to the uncharged polymer, where it cause the polymer chain to flatten at low concentration of salt, and then to fold again under further addition of these salts. Effect of salts on PDMAEMA polymer conformation has been found to be efficient in growth of aggregation for the cationic polymer. However, salts like sodium chloride, sodium bromide and calcium bromide, has a different effect on the polymer conformation which exist in a coiled state, as they unfold the coiled polymer (at high pH) at low concentrations of them and refold it at high concentration.

The interactions between polyelectrolytes and the oppositely charged surfactant micelles have been investigated using fluorescence technique, in order to understand the conformation and the dynamics of these polyelectrolytes. Addition of cationic micelles (CTAC) to anionic PAA polymer (at high pH), and anionic micelles(SHS) to cationic PDMAEMA polymer(at low pH), change the conformation form of the polymers from an expanded chains to a collapsed structure, as the electrostatic forces assume to play the main role in such interactions. Whereas, the hydrophobic forces control the interactions in polymer/micelles system when the polymers adopt a coiled conformation.

Chapter 1 **Introduction**

This work is concerned with the fluorescence analysis of poly(dimethylamino ethyl methacrylate) (PDMAEMA) and poly (acrylic acid) (PAA) systems in aqueous solutions. Fluorescence techniques, including steady state, excited-state life time and time resolved anisotropy measurements (TRAMS) will be used to study the conformational behaviour of these synthetic polyelectrolytes in aqueous media. The effects of variables such as pH and salt content on the chain dynamics will be investigated. The interactions of the cationic (PDMAEMA) and anionic (PAA) polymers with the oppositely charged surfactant micelles will be also investigated. These fundamental studies are of importance in manipulating macromolecular characteristic for industrial applications.

The aim of this chapter is to present a short review on the chemistry of poly(dimethylamino ethyl methacrylate) (PDMAEMA) and Poly (acrylic acid) (PAA), and on the physicochemical behaviour of these polymers in aqueous solution. Synthesis of water-soluble fluorescently labelled polyelectrolytes is illustrated as well as the background on photophysics. Fluorescence techniques that are used in this project are also reviewed, as these topics need to be included to provide better understanding of the conformational behaviour of pH responsive polyelectrolytes (PDMAEMA and PAA) in aqueous solution and upon interacting with salts and with surfactant micelles. The previous studies of the interactions of the surfactants with polyelectrolyte are also reviewed. The final sections present the aim and thesis objectives.

1.1 Polyelectrolytes

Polyelectrolytes can be defined as macromolecules with ionisable repeat units, which can consequently display a pH-dependent behaviour when dissolved in aqueous solution. These pH- responsive polymers are classified to weak poly-acids (such as PAA) and weak poly-bases (such as PDMAEMA) [1]. The poly-acidic behaviour of PAA causes conformational changes of the polyelectrolyte chain; from a coiled shape at low pH, below pKa of PAA (~4.5), to an extended state at high pH values as a result of repulsive interactions between carboxylate anions dominate (COO^-) [2-3], Figure 1.1b represents the chemical structure of PAA. On the other hand, PDMAEMA polymer is based on amino-monomer (dimethylamino ethyl methacrylate), it behaves unlike poly-acids [4]. At pH lower than pKa of PDMAEMA (~7.5) [5] amino-monomers are protonated and the polymer chain expands to an open conformation as a result of repulsive forces of positively charged ammonium groups. At pH values above the pKa value, amino side chains become neutral and the polyelectrolyte adopts a coiled conformation [6], Figure 1.1 a represents the chemical structure of PDMAEMA.

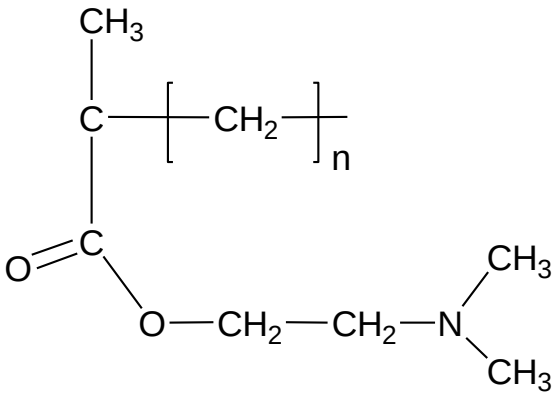

Figure 1.1a chemical structure of PDMAEMA

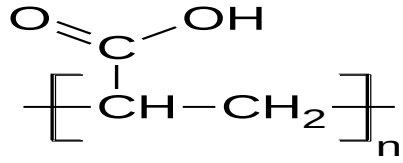

Figure 1.1b chemical structure of PAA

In this work the conformational behaviour of both polyelectrolytes, PDMEAMA and PAA, will be investigated at different pH values by using fluorescence technique, including steady state excited-state life time and TRAMS.

1.1.1 Poly (dimethylamino) ethyl methacrylate (PDMAEMA)

Dry PDMAEMA is a brittle white solid and is nontoxic unlike the monomer 2 (dimethylamino) ethyl methacrylate. The dimethylamino ethyl methacrylate monomer is readily polymerisable, which provides a technique of incorporating amino groups into polymeric systems. The occurrence of the amino group provides the cationic characteristic that allows the following properties: improved binding of co-polymers to a variety of materials, increased compatibility to other polymer systems, thermal stability of synthetic fibers, photographic emulsions and augmented dye ability. The adhesion of resulting polymer film to the masonry and cellulosic substrate can markedly be improved using DMAEMA in latex solutions [7].

PDMAEMA can be classified as a water soluble cationic polymer and the reactive repeat unit is an amino functional group. Viscometric [4] technique on the PDMAEMA reveal that the polyelectrolyte undergoes a change in conformation from an expanded structure at acidic pH,hence the amine unit is protonated, to a collapsed structure at a basic pH. As a result, the expansion of the polymer coil increases as the degree of ionization increases. The conformations of PDMAEMA at low and high pH values are depicted in Figure 1.1.2.

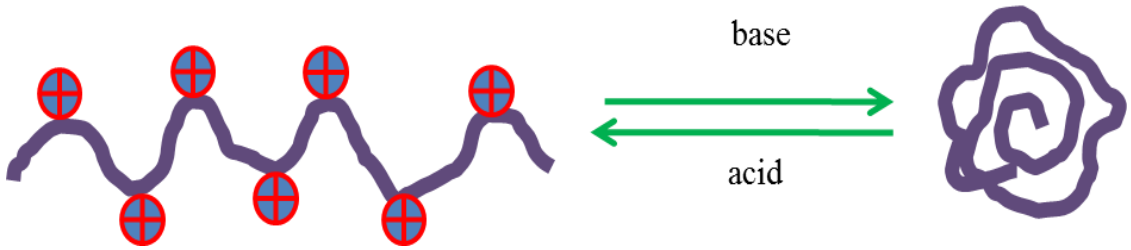

Figure1.1.2. A schematic representation of the conformations of PDMAEMA at low and high pH

The titration behaviour for the high molar mass PDMAEMA found that the pKa of the polyelectrolyte is lower than that of a low molar mass analogue. This is due to the intramolecular association between the carbonyl and the amino groups [8],[9]. It also has been reported [10] that the long chains involving the amine groups in the DMAEMA repeat unit can interact in different cyclic conformations as shown in figure 1.1.3. In conformation 1, the ionised form of the polymer would be stabilised through hydrogen bonding which

raises the pK_a. This does, however, require the side group to already be ionised. Conformation 2 on the other hand, delocalises the free electron pair of the amine making it unavailable for protonation and thus the pK_a is instead lowered

.

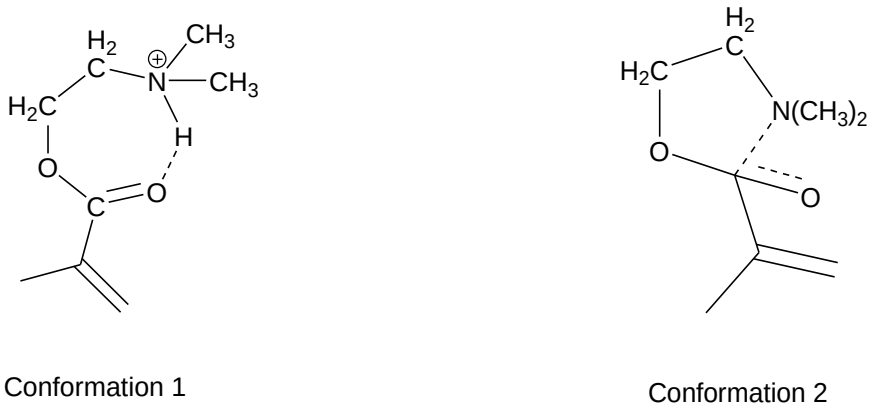

Conformation 1 Conformation 2

Figure 1.1.3. Side chain possible conformations of the DMAEMA monomer side chains that show the otential for some stabilisation that could alter the PDMAEMA pKa. In conformation 1 where the monomer is already protonated there is the potential for hydrogen bonding within the side chain stabilising the monomer electronic structure. Alternatively in conformation 2 interaction of the nitrogen lone pair with the carboxyl group could provide stabilisation of the electronic structure.

Besides the pH response of PDMAEMA chain [4], the polymer chains can respond to the temperature of its surrounding. It was found that [11-12]the PDMAEMA exhibited a Lower Critical Solution Temperature (LCST) around 50°C in water. The LCST is the precise temperature at which the balance of hydrophilic and hydrophobic interactions in the system tips from holding the polymer in an extended open conformation to allowing the polymer to collapse into a tight coil. A similar polymer PNIPAM is a temperature responsive polymer system which exhibits an open, uncoiled state at low temperatures and at temperatures above its Lower Critical Solution Temperature or LCST. For PNIPAM this occurs around 32°C at which it forms a collapsed coil like conformation which aggregates together. This response comes about through a balance of backbone hydrophobic interactions and hydrophilic interaction of the pendant groups. PNIPAM has a drastic enough difference between its two stable states that a visual difference is seen. As the temperature is increased above PNIPAM's LCST a clear solution will turn visibly cloudy.

1.1.2 Poly (acrylic acid) (PAA)

Poly (acrylic acid) (PAA) is a water soluble polymer contains a carboxyl group as repeat unit see Figure 1, this acidic moiety makes it a pH sensitive polyelectrolyte was [13]. It is known that[13] PAA chain undergoes a conformational change, when the pH of the solution is changed. At low pH values the PAA chains are coiled, with increasing pH the chains expand to form an open structure [13]. Both potentiometric and viscometric techniques indicate a smooth transformation from a statistical coil to an extended shape as the pH is increased[14].

On increasing pH the carboxylic acid repeat unit in PAA dissociates to form a negatively charged carboxylate anion, as shown in equation 1.1.2-1. As the poly(acrylic acid) backbone remains hydrophobic at low and high pH values, the COOH groups change as their functionality alters with pH, this amphilic nature of the polymer dictates any conformational changes occurs due to the change in solution pH [3].

$$RCOOH \leftrightarrow RCOO^- + H^+ \qquad \text{1.1.2-1 Equation}$$

It has been demonstrated that [15] the PAA conformational change occurs between pH 4 and 6 [15]. Below pH 4 the collapsed coil reduces the contact between hydrophobic units and the aqueous phase. With increasing pH the repulsive interactions between the negative carboxylate anions turn the polyelectrolyte chain to an expanded water swollen state.

1.1.3 PDMAEMA and PAA applications

PDMAEMA can be used as a homopolymer and as a part of a copolymer in many applications, such as paper making, mineral processing [16], water treatment, modification of natural rubbers [17] and a number of applications related to environmental protection

[18]. There are also a number of further potential applications under investigation such as using the polymer as a sensor [19] and drug delivery systems [20-21].

PAA has a number of uses including acting as a dispersion agent for chemicals such as TiO_2 and $CaCO_3$, thickening agents or adhesives [22]. There has been a particular study on the use of AA containing polymers as replacements for phosphate based detergents for the chelation of calcium. PAA is being considered over other replacement detergents as it also shows dispersion properties [23].

1.2 Fluorescence Studies of poly(2-(dimethylamino ethyl methacrylate) and of poly(acrylic acid)

Further research in this field include fluorescence spectroscopic measurements, which revealed that PDMAEMA undergoes a change in conformation using water-soluble probe dispersed in PDMAEMA [8, 14]. At pH values less than 7 [4, 24], a gradual repulsion between the positive charges when the amino group is protonated serves to expand the coil. On the other hand, when pH levels exceed eight, the amine unit is deprotonated and this results in dominating of hydrophobicity which eventually causes the collapse of the chain. A binding experiment which uses methyl orange (MO) has indicated [4] that PDMAEMA undergoes a conformational transition between pH 7 and pH 9 from extended to coiled which is in agreement with the $pk_a$of the polymer from independent investigations of the titration behaviour [25]. The actuality of the binding strength of the fluorophore which was maximised at pH8 was caused by two possible effects : 1) at pH7, the polyelectrolyte is positively charged, consequently, a strong binding to the negatively charged MO occurs and 2) by pH8.5, the hydrophobicity of PDMAEMA increases due to the reduction in the degree of ionisation. Therefore, the attraction between the MO and the polymer increases. A like behaviour in characterization of fluorescence of toluidinyl naphthalene sulfonic acid (TNS) which is a negatively charged probe, was observed after dispersion in PDMAEMA. The emission intensity from (TNS) was at the highest intensity at pH8.5. Here, PDMAEMA exists in a hydrophobic structure, therefore, attraction between the TNS and the polymer increases. The maximum dispersion for TNS/PDMAEMA was observed below pH8, when PDMAEMA is a protonated polymer,

hence, the enhancement of binding between the protonated polymer and negative charged probe occurs [4].

PAA is a common polyacid [26]that has been studied using fluorescence techniques. Francoise Winnik *et al.*, for example, used pyrene as a bound label for steady-state measurements[26] . Soutar and Swanson studied PAA using multiple techniques including time-resolved anisotropy on an acenapthylene system in both aqueous solution and methanolic [27-28]media.

The fluorescence behaviour of poly acrylic acid systems is complicated, owing mostly to the interactions between water and PAA and the influence of intramolecular hydrogen bonding at partial ionisation. As a result, the fluorescence decays are non-exponential due to the large number of microenvironments that can be created in PAA system [28].

In this project, a different approach has been adopted, using covalently bound fluorophores to introduce luminescence into the polymer. In other words, the label will be chemically attached to the sample. This will allow monitoring of the tagged site directly using TRAMS measurements.

1.3 Fluorescence Probes

As most polyelectrolyte are non-fluorescent (such as dimethylamino ethyl methacrylate (PDMAEMA), luminescence has been introduced to them in main general ways. These are either during polymerization or post-synthesis. Using the post-synthesis approach, certain polyelectrolytes can soubise low mass organic molecules (probes) during the coiled conformation in aqueous solution. Changing the pH level of the polyelectrolyte solution, results in the release of the doped fluorescent material, hence revealing information about the environment and the conformation of the polyelectrolyte. This approach has proved to be successful in providing information pertinent to the solution behavior of polyelectrolytes at the molecular level when the solution conditions (pH levels for example) allow for the probe to solublise [29-32].

Labeling, the introduction of a covalently bounded fluorophore, of polyelectrolytes is the second approach used to introduce luminescence [29-32]. Labels are attached to a specific region of the polyelectrolyte and so enable the study of these regions over a whole range of pH levels. The ratio of doping is in the range of 1:100 of doped fluorophore monomer to electrolyte repeat unit. This low doping ratio is used so that the doping material does not affect the polyelectrolytes properties and behavior.

Each of the above approaches has its merits. However, probes can suffer sequestering in the hydrophobic and hydrophilic regions of the polyeletrolytes. Also, probes are used in the polyelectrolytes aqueous phase only [14]. In contrast to that the labeling approach can be used over the whole range of pH and can be used to study specific regions on the polyelectrolytes directly [14, 29-33].The fluorescent labels applied in this project are acenaphthylene (ACE) and anthryl methylmethacrylate (AMMA).

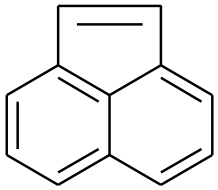

Acenaphthylene (ACE)

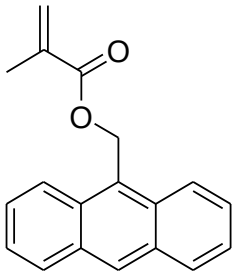

9-Anthryl methylmethacrylate (AMMA)

Figure 1.3 Fluorescent labels applied in this project

ACE binds to the polymer backbone by formation of five membered ring [14]. This forms two covalent bonds meaning that ACE cannot rotate around its axis and therefore any motion of the label is directly related to that of the polymer. In contrast, AMMA attach to the polymer backbone by forming a single bond, which rotate freely around its axis. The speed of rotation depends upon the viscosity of the surrounding environment. When the polymer is collapsed this will lead to a difficulty in the label dynamics and this will change its fluorescence relative to the case when it can rotate freely [34].

1.4 Photophysics and Photochemical Processes

Reaction can be initiated by absorption of radiation (UV-visible light). Photophysics is one natural trend in which upon absorption of light no change takes place, therefore we can use this process to monitor molecular processes, such as luminescence (emission of light) and quenching process (interaction with another chemical species causing a reduction of the intensity of the emission of light) [35]. Photochemical process is another possible process in which chemically distinct products are formed. Figure 1.4-1 illustrates these several processes that can occur from activation of excited state:

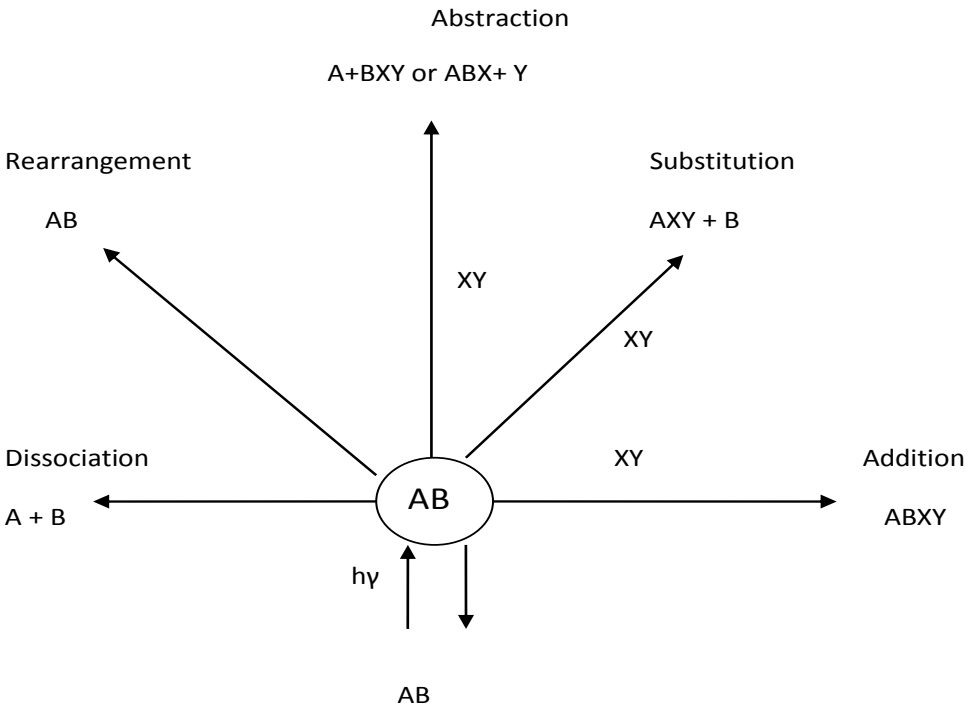

Figure 1.4:1 Light excitation of a molecule and deactivation of the electronically excited state.

1.5 Principles of Luminescence

Luminescence refers to the process of electronically excited states which cause light emission from a substance [36]. Singlet states, when excited, mean the electron in the excited orbital is paired with the second electron in the ground state orbital due to their opposite spin. Photon emission occurs when the excited electron returns to the ground state and this is referred to as fluorescence, the other being phosphorescence. The Jablonski Diagram is a convenient way of summarising the processes that occur between the absorption and emission of light. There are several forms of the Jablonski Diagram which are used to expound various molecular processes that can occur in excited states. Examples include quenching energy transfer and solvent interaction. A typical Jablonski Diagram is shown in figure 1.4.1-1, the lowest energy (singlet ground), first and second electronic states are denoted as S_0, S_1, S_2, respectively of each electronic of the energy levels. There are a number of vibrational energy levels in which the fluorophores can exist, depicted by 0,1,2 .The transitions between various vibrational levels (and rotational levels) are possible, so the fluorophores can exist in vibrational and rotational excited states.

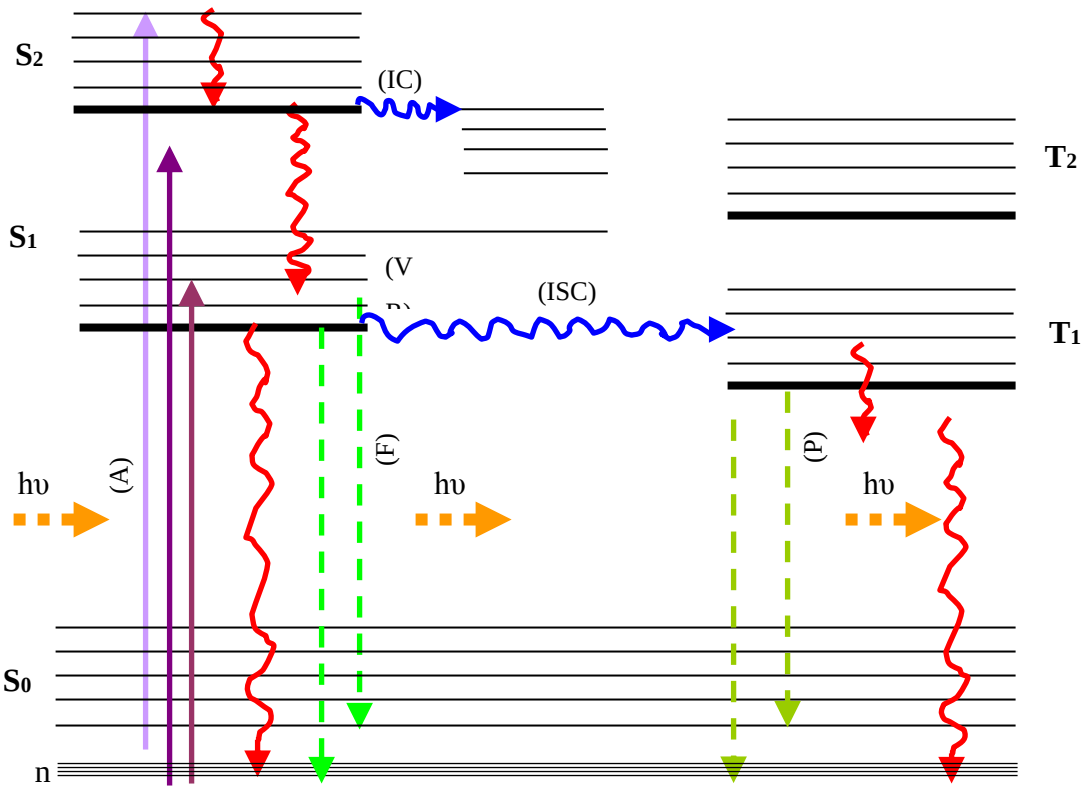

Figure 1.4.1-1: The Jablonski diagram ((IC) is the internal conversion, (ISC) is the intersystem crossing, VR is the vibrational relaxation and hυ is the fluorescence radiation).

Following light absorption, various molecular processes usually occur. A probe is usually excited to some higher vibrational level of either S_1 or S_2 [37]. In condensed phases, the process of internal conversion (IC), which generally occurs within 10ns rapidly succeed in relaxing the molecule down to the lowest vibrational level of S_1. The return to various vibrational levels of S_0 (radiative transitions) results in the vibrational structure in the emission spectrum. In condensed media, emission spectrum occurs at energies lower than that of the absorption band. Another non-radiative transition is that of intersystem crossing (ISC). It is an Iso-energetic transition involving a spin conversion to population of the first triplet state T. The return to the lowest energy ‘’ground state’’ from T is termed phosphorescence. This is shifted to longer wave lengths (lower energy) when comparing to the fluorescence, transition to the singlet ground state being forbidden. Consequently the emission rate is slow. Molecules which have heavy atoms, such as bromine and Iodine are frequently phosphorescent.

1.5.1 Fluorescence lifetime and the quantum yield

The amount of fluorescence observed depends on relative rates of several unimolecular processes which can be illustrated by the following equations:

$$^1\mathbf{A} \xrightarrow{\mathbf{hv}} {}^1\mathbf{A}*$$

Absorption Equation 1.5.1-1

$$^1\mathbf{A}* \xrightarrow{\mathbf{KF}} {}^1\mathbf{A} + \mathrm{hv}$$

Fluorescence Equation 1.5.1-2

$$^1\mathbf{A}* \xrightarrow{\mathbf{KIC}} {}^1\mathbf{A}*$$

Internal conversion Equation 1.5.1-3

$$^1\mathbf{A}* \xrightarrow{\mathbf{KISC}} {}^3\mathbf{A}*$$

Intersystem crossing Equation 1.5.1-4

Of the spectrofluorometer the fluorescence analysis occurs systematically. Firstly, the light beams enter through an excitation monochromator, this allows the selected excitation wavelength to pass through. Gratings then remove stray light and the excitation wavelength is allowed to pass towards to the sample cuvette. Here the sample is excited and emission occurs. Subsequently, the fluorescence is then detected at a right angle to the excitation wavelength so that the sensitivity of the fluorescence measurement is enhanced. The desired emission wavelength is selected through the emission monochromator. Depending on what is being measured, the photomultiplier tubes sense and quantify the fluorescence. Lastly, the fluorescence passes through the amplifier and the computer represents the output spectrally.[37] Using the steady state spectrofluorometer, two kinds of spectra can be recorded. An excitation spectrum represents the relative absorption of the sample at each excitation wavelength and is measured when the excitation wavelength is fixed. The slit width determined the wavelength intervals [37].

In this thesis, the fluorescence steady state excitation and emission spectra were recorded on a fluoromax-4 spectrofluorometer.

1.5.2 Fluorescence lifetime measurements

Lifetime measurements are more advantageous than steady state measurements. They contain more information that is lost in steady state data. For instance, the fluorescence lifetime of the fluorophore is sensitive to its environment. This sensitivity can be informative concerning the conformation of a polyelectrolyte in aqueous solution [38-41]. For example, if we have only one fluorophore in the sample, we may have two different types of excited states present in two different environments. On the other hand, the steady state intensity will only reveal intensities of these two decay times.

As mentioned previously, life time measurements require a pulsed excitation source. In fact there are two methods to measure time-resolved fluorescence; the first one being the time-domain method and the second being the frequency-domain method[37]. In this project we are interested in the time- domain or (single photon counting) (SPC). In this latest method the sample is excited by a short pulse of light with a pulse width shorter than the decay time **τ** of the sample. Following the excitation pulse the intensity which depends on time is measured, and the fluorescence life time is calculated from the slope of a plot of log (I) versus t [37] as illustrated in figure 1.5.2.1:

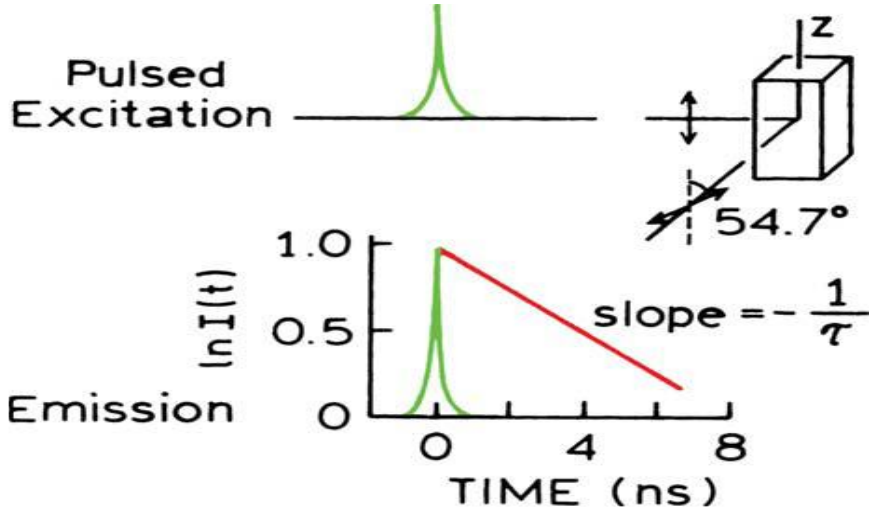

1.51.5.2-1: The time-domain lifetime measurements

1.5.3 Fluorescence quenching phenomenon

A variety of substances known as quenchers such as oxygen, halogens, amines, are capable of decreasing the fluorescence properties, intensity of fluorescence (I), quantum yield (Q), and life time (T) [37]. Such decreases in the intensity are known as quenching. This process may occur through different mechanisms. Static quenching is a process that occurs too fast. It happens when fluorescence combines with a quencher to form a complex in the ground state. When this complex (FQ) becomes excited, it will relax to the ground state without emission of light. Dynamic quenching is another type of mechanism that influences the deactivation of the excited state. During collisional quenching the excited fluorescence transfer its energy to the quencher over very small distances, followed by a decrease in the fluorescence properties. This process can be described using the Stern-Volmer equation (1.5.3.1):

$$I_0/I = \Phi_0/\Phi = \tau_0/\tau = 1 + K_q[Q] \qquad \text{Equation 1.5.3-1}$$

Here, I_0, I, Φ_0 and Φ are the intensity and quantum yield in the absence and presence of a quencher at a certain concentration. The unquenched lifetime is represented by τ_0. The bimolecular quenching constant (K_q) reflects the sensitivity of the probe within macromolecule to quencher. When the value of K_q is low the hyper coiled conformation enhances the degree of protection for the excited fluorophore from the water soluble quenching [42]. A large value of K_q is found when the probe is injected into solution (direct contact between $F^*$and Q). This unexpected decrease in the fluorescence intensity is consistent with the formation of the expanded structure. Therefore, this kind of process can be informative with regards to the conformational switch of the polyelectrolyte.

1.5.4 Nonradiative energy transfer

Fluorescence nonradiative energy transfer (NRET) measurements can be applied with the combination of two distinct fluorophores in the investigated polymer in order to measure the distances between two sites on the polyelectrolytes [43]. It would, therefore, provide information regarding the conformational switch in the macromolecule. This

phenomenon can be distinguished from fluorescence quenching in that NRET is effective over much larger distances (up to 10 nm). As mentioned previously, nonradiative energy transfer measurement is formed by the presence of two different molecules, the donor molecule (D) transfers energy to another molecule known as the accepter (A) molecule:

$$D^* + A \longrightarrow D + A^* \qquad \text{Equation 1.5.4-1}$$

This type of energy transfer is enhanced by a good overlapping of fluorescence spectrum of D and absorbance spectrum of A. As the efficiency of energy transfer is dependent on the distance between donor and acceptor, there are two approaches for estimation of the distance.

The first approach is to use steady state measurements data as described by the following equation:

$$ET = 1 - {\Phi^F}/{\phi^0} \qquad \text{Equation 1.5.4-2}$$

Here, ET is the transfer efficiency, $\Phi^F$and ϕ^0 are the quantum yield in the presence and absence of acceptor respectively.

The second approach uses excited state life time data as described by the equation below:

$$ET = 1 - <\tau_{ET}> / <\tau_D> \qquad \text{Equation 1.5.4-3}$$

Where τ_{ET} and τ_D are the average life time of the donor in the presence and absence of the energy transfer respectively. The distance between D-A, then can be calculated with the following equation:

$$ET = \frac{R_0^6}{R_{0\ +r^6}^6} \qquad \text{Equation 1.5.4-4}$$

Where R_0 is the Forster distance (critical separation distance). This is defined as the distance which is equal to the distance between donor and accepter (r) and this is due to the equivalence between the rate of transfer and the decay rate of the donor. In this case ET is 50%. Consequently, incorporation of two fluorophores as a donor and an acceptor to a macromolecule (Figure 1.5.4.1) allows investigation the conformational behaviour of polymer in a bulk solution as a function of pH. An enhancement in energy transfer as the pH is

decreased demonstrates that the distance between the donor and acceptor has declined representing a coiling in the polymer chain.

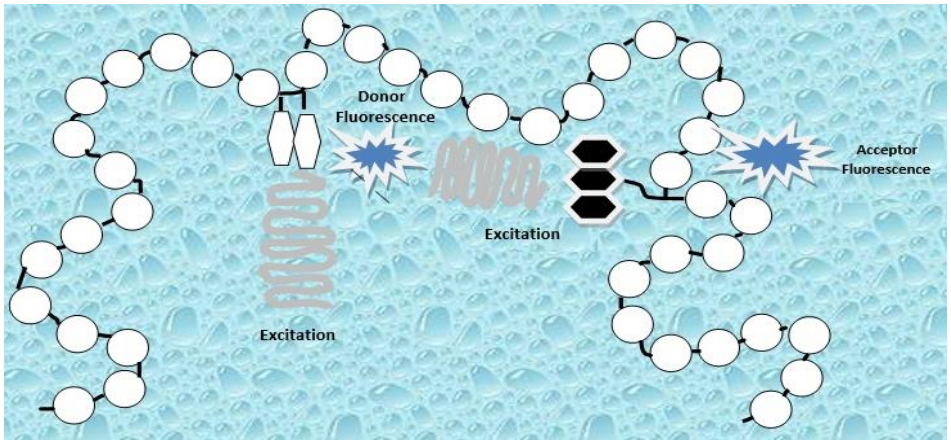

Figure 1.5.4.1. The principle behind fluorescence resonance energy transfer in a polymer chain.

1.5.5 Time-resolved anisotropy measurements (TRAMS)

Time-resolved anisotropy measurement is an additional technique that will be used to provide extra information on the segmental dynamics of the polymers in aqueous solution [14, 27]. Since a fluorophore is chemically attached to the polymer backbone, the mobility of the fluorophore is considered to reflect motion of the tagged site of the macromolecules[27]. In this type of experiment, vertically polarised light is used to photo select fluorophores which are in a parallel orientation to the polarization of the incident light. In fact, these chromospheres will be preferentially excited. The intensity of the emission can then be measured through a polariser. When the polariser is vertical to the polarised excitation the result intensity is called I||. Similarly when the polarized radiation is oriented horizontally to the direction of the polarised excitation the intensity is known as $I^{\perp}$ [37]. The extent of polarisation of the emission is known as anisotropy (r)

Information related to the molecular motion can be obtained by looking at these two different decays of anisotropy. In other words, we can monitor loss of r as a function of

time, r(t). Hence, the time-dependent anisotropy r(t) is estimated from these two distinct intensities values using the following formula:

$$r(t) = \frac{I_{||}(t) - I_{\perp}(t)}{I_{||}(t) + 2I_{\perp}(t)}$$ Equation 1.5.5 1

The raw anisotropy data r(t) can be modelled using exponential function. For example, for single molecular motion:

$$r(t) = r_0 \exp(-t/\tau_c)$$ Equation 1.5.5-1

Here r_0 is the intrinsic anisotropy –spectroscopic property and τ_c is the rotational correlation time which reflects the motion of macromolecule. Figure 1.5.5.1 shows the decay of anisotropy:

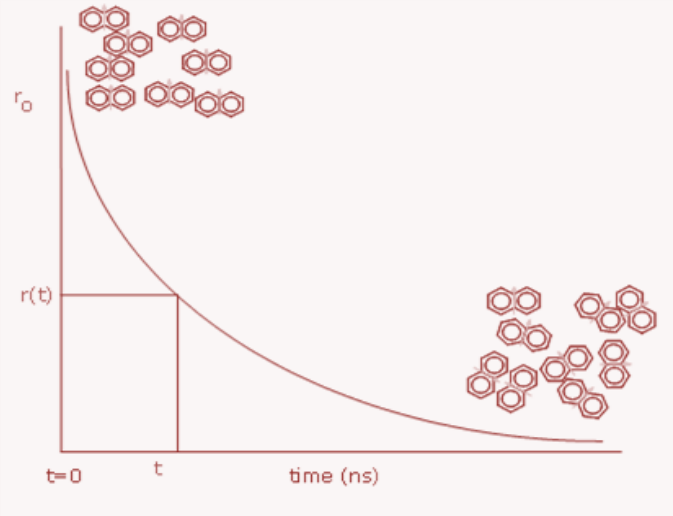

1.5.5-1Schematic representation of time- resolved anisotropy process, a measure of how fast the order is lost.

For this project, an Edinburgh instruments 199 fluorescence spectrophotometer was used to measure the fluorescence anisotropy of fluorescent samples and a schematic illustration of this spectrometer is presented in Figure 1.5.5.2

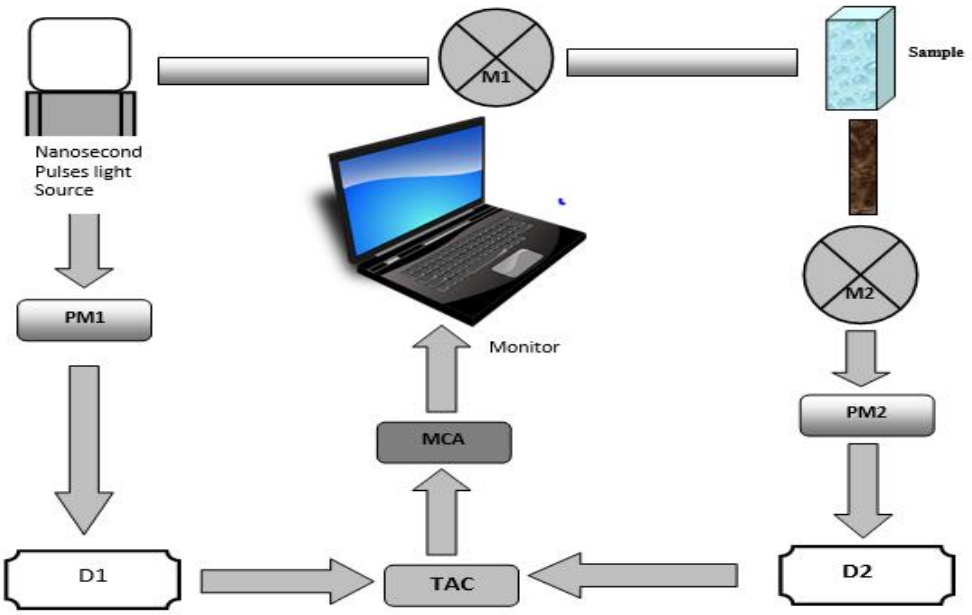

Figure 1.5.5.2 Schematic diagram of the Edinburgh Instruments 199 fluorescence spectrometer.

Analysis is initiated when the light generated by an IBH nano LED pulsed diode, used as an excitation source, is passed through an excitation monochromator (*M1*) where a specific wavelength is picked out to excite the sample. Then the fluorescence generated passes through an emission monochromator (*M2*), where a desired wavelength is selected and is incident on the stop photomultiplier (*PM2*). This signal, following discrimination by (*D2*), stops the generation of voltage in the time-to-amplitude converter (*TAC*). The voltage can be used to determine the time difference between the start and stop pulses.

Output from the *TAC* is deposited in a multi-channel analyser (*MCA*) and is repeated several times. The collection of data produces a curve of fluorescence counts against time in channels as shown in Figure 1.5.5.2 Due to the stop photomultiplier receiving only the first photon from the sample after each pulse, the accumulation of such photons after every pulse gives a true decay curve only when one (or less) fluorescent photon can reach the stop photomultiplier following every pulse.

1.6 Studies of the interactions of the surfactants with polyelectrolytes

Other studies that area related to polymer/surfactant complexes have considered either interactions between polyelectrolytes and oppositely charged surfactant monomers/micelles, or between non-ionic macromolecules with ionic surfactant micelles. Usually, the electrostatic forces provide the main effect in these interactions and the hydrophobic forces are secondary in importance.[44]

Hoffman & Stayton, (2004)[45], conducted a study on binding of oppositely charged surfactants to poly(methacrylic acid) including "poly(methyl acrylic acid) (PMAA), poly(acrylic acid) (PAA), poly(propyl acrylic acid), poly(butyl acrylic acid as well as poly(ethyl acrylic acid) " which highlighted their pH dependent membrane destabilizing activity. The result predicted that the chain length of hydrophobic alkyl group increased based on single methylene unit, and resultantly the value of the constant increased.

Furthermore, Yoshida & Dubin, (1999) [46], in a bid to study the effect of polymer charge, varying pH created an interaction between PAA and cationic mixed micelles of n-hexadecyltrimethyl ammonium chloride. The polymer linear charge density, micelle surface charge density and the ionic strength and the Debye–Hückel parameters are the variables that control the electrostatic process of complex formation. The degree of ionization of the polymer carboxylic acid groups and the micellar mole fraction of ionic surfactant is one of the basic aspects that determines these variables. The study indicated that electrostatic forces control the interaction between the polymer and micelle. The simultaneous increase in pH shows that hydrogen bonding dominates the interaction at low pH (Yoshida & Dubin (1999).

The reaction of PAA with poly(acrylamido-2- methylpropane sulfate) in NaCl and tetramethylammonium chloride showed that sodium ions bind well to PAA, and this reduces its effective polymer charge density. Lee & Kim, (2012) [47], also studied the effect of surfactants on polymers including P(NIPAM-coDMAEMA and PNIPAM. They observed the similar characteristics in both polymers during the phase of transition.

Taktak et al. (2015) [48]also prepared multi-responsive copolymers including DMAEMAco-MEMA using free radical polymerization method. They found that pH-

dependent polymers held a tendency to shrink and swell due protonation and deprotonation. The reaction of DMAEMA with hydrophobic polymers exhibit a domain of hydrogel structure, and consequently, DMAEMA showed a sharp response to pH and temperature.In addition, the interactions between polysaccharide alginate with charged ionic surfactants in an aqueous medium with pyrene as a probe was also studied by Neumann & Iamazaki.(2003) [44]and the hydrophobicity of the medium was measured at the pH of 6 with respect to the dependence of *the* I_1/I_3 ratio of the pyrene emission. This also reduces the concentration of the alginate decreases. This trend indicates the division of the polymer chain hydrophobic microdomain and the aqueous medium. An increase in the concentration of the alginate causes an upsurge in the polymeric hydrophobic microdomains and consequently the highly hydrophobic pyrene molecules will move to the active spot. The electrostatic character was observed to be present in the main initial interaction between the alginate and the surfactant of opposite charge as well as between the charged center on the macromolecular chain and the surfactant's charged head. It appears that hydrophobic interaction plays little or no role in these systems and also longer chain surfactants showed stronger interactions. Additionally, very weak interactions were observed for the polyelectrolyte and surfactants of the same charge. According to Schillen et al. (2000) [49], poly(acrylic acid) can be evaluated based on covalent bonding with a fluorescent hydrophobic chromophore, naphthalene attached randomly on the polymers. They studied polymer, PAAMeNp-34 with steady state fluorescence spectroscopy in methanol at varying pH that shows a fluorescence emission spectra of both Np monomers and Npexcimer with respective intensities of I_M as well as I_E. The association of the Np groups determined excimer emission based on hydrophobic interaction. The intensity ratio (I_E/I_M) reduces in the pH range due to repulsive electrostatic forces that dominate the hydrophobic interaction in the Np groups in the aqueous solution of PAAMeNp-34. Consequently, the polymer chain expands a result of the intrapolymer repulsion that occurs between the carboxylate groups. Moreover, the polymer – surfactant association results in disturbance of the Np-Np interaction. These results are an obvious change in the fluorescence emission, and consequently, the concentration of the surfactant is increased. The structure of polymers/surfactants formed by poly(2-(dimethylamino)ethyl methacrylate) and sodium dodecyl sulfate exist between lignin and PDMAEMA due to the miscible polymer blend system (Goa et al., 2015) [50]. Goa et al. (2015) mixed a weak polyacid softwood kraft

lignin (SKL) with weak polybase (PDMAEMA, and PDMAEMA-*co*PEO-*co*-PDMAEMA copolymer) in order to prepare lignin-based hydrogels. Self-assembled reversible pH-responsive hydrogen is formed by the augmentation of the weight ratio of SKL/PDMAEMA-based polymers, and the non-covalent interactions between the phenolic hydroxyl groups of SKL and the tertiary amino groups of PDMAEMA. They observed reversible pH that was induced between PDMAEMA and PDMAEMA-*co*-PEO-*co*-PDMAEMA.

1.7 Aims and objectives of the present work

This project will deliver targeted data sets on the pH response of the charged macromolecules by using fluorescence techniques including steady state, lifetime and time resolved anisotropy. these techniques particularly well-suited to elucidate, on a molecular scale, many aspects of more complicated systems such as the interactions of both polyelectrolytes with salts and with surfactant micelles. These fundamental studies are of importance in manipulating macromolecular characteristic for industrial applications. Since the synthetic linear polymers are non-fluorescent, fluorophores such as ACE and/or AMMA will be randomly attached to the polymers backbone.

1.8 General Objectives

.To study conformation changes of fluorescently-labeled polyacid[poly (ACE-PAA and ACE-AMMA-PAA)], as a models of the corresponding hydrophobically-modified polymers, a class of materials of rising practical importance, using fluorescence technique.

.To study conformation changes of fluorescently-labeled polybase [poly (ACE-PDMEAMA and ACE-AMMA- PDMEAMA), as a models of the corresponding hydrophobically-modified polymers, using fluorescence technique

1.9 Specific Objectives

Fluorescence study including steady state, excited-state lifetime and time-resolved anisotropy measurements (TRAMS) on:

.Poly(acrylic acid) solutions in the presence of simple electrolytes such as NaCl, $CaCl_2$, NaBr and $CaBr_2$.

Poly (acrylic acid) solutions in the presence of oppositely charged surfactant micelles (Hexadecyltrimethylammonium chloride).

Poly (dimethylamino) ethyl methacrylate (PDMEAMA) solutions in the presence of simple electrolytes such as NaCl, $CaCl_2$, NaBr and $CaBr_2$.

Poly (dimethylamino) ethyl methacrylate (PDMEAMA) solutions in the presence of oppositely charged surfactant micelles (Sodium hexadecyl sulphate).

Chapter 2 **Experimental**

2.1 Preparation and synthesis of materials for linear polymers

2.1.1 Solvents

- Dioxane (Fischer general grade)
- Methanol (Aldrich general and spectroscopic grade)
- Ethanol (Aldrich general grade)
- Diethyl ether (Aldrich general and spectroscopic grade)
- Hexane (Fischer general and Aldrich spectroscopic grades)
- Water (double distilled)
- Tetrahydrofuran (Fisher general and Aldrich Spectroscopic grades)

2.1.2 General reagents

- Sodium hydroxide (Lancaster)
- 9-anthracenemethanol (2: 97%, Fluka)
- Methacryloyl chloride (>_97%, Fluka)
- Hydrochloric acid (Fluka, ≥ 37%)
- Sodium hydroxide (Sigma-Aldrich, ≥ 97%)
- Sodium chloride (Sigma-Aldrich, ≥ 99.5%)
- Calcium chloride (Sigma, ≥ 96%)
- Sodium bromide (Sigma, ≥ 99%)
- Calcium bromide (Sigma, ≥ 99.89%)
- N,N'-Dicyclohexyl carbodiimide (DCC) (Aldrich, 99%)
- Methacrylic acid (Aldrich, 99%)
- 4-(Dimethyl amino) pyridine (DMAP) (Aldrich, ≥99%)
- Anhydrous sodium sulphate (Sigma-Aldrich, ≥ 99%)
- Hexadecyltrimethylammonium chloride **(**Sigma-Aldrich, ≥ 98%)
- Sodium hexadecyl sulfate

2.1.3 Polymerisation initiator and coupling agents

2.1.3.1 2,2'-Azobisisobutyronitrile (AIBN) (BDH, 97%)

AIBN was recrystallised from diethyl ether as follows. Over a water bath at 30°C, AIBN was dissolved in a minimum amount of diethyl ether in a flask with stirring. The solution was filtered and left to cool before being put in the freezer for about 30 mint. The recrystallised material was then washed with a small amount of diethyl ether and filtered under a vacuum before the entire process was repeated twice more. Following the final recrystalisation the AIBN was dried in a vacuum oven overnight at room temperature. The purified reagent was stored in the freezer at -10°C.

2.1.3.2 4,4′-Azobis(4-cyanovaleric acid) (ACVA) (Aldrich, ≤98%)

Used as received, without any further purification.

2.1.3.3 N-(3-Dimethylaminopropyl)-N′-ethylcarbodiimide hydrochloride (EDC) (Fluka, ≤99.0%)

Used as received, without any further purification.

2.1.4 Fluorescent labels

2.1.4.1 Acenaphthylene (ACE) (Lancaster, 90%)

Acenaphthylene (ACE) was purified by applying the following procedure: Acenaphthene is the major impurity within the provided ACE. This was removed by multiple recrystalisation from methanol followed by vacuum sublimation [51]. The purity of the ACE was tested with a Gallenkampf melting point apparatus. The purity was judged to be 100% based on the documented ACE melt point of 86.5-87 C^0. The purified monomer was stored at -10 C^0.

2.1.4.2 (9-Anthryl)methyl methacrylate (AMMA)

(9-Anthryl)methyl methacrylate (AMMA) was synthesied according to the literature [52], figure 2.1. 27.7 g (0.13 mol) of 9-Anthracenylmethanol was dissolved in 350 mL of tetrahydrofuran (THF). A solution of 11.19 g (0.13 mol) of methacrylic acid in 50 mL of THF was added, and the solution was cooled in an ice-water bath. A solution of 26.82 g

(0.13 mol) of dicyclohexyl carbodiimide (DCC) in 50 mL of THF was added upon stirring followed by a solution of 3.2 g of 4-dimethyl amino pyridine (DMAP) in 50 mL of THF. The reaction mixture was kept in the ice-water bath for 5 min and then for 8 h at room temperature. After this time, thin layer chromatography (TLC) was used to check that all the monomer had been consumed in the reaction. Had all the monomer not been used up the solution would have been left to stir for a longer period, possibly overnight. The resultant solution formed an orange oily liquid and precipitated dicyclohexylcarbamide which was filtered off and washed with 50 ml of THF on the filter. The solvent was evaporated, and the formed suspension was kept in refrigerator for several hours and then at room temperature for 3 days. Distilled water was added to the mixture, followed by diethyl ether in order to extract the organic layer. The liquid was then poured into a separating funnel and the lower aqueous phase was removed, leaving the orange ether layer (containing the product). The ether layer was filtered with a paper filter then washed with 0.5M HCl solution (3 times) followed by a saturated $NaHCO_3$ solution (4 times). The ether solution was finally washed 4 times with distilled water and dried over anhydrous sodium sulphate.

(BDH) for a period of 16 hours at room temperature. The sodium sulphate was filtered off and the ether solution was evaporated off with a rotary evaporator. The resultant product was recrystallised from spectroscopic grade methanol (3 times). After the completion of the recrystallisation the monomer was dried in a vacuum oven at 60^{o}C for several days. The yellow crystalline solid was tested for purity from its melting point (82-83.5^{o}C) and by obtaining its NMR spectrum in $CDCl_3$. After synthesis, the monomer was stored in the freezer at -10^{o}C.

$_1$H NMR (400 MHz, CHLOROFORM-*d*) δ ppm 1.92 (s, 3 H, =C-C**H**$_3$) 5.5(s, 1 H, -C=C**H**) 6.06 (s, 1 H, -C=C**H**) 6.22 (s, 2 H, **Ar**) 7.49 (t, *J*=6 Hz, 2 H, **Ar**) 7.58 (t, *J*=6 Hz, 2 H, **Ar**) 8.02 (d, *J*=8 Hz, 2 H, **Ar**) 8.37 (d, *J*=9 Hz, 2 H, **Ar**) 8.51 (s, 1 H, **Ar**). m/z = 276

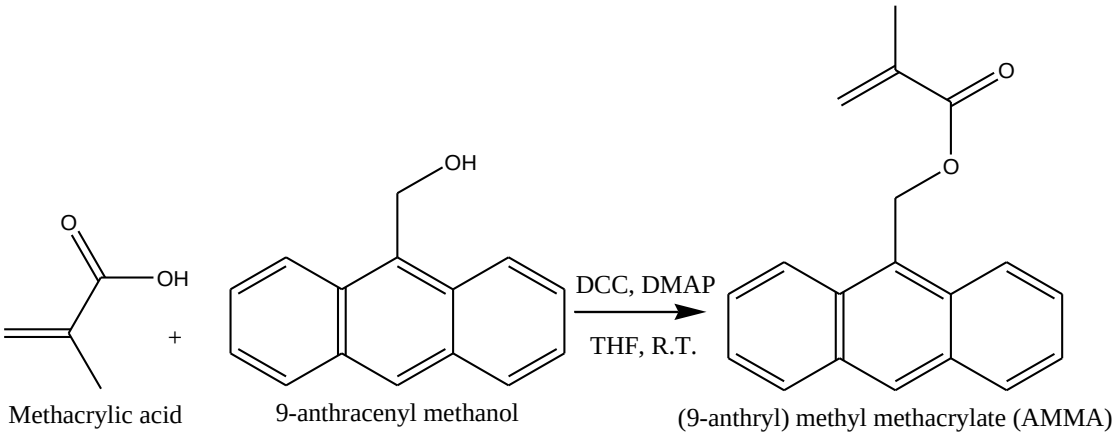

Figure 2.1 Scheme for the synthesis of (9-anthryl)methyl methacrylate (AMMA) .

2.1.5 Monomers

2.1.5.1 Acrylic acid (AA) (Aldrich, 99%)

Prior to use, the monomer acrylic acid (AA) was passed through a vacuum distillation at room temperature to remove the gas phase inhibitors (mono methyl ether hydroquinone) that are included in the supplied material to prevent polymerisation. The distillation was carried out with the distillate flowing into an iced vessel. The purified AA was stored in the freezer at -10C^0.

2.1.5.2 2-(dimethylamino)ethyl methacrylate (98% Aldritch)

Several approaches have been used in attempt to remove polymerisation inhibitor:

Vacuum distillation

Inhibitor removal column

Alumina-based column

2.1.6 Synthesis unlabelled and fluorescently labelled Poly-2-(dimethylamino)ethyl methacrylate preparation

2-(dimethylamino)ethyl methacrylate was polymerised using an AIBN initiated free radical mechanism. This method was chosen because the free radical mechanism results in a polymer which does not contain any potential contaminants that would impede

fluorescence investigations. Polymers were prepared without any fluorescent label or with ACE label and with both ACE and AMMA labels in trace amounts.

Solutions with a monomer to solvent weight ratio of roughly 1: 3 were made using THE as the solvent. The monomer mixes included either 0.5 wt% ACE, 1.0 wt% AMMA or 0.5 wt% ACE and 1.0 wt% AMMA. The AIBN was used at a concentration of 1 g/litre. The polymerisation solution was thoroughly degassed using a freeze-pump-thaw method and then polymerised at 60°C for not less than 16 hours. The polymers were purified by multiple dissolutions (3 times) and subsequent precipitations using THE as the solvent and hexane as the non-solvent, this removes any unreacted monomer and labels which remain dissolved in the THF/hexane mix. The polymer was then dried in a vacuum oven over at least 24 hours before being weighed.

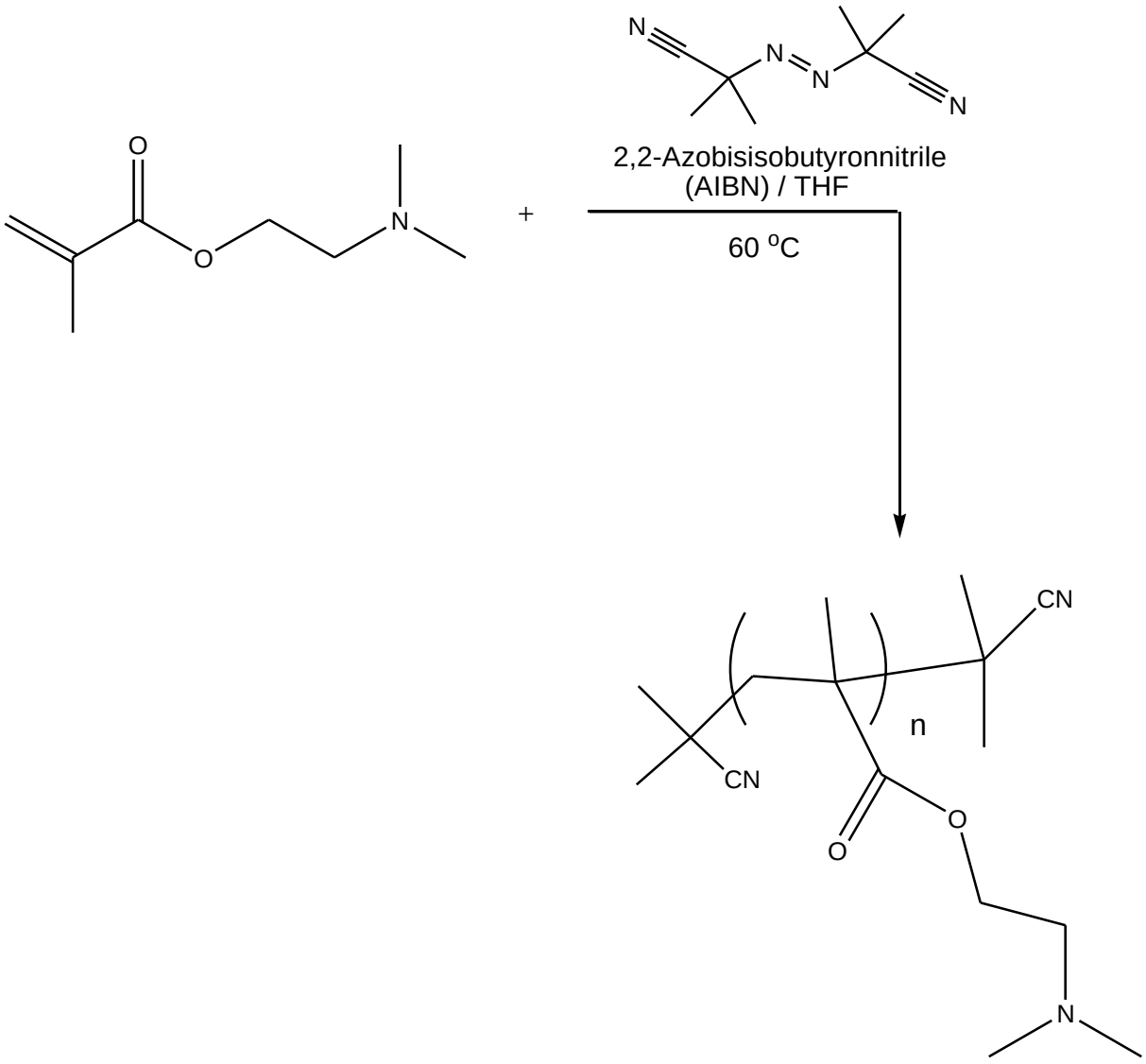

2.1.6.1 Scheme for the radical copolymerisation of dimethylamino ethyl methacrylate (DMAEMA).

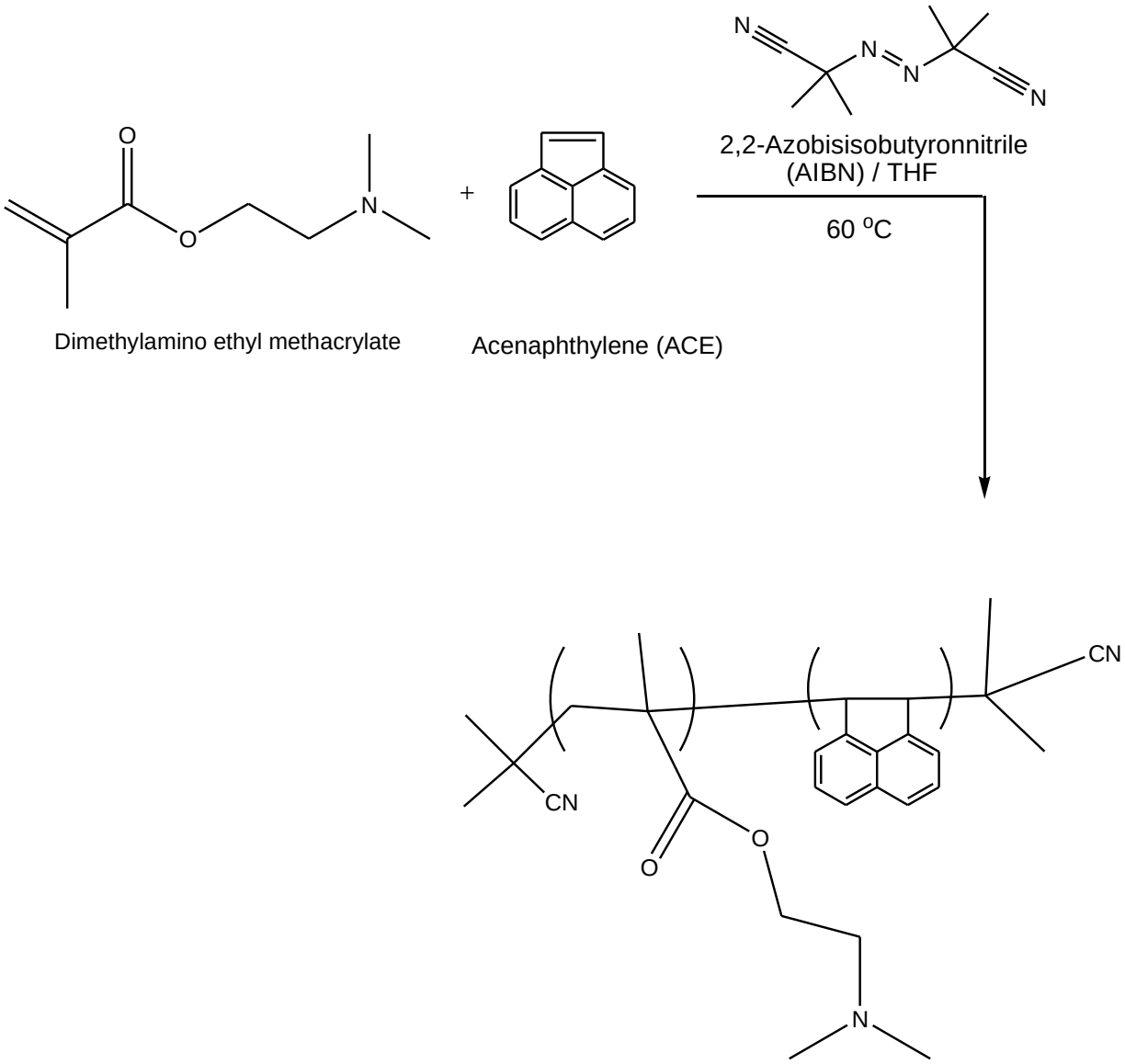

2.1.6.2: Scheme for the radical copolymerisation of acenaphthylene (ACE) and dimethylamino ethyl methacrylate (DMAEMA).

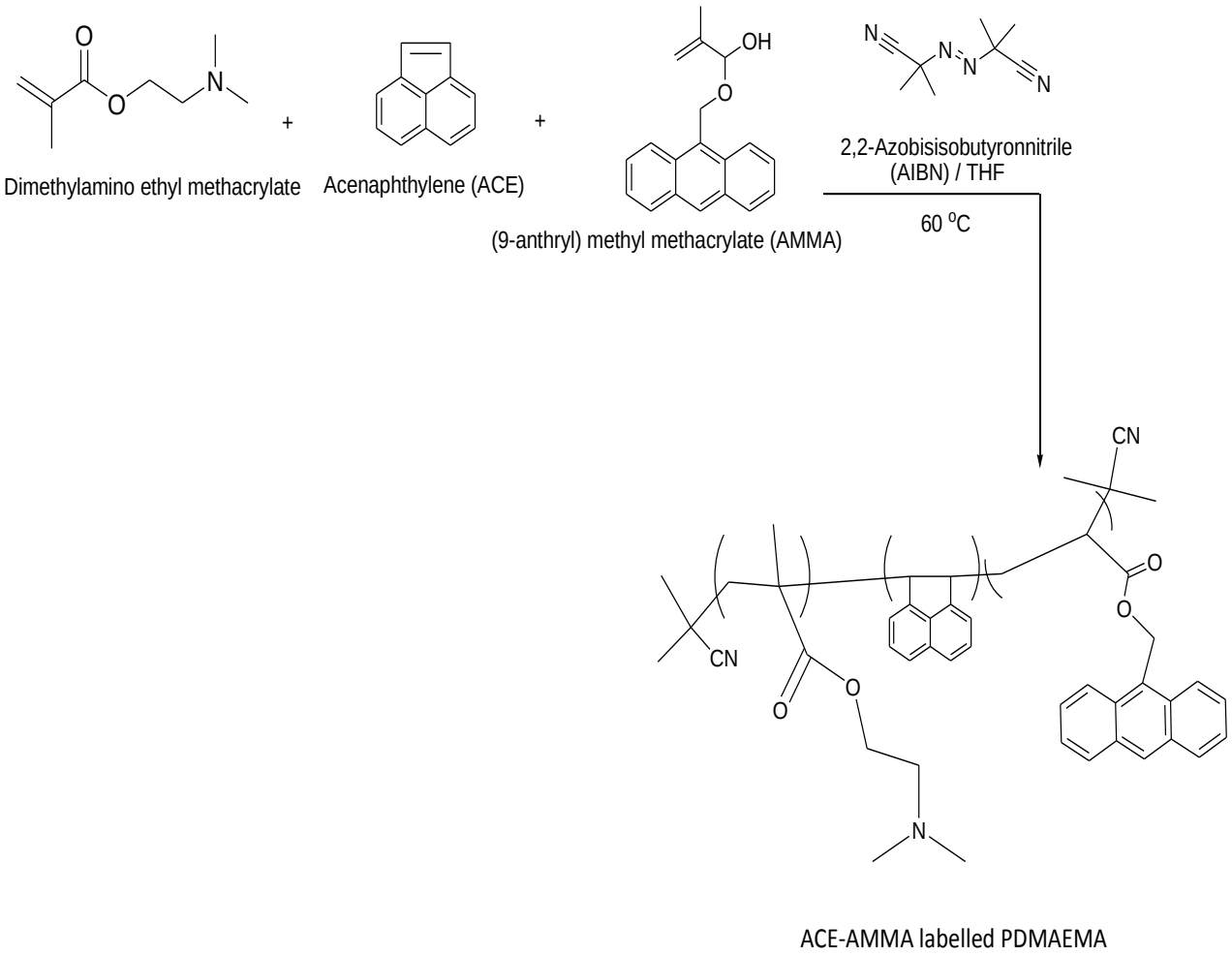

2.1.6.3: Scheme for the radical copolymerisation of ACE and AMMA labelled dimethylamino ethyl methacrylate (DMAEMA).

As a typical polymerisation, below is listed the amounts of reagents used for the synthesis of the ACE labelled PDMAEMA sample:

Solvent used: THF, 20m1
Monomer used: DMAEMA 5.898 g
Label used: ACE 29.6 mg
Initiator: AIBN 30mg
The reaction was left at 60°C for 24 hours.
The resulting polymer, after reprecipitation 3 times as mentioned above, was dried and gave a final weight of 5.216 g and thus a final yield of 88.437%

2.1.7 Synthesis unlabelled and fluorescently labelled Poly-acrylic acid

The PAA-COOH polymer was synthesized by radical polymerization of 5 g of acrylic acid using 0.197 g of the initiator 4,4'-azobis(4-cyanovaleric acid) in 60 mL of 1,4-dioxane under vacuum line for 24 h at 60 °C. The polymer started to precipitate from the reaction solution after about 5 h. The acid-ended polymer was purified by multiple precipitations in ether from methanol.

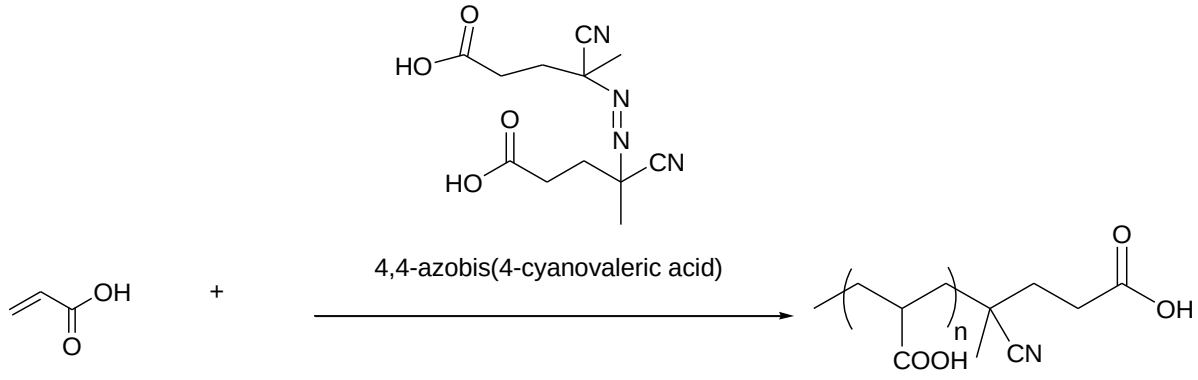

2.1.7.1: Scheme for the radical polymerisation of acrylic acid (AA).

ACE-labelled PAA was also prepared by free radical copolymerization, under high vacuum in dioxane, using purified acrylic acid (2.771g), recrystallised acenaphthylen

(ACE)(0.072g) and AIBN(0.1092g) as initiator at 60 °C for 15h. The labelled polymer was purified by multiple precipitations from dioxane into diethylether.

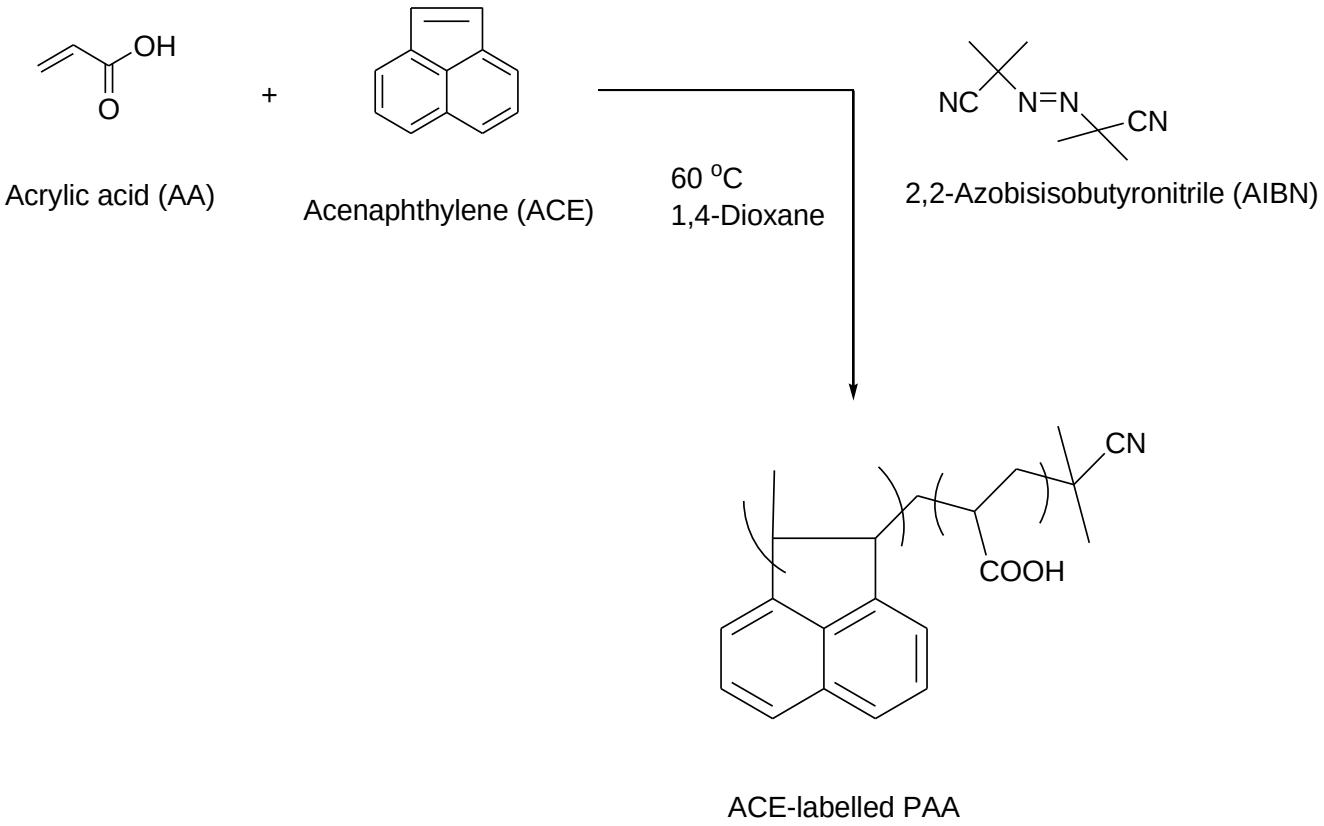

2.1.7.2: Scheme for the radical copolymerisation acenaphthylene (ACE) and acrylic acid(AA).

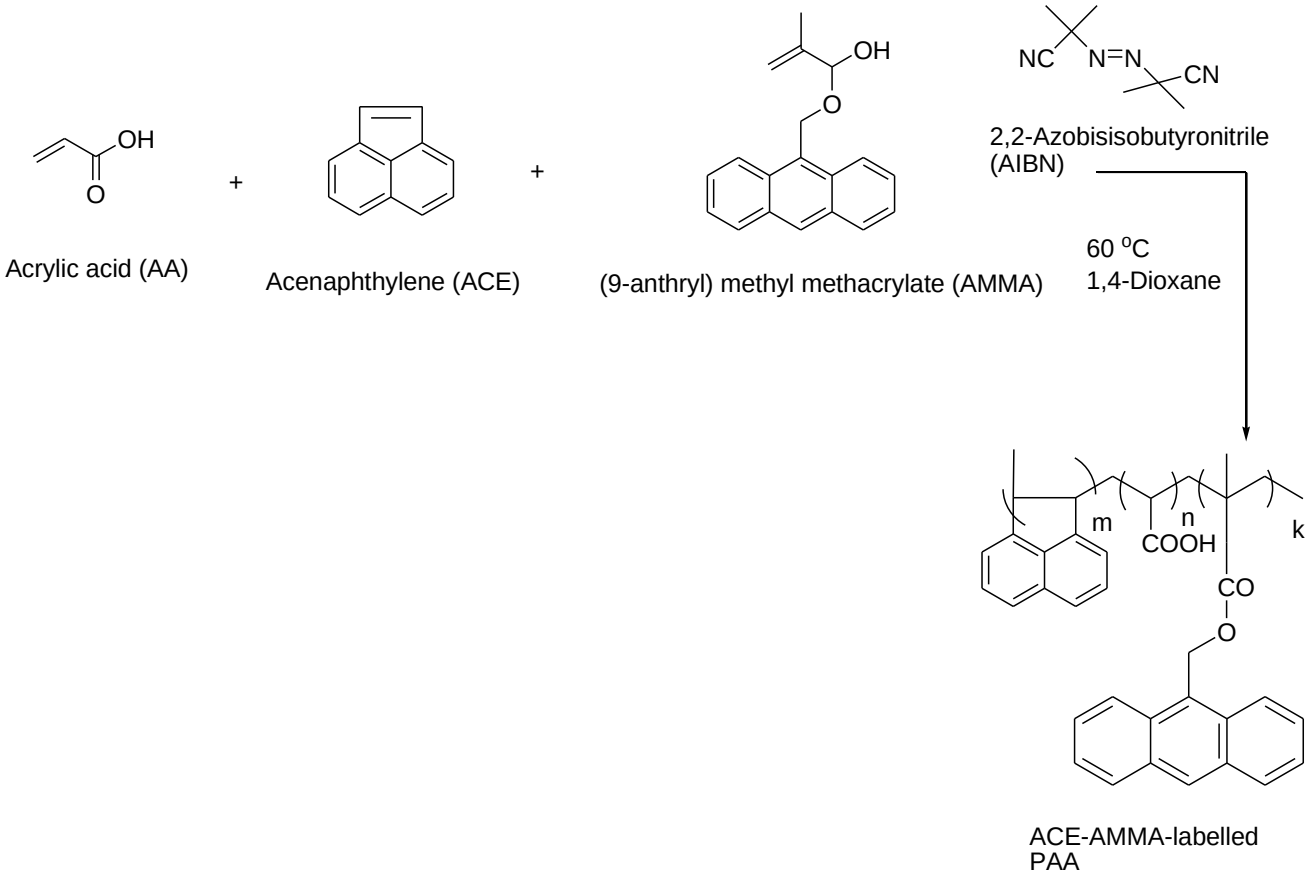

2.1.7.3: Scheme for the radical copolymerisation of acenaphthylene (ACE), (9-anthryl) methyl methacrylate (AMMA) and acrylic acid (AA).

ACE-AMMA-labelled PAA was prepared as above by free radical copolymerization, under high vacuum in dioxane, using purified acrylic acid(2.771g), recrystallised ACE(0.072g), recrystallised AMMA(0.26g) and AIBN(0.1092g) as initiator in 1,4-dioxane at 60 °C for 15h. The doubly labelled polymer was purified by multiple precipitations from dioxane solution into diethylether.

2.2 Characterisation Techniques

2.2.1 Nuclear magnetic spectroscopy (NMR)

To characterise the monomers, synthetic model polymers and biopolymers proton nuclear magnetic resonance ($_1$H NMR) spectra were recorded on a Bruker AC250 sample changer instrument operating at 400 MHz The monomer and polymer samples were prepared in deuterated solvent (20mg/1ml). The 1D ACDlabs program was used to analyse spectrometer data.

2.2.2 Ultraviolet spectroscopy (UV)

To estimate the quantity of fluorescent label ((mol%)fluorophore) in the polymers, ultraviolet (UV) spectra were recorded with a Hitachi U-2010 spectrometer. The scan was done from 800 nm to 200nm with a scan speed of 400nm/min. The slits were set at 2nm. Fluorophores were measured at different concentrations in methanol spectroscopic grade, whereas polymer solutions at 10^{-1} wt% in deionised water were prepared and measured at room temperature.

The mol% of the fluorescent label was calculated by the following equation:

$$(mole)\%_{fluorophore} = \frac{c_{fluorophore}}{c_{fluorophore} + c_{monomer}} \times 100 \qquad \text{Equation 2.1}$$

Where, $C_{fluorophore}$ and $C_{Monomer}$ are the molar concentration of the fluorescent label and the non fluoro-monomer, respectively.

2.2.3 Gel-permeation chromatography (GPC)

Gel permeation chromatography (GPC) was utilized to determine the molecular weight of prepared polymers. Polymer solutions were prepared in (0.2M sodium nitrate and 0.01M sodium hydrogen orthophosphate) mobile phase. The prepared sample was filtered, then placed in a manual injection using 200μl Injecton loop which injected the sample into a pump which was set to a flow rate of 1ml/min. The sample was pumped through (TSKgelGPMPWX), a mixed of polyehelene oxide (PEO) and polyehelene glycol (PEG) standards. An Erma Refractive Index detector was applied.

2.3 Calculations

2.3.1 Yield calculations

Monomer yields were calculated by a simple calculation such that the mass of end material was expressed as a relative percentage of the mass of starting material. Whereas, the macromolecule yields were obtained by expressing the mass of end material as a relative percentage of the monomer and label(s) used in the mixture of reaction.

2.3.2 Fluorescent label content

A more accurate concentration (C) can be determined mathematically from the Beer-Lambert's law for the calibration curve as flows [37]:

$$A = \text{Ɛ}\, bC \qquad \text{Equation 2.3.2.1}$$

Where, A is the absorbance value of fluorophore, $\mathcal{E}$ is the molar absorptivity; b is the bath length of the cell, equal to 1 cm and C the concentration of fluorescent label in solution.

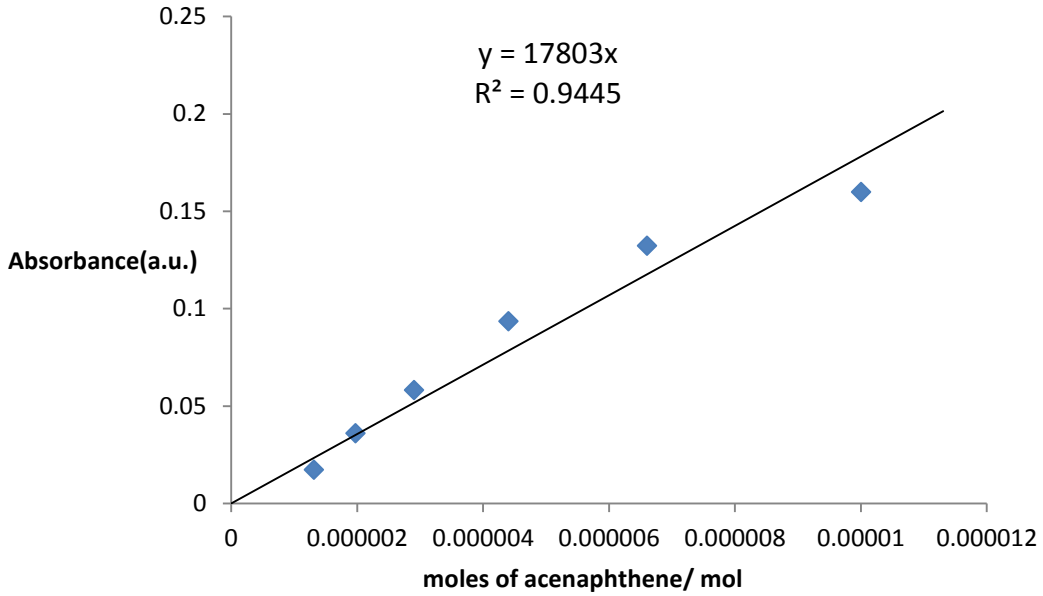

Figure 2.3.2.1 Beer-Lambert's law of acenaphthene at different molar concentration in methanol.

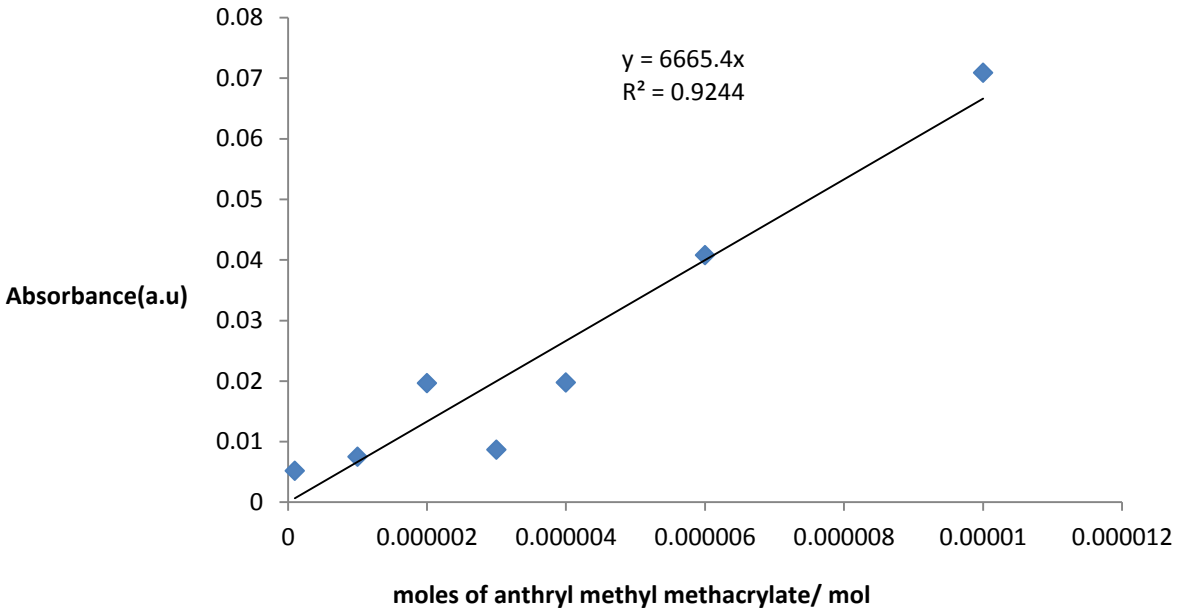

Figure 2.3.2.2 Beer-Lambert's law of (9-anthryl methyl) methacrylate at different molar concentration in methanol

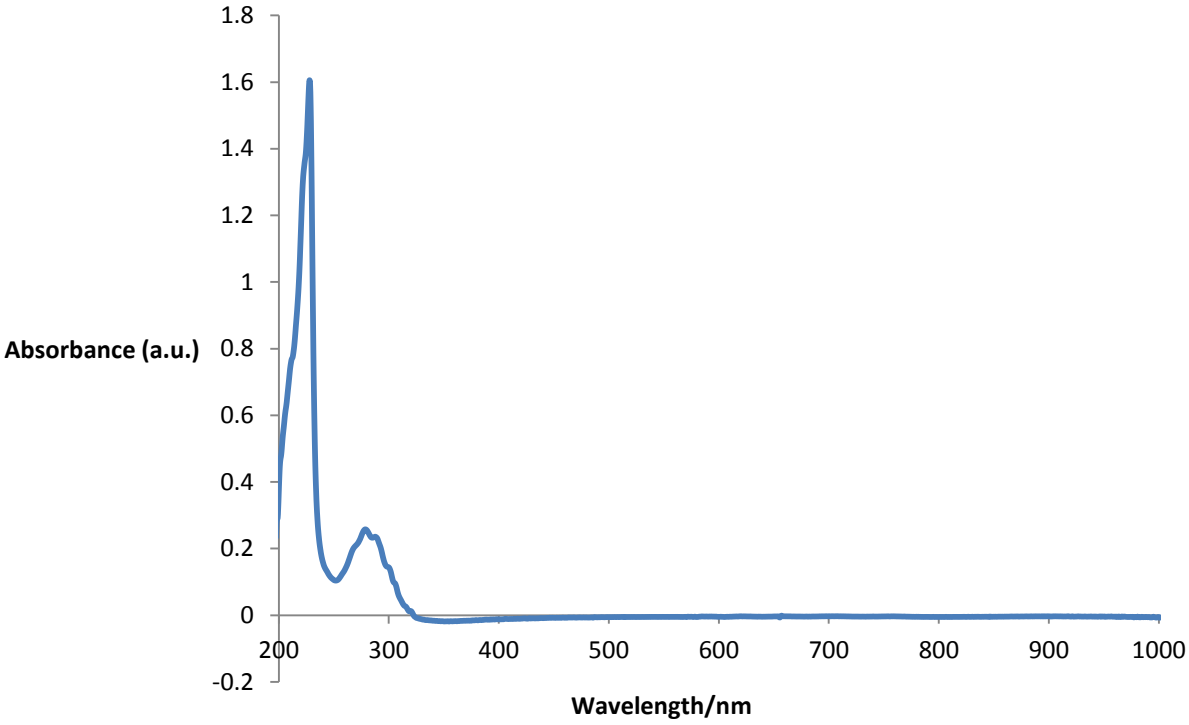

Figure UV-Absorption spectra of 0.1 g/L ACE-labelled PAA.

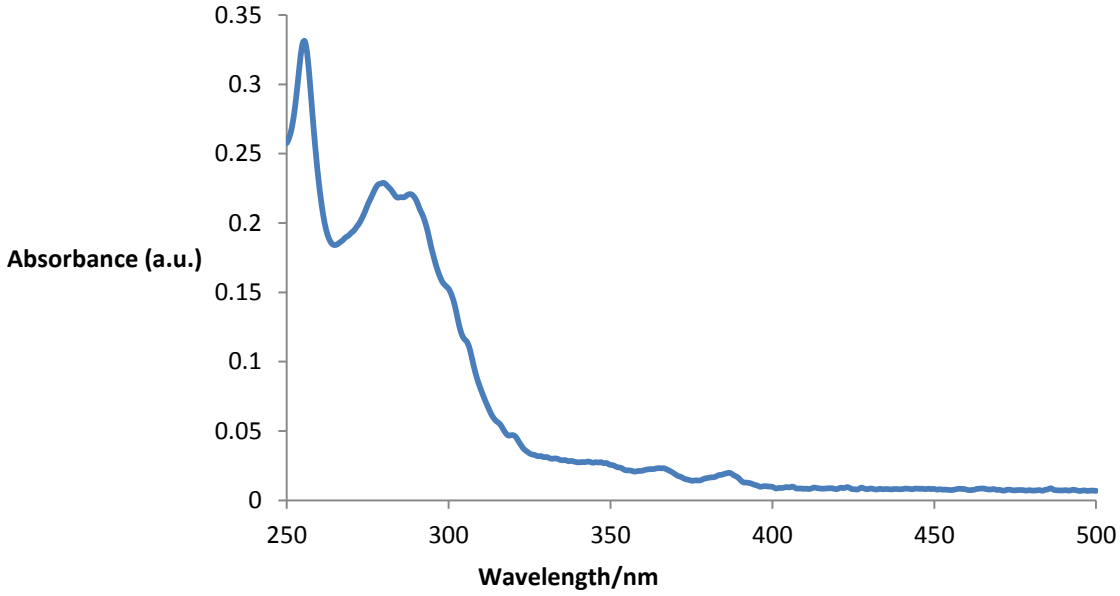

Figure UV-Absorption spectra of 0.1 g/L ACE-AMMA-labelled PAA

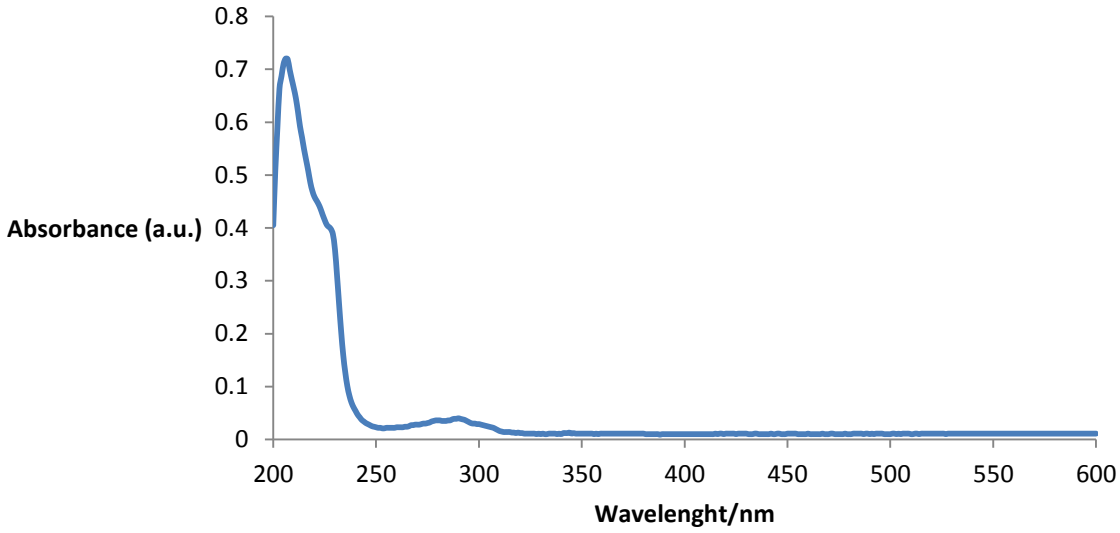

Figure UV-Absorption spectra of 0.1 g/L ACE-labelled PDMAEMA

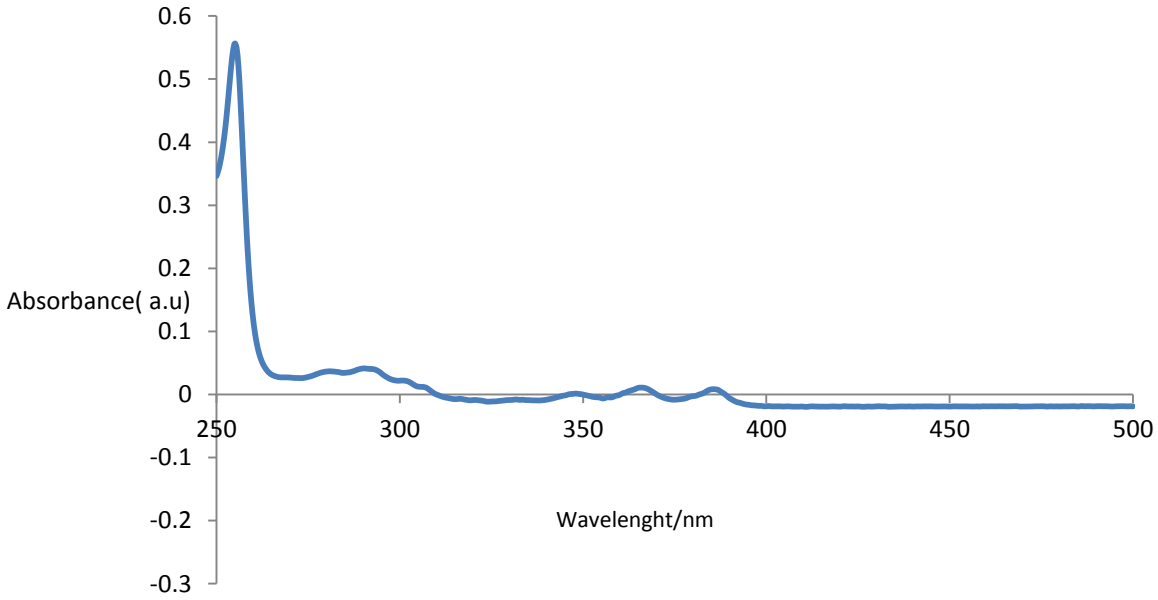

Figure UV-Absorption spectra of 0.1 g/L ACE-AMMA-labelled PDMAEMA

2.4 Results of characterisation:

2.4.1 PDMAEMA- No label

Molecular weight, GPC(RI): Mn: 30791g/mol, Mw: 93795g/mol.

NMR: 1H NMR (500 MHz, DEUTERIUM OXIDE) δ ppm (br, 2H, CH2N), 1.97-2.46 (br, 2H, CH2O), 2.51 (br, 6H, N-(CH3)2), 0.5-1.29 (m, 5H,CH3 and CH2 main chain and backbone). The H1 NMR spectrum was quite informative, viewing the typical H1 NMR of unlabelled PDMAEMA. Additionally, the 1H NMR spectrum showed that no monomer was found.

2.4.2 PDMAEMA-ACE

Yeild: 88.004%

Fluorescent label content: (mol %)$_{ACE}$ 0.61311 mol%

Molecular weight GPC(RI): Mn: 17368g/mol, Mw: 46330g/mol.

NMR: 1H NMR (500 MHz, DEUTERIUM OXIDE) δ ppm 3.84-4.36 (br, 2H, CH2N), 1.97-2.46 (br, 2H, CH2O), 2.51 (br, 6H, N-(CH3)2), 0.5-1.29 (m, 5H,CH3 and CH2 main chain and backbone) 6.85-8.45 (br. m., 15 H, Ar). The H1 NMR spectrum was quite informative, viewing the typical H1 NMR peaks of PDMAEMA and a broad peak in the aromatic region is supposed to the acenaphthene ring.

2.4.3 PDMAEMA-ACE-AMMA

Yield: 69.124%

Molecular weight: Because of solubility issues a molecular weight for ACE-AMMA-PDMAEMA was not achieved, there may be other molecular weight determining techniques that could be used however the macromolecule was insoluble in the solvent systems for the three available GPCs at the masses required. However, this polymer still soluble in aqueous solutions at the concentrations required for the fluorescence studies and so may still be employed.

Fluorescent label content: (mol %)$_{ACE}$ 0.4018 mol%,

Fluorescent label content: (mol %)$_{AMMA}$ 0.257 mol%

NMR1H NMR (500 MHz, DEUTERIUM OXIDE) δ ppm 3.84-4.36 (br, 2H, CH2N), 1.97-2.46 (br, 2H, CH2O), 2.51 (br, 6H, N-(CH3)2), 0.5-1.29 (m, 5H,CH3 and CH2 main chain and backbone) 6.98-8.99 (br. m., 15 H, Ar). The H1 NMR spectrum was quite informative, viewing the typical H1 NMR peaks of PDMAEMA and a broad peak in the aromatic region is supposed to the acenaphthene and anthracene rings.

2.4.4 PAA-No label

Yeild: 83.98%

Molecular weight GPC(RI): Mn: 15043g/mol, Mw: 146216g/mol

NMR: 1H NMR (500 MHz, DEUTERIUM OXIDE) δ ppm 1.29-2.15(br. m, 2 H , b:C-CH2 backbone) 2.96-2.56 (br. m, 1 H, a:HOOC -CH). The H1 NMR spectrum was quite informative, viewing the typical H1 NMR of unlabelled PAA. Additionally, the 1H NMR spectrum showed that no monomer was found.

2.4.5 PAA-ACE

Yeild: 87.966%

Fluorescent label content: (mol %)$_{ACE}$ 2.28 mol%

Molecular weight GPC(RI): Mn: 17368g/mol, Mw: 46330g/mol.

NMR: 1H NMR (500 MHz, DEUTERIUM OXIDE) δ ppm 1.29-2.15(br. m, 2 H , b:C-CH2 backbone) 2.96-2.56 (br. m, 1 H, a:HOOC -CH) 6.98-7.82 (br. m., 6 H, Ar). The H1 NMR spectrum was quite informative, viewing the typical H1 NMR peaks of PAA and a broad peak in the aromatic region is supposed to the acenaphthene ring.

2.4.6 PAA-ACE-AMMA

Yeild: 86.866%

Fluorescent label content: (mol %)$_{ACE}$ 1 mol%

Fluorescent label content: (mol %)$_{AMMA}$ 0.257 mol%

Molecular weight GPC(RI): Mn: 2333g/mol, Mw: 28580g/mol

NMR:1H NMR (500 MHz, DEUTERIUM OXIDE) δ ppm 1.30-2.06 (br. m, 2 H, C-CH2 backbone) 2.15-2.65 (br. s., 1 H, HOOC -CH) 6.9-7.8 (br. m., 15 H, Ar). The H1 NMR spectrum was quite informative, viewing the typical H1 NMR peaks of PAA and a broad peak in the aromatic region is supposed to the acenaphthene and anthracene rings.

2.5 Fluorescence Measurements

2.5.1 Preparations of samples for photophysics studies

To obtain a consistent polymer concentration in solutions for photophysics studies a stock solution of polymer in distilled water at a concentration of 0.1 g in 100m1 was made. Each time a solution was required for fluorescence studies 1 ml of this solution was removed to make up to l 0 ml to give a concentration of 10^{-2}wt%. The pH of these solutions was controlled by addition of HCl and NaOH.

2.5.2 Fluorescence steady state measurements

Fluorescence steady state measurements were carried out on Spectrofluorometer FluoroMax®-4**.** For all ACE and AMMA labelled polymers the excitation wavelength was 290 nm and the emission range was 330-500 nm to detect both donor and acceptor. An emission range of 380-500 nm and excitation wavelength of 370nm was applied to detect AMMA only. Emission and excitation slits were set on 2.5. seven accumulation scans were made seven times for each reading to ensure smooth spectra.

2.5.3 Fluorescence lifetime and time resolved measurements

Fluorescence excited state lifetime and time resolved measurements were carried out via an IBH 5000 system and Edinburgh Instruments 199 Fluorescence Spectrometers, respectively. Samples were excited at 290nm with the monochromator set to detect fluorescence at 340nm to detect ACE. The range was 200ns for ACE samples, and 30,000 counts were obtained for each sample in lifetime measurements, whereas 20,000 counts were obtained for time resolved measurements. A prompt was run after each sample to take into account scattered light from the source during fluorescence examination.

Chapter 3 Fluorescence investigations of the solution behaviour of pH responsive polymers

In this chapter, the fluorescence techniques such as steady state, excited state lifetime and time resolved anisotropy are applied to study the effect of pH on the conformational behaviour of singly and doubly labelled poly(acrylic acid) and poly (dimethylamino ethyl methacrylate).

3.1 Conformational Behaviour of ACE-labelled PAA as a Function of pH

The effect of changes in pH on diluted aqueous solution of ACE-labelled PAA was studied. The fluorescence steady state, the fluorescence exited state lifetimes and the fluorescence time-resolved anisotropy data was collected for this polymer at different pH values.

3.1.1 Fluorescence steady state spectra of ACE- labelled PAA as a function of pH

Figure 3.1 shows a plot of a measured steady-state fluorescence emission spectra of 10^{-2} wt% aqueous solution of ACE-labelled-PAA over a 2-11 range of pH values. In this solution acenaphthylene fluorophore (ACE) label is responsible for the fluorescence emission spectra.. The observed emission spectrum is well known for the ACE fluorophore and characterised by a structured band centred at 340nm when excited by 290 nm. The measurement shows that the maximum emission peak position is independent of the pH value of the polyelectrolyte solution. This is confirmed by the lack of marked difference in the position of the maximum emission peak of the spectra when the pH of the solution was varied. This suggests that there is no significant dependence of the fluorescence intensity of ACE label on the structural conformation of the polymer chain to which it is covalently linked.

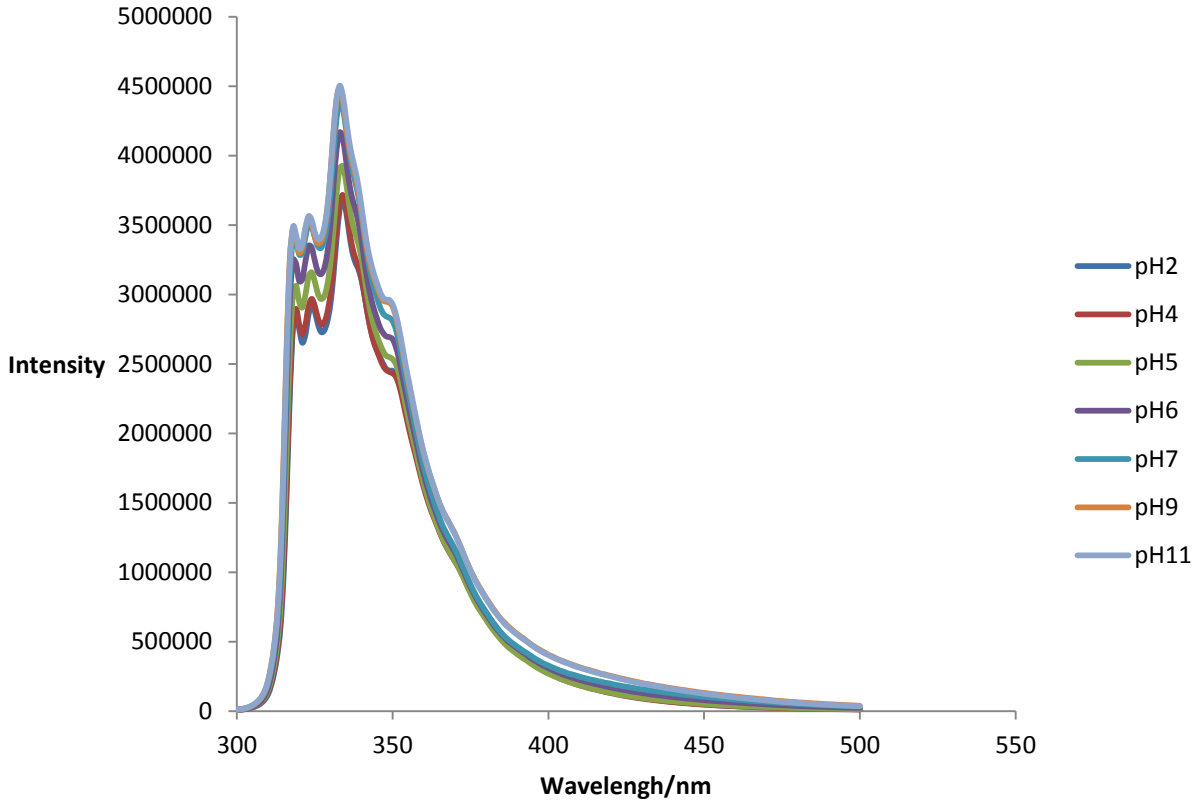

Figure 3.1: Steady-state fluorescence emission spectra of 10^{-2} wt% ACE-labelled PAA in aqueous solution at different pH (λex = 290 nm).

3.1.2 Fluorescence exited state lifetimes of ACE- labelled PAA as a function of pH

From the fluorescence intensity decays for 10^{-2} wt% ACE-labelled-PAA over a pH range (Figure 3.2), it was observed that at high pH (pH > 4), the ACE-labelled polymer showed shorter duration decays compared to those at lower pH values. This could be attributed to the fact that polyelectrolyte chains begin to deprotonate at this pH level, adopting a partially expanded form, due to the repulsive electrostatic force among the ionized carboxylic moieties (COO^-) [2]. In acidic conditions, the lifetime decays of the ACE labels are longer than their lifetime decays in basic conditions since the polymer chains are partially collapsed due to the deprotonation of carboxylate groups of PAA[2]. This is consistent with solubilisation of ACE in the protective domains of the coiled chain.

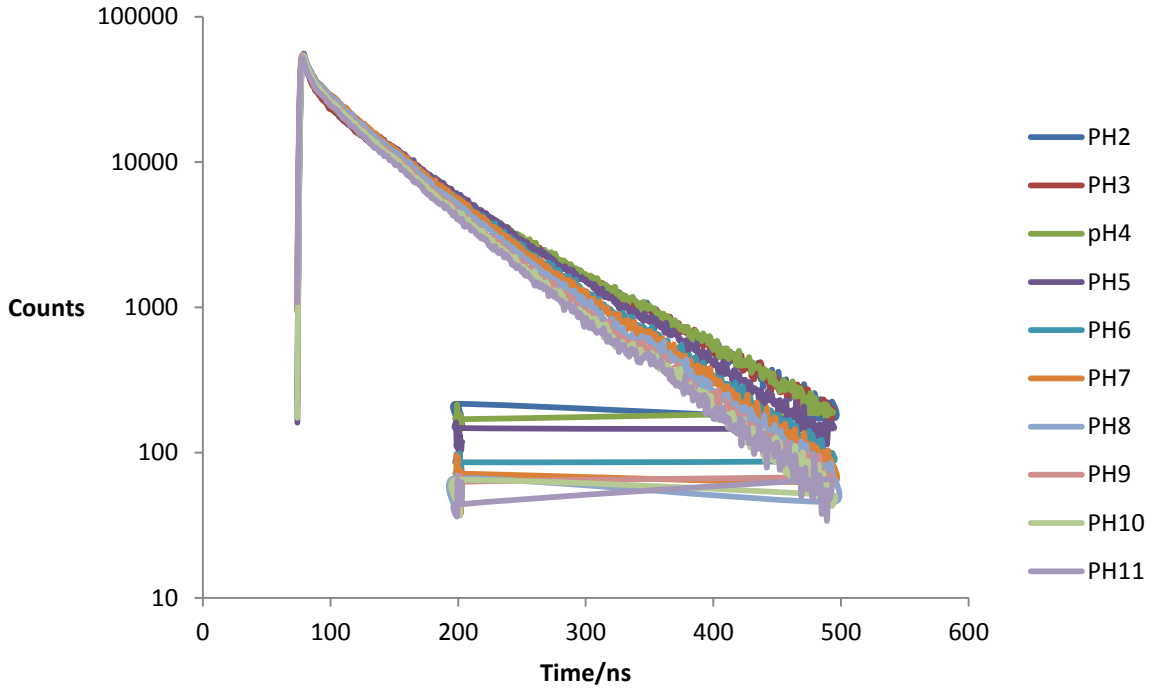

Figure 3.2 Fluorescence intensity decays as a function of pH for 10^{-2} wt% solution ACE-labelled PAA in water

Fluorescence excited state analysis was carried out by fitting the raw data to mathematical functions. The statistical value A chi square statistic is a measurement of how expectations compare to results. The data used in calculating a chi square statistic must be random, raw, mutually exclusive, drawn from independent variables and drawn from a large enough sample. If χ^2 is close to unity, then we have chosen a good fit. However, single exponential fit was unsatisfactory, since it generated large χ^2 values (Eqn 3.1). To improve these values, a double exponential fit was applied to all raw fluorescence intensity decay data (Eqn 3.2). Single and double exponential fits can be expressed as follows:

$$I(t) = A + B\, exp^{-t/\tau_f} \qquad \text{(Single exponential fit)} \qquad \text{Equation 3.1}$$

$$I(t) = A + B_1\, exp^{-t/\tau_{f1}} + B_2\, exp^{-t/\tau_{f2}} \qquad \text{(Double exponential fit)} \qquad \text{Equation 3.2}$$

Where A and B are constants, t is time and the τ_f components represent the fluorescence excited state lifetimes. The τ_{f1} component is usually in the nanoseconds range, while τ_{f2} is

in 10^{-10} seconds range. From this, it can be deduced that the decay has two components, a longer decay component followed by a relatively short decay component. Figure 3.3 shows a sample of fluorescence intensity decay with its fit and residuals data of ACE-PAA. Eqn 3.3 can be employed to determine the average excited state fluorescence lifetime $< \tau_f >$.

$$< \tau_f >= \sum B_i \tau_i^2 / \sum B_i \tau_i \qquad \text{Equation 3.3}$$

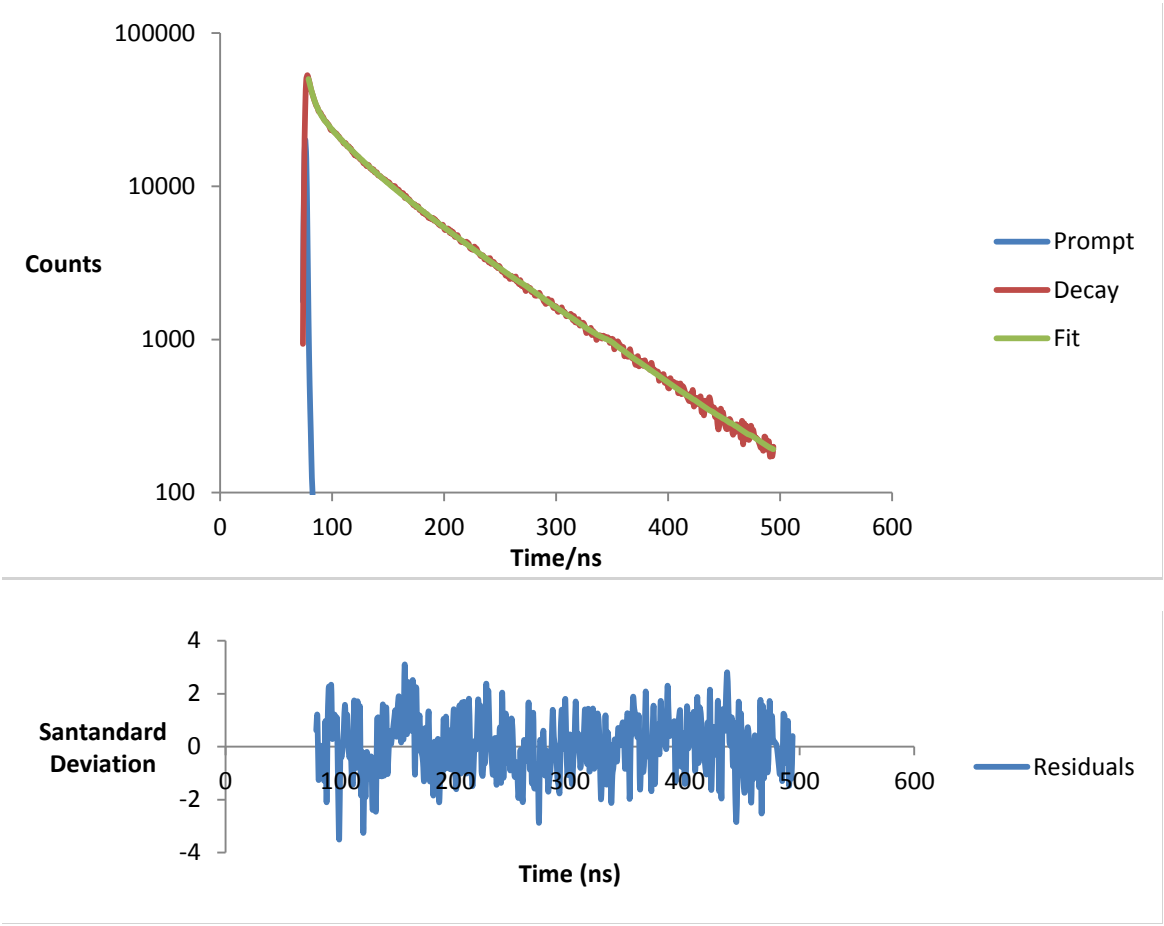

Figure 3.3: Fluorescence intensity decay of 10^{-2} wt% ACE-labelled PAA in aqueous solution with pH value 3, prompt and the associated double-exponential fit and distribution of residuals. (λex = 295 nm and λem=350nm).

The average ACE emission lifetimes at 340 nm from ACE-PAA as a function of pH were determined (Figure 3.4). At low pH (pH < 4) the average lifetime values are longer, suggesting that the polymer collapsed at these pH values, and as the ACE labels are the exposed to hydrophobic environment and become more solubilised, enhancing their decay lifetimes (ca 27 ns). A marked decrease in these values (ca 21 ns) was noted at higher pH (pH > 4) values and this is because of the polymer chains are expanded due to the electrostatic repulsion, which occurs between the carboxylate anion groups[2]. As a result, the hydrophobic label exposes to hydrophilic environment and becomes insoluble.

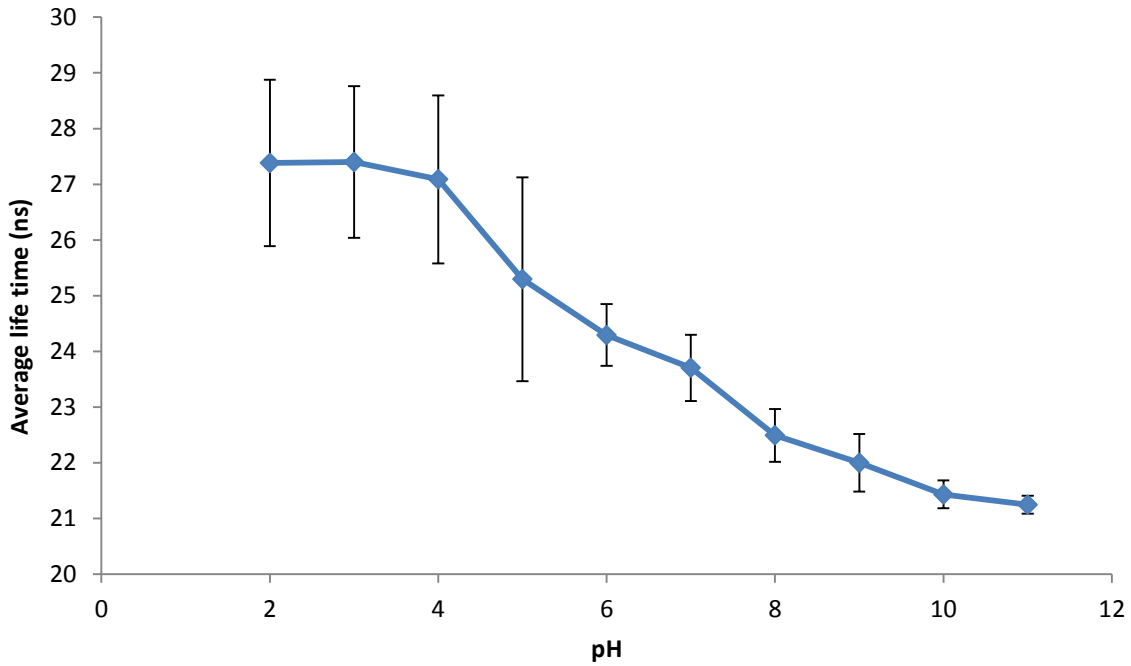

Figure 3.4: Fluorescence excited-state average lifetime as a function of pH for 10^{-2} wt% solution ACE labelled PAA in water.

3.1.3 Fluorescence Time-resolved anisotropy measurements (TRAMS) of ACE labelled PAA as a function of pH

Fluorescence time-resolved anisotropy measurements (TRAMS) were carried out to determine the change in the mobility of the poly (acrylic acid) PAA chain. The correlation time of the fluorophore ACE was estimated as the measure of the motion of the polyelectrolyte chain. Parallel and perpendicular fluorescence decays were generated after excitation at 295 nm with vertically polarized light and analysed at 350 nm from ACE-labelled PAA in aqueous solution (Figures 3.5 and 3.6). This led to the anisotropy decay of the ACE-PAA polymer as shown by a selective samples for pH 3 and pH 8 values on Figure 3.7. Shortly after excitation, the two polarized fluorescence decay curves were superimposed on each other for there were no overall restrictions in rotation for the expanded PAA chains (Figure 3.5). It was observed that the anisotropy decay quickly decayed to zero (the red curve in Figure 3.7). Once the pH value was decreased to 3, the motion of ACE label was hindered by the collapse of PAA chain, and a tramline gap was generated between the two polarized decays for a slower time, as depicted in Figure 3.6. As a result, the anisotropy decay did not reach the zero for a longer period (the blue decay in Figure 3.7). A direct analysis, using a single exponential function, was applied to fit the anisotropy decays curves (see Figure 3.8), which can reflect the polymer backbone motion. These TRAMS results reveal an obvious differentiation between the collapsed and expanded shapes of PAA polymer.

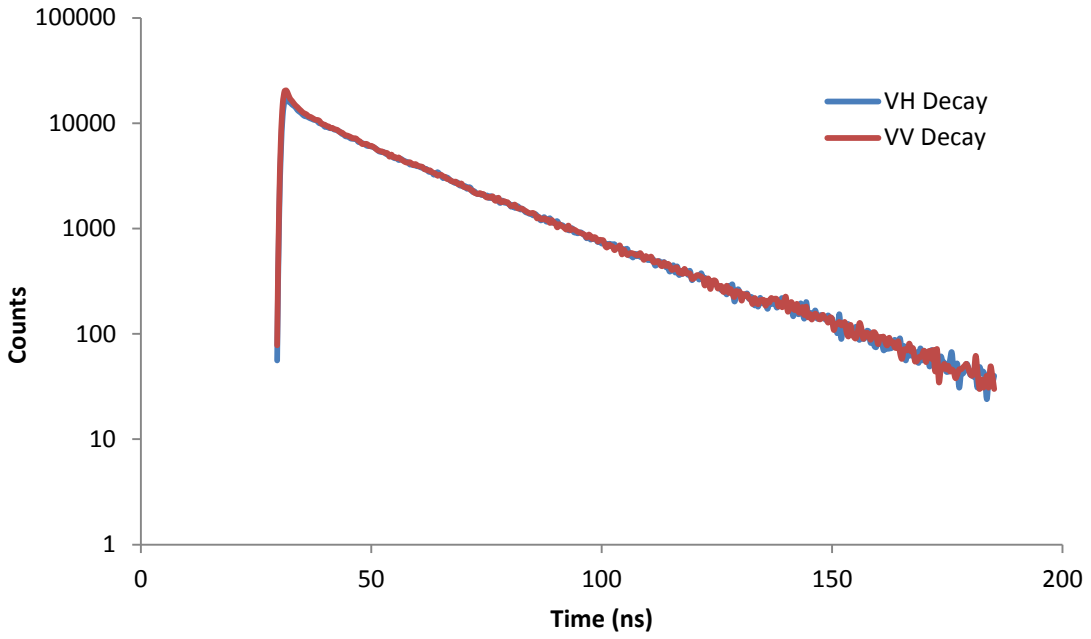

Figure 3.5: Parallel (red curve) and perpendicular (blue curve) fluorescence intensity decay curves following excitation with vertically polarized light (λex = 295 nm) analysed at 350 nm from 10^{-2} wt% ACE-labelled PAA in aqueous solution at pH = 8.

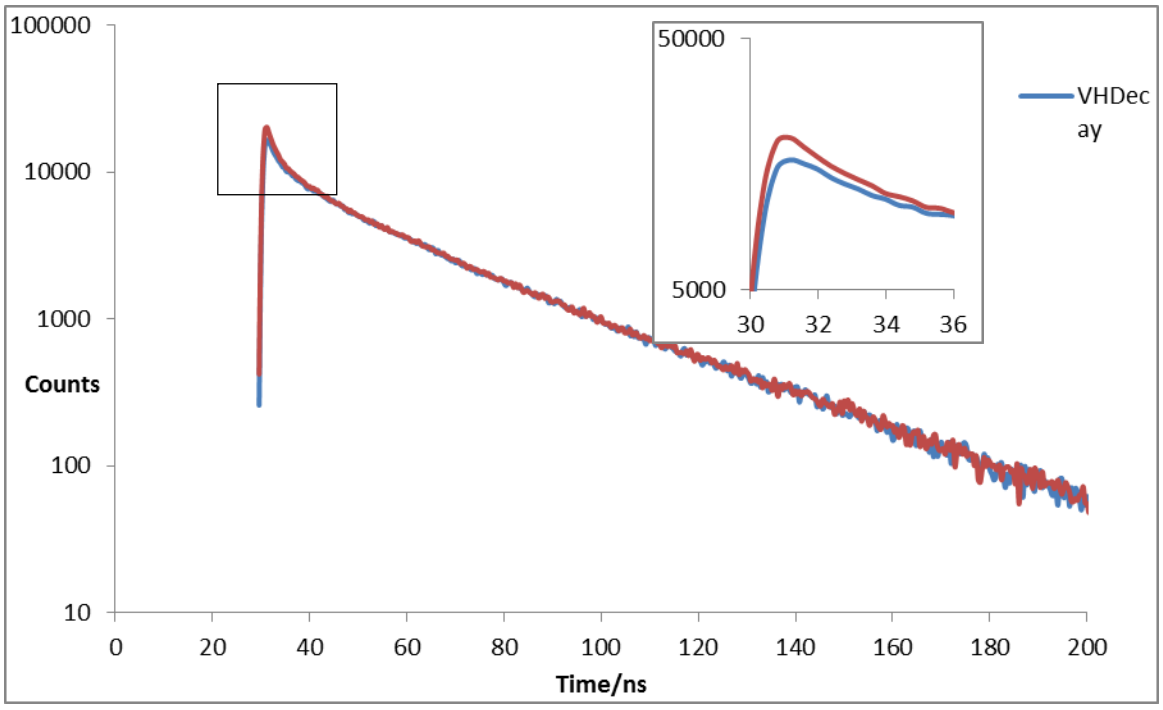

Figure 3.6: Parallel (red curve) and perpendicular (blue curve) fluorescence intensity decay curves following excitation with vertically polarized light (λex = 295 nm) analysed at 350 nm from 10^{-2} wt% ACE- labelled PAA in aqueous solution at pH = 3.

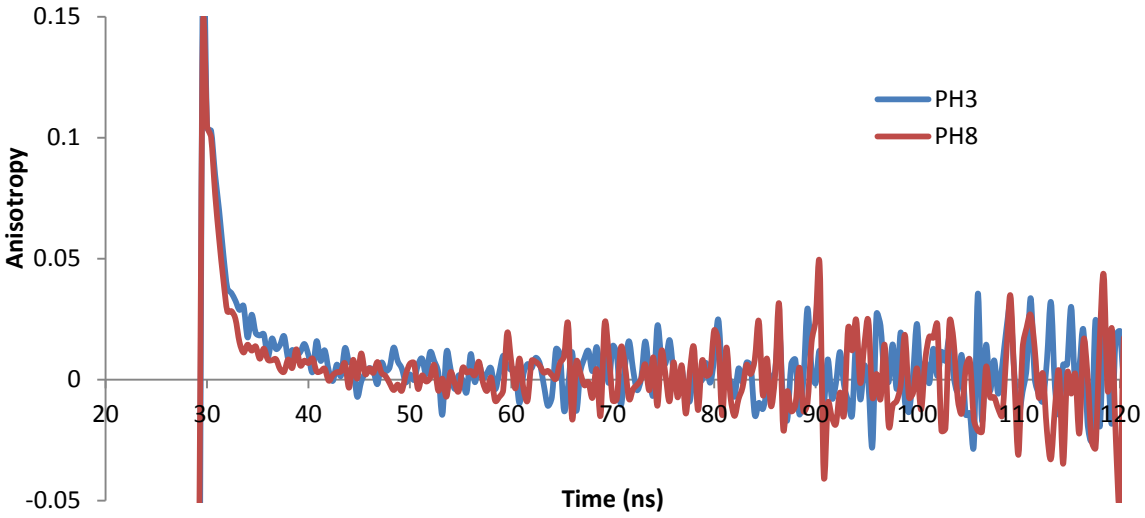

Figure 3.7: Fluorescence time-resolved anisotropy decays of 10^{-2} wt % ACE-labelled PAA in aqueous solution at pH 3 (blue curve) and pH 8 (red curve) (λex = 295 nm and λem = 350 nm).

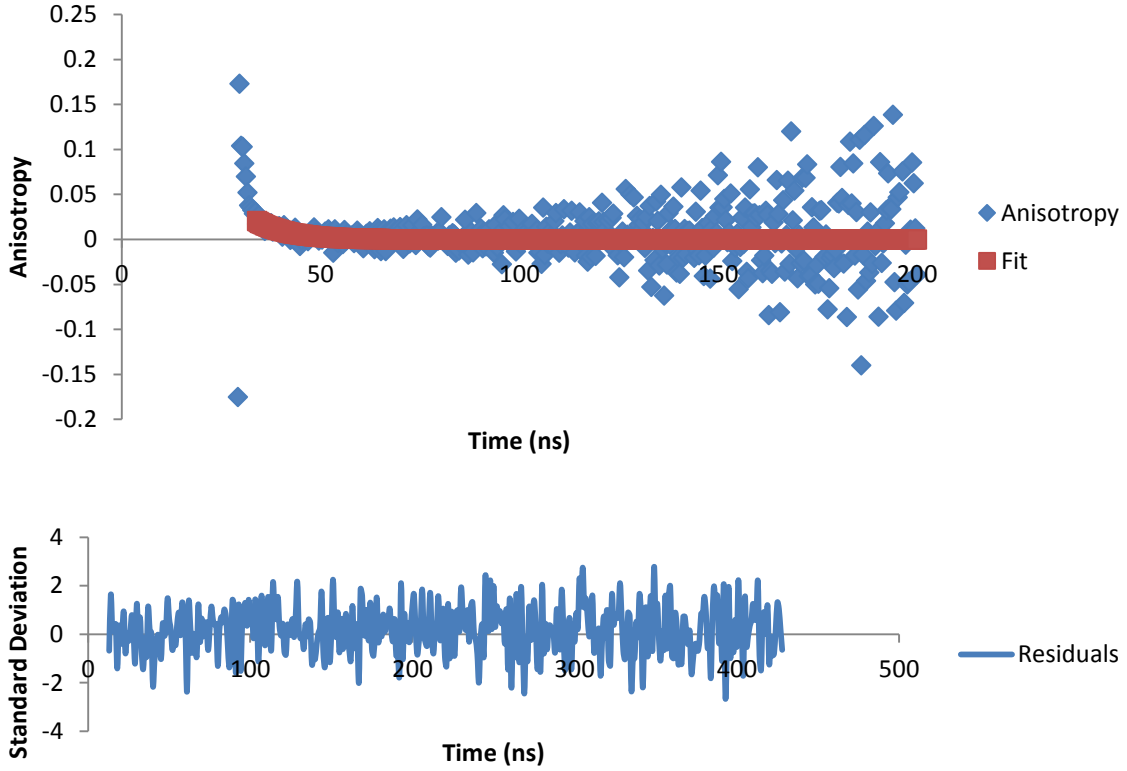

Figure 3.8: Decay of anisotropy, r(t), of 10^{-2} wt% ACE-labelled PAA in aqueous solution at pH 3, and the associated single-exponential fit with the distribution of residuals. (λex = 295 nm and λem = 340 nm).

Figure 3.9 shows the τ_c of ACE-PAA as a function of pH. A maximum increase in correlation time value was recorded at pH 2 (ca 7.8 ns). This value decreased to a minimum (ca 2 ns) at pH 11. It can be hypothesized that an increase in correlation time values occurs because of ACE label rotation about an axis defined by the single bond, linking the ACE label to the macromolecule backbone. In addition, it can be expected that at low pH the polyelectrolyte chain will move more slowly. This could be attributed to an aggregation in the chain, in which hydrogen bonding between carboxylic groups and any remaining carboxylate ions enhances the rigidity of the PAA chain [53-54], which led to an increase in the rotational correlation time. On the other hand, in basic media a relatively expanded shape is dominate, which makes the label rotate faster, hence a short correlation time is recorded. It has been reported in the literature that as pH increases, PAA chain switches from a collapsed coil to an expanded chain [3, 14]. Potentiometric titration has been utilised to study the coiling and unfolding behaviour of the linear PAA polymer chain [55], and determined by optical density (OD) measurements as a function of pH [1].

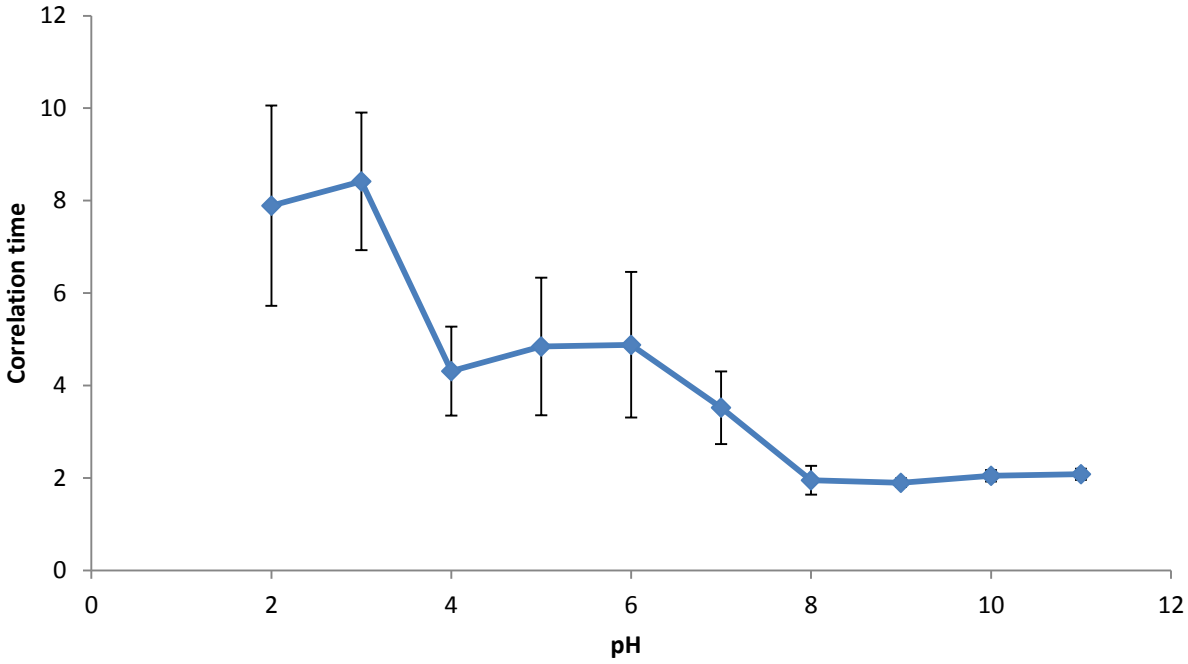

Figure 3.9: Correlation times (τ_c) for molecular segmental motion of 10^{-2} wt% ACE-labelled PAA in aqueous solution at different pH values. (λex = 295 nm and λem = 340 nm).

3.2 Conformational Behaviour of ACE-AMMA-PAA as a Function of pH

In this section, the conformation behaviour of a fluorescently doubly labelled PAA polymer is investigated as a function of pH. Fluorescence spectroscopy includes steady state and excited state lifetime, applied for such investigation.

The measuring of distance distribution of fluorescently doubly labelled PAA (where the average lifetimes for singly and doubly labelled polymer is used) to investigate the conformational change (aggregation and expansion) is the aim of this experiment.

3.2.1 Fluorescence steady state spectra of ACE-AMMA-PAA as a function of pH

In order to investigate the single macromolecule conformational behaviour, a 10^{-2} wt% of polymer concentration dilute is used [56]. An emission scan of ACE-AMMA-labelled-PAA in aqueous solution as a function of pH is graphed on Figure 3.10. The excitation wavelength was fixed at 290 nm, which is a characteristic of the ACE label (donor). The performed emission scan included the emission wavelengths of ACE (~340 nm) and AMMA (~420 nm).

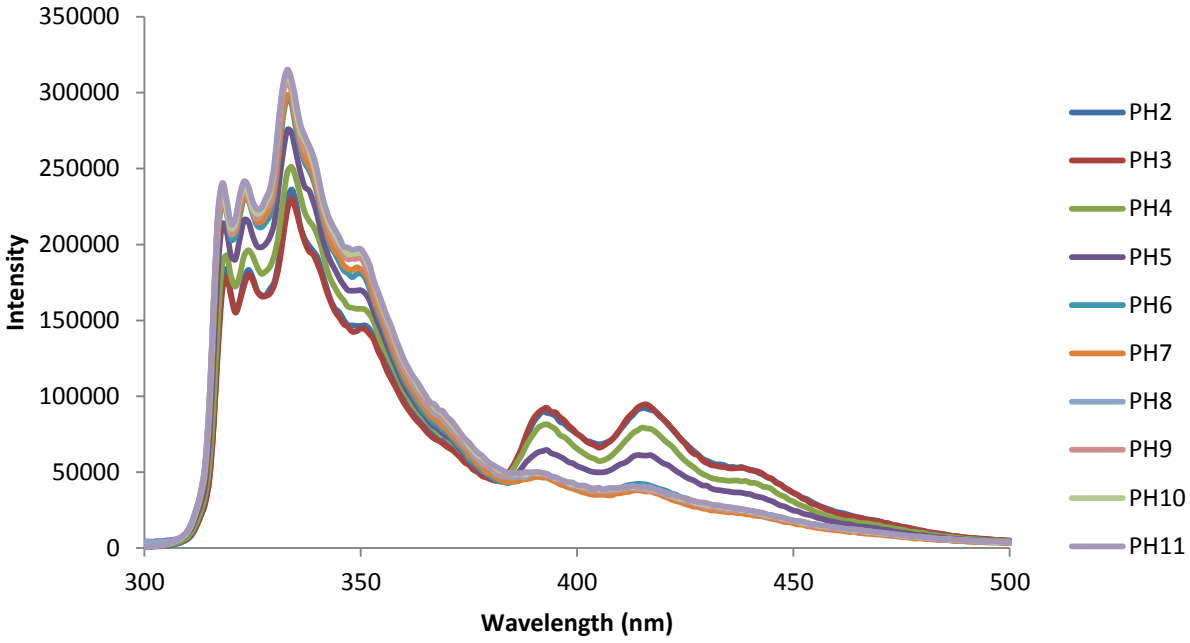

Figure 3.10: Emission scan in a range equal to 300-500 nm at fixed excitation λex= 290 nm for ACE-AMMA-PAA (10^{-2} wt% in water) at different pH values.

The ACE label (donor) and AMMA (acceptor) were observed to emit at ~340 nm and ~420 nm respectively, when the excitation level is set to 290 nm. The emission of the acceptor could be attributed to either direct absorption at 290 nm and/or some energy transfer (ET) from the excitation from the donor molecule. The ACE emission peak decreased in acidic media (pH < 7) presumably because of excitation of the AMMA fluorophore, whose emission increases because of ET from donor. This transition in the energy indicated that the distance between the donor and the acceptor became shorter in the acidic media in comparison to the basic media, further confirming that the polymer chain existed in a collapsed shape due to the protonation process (Figure 3.10).

In contrast, the AMMA emission peak was quenched under basic conditions, and any observable peaks could be attributed to a direct excitation of an acceptor molecule rather than ET, which cannot occur when the polyelectrolyte chain exists in an expanded form due to the repulsion of carboxylic groups (Figure 3.10).

Experimentally, the energy transfer efficiency (*ET*) has been calculated as a function of pH from the maximum fluorescence intensity peaks of ACE-AMMA-PAA emission spectra, as shown in the following equation:

$$ET = \frac{\text{Enhanced acceptor emission}}{\text{Quenched donor emission}} = \frac{I_{A\,(\lambda_{max=420\ nm}}}{I_{D\,(\lambda_{max=340\ nm}}} \qquad \text{Equation 3.4}$$

Where ET is energy transfer efficiency, I_A represents the maximum fluorescence intensity peak of the acceptor and I_D is the maximum fluorescence intensity peak of the donor.

As the pH level was gradually adjusted to more acidic medium, an increase in the I_A/I_D ratio was observed. This increase is possibly due to the formation of a collapsed form of the polymer. On the other hand the ratio decreased under basic conditions promoting the unfolding of the polymer chain to an expanded form hypothesis (Figure 3.11). In particular, at pH 2 and 3, the ratio is at maximum ~0.45 indicating ~45% efficiency of ET in the partially coiled form of the poly (acrylic acid) PAA chain, since at theses pH values the vast majority of the carboxylate groups are deprotonated [2]. At pH values between 4 and 6, a transition in conformation occur leading to a decrease in I_A/I_D ratio. This means that some of the carboxylic groups become deprotonated and accordingly bear a negative charge, which in turn leads to a partially expanded form [2]. In the same manner, the ratio declines to ~0.1 in pH >7, which suggests that the polyelectrolyte chain exists largely in a more expanded form at strong basic media, due to more carboxylic groups being protonated to form negative charges.

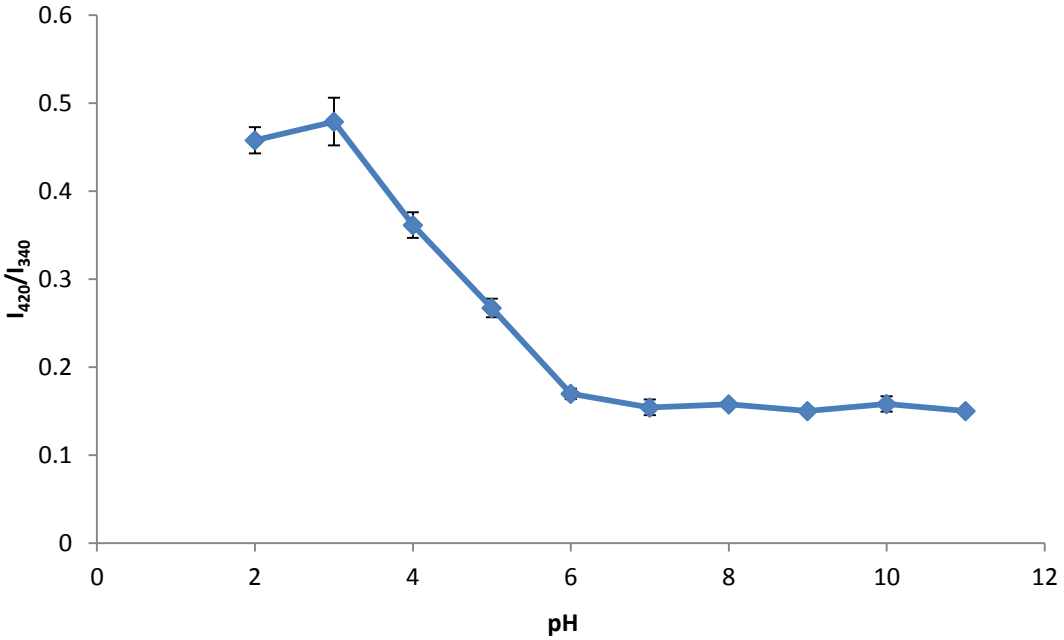

Figure 3.11: Ratio of emission at λem = 420nm (AMMA) to emission at λem = 340nm (ACE) exciting at 290 nm with varying pH for 10-2 wt% from ACE-AMMA-PAA in water.

3.2.2 Fluorescence exited state lifetimes of ACE-AMMA-PAA as a function of pH

To further investigate the phenomenon of energy transfer (ET), which provides us with more information about the distance distribution of a polymer chain, ACE fluorescence decays were collected over the whole pH range for ACE-AMMA-PAA as previously collected data for a singly labelled polymer. A triple exponential function of the form of Equation 3.5 was applied to adequately interpret the fluorescence decay data when energy transfer occurred under acidic conditions, while in basic media the use of a double exponential (Equation 3.2) was enough to fit the decay data. The average lifetimes were calculated using Equation 3.3.

$$I(t) = A + B_1 \, exp^{-t/\tau_{f1}} + B_2 \, exp^{-t/\tau_{f2}} + B_3 \, exp^{-t/\tau_{f3}} \qquad \text{Equation 3.5}$$

By comparing the average lifetimes for ACE-PAA and ACE-AMMA-PAA, it was noted that $< \tau_f >$ values were lower for the donor in the presence of AMMA than for ACE without acceptor (Table 3.1). At pH 2, the ACE fluorophore in ACE-PAA remained excited for ~3 ns longer than the donor in ACE-AMMA-PAA. This indicates that the maximum efficiency of energy transfer occurred when the polymer chain was collapsed at low pH values.

Table 3.1: Average lifetimes $< \tau_f >$ comparison for ACE-PAA and ACE-AMMA-PAA samples in aqueous solution at different pH values.

pH	$<\tau_f>$ (ns)/ACE-PAA	$<\tau_f>$ (ns) ACE-AMMA-PAA
2	27.3	24.6
3	27.3	24.6
4	27.0	24.3
5	25.2	23.3
6	23.3	22.1
8	22.4	22.0
9	22.0	21.9
10	21.4	21.2
11	21.2	21.2

As seen in Table 3.1, no significant differences in average lifetime values of ACE in ACE-PAA and ACE-AMMA-PAA polymers were observed when the pH varied from 8 to 11. This pH range values are higher than the expected conformational transition pH value for the PAA polymer where a higher expansion of the polyelectrolyte chain occurs because of the electrostatic repulsions of the negatively charged COO- groups [2]. The repulsions lead to the expanded form of the polymer chains which increases the distance between the donor and the acceptor preventing any significant energy transfer.

Figure 3.12 shows a plot of the average lifetimes for the ACE-PAA and ACE-AMMA-PAA data (Table 3.1) against the corresponding pH values. Both curves display a similar pattern to the graph obtained from the I_A/I_D ratio against pH values (Figure 3.11). This suggests that the shape of the plot may also be attributed to the conformational transition occurring for the PAA chain when the pH value is changed. This transition goes from a partially expanded chain at high pH (where short $< \tau_f >$is recorded), to a partially

collapsed form at low pH (where longer $< \tau_f >$ is recorded). This similarity for double and single labelled polymers suggests that the attachment of the covalently bounded AMMA does not affect the conformational behaviour of the poly (acrylic acid) chain.

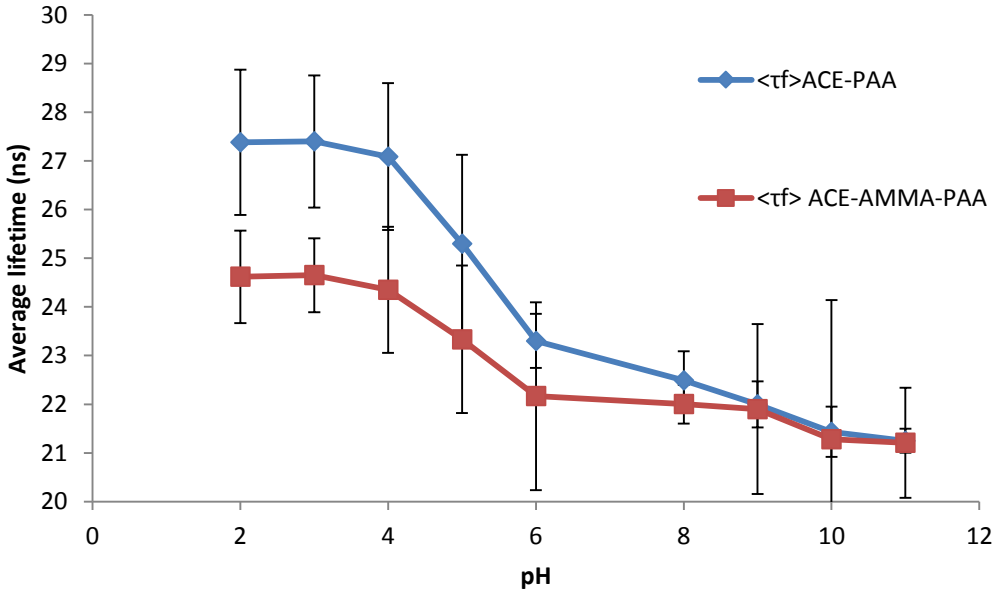

Figure 3.12: Average donor lifetime $< \tau_f >$ for ACE-PAA and ACE-AMMA-PAA as a function of pH (λex = 295 nm and λem = 340 nm).

When donor-acceptor pairs are randomly attached to the polyelectrolyte chain, the distribution of distances between such pairs is related to the chain dimensions. Since fluorescence steady-state data cannot be used to measure the distance distribution of fluorescently doubly labelled polymer, average lifetimes for ACE-PAA and ACE-AMMA-PAA were used to determine such distribution, as described in Eqn 3.7:

$$r^6 = (R_0^6 \,/\, \mathrm{ET}) - R_0^6 \qquad \text{Equation 3.7}$$

where r is the actual separation distance in a particular system, R_0 the distance for ACE-AMMA pair involved in our studies (2.3 nm) [14], and ET is the energy transfer efficiency, which can be determined, using the following equation:

$$ET = 1 - \frac{<\tau_{ET}>}{<\tau_D>} \qquad \text{Equation 3.8}$$

Where $< \tau_{ET} >$ represents the average lifetime of the ACE-AMMA-PAA and $< \tau_D >$ represents the average lifetime of the ACE-PAA.

The actual separation distance in the poly(acrylic acid) PAA chain as a function of pH is show on Table 3.2. As expected, a decrease in the separation distance between the donor and acceptor is noted when the pH is decreased which indicated that the polymer chain was in a collapsed form. On the other hand, increasing the pH level caused the polymer (PAA) to take an expanded form which led to an increased separation distance between the labels. An average separation distance of (ca. 3.6 nm) between the donor and accepter labels was observed at around pH 6. This separation distance is within the Förster distance for donor-to-acceptor energy transfer [37] consistent with a collapsed coiled form. Above pH 6, the PAA polymer expands and the distance between the labels is greater than that over which NRET occurs.

Table 3.2: The distance between donor and acceptor as a function of pH.

pH	r (nm)
2	3.5
3	3.6
4	3.5
5	3.6
6	4.7
8	4.7
9	6.1
10	5.6
11	7.0

In summary, Poly acrylic acid in an aqueous acidic solution forms a collapsed structure, this is supported by: an apparent decrease of energy transfer with an increase of pH, the increase in AMMA label emission intensity relative to ACE label emission and the decrease in ACE label lifetime above pH 4. TRAMS measurements show that poly acrylic acid has a conformational change from a coiled shape at low pH and has a water swollen state between pH4 to 6 before switch to a more extended state at a higher pH values as a result of repulsive interactions between carboxylate anions dominate.

PAA only exhibits partial coiling, which is shown by the distance between labels being bigger than what NRET occurs, even at low pHs and pH 11 the labels are not predominately close.

3.3 Conformational Behaviour of ACE-labelled PDMAEMA as a Function of pH

Similarly to section 3.1, the effect of pH on diluted water solution of ACE-labelled PDMAEMA was investigated by the fluorescence principle. Since fluorescence data includes steady state, exited state lifetimes and time-resolved anisotropy was collected for this macromolecule at different pH values.

3.3.1 Fluorescence steady state spectra of ACE-labelled PDMAEMA as a function of pH

Steady state spectroscopy analysis on an ACE labelled PDMAEMA sample across a pH range showed a decrease in the intensity of emission of the sample when excited at 290 nm as the pH increased to more basic conditions. This was most notable above pH 6 where the intensity dropped markedly (Figure3.13). This could be attributed to fluorescence quenching that occurs in the system promoted by the aqueous environment. However, it is also expected that the PDMAEMA polymer would adopt a coiled conformation at high pH which could prevent access of water molecules to the fluorophore and hence reduce quenching from this source. Therefore, the observed quenching of the ACE emission must come from within the polymer system itself, presumably from the pendant amine groups of the polymer as previously reported [57]. This would be consistent with the polymer system adopting a more coiled conformation as the pH level increases, thus bringing the label into contact with the quencher (amine group) and lowering fluorescence intensity.

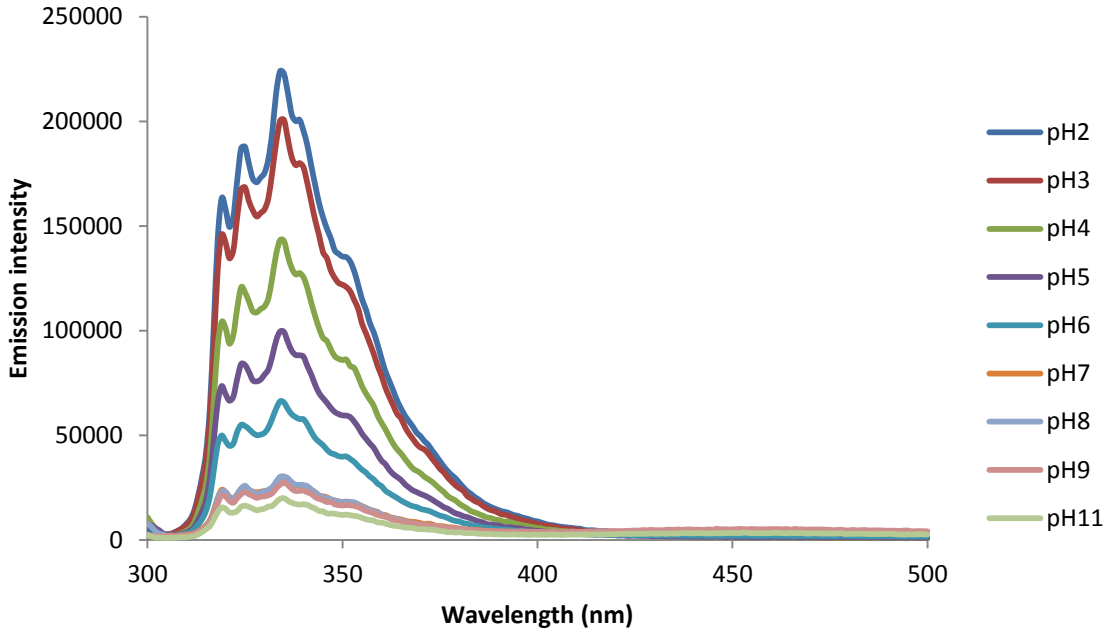

Figure 3.13: Fluorescence emission scan in a range equal to 300-500 nm at fixed excitation λ_{ex} = 290 nm for ACE- labelled PDMAEMA in water (10^{-2} wt %) at different pH values.

It is observed that the emission spectra of 10^{-2} wt% ACE-PDMAEMA at high pH (Figure 3.14) had an additional peak at 450 nm. This peak refers to the hydroquinone mono methyl ether, which is added to monomer (DMAEMA) as an inhibitor [58].The mere fact that we can see emission at high pH rather than at low pH is consistent with the collapsed structure at high pH and possibly reflects enhanced energy transfer.

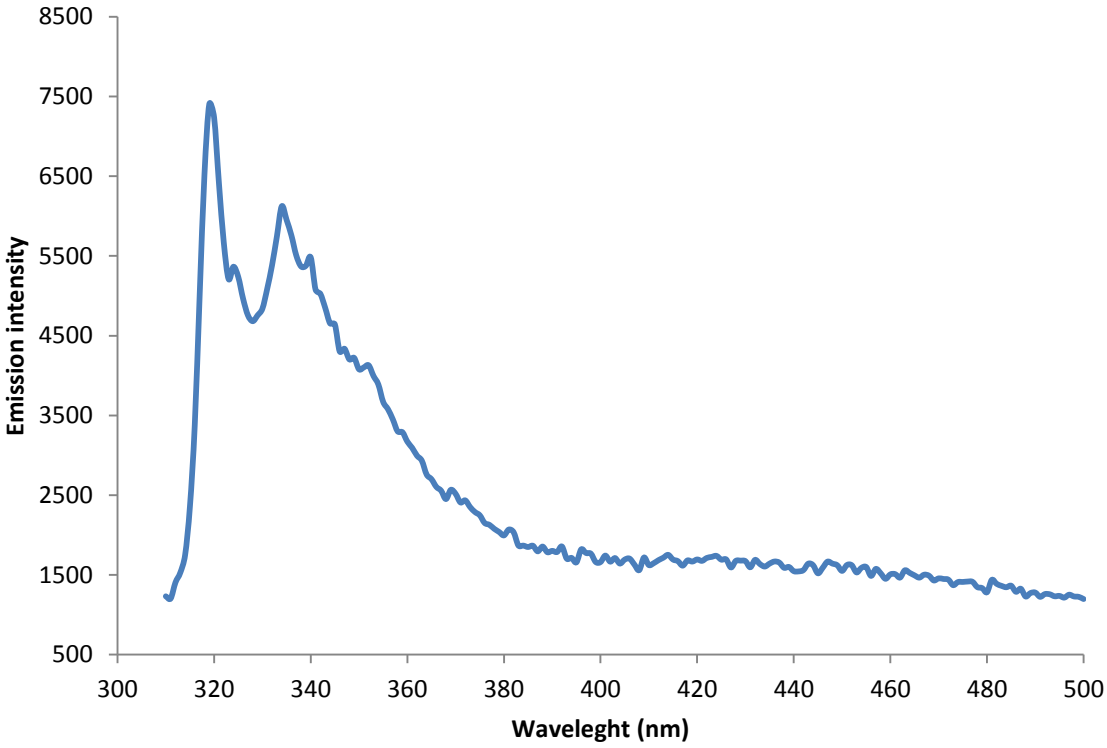

Figure 3.14: Fluorescence emission at fixed excitation λex = 290 nm for ACE- labelled PDMAEMA in water (10-2 wt%) pH11.

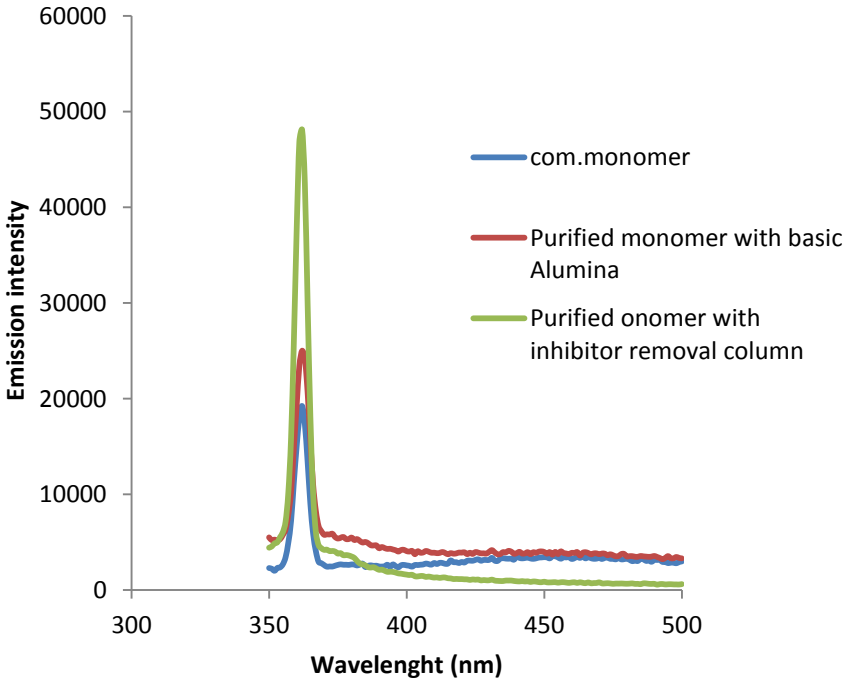

Figure 3.15: Steady-state fluorescence emission spectra of the commercial monomer (DMAEMA) and purified monomers. (λex = 330nm)

Figure 3.15 shows the steady-state fluorescence emission spectra of a commercial monomer (DMAEMA), a purified monomer with a basic alumina column and purified monomer with an inhibitor removal column. It is clear that purifying the monomer using an inhibitor removal column is more efficient (in removing the inhibitor) than alumina column.

A plot of the peak emission intensity values (the maximum fluorescence intensity peaks of ACE-PDMAEMA versus pH shows that the emission intensity was observed to reach a maximum drop at pH ~7 (at the pKa of the polymer) (Figure3.16). This drop along with internal quenching implies that coiling becomes tight beyond this pH. A very small change in emission intensity was observed at pH levels between pH 8 and 11 presumably because the polymer had achieved a fully coiled state by this stage.

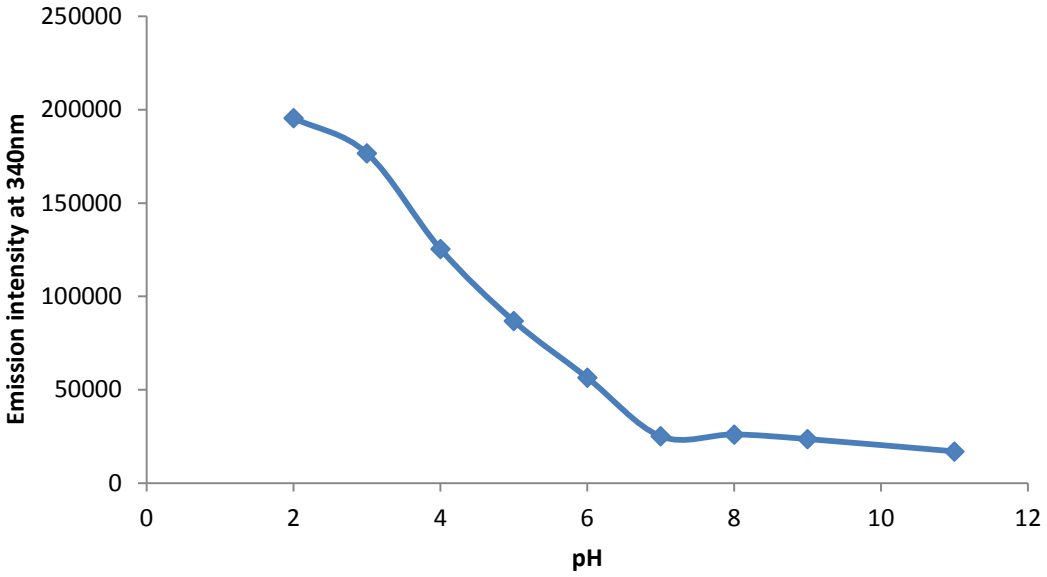

Figure 3.16: A plot of the peak emission intensities (observed at 337 nm) for an ACE labelled PDMAEMA sample in aqueous solution across a pH range when excited at 290 nm.

3.3.2 Fluorescence exited state lifetimes of ACE- labelled PDMAEMA as a function of pH

Figure 3.17 shows a fluorescence intensity decays for 10^{-2} wt% ACE-labelled-PDMAEMA over a pH range of 2-11. From the data it can be observed that at basic pH levels (high pH), the ACE-labelled polymer PDMAEMA shows shorter time duration decays compared to that of low pH levels. This could be attributed to the fact that the polyelectrolyte exists in a coiled conformation (due to the low degrees of ionisation), thus bringing the ACE label in to contact with the quencher (amine group) and hence make their fluorescence intensity lower (quenched). On the contrary, at low pH, such decays become longer than those in basic conditions. At low pH the PDMAEMA polymer adopts an extended water-swollen conformation. This expanded form allows the donor (ACE) to be far from the quencher (amine group). Hence, the lifetime decay of the polymer is consequently longer as reflected by the transient fluorescence.

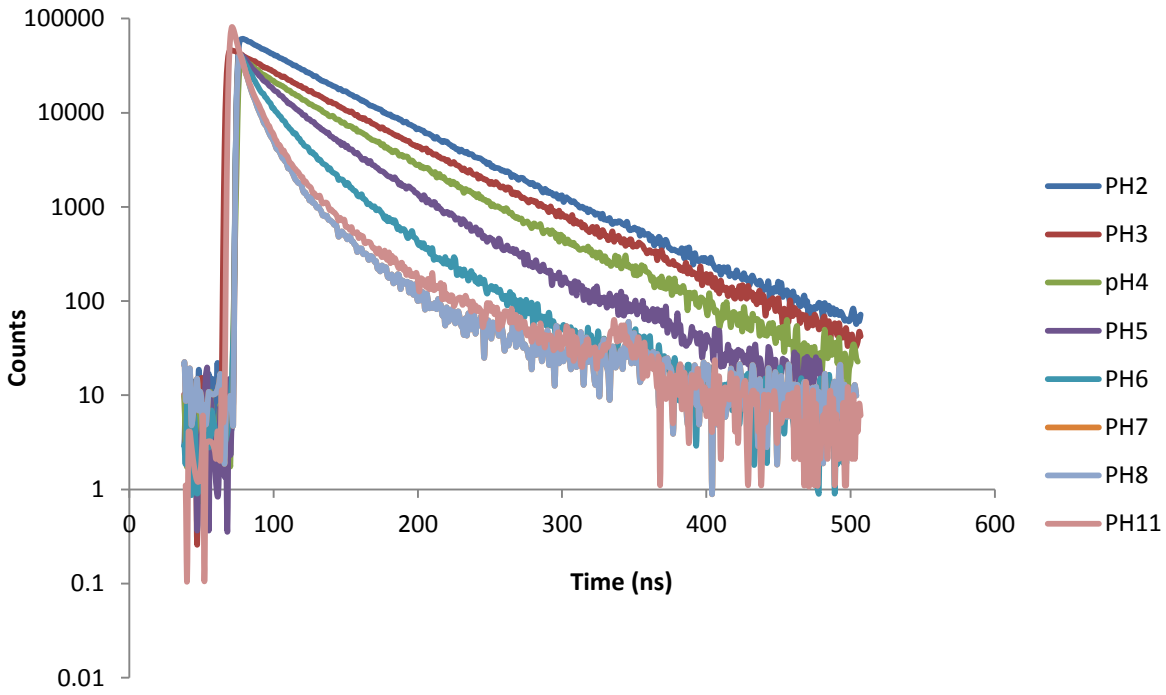

Figure 3.17: Fluorescence intensity decays as a function of pH for ACE-labelled PDMAEMA in water (10-2 wt %)

It has been previously shown in literature [59] that the lifetime decay of an excited ACE label in aqueous media is sensitive to the polymer conformation. In particular, this is because of the unlikelihood that the label will exist in only one environment as the polymer conformation changes. The analysis of fluorescence decay data shows that the fluorescence decay for ACE-PDMAEMA appears to be complex across all pH values tested. The data at low pH values was modelled using a double exponential fit (equation 3.2) while triple exponential fit was used for high pH values data (Equation 3.5). An average value for the lifetime of the polymer which was obtained from equation 3.3, then allowed easy comparison between one pH and another. The residuals plotted showed that the double and triple exponential mathematical models provided good fits to the lifetime data (Figures 3.18 and3.19). Furthermore, the fact that χ_2 values are close to unity provides statistical confidence in the models used.

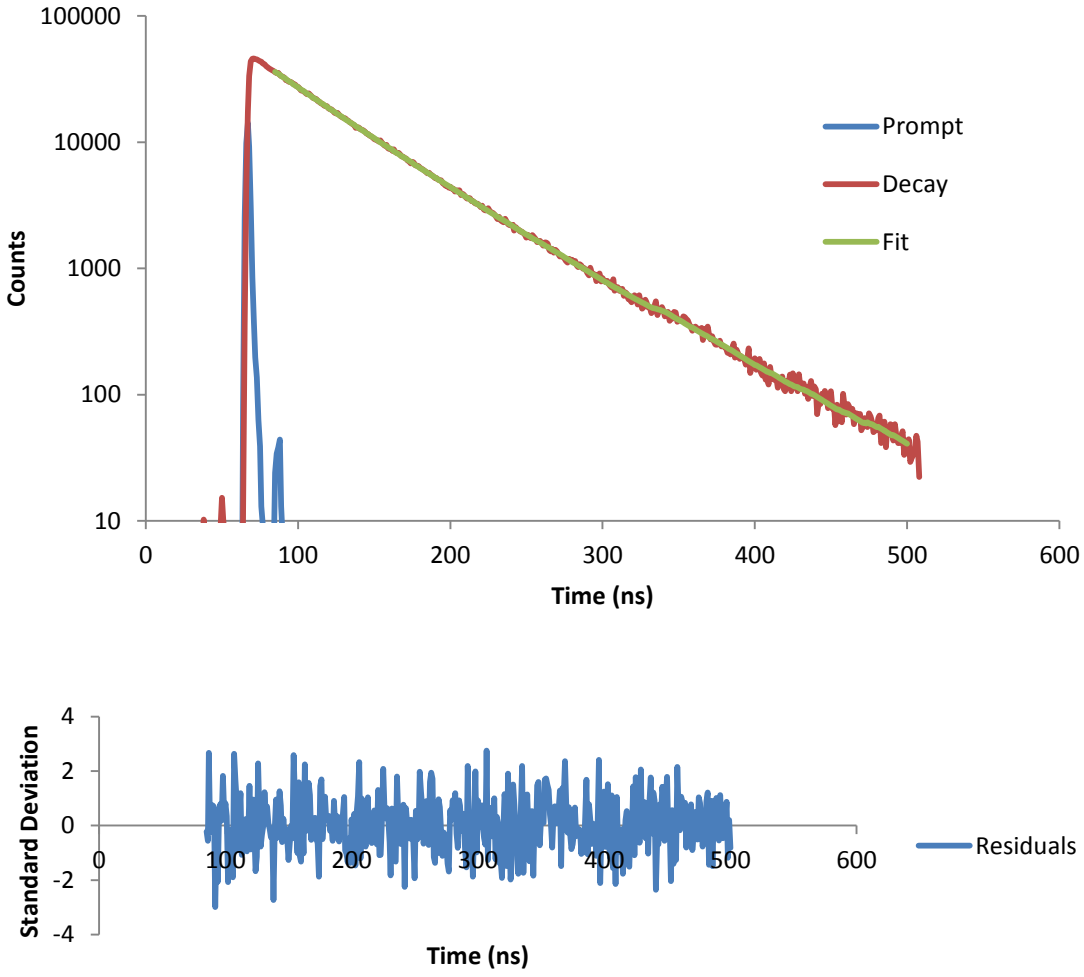

Figure 3.18: Fluorescence intensity decay of 10^{-2} wt% ACE- labelled PDMAEMA in aqueous solution at pH 3, prompt and the associated double-exponential fit with the distribution of residuals (λ_{ex} = 295 nm and λ_{em} = 340 nm).

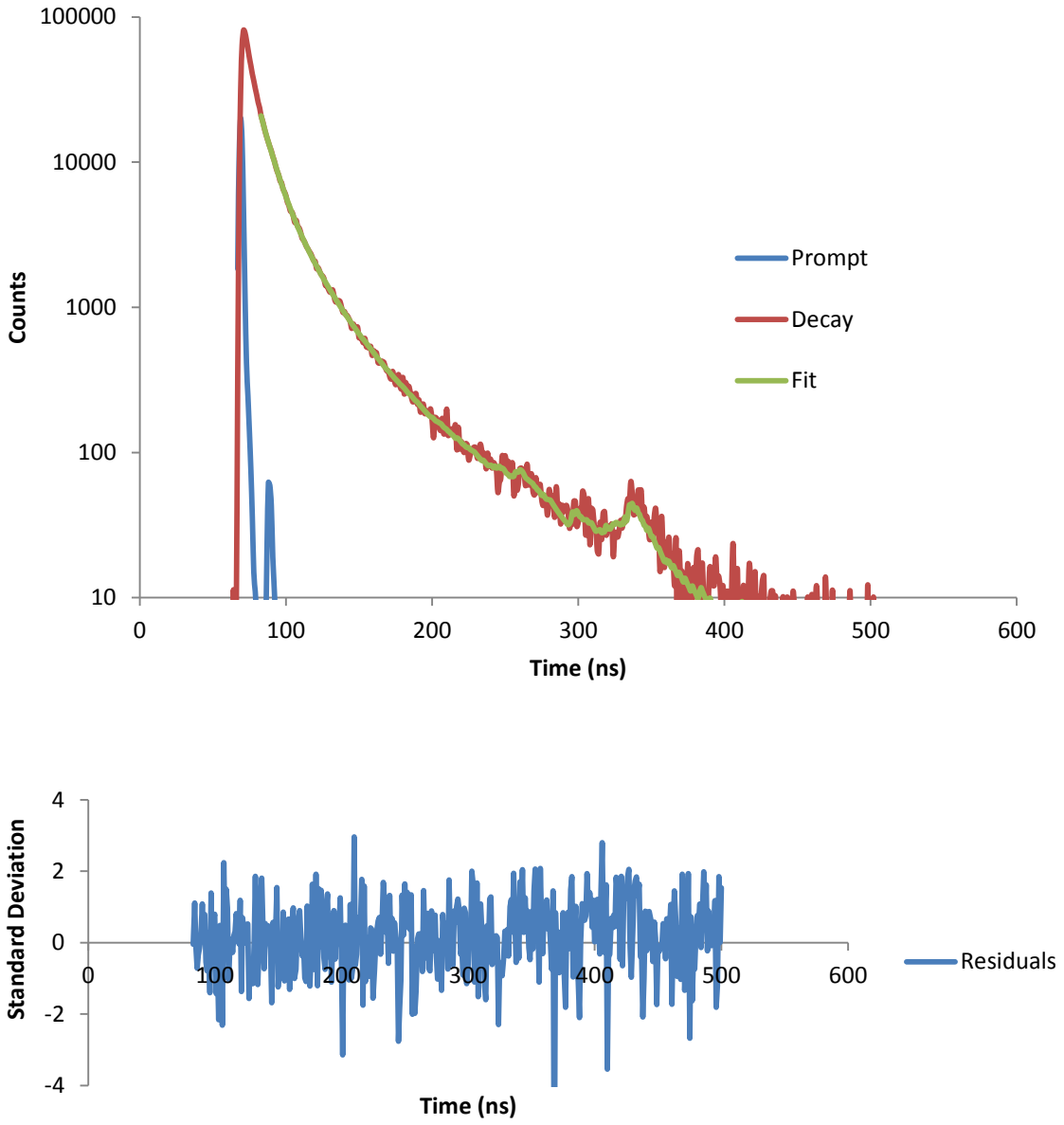

Figure 3.19: Fluorescence intensity decay of 10^{-2} wt% ACE- labelled PDMAEMA in aqueous solution at pH 11, prompt and the associated triple-exponential fit with the distribution of residuals (λex = 295nm and λem=340nm).

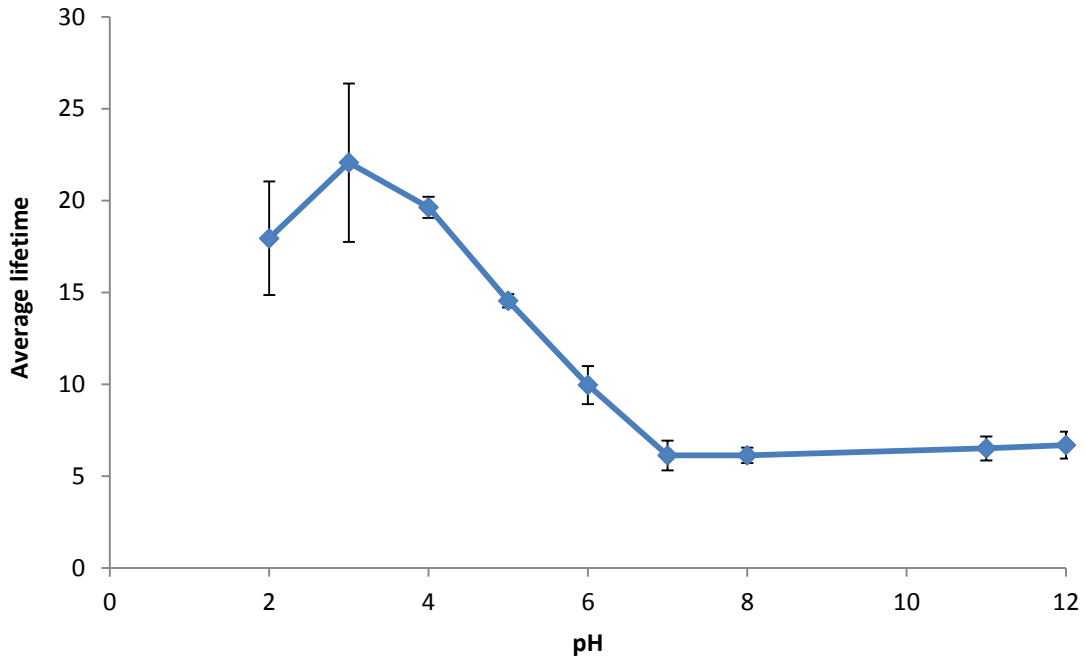

Figure 3.20: Fluorescence excited-state average lifetime, as a function of pH for ACE- labelled PDMAEMA in water (10-2 wt%).

Figure 3.20 shows the average lifetime emission for the ACE label at 340 nm from the ACE-PDMAEMA as a function of pH data. The longest average lifetime values (ca. 20 ns) suggests that the polymer expanded at low pH values and hence led to an increase in the distance between the ACE labels and the amine group which consequently led to the enhanced lifetime decays due to the reduced quenching from the amine group. A marked drop in the lifetime values (ca 6.6 ns) can be observed at higher pH levels. This is presumably because the polymer chains were collapsed due to the deprotonation leading to shortened distances and hence higher quenching by the amine group.

3.3.3 Fluorescence Time-resolved anisotropy measurements (TRAMS) of ACE-labelled PDMAEMA as a function of pH

The chain mobility of PDMAEMA in aqueous solutions was examined using the TRAMS technique. The correlation time of the ACE label was estimated as the measure of the motion of the polyelectrolyte chain.

For the time-resolved anisotropy analysis, parallel and perpendicular fluorescence decays were generated from ACE-labelled PDMAEMA and analysed at 340 nm after excitation with a vertically polarized light in aqueous solution. This contributed to resolve the anisotropy decay of the ACE labelled PDMAEMA polymer. It was observed that a long duration anisotropy decay was obtained at pH 11 compared to pH 2. This difference in anisotropy decay duration indicated that the mobility of the polyelectrolyte was restricted when the PDMAEMA chain is coiled in basic media (Figure 3.21).

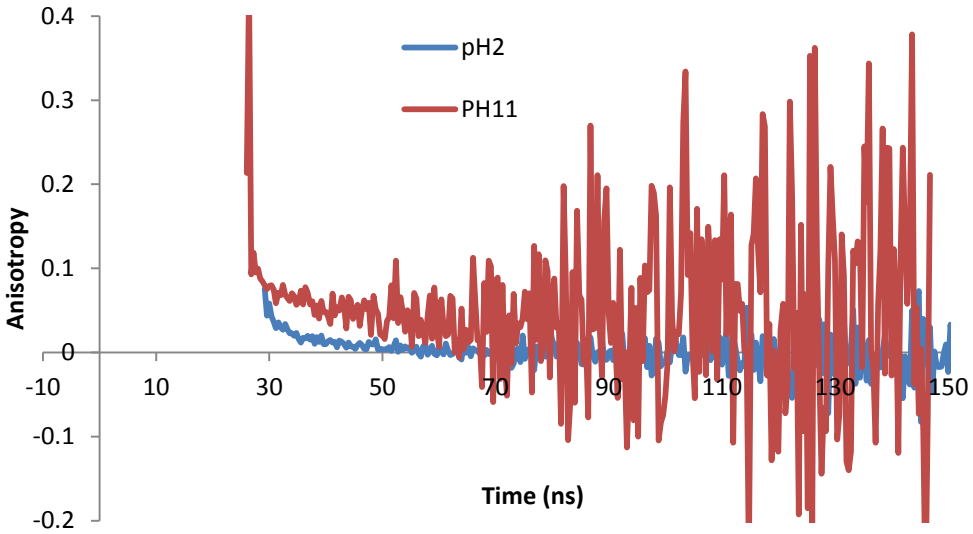

Figure 3.21: Decay of anisotropy, r(t), of 10^{-2} wt% ACE-labelled PDMAEMA in aqueous solution at pH 2 (blue line) and pH 11(red line). (λex = 290 nm and λem = 340 nm).

Direct analysis using a single exponential function was applied to fit the anisotropy decay curves (Figure 3.22), which reflect the macromolecule backbone motion. These TRAMS results revealed an obvious differentiation between the collapsed and expanded forms of the macromolecule.

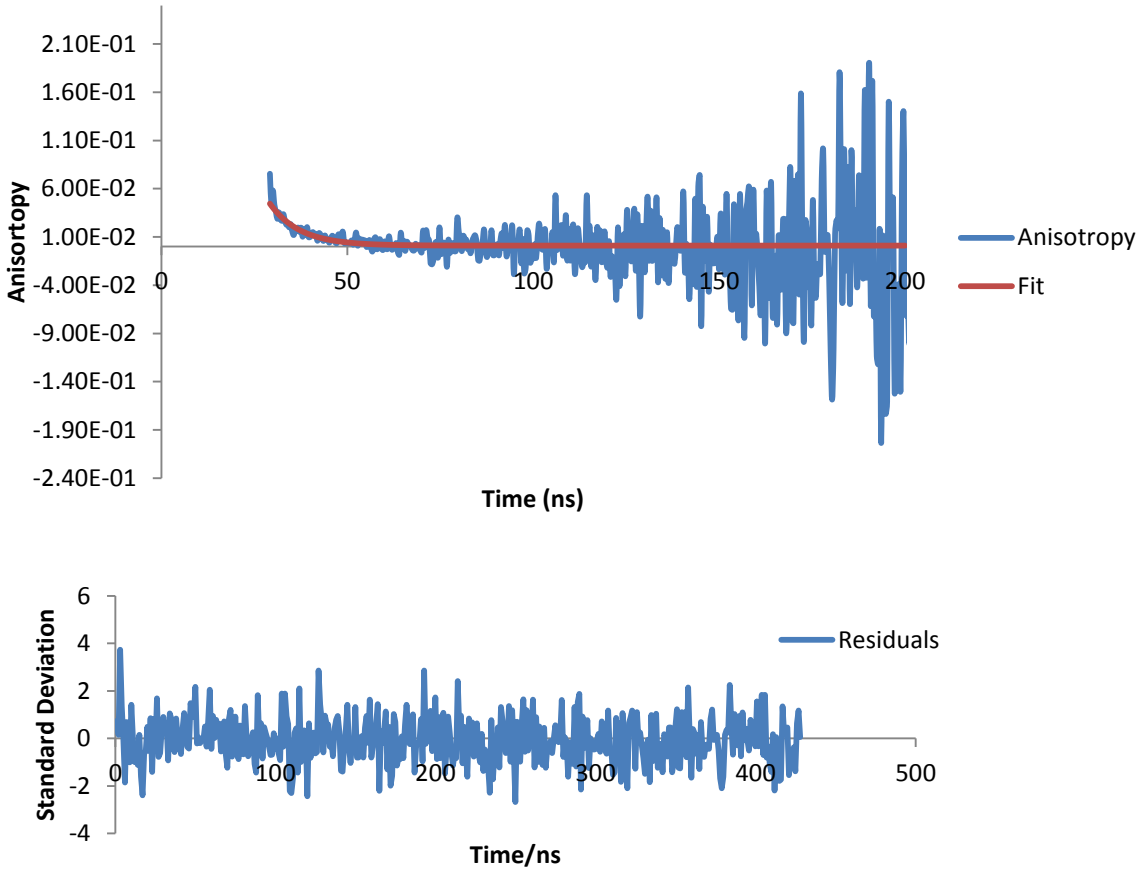

Figure 3.22: Decay of anisotropy, r(t), of 10^{-2} wt% ACE-labelled PDMAEMA in aqueous solution at pH 3, and the associated single-exponential fit with the distribution of residuals. (λex = 295 nm and λem = 340nm).

Figure 3.23 shows the rotational correlation time of ACE-PDMAEMA polymer as a function of pH value. It can be observed that the polymer undergoes a transition between pH 7 and pH 9 from an extended form to a compact coil form. In particular, a minimum decline in correlation time value is observed at pH 2 (ca 8 ns) and increased to a maximum of (ca 27 ns) at pH 11. This increase in correlation time at high pH values may have been due to the deprotonation of the amine units allowing hydrophobic forces of attraction to dominate and collapse the ACE-PDMAEMA chain, resulting in a slower rotation of the labels in the solution. Whereas in acidic media, an expanded form of the polymer is dominant. This is due to the mutual repulsion forces among the positive charges in the

protonated structures and hence inducing an expansion of the coil. This forces a fast rotation of the labels which yielded a small correlation time. This is consistent with the literature that the PDMAEMA chain undergoes a switch from an expanded chain to a collapsed coil form as the pH level increases [60] This behaviour is characterised by potentiometric titration for the linear PDMAEMA chain [61].

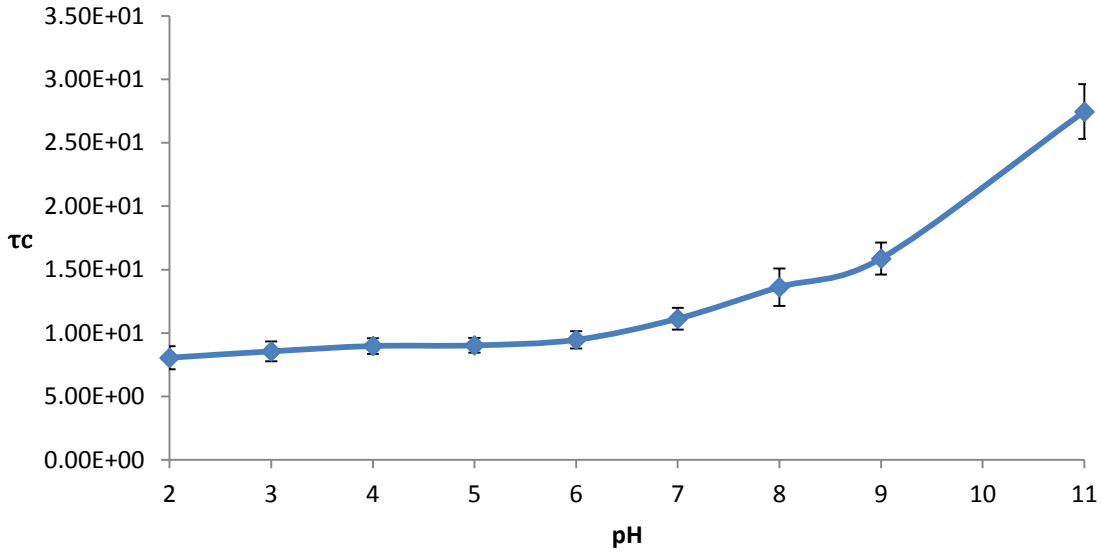

Figure 3.23: Correlation times (τc) for molecular segmental motion of 10-2 wt% ACE-labelled PAA in aqueous solution at different pH values. (λex = 295 nm and λem = 340nm).

3.4 Conformational Behaviour of ACE-AMMA labelled PDMAEMA as a Function of pH

The effect of pH, on the conformation behaviour of PDMAEMA is investigated by the Fluorescence Resonance Energy Transfer principle. Since fluorescence data, includes steady state and excited state lifetime, is applied to investigate the conformations of PDMAEMA at different pH values.

Again, the measuring of distance between donor and acceptor of ACE-AMMA- PAA is applied to investigate the conformational change (aggregation and expansion).

3.4.1 Fluorescence steady state spectra of ACE-AMMA-PDMAEMA as a function of pH

Steady state spectra data was measured and collected from PDMAEMA samples labelled with both an ACE label acting as a donor and an AMMA label acting as an acceptor, in aqueous solution (Figure 3.24). The figure shows a substantial drop in the emission intensity of the ACE label at 340 nm as the pH level is increased while it shows insignificant drop in the emission intensity level of the AMMA label at 420 nm.

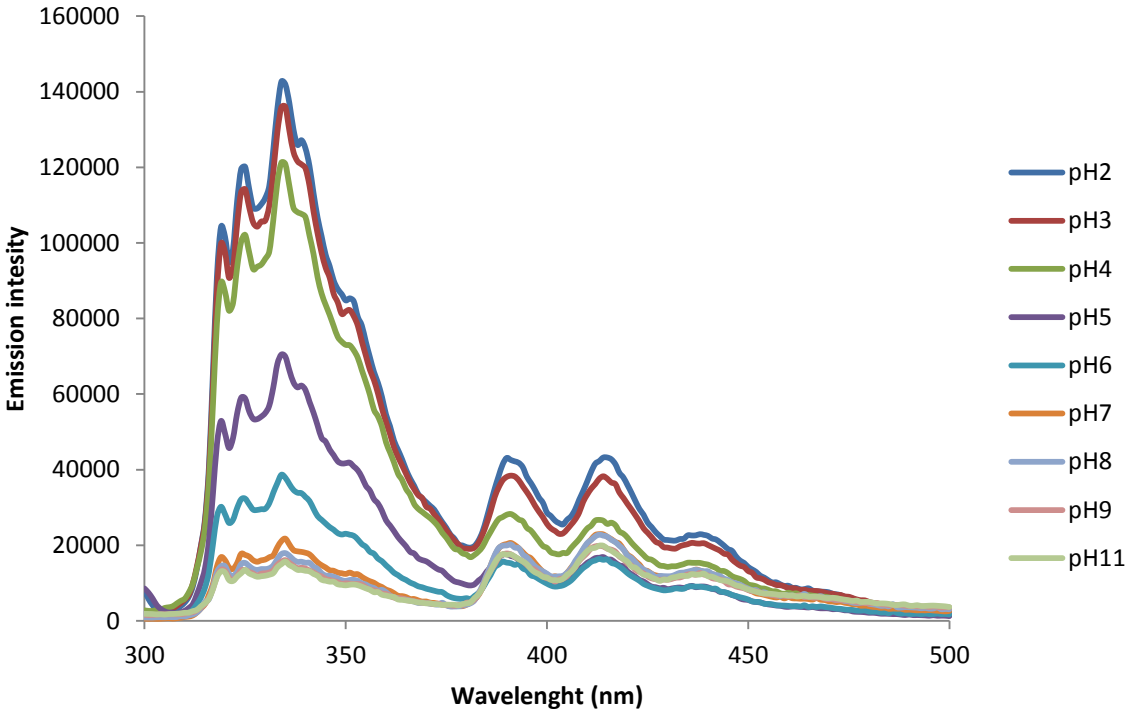

Figure 3.24: Emission scan in a range equal to 300-500 nm at fixed excitation λex = 290 nm for ACE-AMMA-PDMAEA (10^{-2} wt % in water) at different pH values.

It was inferred from the substantial drop in the intensity for the ACE label at 340 nm that energy is transferred from the ACE label to the AMMA label as quenching by the internal amine groups of the polymer should affect both labels to the same extent. This was observed when the ACE-AMMA-PDMAEMA polymer sample was excited at 370 nm leading to the increase in fluorescence intensity of the AMMA label (Figure 3.25). The emission intensity from the anthryl label is decreased as pH level switched from high pH values to low pH values in a manner similar to that of the ACE labelled sample. From this it is deduced that the insignificant decrease of the intensity of the AMMA label in the ACE-

AMMA-PDMAEMA sample is attributed to energy transfer from the ACE label to the AMMA label at high pH values. This provides evidence that the deprotonated amine unit must have acted as the quencher at high pH values. This inference would be fitting because, despite the fact that PDMAEMA should in theory coil as the pH value of the solution increases, there was a decrease in the emission intensity of the directly excited AMMA label, which was not quenched by the ACE label. This means that with the aqueous media being more excluded in this conformation, something in the polymer chain itself acted as a quencher, most likely the amine group.

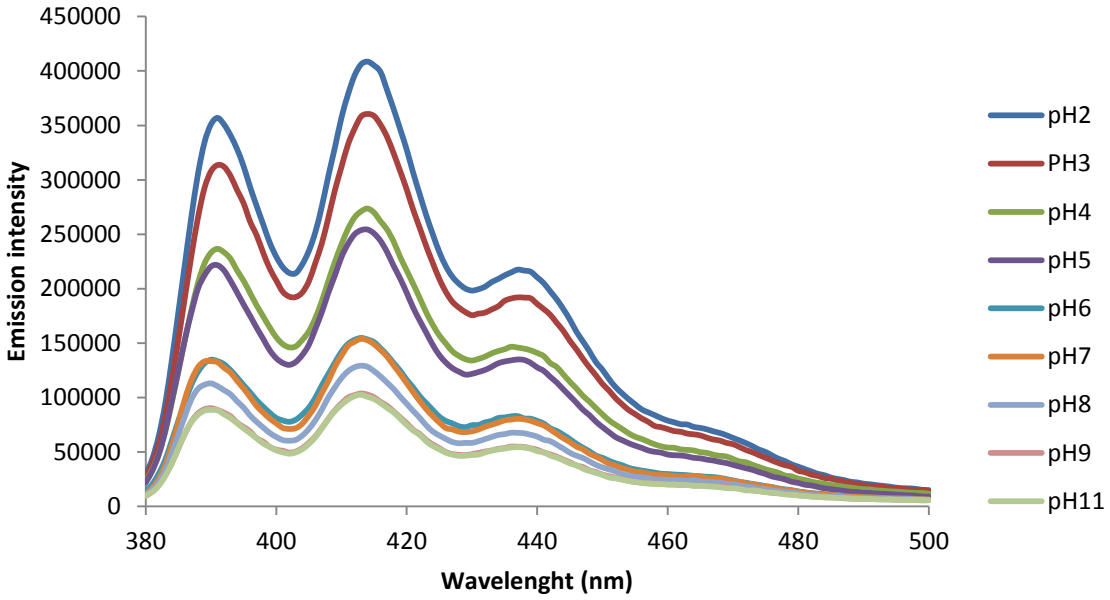

Figure 3.25: Example steady state emission spectra for an ACE-AMMA labelled PDMAEMA sample in aqueous solution when excited at 370 nm at different pH values.

Figure 3.26 shows a plot of the ratio of the intensity of emission for ACE-AMMA-PDMAEMA polymer sample at 420 nm (AMMA) and 340 nm (ACE) upon excitation at 290 nm. It can be observed from the figure that the ratio of the acceptor peak to donor peak increases as the pH value increased to the collapsed form of the polymer while the ratio decreased when the pH value decreased to a value that resulted in an expanded polymer form.

The AMMA (I_{420}): ACE (I_{340}) emission intensity ratio began to increase from pH 7, around the pKa of the PDMAEMA polymer system indicating that the energy transfer in the coiled

form of the polymer chain occurred as the amine groups are deprotonated[14]. Before the transition in conformation occurred, (pH < 7), a marked decrease in the ratio cab be observed. This means that some of the amine groups became protonated and accordingly bear a positive charge, which in turn led to an expanded form.

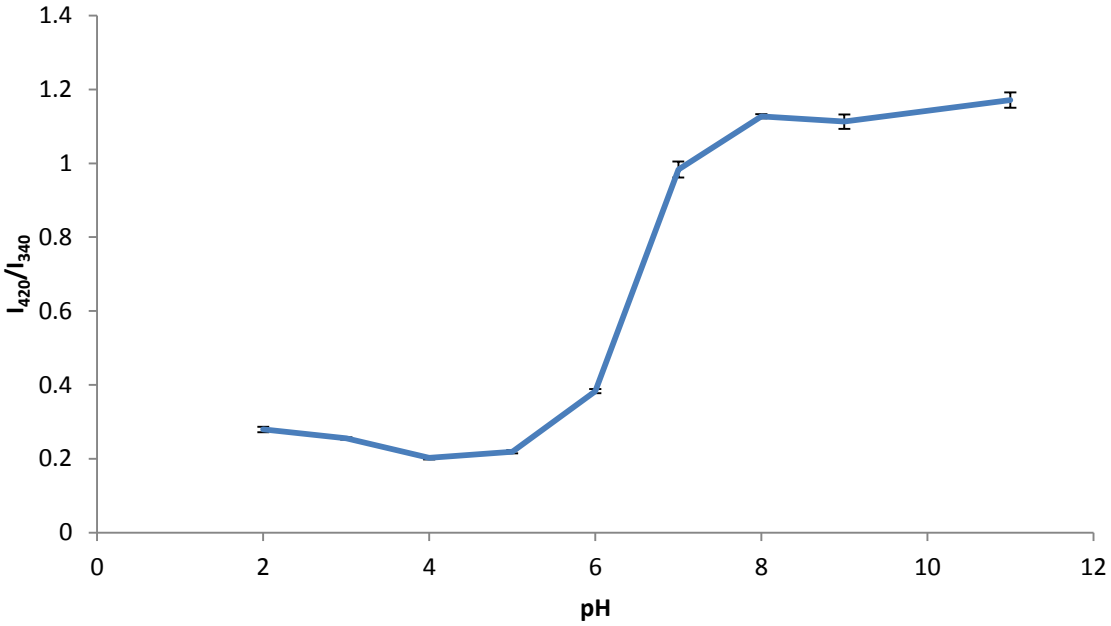

Figure 3.26: Ratio of emission at λ_{em} = 420 nm (AMMA) to emission at λ_{em} = 340 nm (ACE) exciting at 290 nm with varying pH for 10^{-2} wt% from ACE-AMMA-PDMAEMA in water.

3.4.2 Fluorescence exited state lifetimes of ACE-AMMA- PDMAEMA as a function of pH

ACE fluorescence emission decay data was collected over the whole pH range for ACE-AMMA-PDMAEMA in a similar way to the previously collected data for the singly labelled PDMAEMA polymer (Section 3.3.2). Under basic conditions, a triple exponential function of the form (Equation 3.5) was used to adequately interpret the fluorescence decay data when energy transfer occurs, while at an acidic media the use of a double exponential (Equation 3.2) was enough to fit the decay data. The average lifetimes were calculated using Equation 3.3.

The average decay lifetimes for ACE-PDMAEMA and ACE-AMMA-PDMAEMA are recorded in Table 3.3. It can be seen from Figure 3.27 that the $< \tau_f >$ values are slightly lower for the donor at pH values >7 in the presence of AMMA than for ACE

without the acceptor. This indicates that the maximum efficiency of energy transfer occurres when the polymer chains was in collapsed form at high pH values. On the other hand, the average lifetime values at pH < 8 (which is around the conformational transition pH value) are a little bit higher for the donor in the presence of the AMMA than for ACE without acceptor. In this range of pH values, higher expansion of the polyelectrolyte chain occurs because of the electrostatic repulsions of the positively charged amine groups. As a result, the distance between the donor and the acceptor is longer and thus no significant energy transfer was observed.

Table 3.3: Average lifetimes $< \tau_f >$ comparison for ACE-PDMAEMA and ACE-AMMA- PDMAEMA samples in aqueous solution at different pH values.

pH	$< \tau_f >$ (ns) ACE-PDMAEMA	$< \tau_f >$ (ns) ACE-AMMA-PDMAEMA
2	17.95	21.62
3	22.07	21.65
4	19.64	20.43
5	14.55	14.64
6	9.96	9.8
7	6.13	6.14
8	6.13	5.65
11	6.51	5.42
12	6.69	5.51

The average lifetimes as a function of pH for ACE-PDMAEMA and ACE-AMMA-PDMAEMA are plotted in Figure 3.27 The graph shows the conformational transition of the PDMAEMA as the pH level increased from low pH values with expanded PDMAEMA form (the label away from quencher at low pH) to a collapsed PDMAEMA form at high pH values (the label closer to the quencher), hence shorter $< \tau_f >$ is observed.

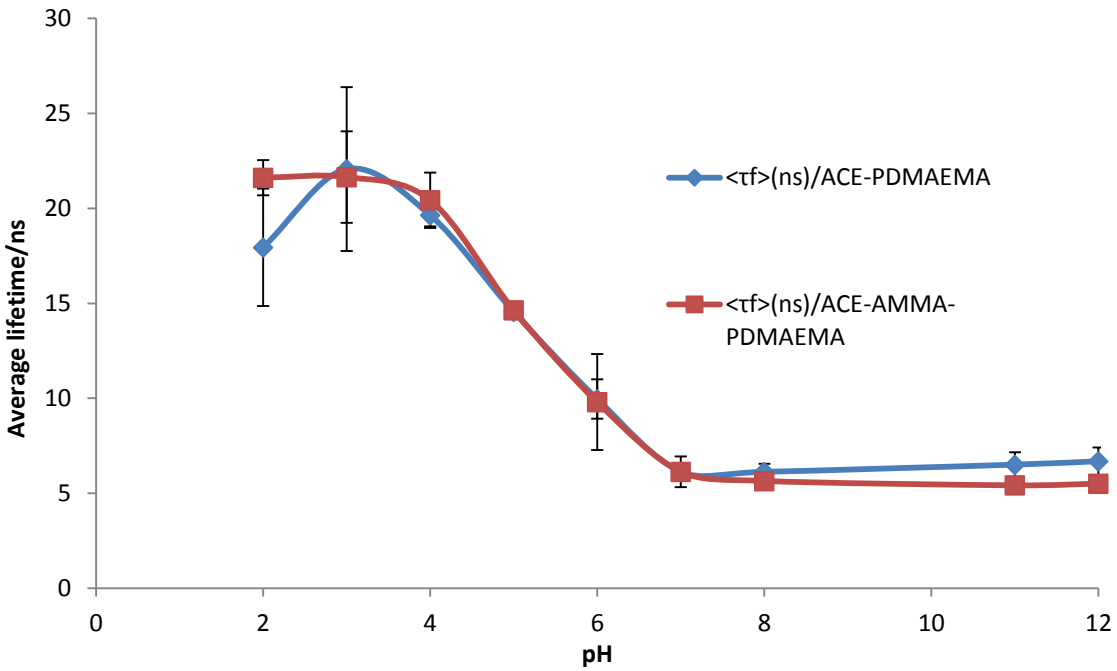

Figure 3.27: Average donor lifetime $< \tau_f >$ for ACE-PDMAEMA and ACE-AMMA-PDAEMA as a function of pH (λex = 295 nm and λem = 340 nm).

Average lifetimes for ACE-PDMAEMA and ACE-AMMA-PDMAEMA were used to determine the distribution of distances between the donor-acceptor pairs, which is related to the chain dimensions as described in equation 3.7. Table 3.4 presents the actual separation distances in the PDMAEMA chain at the higher range pH values. In particular it has been found that at pH 8, the distance between ACE and AMMA was 3.77 nm, which is within the Förster distance for donor-to-acceptor energy transfer [37]. At pH $\leq$ 7 (below the transition point) the distance cannot be determined due to the separation distance is believed to be more than 10 nm, which is completely out of ET range.

Table 3.4: The distance between donor and acceptor as a function of pH

pH	r (nm)
8	3.7
9	3.3
11	3.2
12	3.2

In summary, an increase of fluorescence intensity and lifetime was resulted with decrease of pH for PDMAEMA in aqueous solution. This implies that as the donor label becomes distant from the internal quencher (amine group), there was an expansion of the polymer chain. Moreover PDMAEMA in aqueous solution, showed that with increasing pH an increase in the amount of energy transfer between donor and acceptor labels was resulted. TRAMs studies support this collapse of polyelectrolyte backbone, showing a decrease in the segmental mobility at the same pH range.

Chapter 4 **Fluorescence investigation of pH responsive polymers in the presence of various salts**

4.1 Fluorescence investigation of poly (acrylic acid) PAA in the presence of various salts

The concentration of salt and cations are found to have a different impact on poly acrylic acid conformation, which is also dependent on the solution's salt type that is present. Different cations in the solution have different influences, this may be due to the difference of being monovalent or divalent cations. Divalent cations, for example Ca^{2+}, have a higher charge and so a higher attractive interaction would occur with deprotonated carboylate groups. The fluorescence techniques is used to compare how these salts affect the PAA coiled polyelectrolyte chains and is used for comparative analysis. Results from this experiment showed that monovalent and divalent cations have different effects. The difference is particularly shown by the effect of monovalent cations, sodium bromide and sodium chloride on PAA compared to divalent cations, calcium bromide and calcium chloride on PAA.

4.1.1 Fluorescence steady state spectra of ACE-AMMA labelled PAA in the presence of NaCl as a function of pH

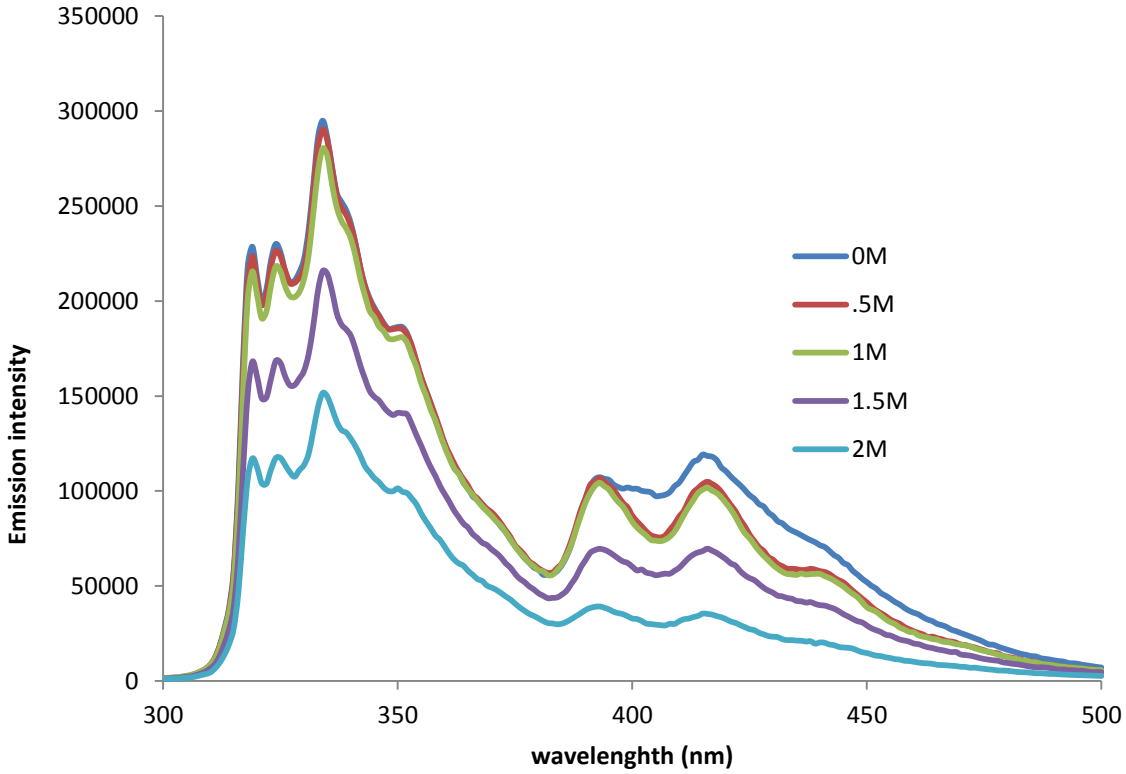

Figure 4.1 Emission scan in a range equal to 300-500 nm at fixed excitation λ_{ex} = 290 nm for ACE-AMMA-PAA sample in aqueous solution at pH 3 and varying NaCl concentration.

Figure 4.1 shows the emission spectra for an ACE-AMMA labelled PAA sample at pH 3 with different NaCl concentrations. The figure shows a decrease in emission intensity of both donor and acceptor labels as the NaCI concentrations were increased. The graphs indicate that the entire system is being quenched. It also suggests that the addition of the salt to a coiled polyelectrolyte (pH3) led to the unfolding of the coiled polymer at all concentration of salt and possibly quenched the labels by an aqueous environment.

Poly (sodium styrene sulfonate) PSS is similar to PAA in being a negatively charged polyelectrolyte in aqueous solutions, however it is stronger polyelectrolyte than the PAA. It is reported in the literature that the fluorescence emission data collected from a DPA(Cryo Disbosable Probe Adaptor)-labelled PSS sample quenched with thallium cation (TI^{+}) showed an extended PSS conformation in the presence of low concentrations

of salt [14]. Figure 4.2 show a slight decrease in the emission intensity of the ACE label at pH 11 as NaCl concentration is increased, and no significant change in the AMMA emission intensity.

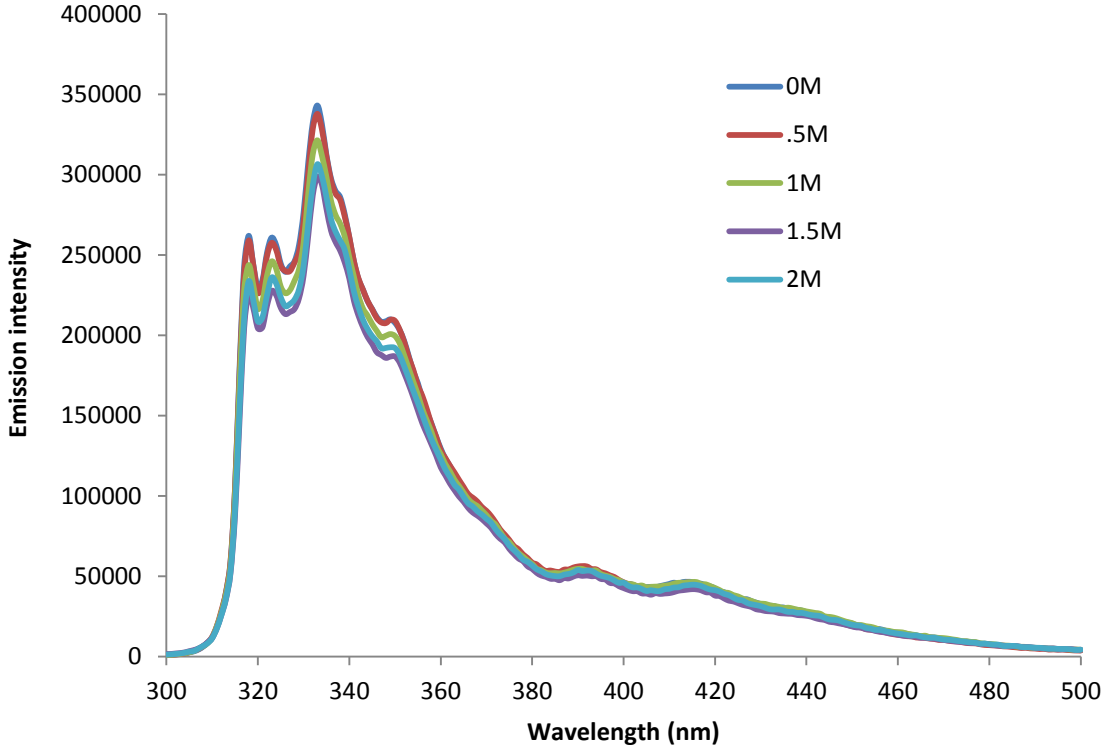

Figure 4.2: Emission scan in a range equal to 300-500 nm at fixed excitation λ_{ex}= 290 nm for ACE-AMMA-PAA sample in aqueous solution at pH 11and varying NaCI concentration

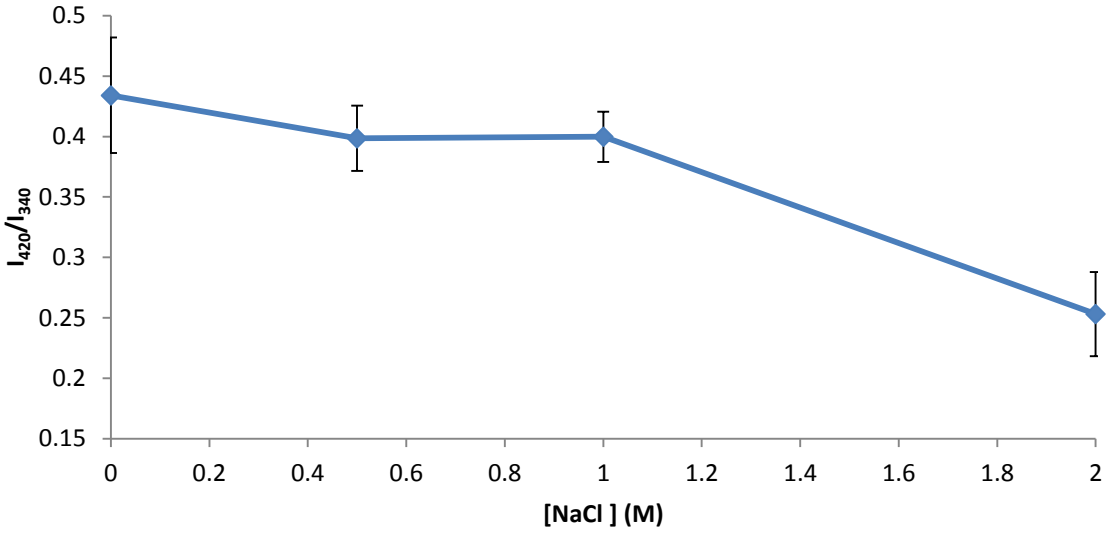

Figure 4.3: Fluorescence emission intensity ratio, I_A/I_D of 10^{-2} wt% ACE-AMMA-labelled PAA as a function of NaCl concentration at pH 3 (λ_{ex} = 290 nm).

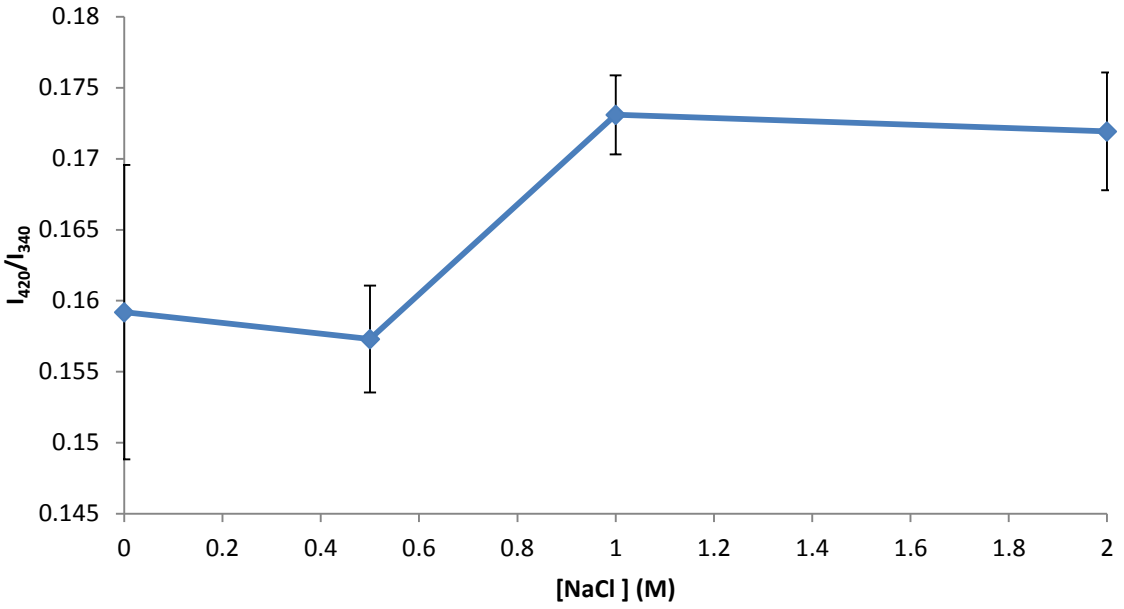

Figure 4.4: Fluorescence emission intensity ratio, I_A/I_D of 10^{-2} wt % ACE-AMMA-labelled PAA as a function of NaCl concentration at pH 11 (λ_{ex} = 290 nm).

The energy transfer efficiency (ET) as a function of the NaCl concentration is shown for pH 3 on Figure 4.3 and for pH 11 on Figure 4.4. It can be seen from figure 4.3 that the acceptor to donor ratio decreased considerably as the NaCl concentration increased from 1M to 2M. This suggests that the coiled polymer expanded when NaCl salt was added. On the other hand, this ratio increased as the NaCl concentration increased at pH 11 (Figure 4.4), In this case the increase in the ET suggests that the polymer chain collapsed when Na^+ ions were added. Possibly, the anionic carboxylate groups of Poly(acrylic acid) with its expanded chain were neutralized by Na+ cations [54] leading to a coiled conformation with a shorter distance between the acceptor and the donor labels and hence an increase in the energy transfer as indicated by the emission intensities.

Figure 4.4 shows the energy transfer ratio graph for pH 11. At 1M and 2M NaCl concentrations the energy transfer ratio is at a maximum value (~0.17) indicating ~17% energy transfer efficiency in the relatively coiled form of the PAA chain. This increase in energy transfer efficiency is due to the high concentration levels of Na^+ ions where several of the negatively charged carboxylate groups are neutralised by the sodium cations Na^+ [54].

In contrast, the ratio dropped to ~0.157 at low NaCl concentration (0.5 M) suggesting that the macromolecule chain largely existed in an expanded form compared to the zero concentration case when the PAA in water.

4.1.2 Fluorescence excited state lifetimes of singly and doubly labelled PAA in the presence of NaCl as a function of pH

The lifetime data of the ACE labelled PAA polymer in the presence of sodium chloride (NaCl) was best modelled by a triple exponential data model (Equation 3.5). Three average lifetimes fits for pH 3, pH 6 and pH 11 were then analysed and compared (Figure 4.5). The used data model gave the closest fit for the lifetime values with χ^2 value close to unity and small standard deviation (Figure 4.6).

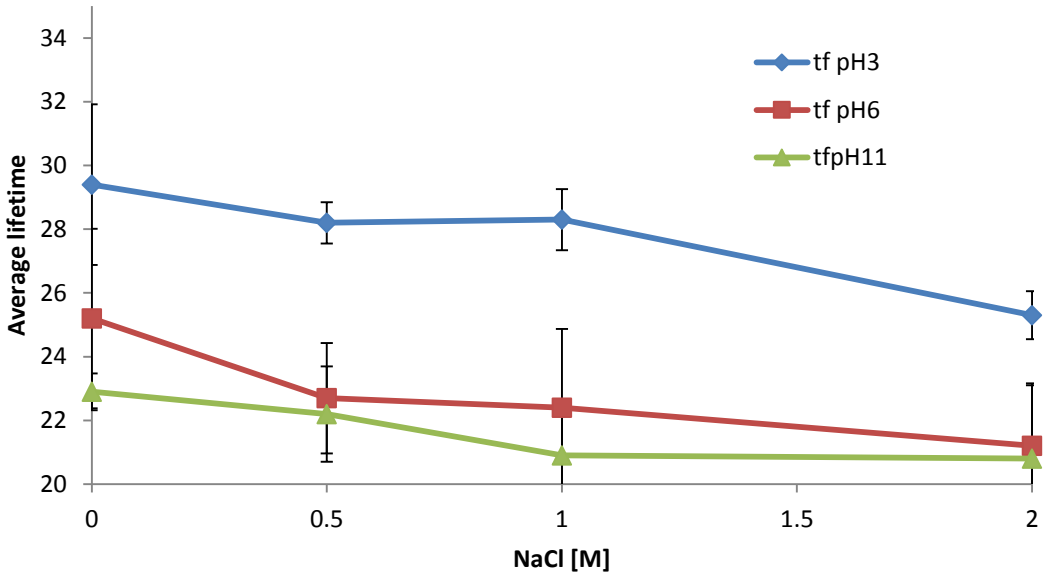

Figure 4.5: A plot of the average lifetime values obtained for ACE-PAA in aqueous solution at three different pH values with increasing NaCl concentration when excited at 290 nm and observed at 340 nm.

Figure 4.5 shows the average ACE lifetimes values for ACE-PAA plotted against [NaCl] concentration levels. Addition of salt resulted in a decrease in the lifetime for all pH values. This decrease became more substantial in the doubly labelled ACE-AMMA system (Figure 4.7). There is a slight decrease in the lifetime at 0.5 M to 1 M of NaCl at pH 3. The decrease became more pronounced at 2 M. This could be attributed to quenching of the

system by the aqueous media resulted from the expansion of the polymer from the coiled conformation state.. A substantial decrease in the lifetime values at pH 6 (more expanded polymer form) indicating that the system was coiling and the ACE fluorescence was being quenched. This behaviour has been previously observed prominently in fluorescence quenching experiments that investigated the behaviour of PMAA in aqueous solutions where the degree of "openness" or "compactness" of the PMAA polymer chain can be inferred. Also, it is reported that positively charged species such as TI^{+} [62],[63] or Cu^{+2} [64], [63] are used to quench the fluorescence from labeled PMAA polymer samples with results of low kq (bimolecular quenching constant) values at low pH. This implies that the cations experience a largely aqueous environment as they diffuse toward the excited state and would be consistent with an expanded polyelectrolyte coil under these conditions. In contrast, at higher pH values, more efficient quenching occurred than that of a diffusion-controlled process. This behavior of PMAA polymer which also has been observed in other works (see for example [62],[63-64] points to the existence of carboxylate anions under these conditions: the cations cluster around the poly salt form forming a high local concentration of quencher around the label (higher than the nominal bulk quencher concentration in solution). In respect of this study, it can be said that Na^{+} ions may have acted as a quencher leading to the decrease in the lifetime observed for all pH values.

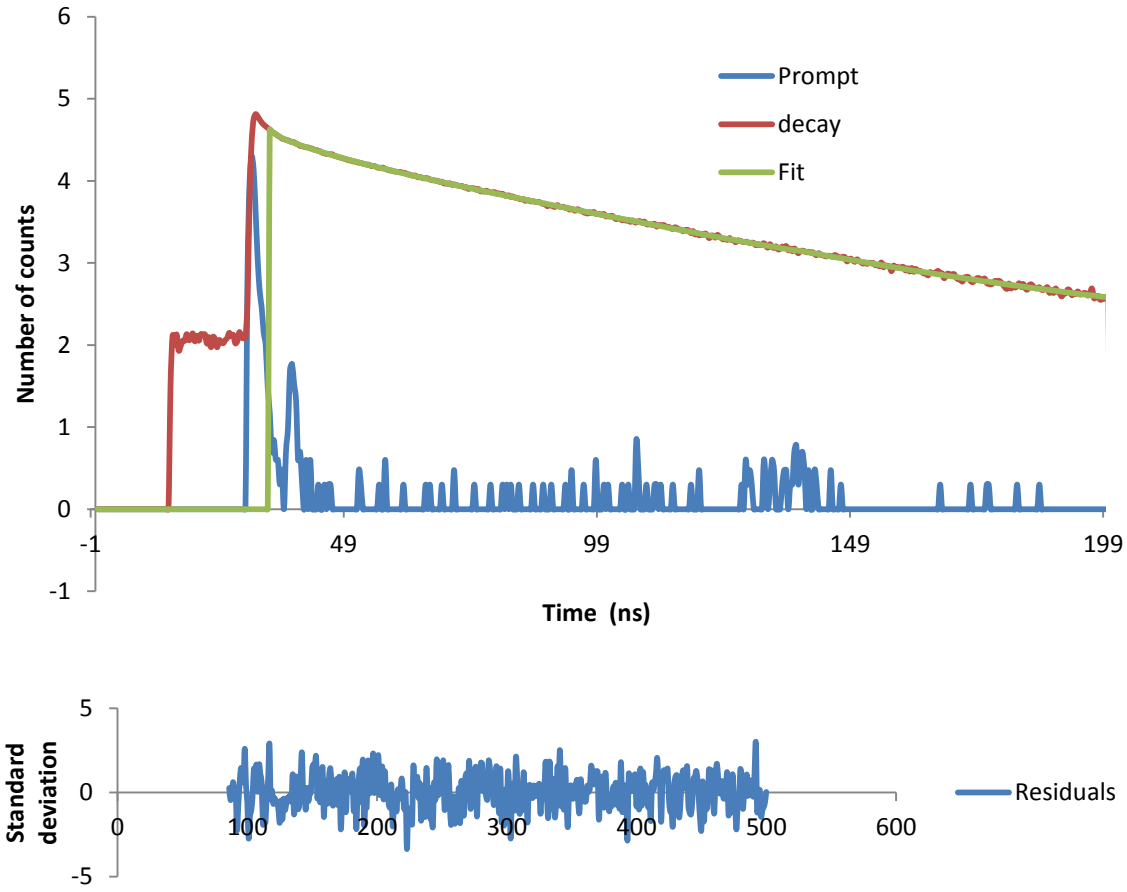

Figure 4.6: A fluorescence decay with corresponding mathematical fit (shown in green) and a plot of the resulting residuals for ACE-PAA in aqueous solution of pH 3 with 0.5 M of NaCl.

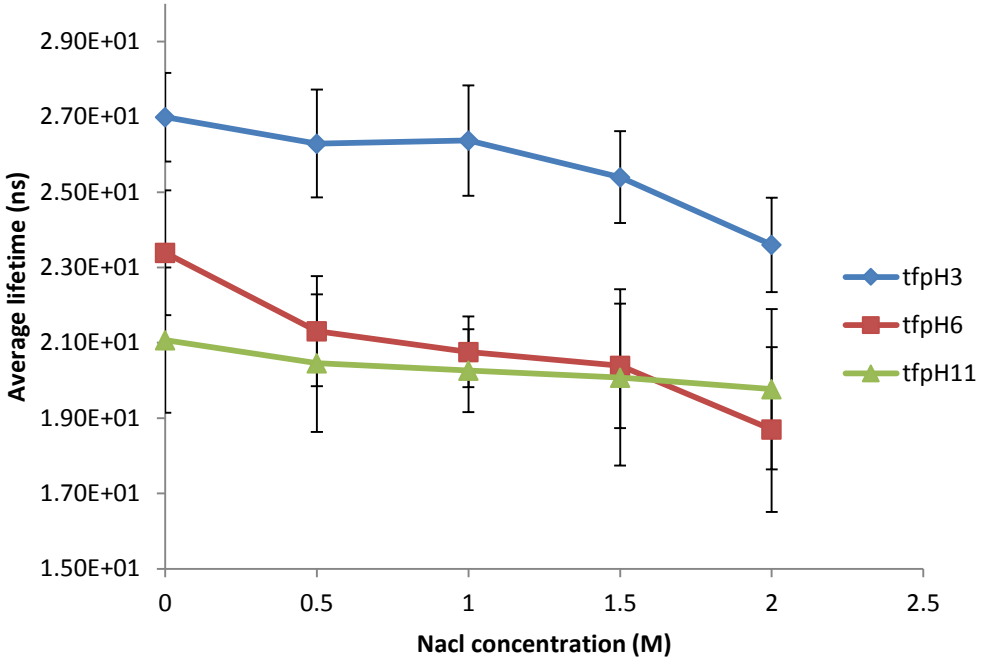

Figure 4.7: A plot of the average lifetime values obtained for ACE-AMMA-PAA in aqueous solution at three different pH values with increasing NaCl concentration when excited at 290 nm and observed at 340 nm.

The curve at pH 3 (Figure 4.7) displays a similar pattern to that obtained from the I_A/I_D ratio against [NaCl] (Figure 4.3). Therefore, the shape of the plot may also be attributed to the conformational transition occurring for the Polymer chain. Such a transition went from a relatively collapsed chain at zero [NaCl] where a longer $< \tau_f >$ was recorded, to a relatively expanded form at higher [NaCl] which resulted in a shorter $< \tau_f >$ this suggests that the opening of the PAA polymer coil enabled increased quenching by the aqueous media. On the other hand, figure 4.4, the opposite pattern was obtained from the I_A/I_D ratio against NaCl concentration at pH 11 However, the shape of the plot could be attributed to the fact that a conformational transition occurred to the PAA chain when the concentration of the sodium chloride was increased. This transition is believed to go from a partially expanded chain at zero NaCl concentration yielding longer$< \tau_f >$, to a partially collapsed form at higher concentration of NaCl. Figure 4.7, also shows an average lifetime slightly quenched to ~20.8 ns. This average lifetime level could be attributed to the binding of the Na^+ ions to the PAA polymer which led to a collapsed PAA polymer state and

consequently quenching the label in addition to the energy transfer to the acceptor. The curve at pH 6 showed a similar behaviour to that observed for the curve at pH 11.

Triple exponential fit (Equation 3.5) was used to model the fluorescence decays of ACE-AMMA PAA samples and gave the best fit with statistically χ^2 values close to unity and small residuals standard deviations (Figure 4.8). Again, average lifetime values are used for the purpose of comparison.

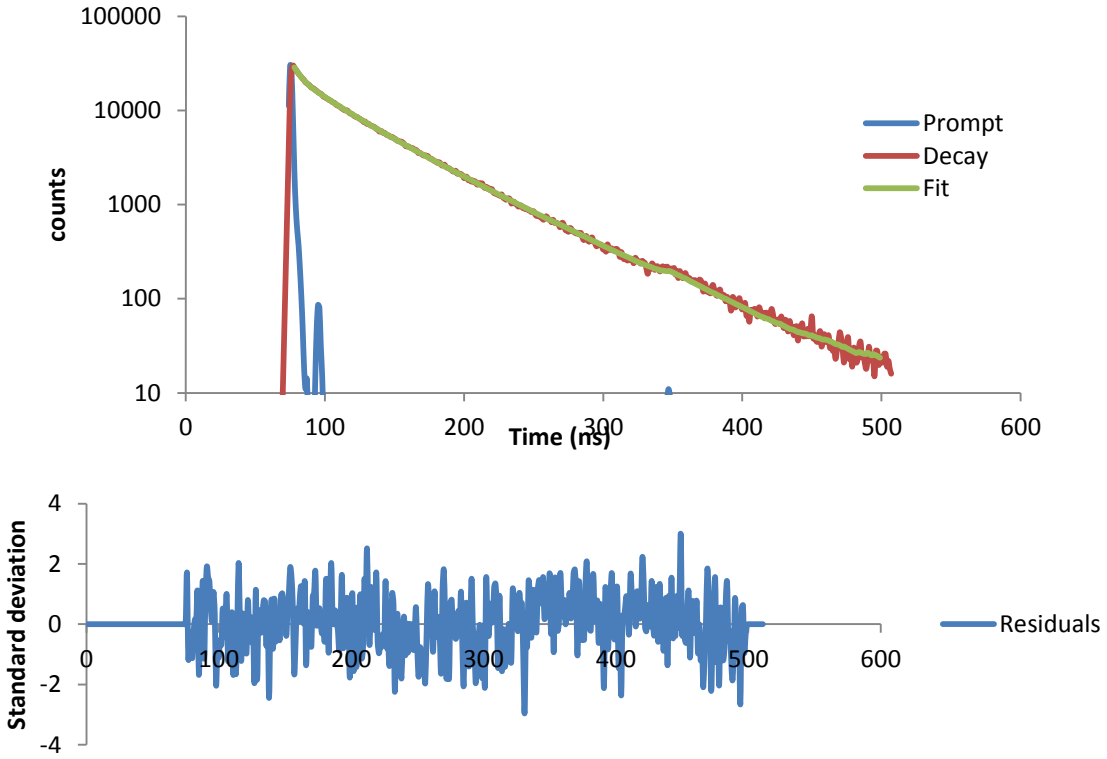

Figure 4.8: A fluorescence decay with corresponding mathematical fit (shown in green) and a plot of the resulting residuals for ACE- AMMA-PAA in aqueous solution of pH 11 with 2 M of NaCl.

The average r values are then estimated for the ACE-AMMA-PAA as a function of [NaCl] and pH via equation 3.7 and 3.8 respectively. Figure 4.9 shows the calculated distance values between the donor and acceptor labels in the double label PAA polyelectrolyte system at varying salt concentrations and pH values.

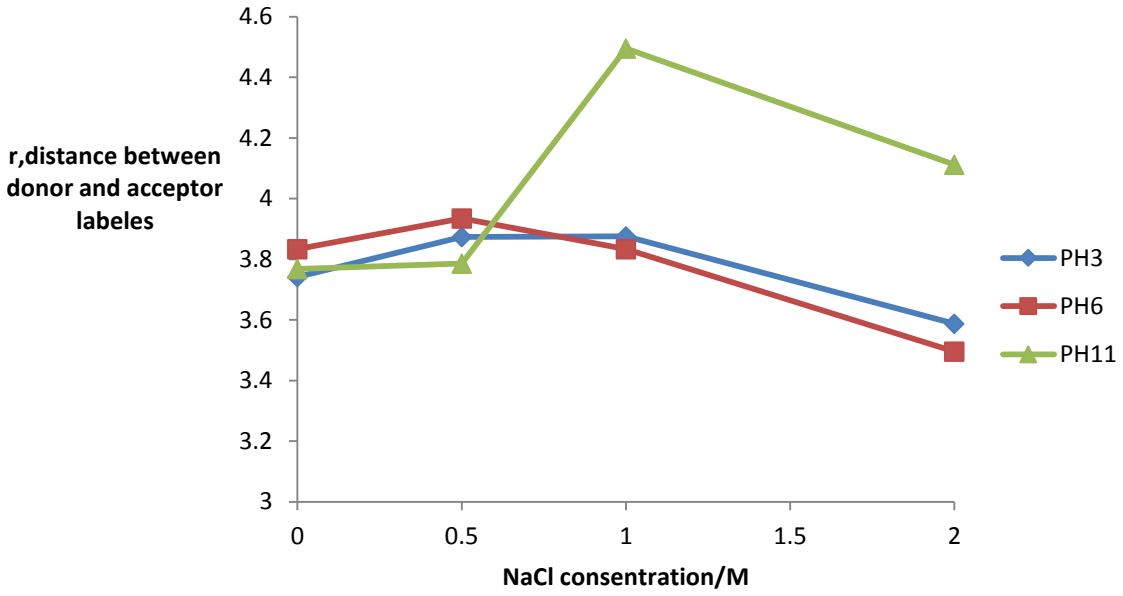

Figure 4.9: Plot of the value r, the distance between ACE (donor) and AMMA (acceptor) labels, as calculated by equation 3.7 for single and double -PAA across a range of pH values and NaCl concentrations.

The label distance r at pH 3 and pH 6 shows an increase at the initial concentration of the salt (i.e. 0.5 M) as might be expected given that the polymer expands at a lower pH values in the presence of a small amount of salt. The distance values are then decrease as [NaCl] increases indicating that the polymer adopt a coiled form at high amount of salt concentration. In contrast to this behaviour, at pH 11 the distance between the labels shows a decrease at small amount of NaCl concentrations, indicating that the polymer adopted a coiled chain. The distance r value is then increased at 1 M suggesting that the polymer adopted an opened chain, at even higher NaCl concentration of salt (2 M) the r value start to drop again indicating that the polyelectrolyte start to adopt a coiled chain at such higher amount of NaCl concentrations.

4.1.3 Fluorescence Time-Resolved Anisotropy Measurements (TRAMS) of ACE-PAA in the presence of NaCl as a function of pH

The interaction between the PAA polyelectrolyte and salt content is accompanied by changes in the mobility of the polymer chain. Techniques like TRAMS, which monitor polymer dynamics, should be useful for investigating the dynamic behaviour of PAA in the presence of NaCl.

Figure 4.10 and Figure 4.11compare the fluorescence anisotropy decays of ACE-labelled-PAA in water in the absence and presence of low and high sodium chloride at pH 3 (acidic condition). At low [NaCl] (Figure 4.10) the anisotropy decays pattern can be attributed to that the polymer underwent a structural change from partially collapsed form to a partially expanded chain form as indicated by the faster decay time. Conversely, the anisotropy slowly decayed to zero at high salt concentration than that in the absence of salt (Figure 4.11).This photophysical behaviour provides an evidence that the PAA adopts a more coiled chain from when the salt is at high concentration under acidic condition in comparison to the case where no salt is present. Hence, a long anisotropy decay was observed.

It is found that, the high ionic strength effects more coiling of the PAA chain while the low ionic strength effects less coiling of the chain as observed for high and low ionic strength cases, this is presumably due to the expanded form of the polymer chain. This observation also has been reported by Major and Torkelson where they examined the effect of coil size and conformation on the fluorescence properties of PSS through the addition of low molecular weight electrolytes [14]. A dramatic increase in excimer formation was observed for solutions of high ionic strength as a consequence of chain contraction. In contrast, smaller effect on the excimer population was reported on addition of low salt concentrations.

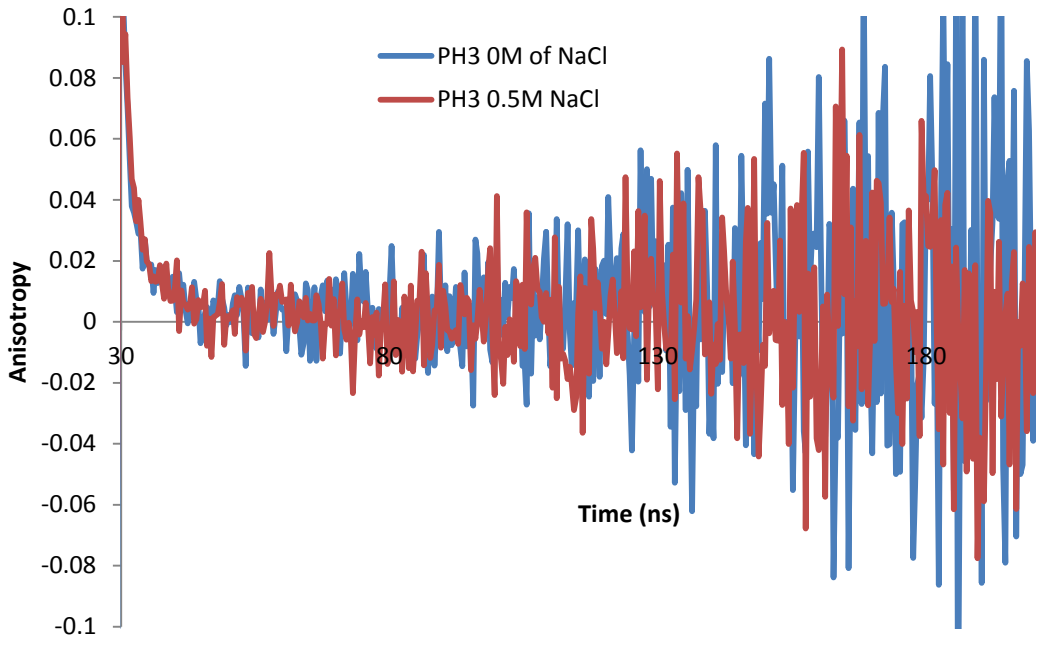

Figure 4.10: Fluorescence time resolved anisotropy data of aqueous ACE-labelled PAA solution (10^{-2} wt %) in the absence of sodium chloride (blue line) and at the sodium chloride concentration of 0.5M at pH 3 (λ_{ex} = 295 nm and λ_{em} = 340 nm).

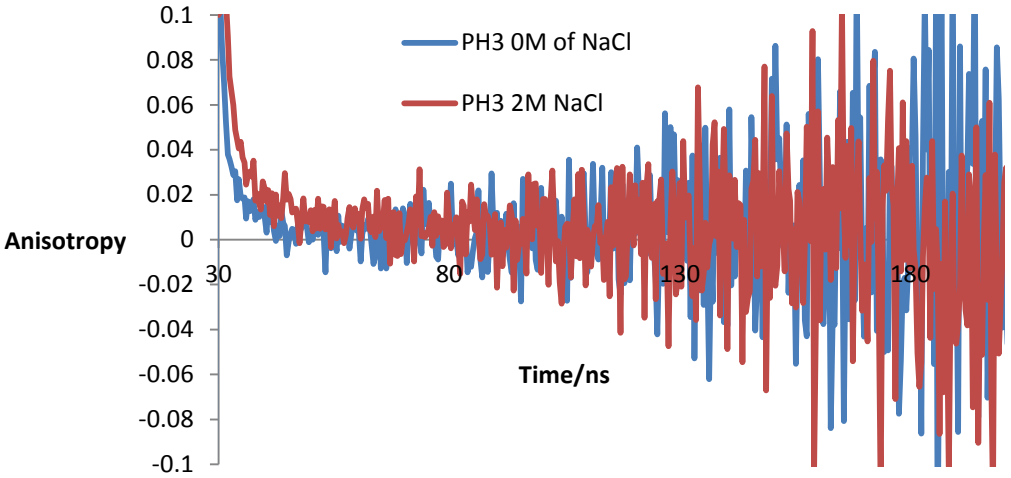

Figure 4.11: Fluorescence time resolved anisotropy data of aqueous ACE-labelled PAA solution (10^{-2} wt %) in the absence of sodium chloride (blue line) and at the sodium chloride concentration of 2M at pH 3 (λ_{ex} = 295 nm and λ_{em} = 340 nm).

Figure 4.12 presents the anisotropy decays of ACE- PAA in the presence and absence of NaCl at pH 6. It is found that the anisotropy time decay in the presence of NaCl salt took longer time decay than the case where the NaCl is absent. This is possibly due to the interaction occurring between the Na^+ ions and the COO^- of the PAA [54] leading to the collapse of the PAA polyelectrolyte chains, which in turn inhibited the motion of the ACE-PAA chain and hence the slow decay. This in agreement with the static and dynamic light scattering study [65], which was applied to characterise a variety of poly (acrylic acid) PAA samples in dilute aqueous solutions with added NaCl. It was found that an increase in the NaCl concentration led to a decrease in the hydrodynamic radius of PAA chain.

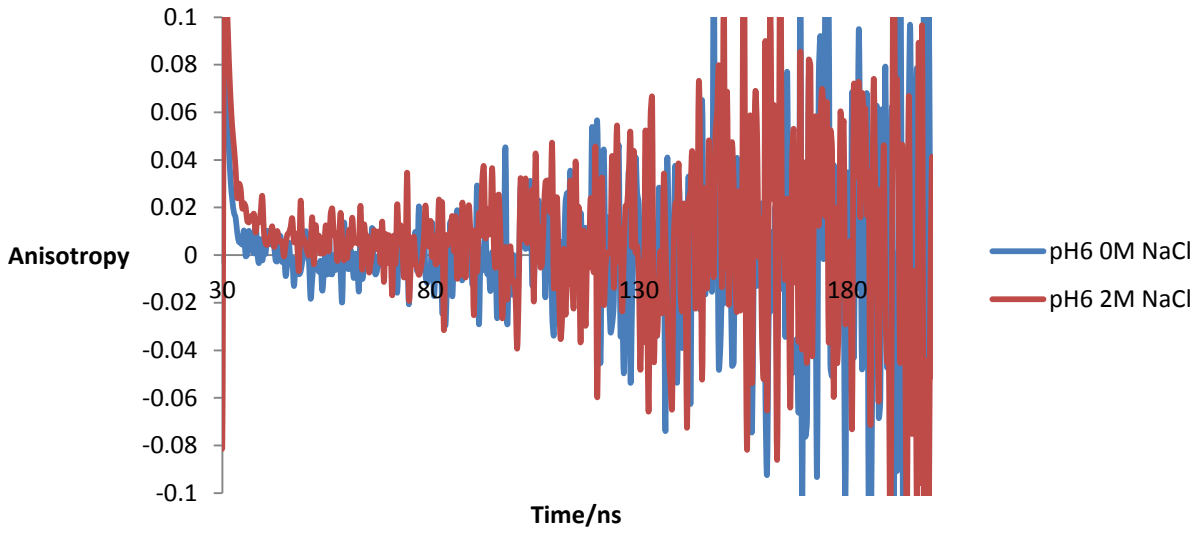

Figure 4.12: Fluorescence time resolved anisotropy data of aqueous ACE-labelled PAA solution (10^{-2} wt%) in the absence of sodium chloride (blue line) and at the 2 M [NaCl] at pH 6(λ_{ex} = 295 nm and λ_{em} = 340 nm).

Correlation times derived from mathematical analysis of anisotropy decays of ACE-PAA was best fitted using a single exponential function to determine the correlation time values in nanoseconds. The correlation time data is plotted on Figure 4.13 as a function of both pH and salt content.

In general, the τ_c values at pH 3 and pH 6 increased as the amount of salt NaCl increased (i.e. 1M and 2M). This trend indicates that the polymer underwent a conformational collapse as the concentration of NaCl salt increased at these values of pH.

However, the correlation time at pH3 and pH6 initially decrease after the initial addition of NaCl (0.5 M) which indicate that the polymer chains become expanded.

At higher pH values, the correlation time slightly increase at the initial addition of the NaCl salt and then drops slightly at 1 M, before starting to increase again at high concentration of NaCl although with less rate than the initial rate. It is worth noting that the aggregation generated by the binding of Na^+ ions to COO- ions for expanded polymer chains is more noticeable at pH6 than pH11.

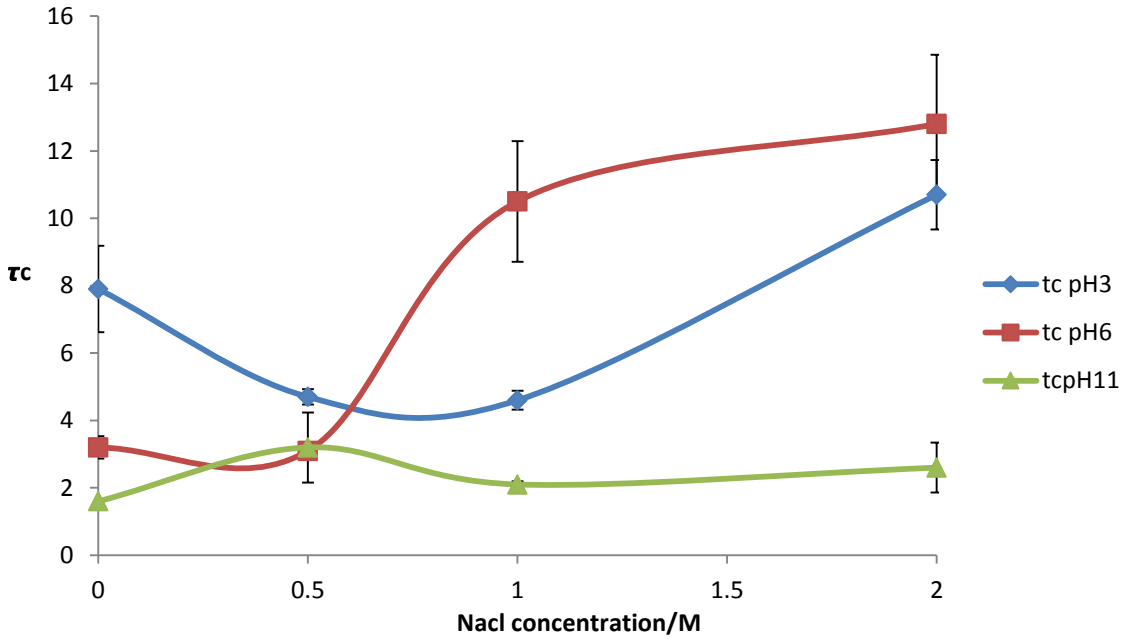

Figure 4.13: A plot of correlation time against NaCl concentration for three ACE labelled PAA samples in aqueous solution at three different pH values when excited at 290 nm and observed at 340 nm.

4.1.4 Fluorescence steady state spectra of ACE-AMMA labelled PAA in the presence of $CaCl_2$ as a function of pH

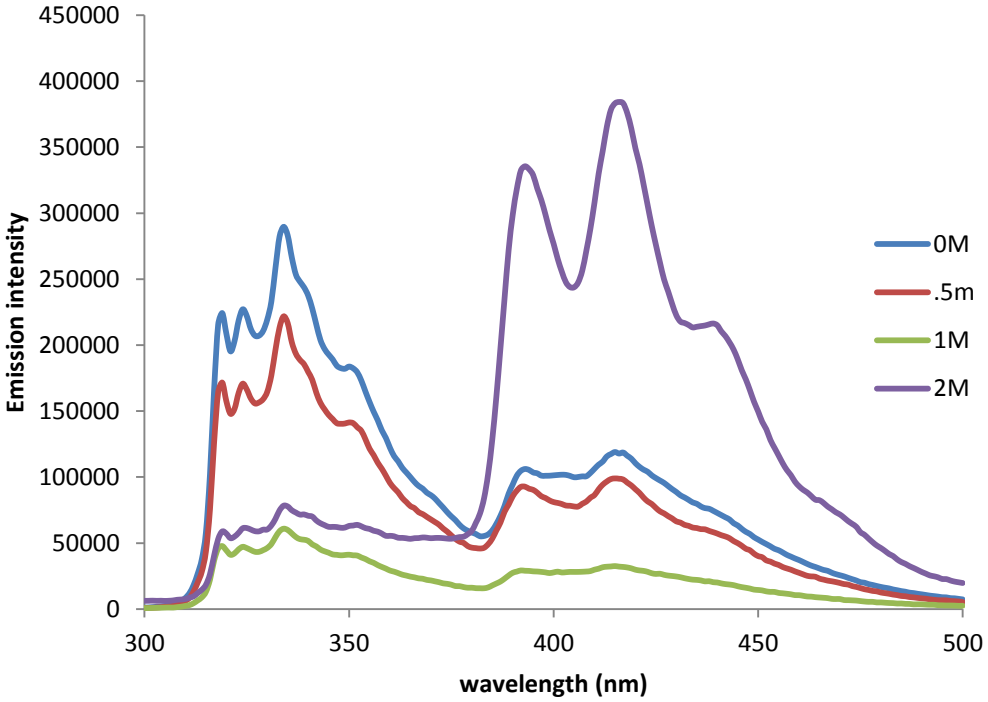

Figure 4.14: Emission scan in a range equal to 300-500 nm at fixed excitation λ_{ex} = 290 nm for ACE-AMMA-PAA sample in aqueous solution at pH 3 and varying $CaCl_2$ concentration

Steady state emission spectra of an ACE-AMMA labelled Poly(acrylic acid) sample against a range of $CaCl_2$ concentrations at pH 3 showed a great decrease in the emission intensity (at 340 nm) of the naphthyl label with increasing calcium chloride concentration (Figure 4.14). The relative emission from the anthryl label centred at 410 nm is also decreased. However, at concentration of 2 M, this emission is greatly increased indicating a selective quenching of the donor emission, a quenching of the entire system, or that the polymer collapsed leading to energy transfer between the two labels.

It can be observed from Figure 4.15 (high peak at 340 nm) that the ACE-AMMA-PAA adopted an expanded conformation at pH 11 in the absence of $CaC1_2$; this expansion is a consequence of the charge repulsions between carboxylate anions. The fluorescence spectra from the polymer (in the absence of $CaC1_2$) showed emission largely from ACE suggesting that energy transfer is minimal under these conditions. Increasing the concentrations of $CaC1_2$ served to reduce the naphthyl emission with a corresponding increase in anthryl fluorescence; this is presumably due to the attraction of the Ca^{2+} ions

complex to the carboxylate anions and hence collapsing the polymer chain and therefore increasing the degree of energy transfer in the process.

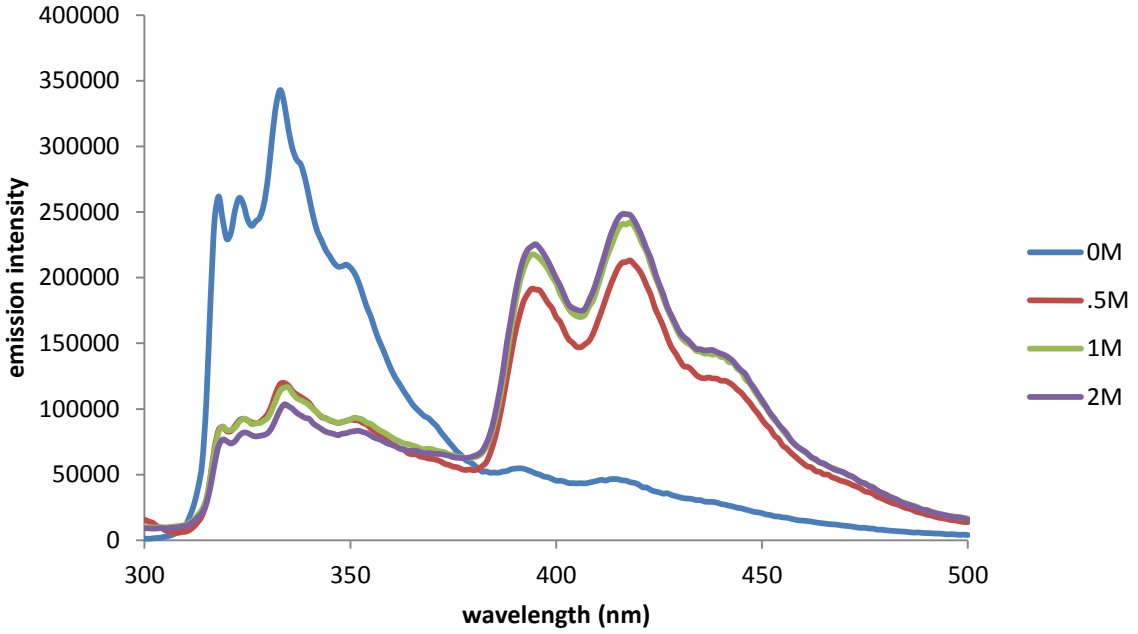

Figure 4.15: Emission scan in a range equal to 300-500 nm at fixed excitation λ_{ex} = 290 nm for ACE-AMMA-PAA sample in aqueous solution at pH 11 and varying $CaCl_2$ concentration

There is a general increase in the I_A/I_D ratio with the increasing concentrations of the calcium cations as can be seen on Figure 4.16 and irrespective of the pH value. This is consistent with a conformation of a collapsed PAA polymer chains. A slight increase in the ratio was observed for the sample at pH 3 between 0.5 M and 1 M of $CaC1_2$ salt concentration. The I_{420}/I_{340} ratio then markedly reached a maximum of ~3. This suggests that the anthryl label gets close to the naphthyl label when Ca^{2+} ions are added. At pH 6, there is a slight increase in the ratio at the initial low concentrations of $CaCl_2$ which then dramatically rose to ~2.2 when the concentration of the $CaC1_2$ is increased to 1. With increasing the pH level to 11 it is very noticeable from Figure 4.16 that a significant increase in the ratio at the low concentration levels of the $CaC1_2$ salt but no significant change in the ratio value at higher amount of salt. The figure also shows that the I_A/I_D ratio at pH 11 (and for all the salt concentrations) is slightly greater than the I_A/I_D ratio at pH 6, however in the absence of the salt the ratio at pH 11 is less than that of pH 6. This gives an indication that the polymer underwent a conformational transition from an expanded

polyelectrolyte chain to a collapsed form at pH 6 and pH 11. This transition is due to the electrostatic bonding of the COO^- groups with the Ca^{2+} ions leading to chain aggregation.

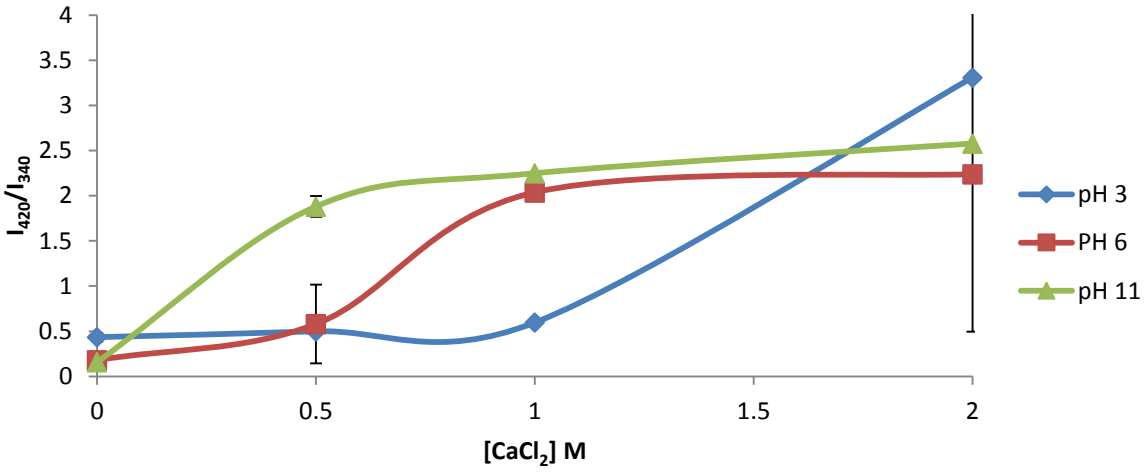

Figure 4.16: Fluorescence emission intensity ratio, I_A/I_D of 10^{-2} wt % ACE-AMMA-labelled PAA as a function of [$CaCl_2$] at different pH values (λ_{ex} = 290 nm)

4.1.5 Fluorescence excited state lifetimes of singly and doubly labelled PAA in the presence of $CaC1_2$ as a function of pH

A triple exponential (Equation 3.5) achieved the best fit to the data obtained for an ACE labelled PAA sample as a function of [$CaC1_2$] at various pH values. The fit gave χ^2values close to unity and a random distribution of residuals as shown on Figure 4.17. The average lifetime was subsequently calculated from equation 3.3, and the resultant data is plotted as a function of calcium chloride concentration as shown on Figure 4.18.

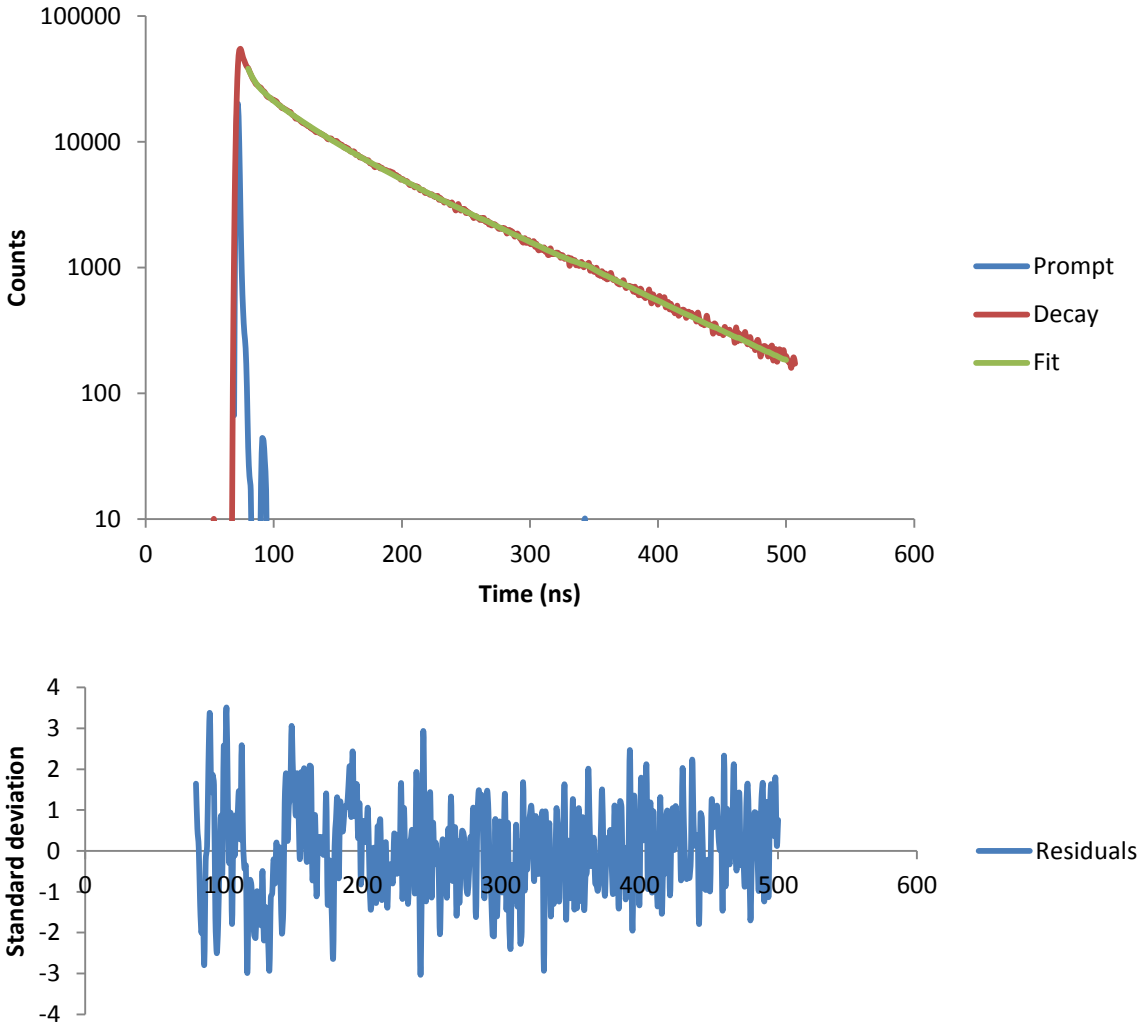

Figure 4.17: A fluorescence decay with corresponding mathematical fit (shown in green) and a plot of the resulting residuals for ACE-PAA in aqueous solution of pH3 with 0.5 M of $CaCl_2$

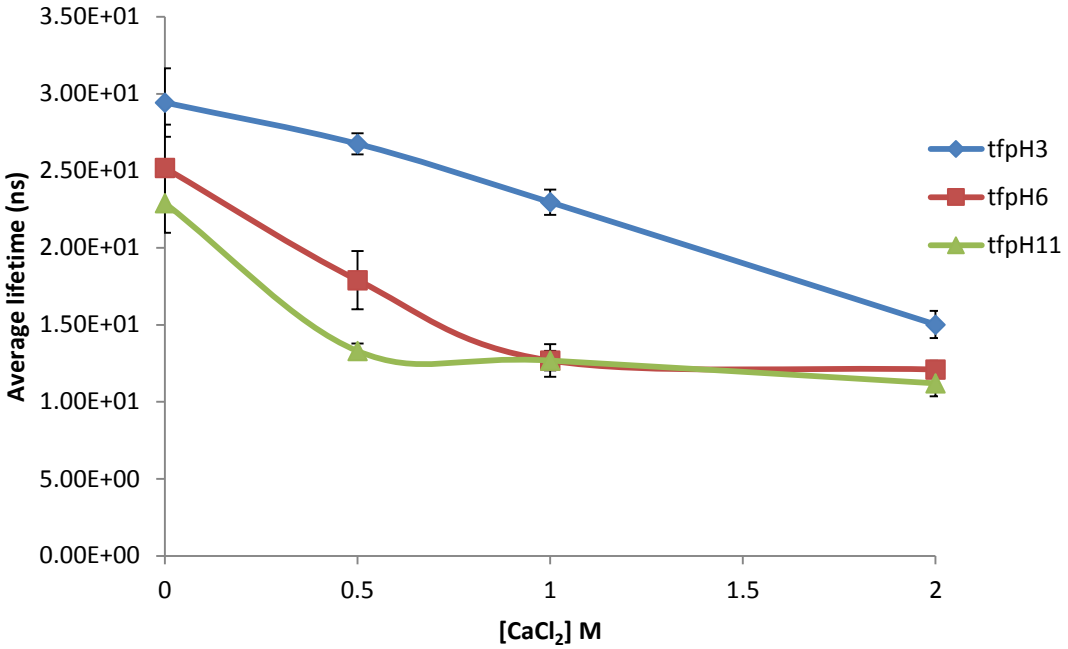

Figure 4.18: A plot of the average lifetime values obtained for ACE-PAA in aqueous solution at three different pH values with increasing $CaCl_2$ concentration when excited at 290 nm and observed at 340 nm.

The average fluorescence lifetime of ACE-PAA at high concentrations of calcium chloride were lower than in the absence of any salt. However, the relative lifetime values as pH increased followed the same pattern of decreasing as the pH level increased. A general decrease in lifetime is apparent with increasing Ca^{2+} concentration, indicating a quenching of the ACE donor by the increased concentration of $CaCl_2$ slat.

At 1 M and 2 M [$CaC1_2$], and a pH of 6, the lifetime values are similar to that of the PAA coil as seen at pH 11. This is a clear indication that addition of calcium chloride to the PAA-ACE solution increased the quenching of the ACE label, thus decreasing the average lifetime as a collapsed conformation is adopted by the PAA chains (possibly due to the binding interaction between Ca^{2+} ions and COO^- ions which in turn led to quenching of the label).

Equation 3.5, for triple exponential functions, is used to model the fluorescence decays of ACE-AMMA PAA samples and it was found to best fit the data statistically. The statistical χ^2 values are close to unity and a good small standard deviation of the residuals values as seen on Figure 4.19. The decrease in the lifetime of the ACE label in PAA-ACE-

AMMA in the presence of $CaCl_2$ is significant compared to that in the PAA-ACE system. The curves at pH 3, pH 6 and pH 11 (Figure 4.20) for the PAA-ACE-AMMA system displays the opposite pattern to that obtained from the I_A/I_D ratio against [$CaCl_2$] (Figure 4.16). This pattern is consistent with an increased quenching of the ACE label as the collapsed conformation is adopted. The shape of the curve at pH 11 could be attributed to the fact that a conformational transition occurred for the polyelectrolyte chain when the concentration of the added salt increased from 0 M to 2 M. This transition goes from a relatively expanded chain conformation at the absence of salt, with a longer average lifetime value recorded (~21 ns), to a partially collapsed form at high $CaCl_2$ concentration level of 2 M. The average lifetime value is quenched to ~ 8.7 ns, perhaps this is due to the collapsing of the polymer chains caused by the high concentration of the Ca2+ ions. This collapse of the polymer chains then led to the quenching of the ACE labels and also to an increased energy transfer to acceptor AMMA. The curve at pH 6 shows a similar behaviour to that of the curve at pH 11, although with a slight higher average lifetime values.

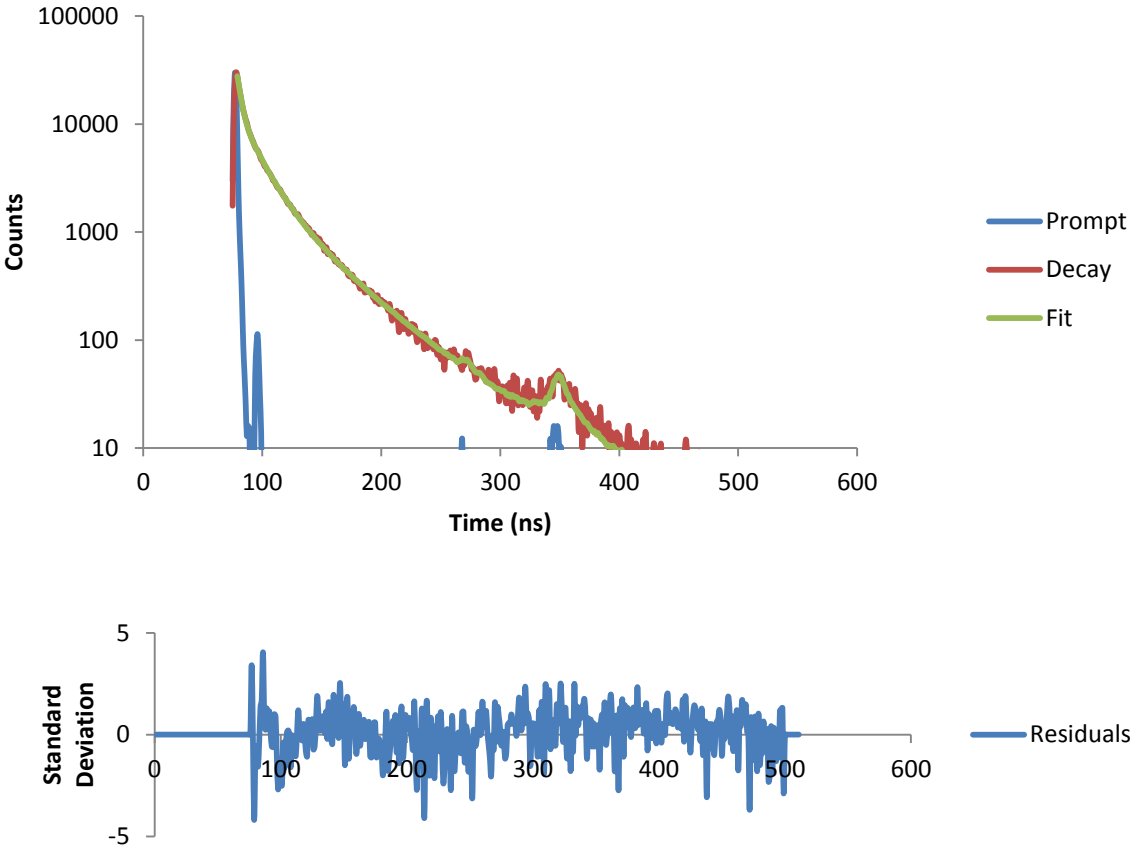

Figure 4.19: A fluorescence decay with corresponding mathematical fit (shown in green) and a plot of the resulting residuals for ACE-AMMA-PAA in aqueous solution of pH 11 with 2 M of $CaCl_2$

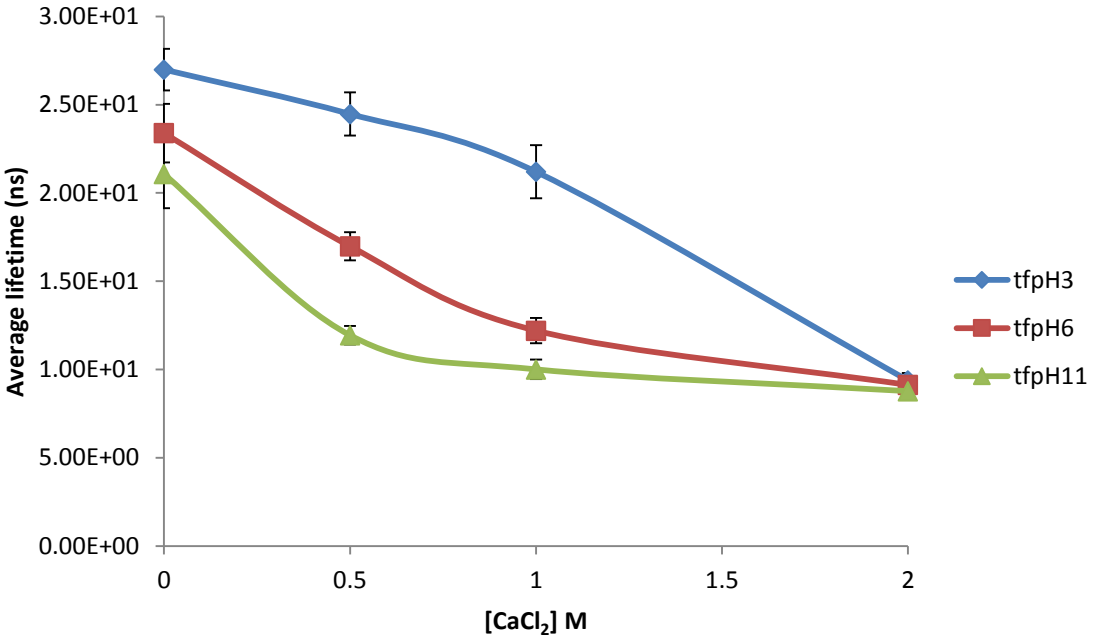

Figure 4.20: A plot of the average lifetime values obtained for ACE-AMMA-PAA in aqueous solution at three different pH values with increasing [$CaCl_2$] when excited at 290 nm and observed at 340 nm.

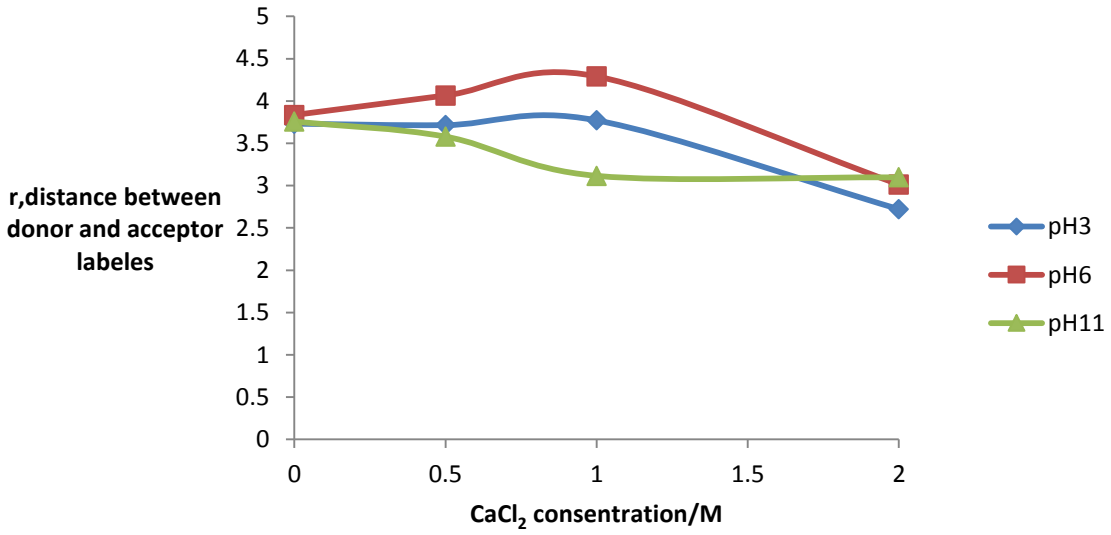

Figure 4.21: plot of the value r, the distance between ACE (donor) and AMMA (acceptor) labels, as calculated by equation 3.7 for single and double -PAA across a range of pH values and $CaCl_2$ concentrations.

The average separation distance, r, between D and A was calculated using equation 3.7 and 3.8 respectively, this data is shown in figure 4.21. At pH3 and 6, there is no important change in the distance between the donor and acceptor at low salt concentration (0.5 M and 1 M), while at high concentration of salt there is a decrease in the distance between labels; which is consistent with a collapsing of the polymer chain. The distance, at pH 11 however shows a decrease between 1 M and 2 M concentrations, suggesting a collapse in the chain as a consequence of the interaction between the carboxylate anion and Ca^{2+} cation.

4.1.6 Fluorescence Time-Resolved Anisotropy Measurements (TRAMS) of ACE-PAA in the presence of $CaCl_2$ as a function of pH

TRAMS were conducted on an ACE labelled-PAA polymer sample with increasing $CaCl_2$ concentration at various pH values in order to study the polymer dynamics. Figure 4.22 compares the fluorescence anisotropy decays of ACE-labelled-PAA polymer for 0 M [$CaCl_2$] (salt free) and 1 M [$CaCl_2$] in water solution with pH 3 (acidic conditions). The figure shows that the anisotropy decays are slightly different. In the presence of the $CaCl_2$ salt case, the anisotropy decays quite slowly to zero in comparison to the free of salt case. This photophysical character is indicative of a more collapsed polymer conformation is adopted by the PAA polymer when the salt is added and hence the longer anisotropy decay.

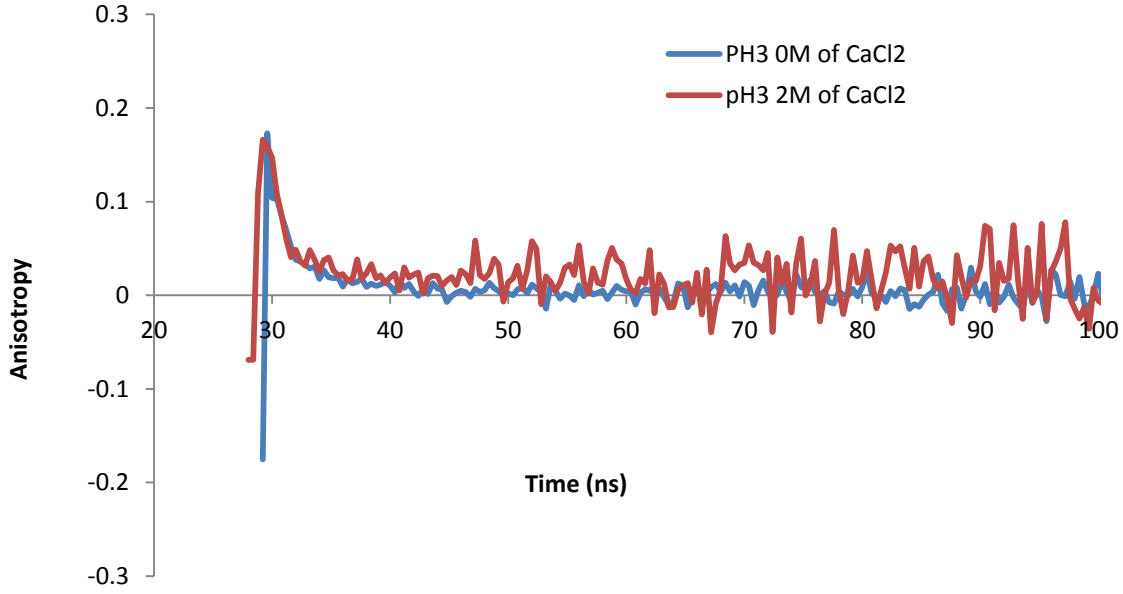

Figure 4.22: Fluorescence time resolved anisotropy data of aqueous ACE-labelled PAA solution (10-2

wt%) in the absence of calcium chloride (blue line) and at the calcium chloride concentration of 2 M at pH 3 (λex = 295 nm and λem = 340 nm).

Figure 4.23 shows that the anisotropy quickly dropped to zero in the absence of $CaCl_2$ for pH11 (basic conditions) levels. The presence of the salt gradually lowered the anisotropy decays to zero. This result is expected and it can be attributed to the interaction that occurred between the Ca^{2+} ions and the two COO^- groups of the PAA polymer [66] . The collapse of the polyelectrolyte chains that resulted from this interaction has led to the insulation of the COO^- group and also reduced the ACE-PAA chains motion and hence the observed anisotropy slow decay. A static and dynamic light scattering study [67]is conducted to interrogate the collapse of the PAA chain in calcium chloride solutions seems to agree with the observed slow decay found in this research study. It is also reported that the bidentate complex formation causes intra-molecular bridging and as result lead to more coil dimensions of the PAA polymer chains

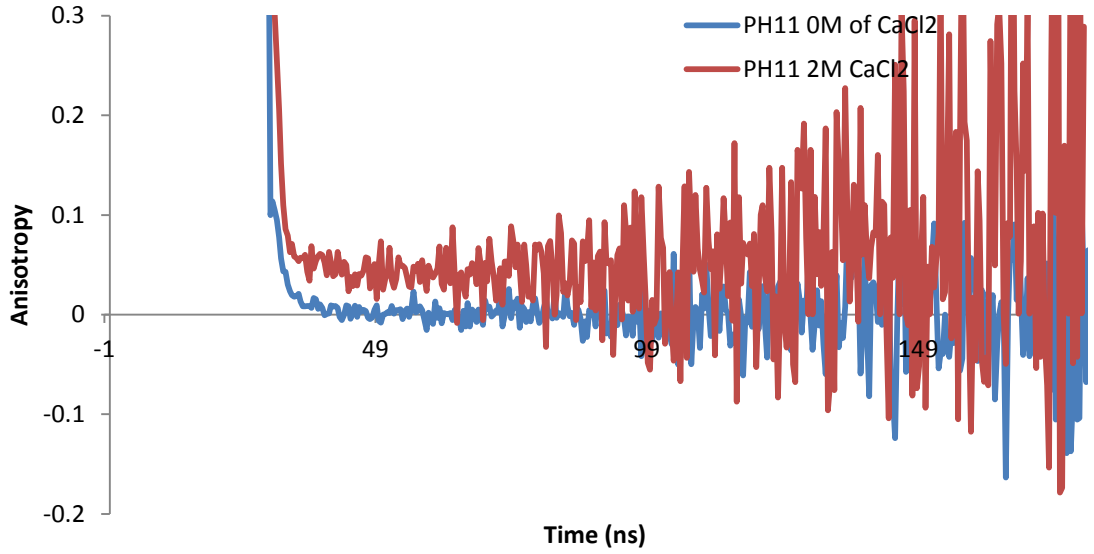

Figure 4.23: Fluorescence time resolved anisotropy data of aqueous ACE-labelled PAA solution 10^{-2} wt%) in the absence of calcium chloride (blue line) and at the calcium chloride concentration of 2 M at pH 11 (λ_{ex} = 295 nm and λ_{em} = 340 nm).

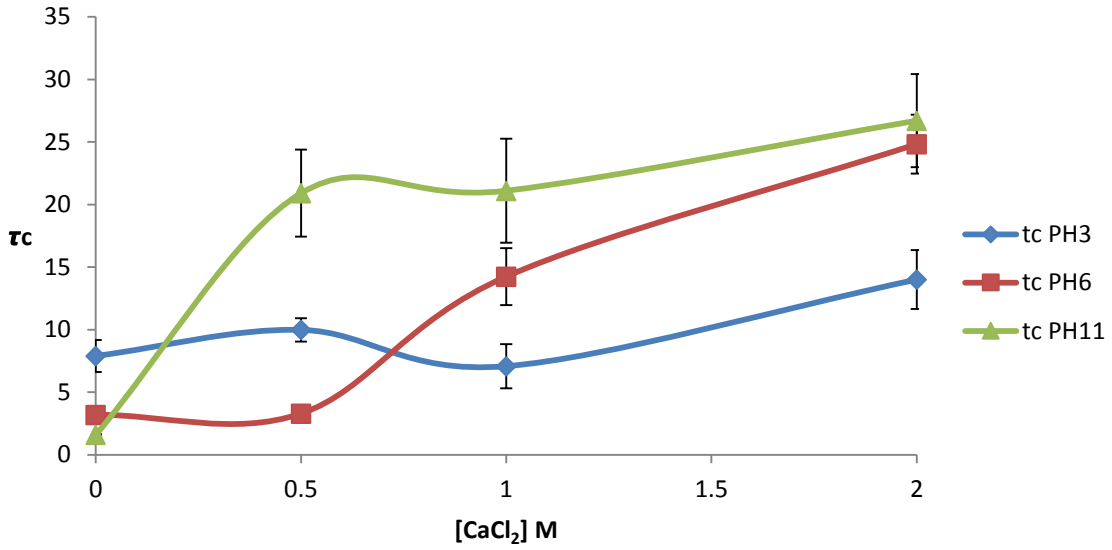

Figure 4.24: A plot of correlation time against $CaCl_2$ concentration for three ACE labelled PAA samples in aqueous solution at three different pH values when excited at 290 nm and observed at 340 nm.

The best fit to the ACE-PAA TRAMS data and irrespective of solution condition was achieved using a single exponential model. The statistical residuals of the fitted data were randomly distributed around zero and with χ_2 values close to unity which provides a good statistical confidence in the quality of the fitted data.

The resultant correlation time data are plotted as a function of $CaCl_2$ concentration at several pH values in figure 4.24. The figure shows a general increasing trend in τ_c values, for all pH levels, as the amount of the salt is increased. This suggested that the mobility of the ACE labels is reduced with the increase of the salt concentration. This is consistent with the findings previously discussed on the energy transfer as the PAA polymer collapse occurred. The increase in τ_c values is more markedly increased at higher pH values which suggested a more efficient complexation between the Ca^{2+} anions and COO- groups.

4.1.7 Fluorescence steady state spectra of ACE-AMMA labelled PAA in the presence of NaBr as a function of pH

Steady state emission spectra (Figure 4.25) of ACE-AMMA-PAA sample across a range of NaBr concentrations at pH 3 level shows that the observed emission intensity level at 340 nm of the naphthyl label decreased with the increase of the NaBr salt concentration.

On the other hand, the emission from the anthryl label centred at 410 nm is slightly enhanced and increased with the increase of the NaBr concentration after an initial drop from the free of salt intensity level. This observation gives an indication of the possibility of energy transfer from the naphthyl label to the anthryl label under these conditions. A relatively high degree of energy transfer was apparent even in the absence of NaBr case which is consistent with a relatively collapsed polymer conformation at acidic condition.

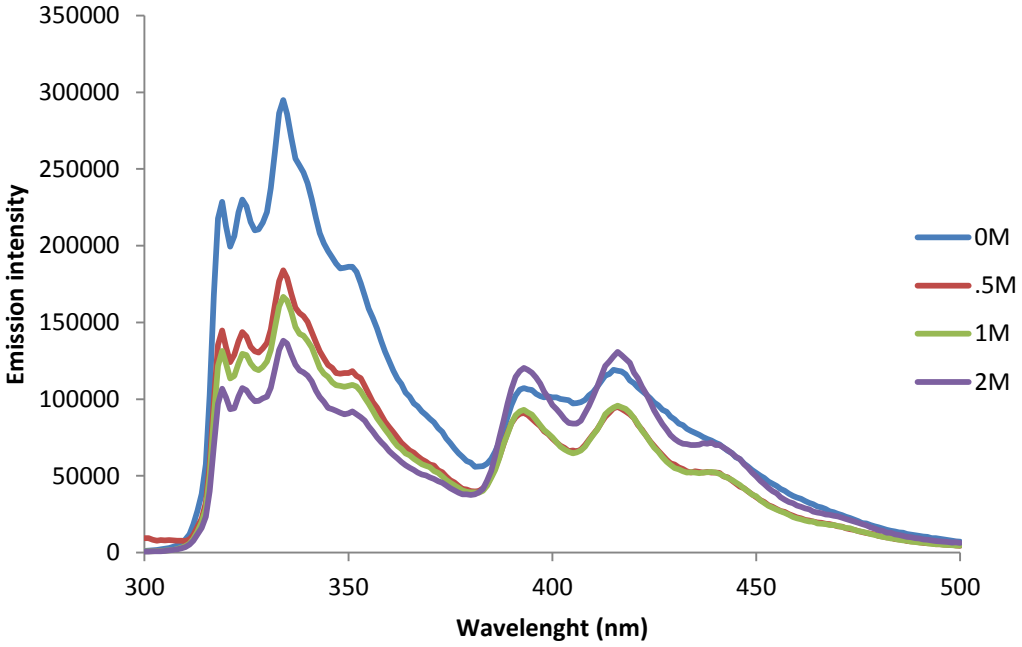

Figure 4.25: Emission scan in a range equal to 300-500 nm at fixed excitation λ_{ex} = 290 nm for ACE-AMMA-PAA sample in aqueous solution at pH 3 and varying NaBr concentration

At pH 11 (basic conditions), there is a significant decrease in the emission intensity of the ACE label accompanied by a slight drop in the AMMA emission as the NaBr concentration increased (Figure 4.26). When the polymer samples at pH 3 and pH 11 are excited with 370 nm, the AMMA label is observed to be stimulated directly as shown on Figure 4.27 and Figure 4.28. The emission intensity from the anthryl moiety is slightly decreased with the increase of the [NaBr] in a manner similar to that of the ACE label. This provides further evidence that some species in the solution, possibly the Na^+ cations, acted as a fluorescence quencher in the acidic and basic conditions.

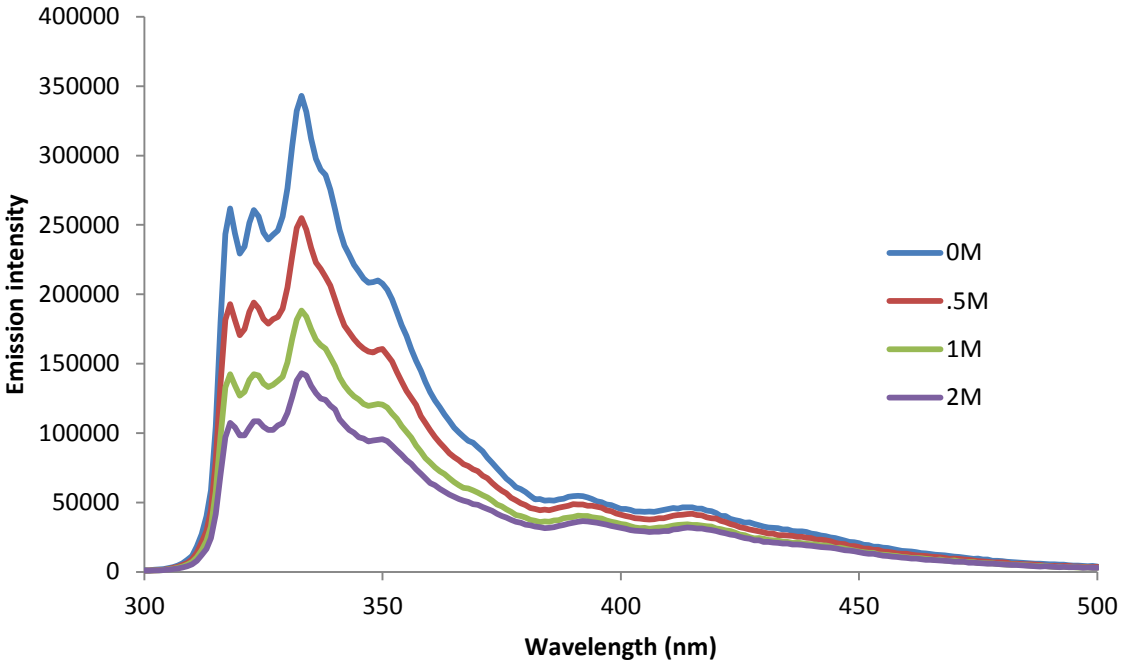

Figure 4.26: Emission scan in a range equal to 300-500 nm at fixed excitation λ_{ex} = 290 nm for ACE-AMMA-PAA sample in aqueous solution at pH 11 and varying NaBr concentration.

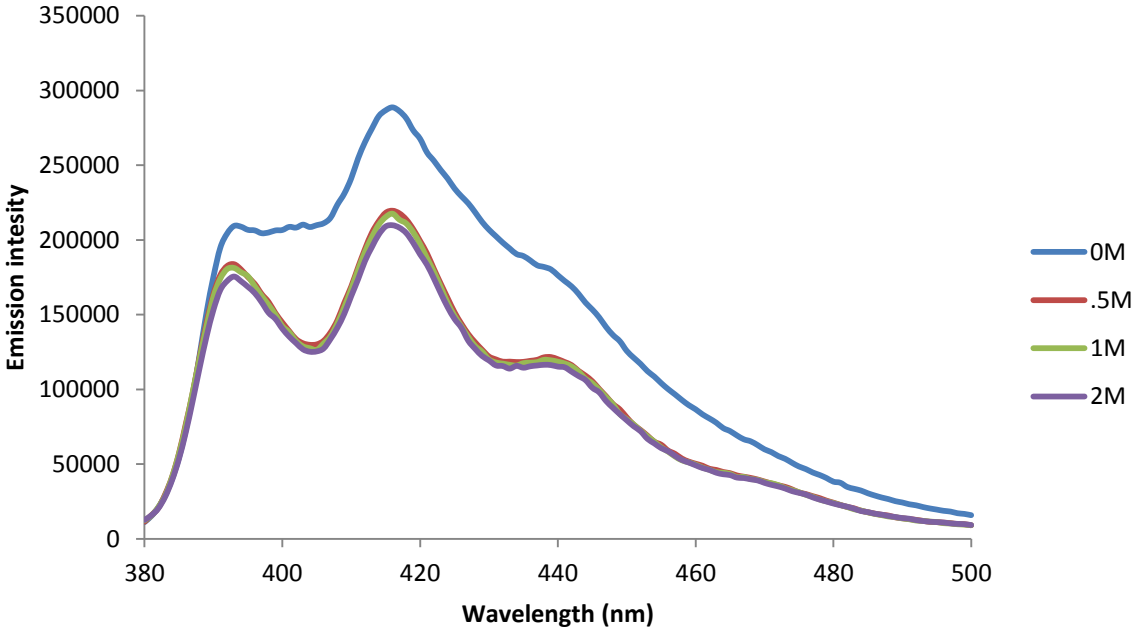

Figure 4.27: Example steady state emission spectra for an ACE-AMMA labelled PAA sample as a function of NaBr concentration when excited at 370 nm at pH 3.

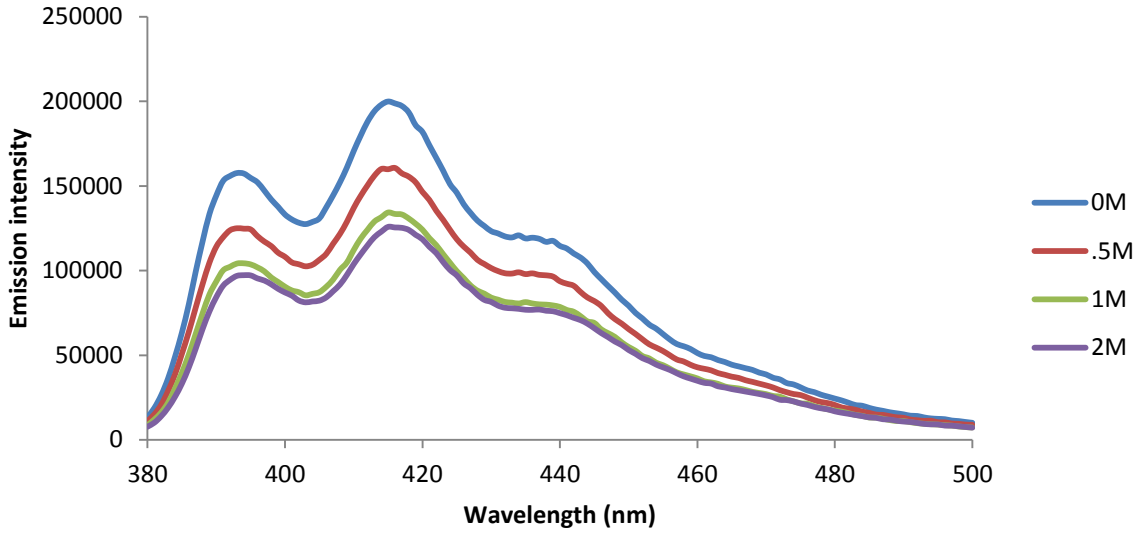

Figure 4.28: Example steady state emission spectra for an ACE-AMMA labelled PAA sample as a function of NaBr concentration when excited at 370 nm at pH 11.

Figure 4.29 and Figure 4.30 show the energy transfer efficiency as a function of the sodium bromide concentration at pH 3 and pH 11 respectively. The fluorescence intensity ratio increases as the NaBr concentration increased. This suggests that the relatively coiled polymer became even tighter with the NaBr concentration increase (Figure 4.29). It is worthy to note that this behaviour of the polymer is opposite to that of the NaCl case discussed previously and in particular this opposite behaviour is caused by the Bromine anion (Br^{-1}) of the NaBr salt. In basic conditions at pH 11 (Figure 4.30) the fluorescence intensity ratio increases with the NaBr concentration increase, however the trend increase is much less than that of the acidic condition case (pH 3). This suggests that the polymer chains have collapsed when the Na^{+} ions concentration is increased, this collapse is possibly due to the neutralization of the anionic carboxylate groups of the Poly (acrylic acid) expanded chains by the Na^{+} cations.

At 2 M NaBr concentration and pH 11 level several of the negatively charged carboxylate groups of the PAA are neutralised by the sodium cations Na^{+}. At this level of concentration the intensity ratio is at a maximum of ~0.22 which means a ~22% energy transfer efficiency in the relatively coiled form of the PAA chains.

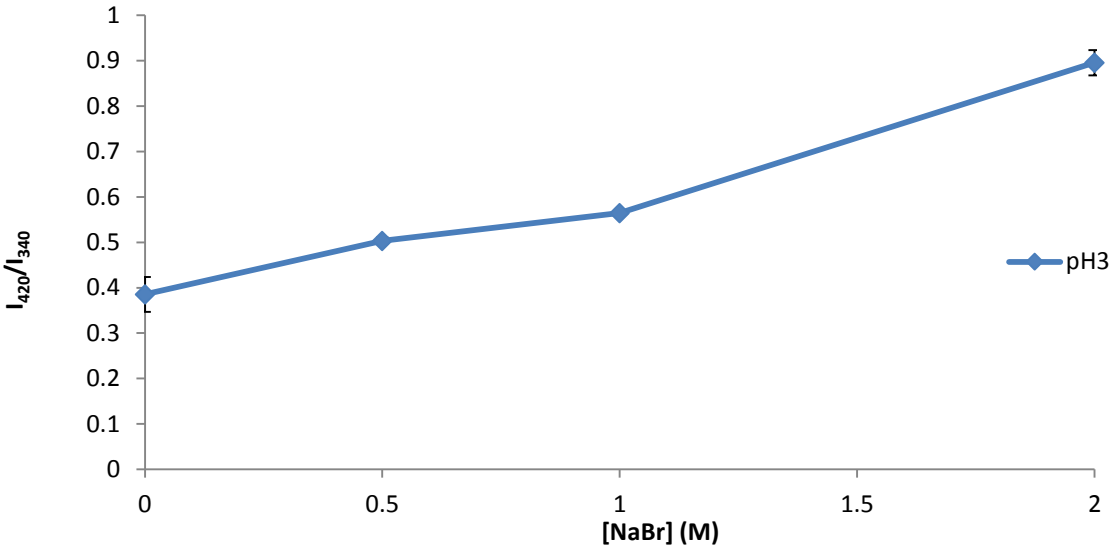

Figure 4.29: Fluorescence emission intensity ratio, IA/ID of 10^{-2} wt % ACE-AMMA-labelled PAA as a function of NaBr concentration at pH 3. (λ_{ex} = 290 nm)

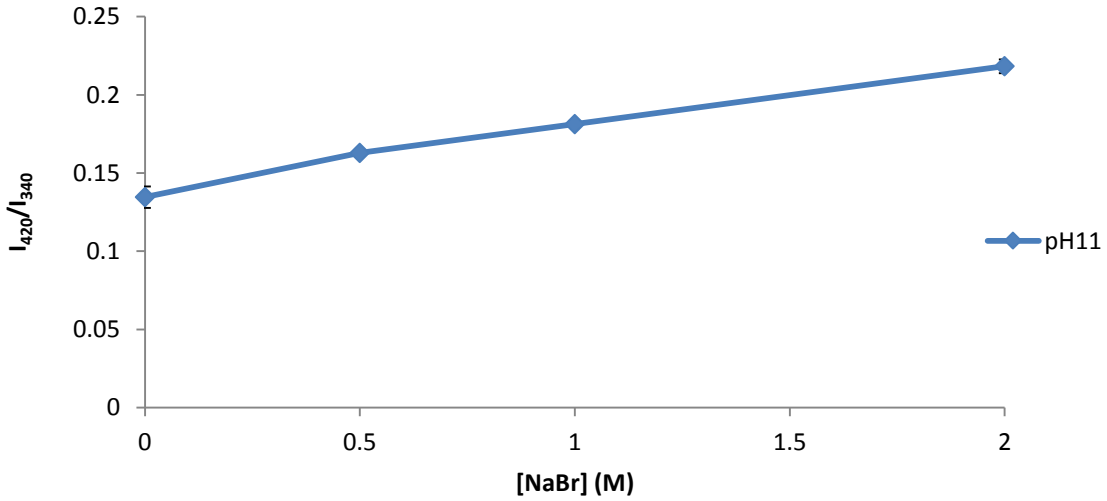

Figure 4.30: Fluorescence emission intensity ratio, IA/ID of 10^{-2} wt % ACE-AMMA-labelled PAA as a function of NaBr concentration at pH 11. (λ_{ex} = 290 nm)

4.1.8 Fluorescence excited state lifetimes of singly and doubly labelled PAA in the presence of NaBr as a function of pH

The triple exponential function (Equation 3.5) was used to model the lifetime values of ACE-PAA in the presence of sodium bromide. It was found to fit best the data sample with χ_2 statistical values close to unity and a small standard deviation in addition to small residual values (Figure 4.32). In the following the average lifetime values are used for the purpose of comparison.

Average ACE lifetimes for the ACE-PAA polymer chains are plotted against [NaBr] as shown on Figure 4.31 The average lifetime of the ACE-PAA fluorescence at low concentrations of NaBr are higher than the average lifetimes at high NaBr concentrations. The graph shows a trend of decreasing lifetime as the concentration of the NaBr increased. The relative lifetime values of the ACE-PAA samples showed a general decrease as the pH values of the solution changed from low to high values. It is similar to the pattern followed with the increase of the [NaBr]: a general decrease in lifetime is apparent with the increase of the Na^+ cations concentration. It was observed that the ACE donor was quenched by energy transfer to the quencher, which may to be Na^+ since the cations have been found to act as a quencher [68].At pH 6, the average lifetime decrease in a manner similar to that observed at pH 11 for all NaBr concentrations. This indicates that the system was coiling at pH 6 and 11, and the ACE fluorescence was being quenched possibly by the binding interactions between the Na^+ ions and COO^- ions.

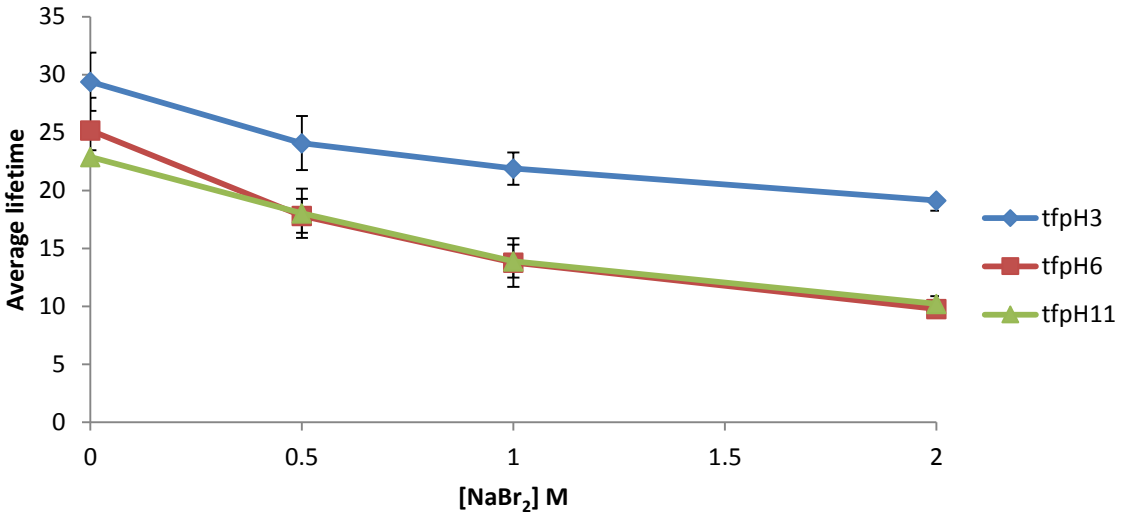

Figure 4.31: A plot of the average lifetime values obtained for ACE-PAA in aqueous solution at three different pH values with increasing [NaBr] when excited at 290 nm and observed at 340 nm.

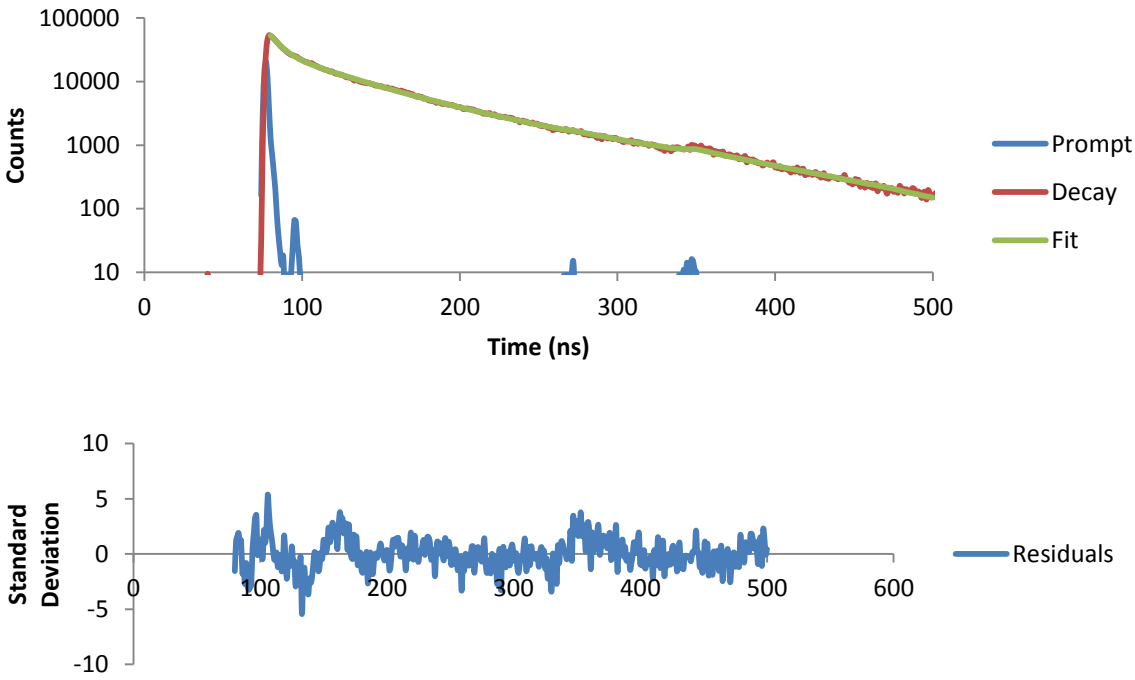

Figure 4.32: A fluorescence decay with corresponding mathematical fit (green fit) and a plot of the resulting residuals for ACE-PAA in aqueous solution of pH 3 with 0.5M of NaBr.

Triple exponential function (Equation 3.5) is used to model the fluorescence decays of the doubly labelled PAA samples. Again it was found to be the best fit. The statistical χ_2 values are found to be close to unity with small standard deviation along with small residual deviations from zero as shown on Figure 4.33. The modelled average lifetime values are used for the purpose of comparison in the following paragraphs.

The lifetime of the ACE label in PAA-ACE-AMMA in the presence of NaBr showed a general decrease at all pH values (Figure 4.34). The lifetime values observed at pH 3 are higher than those recorded at any other pH levels. The average lifetime subsequently decreased with increasing [NaBr] which is consistent with an enhanced energy transfer in the collapsed PAA chains conformation, and in agreement with the steady state experiment.

However, the curve at pH 11 exhibited an opposite pattern of PAA chains behaviour to that observed from the I_A/I_D ratio against NaBr concentration as seen on Figure 4.30. In this sample, the plot pattern could be attributed to the fact that a conformational transition occurred for the polymer chain when the concentration of added sodium bromide was increased. This led to a transition from a partially expanded chain at low NaBr concentration (long $<\tau f>$ is observed), to a partially collapsed form at high concentration of NaBr giving an average lifetime of ~ 9 ns (quenched). This behaviour is perhaps due to the collapse of the polymer that is caused by the high Na^+ ions concentration in addition to an energy transfer from the donor label to the acceptor label. This quenching was found to be more prominent in the case of NaBr salt than the NaCl salt. The curve at pH 6 exhibited a similar behaviour pattern to that of the pH 11 curve.

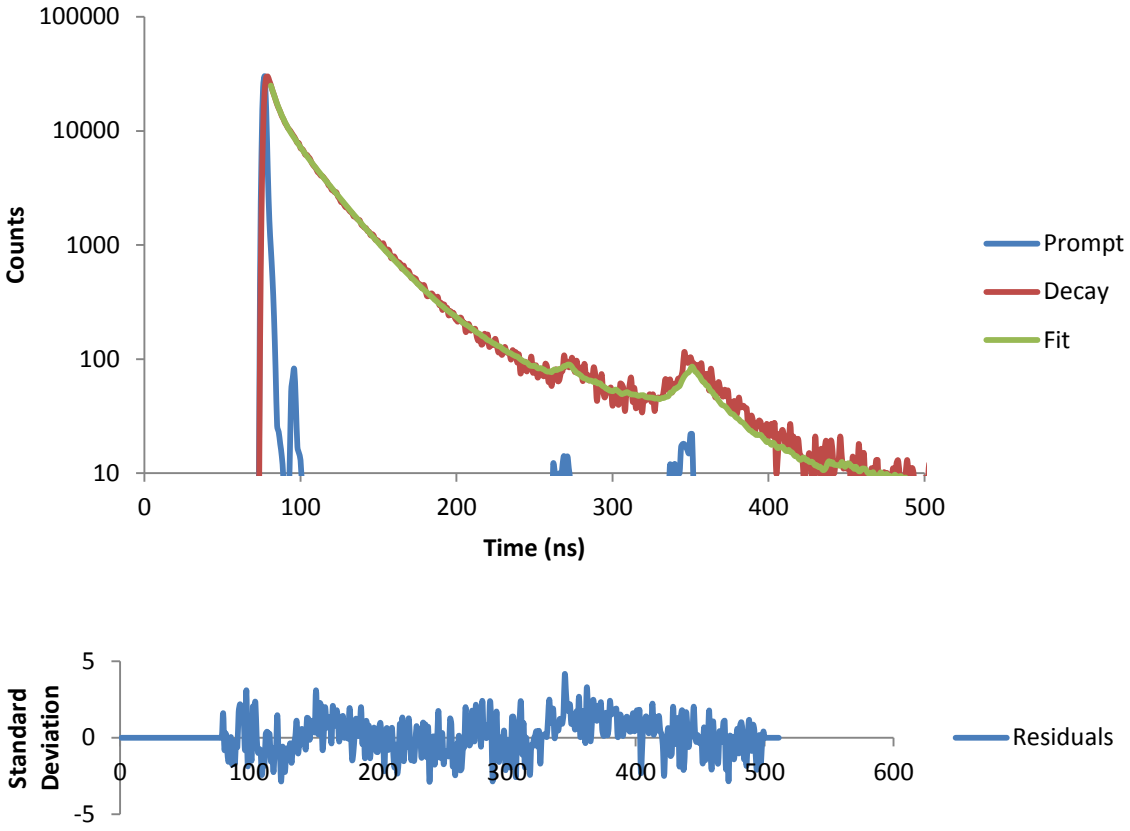

Figure 4.33: A fluorescence decay with corresponding mathematical fit (green) and a plot of the resulting residuals for ACE- AMMA-PAA in aqueous solution of pH 11 with 2M of NaBr.

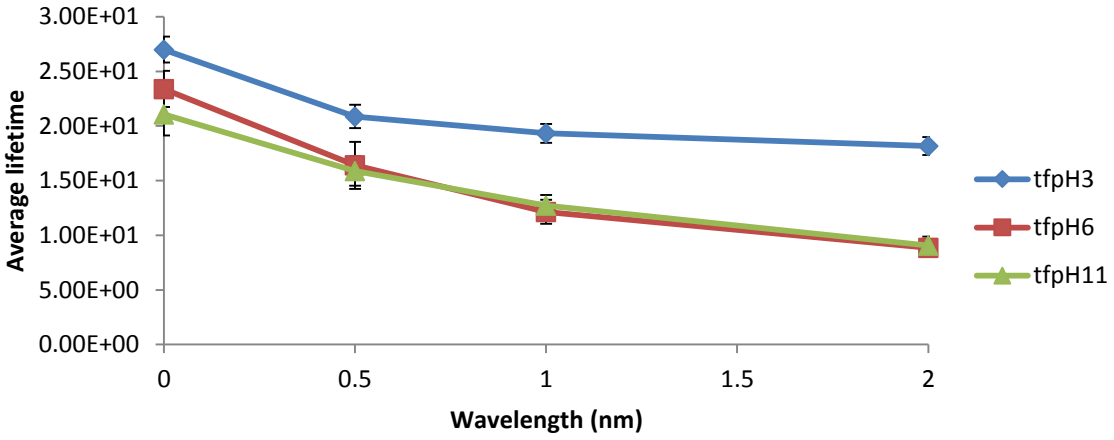

Figure 4.34: A plot of the average lifetime values obtained for ACE- AMMA-PAA in aqueous solution at three different pH values with increasing NaCl concentration when excited at 290 nm and observed at 340 nm.

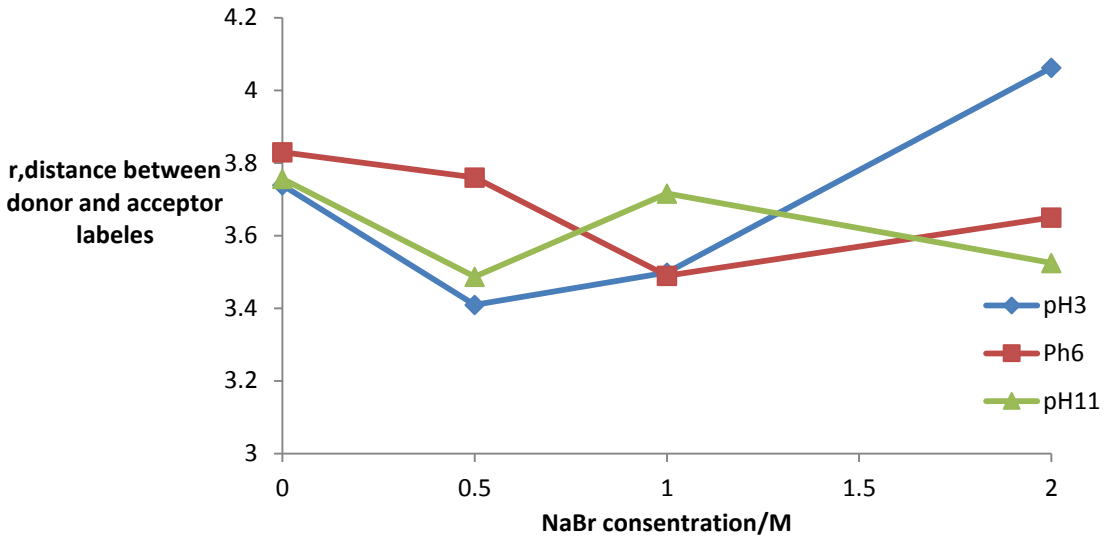

Figure 4.35: A plot of the value r, the distance between ACE (donor) and AMMA (acceptor) labels, as calculated by equation 3.7 for single and double -PAA across a range of pH values and NaBr concentrations.

The r value, at pH 3 and 6 show a decrease between 0.5 M and I M concentrations, indicating a collapse in the system (figure 4.35). With error taken in to account the distance then substantially increase upon large addition of NaBr.

The distance between the donor and the acceptor labels at pH 11 shows a noticeable increase with rising NaBr concentrations up to I M after the initial decrease and then a decrease in the inter label distance can be seen as the concentration promote to 2 M. Clearly collapse of the chain has took place under these conditions as the carboxylate anion charge is screen by the Na^+ cation indicating collapse as a result of increased the hydrophobic attraction.

4.1.9 Fluorescence time-resolved anisotropy measurements (TRAMS) of ACE-PAA in the presence of NaBr as a function of pH

Interactions between polyelectrolyte and salt content have been shown to be accompanied with changes in the mobility of the polymer chains. Techniques like TRAMS, which monitor polymer dynamics, should be useful for investigating the dynamic behaviour of the PAA polymer chains in the presence of NaBr.

Figure 4.36 compares the fluorescence anisotropy decays of the ACE-PAA polymer in aqueous solution in the absence and presence of sodium bromide at pH 3 (acidic condition). The figure shows the anisotropy decays slightly slower in the presence of NaBr in comparison to the decay of the anisotropy in the free of salt conditions at the same pH 3 level. This photophysical behaviour give evidence of the PAA polymer chains collapse in the presence of the NaBr salt at pH 3 level which leads to lower mobility and therefore the observed long anisotropy decay.

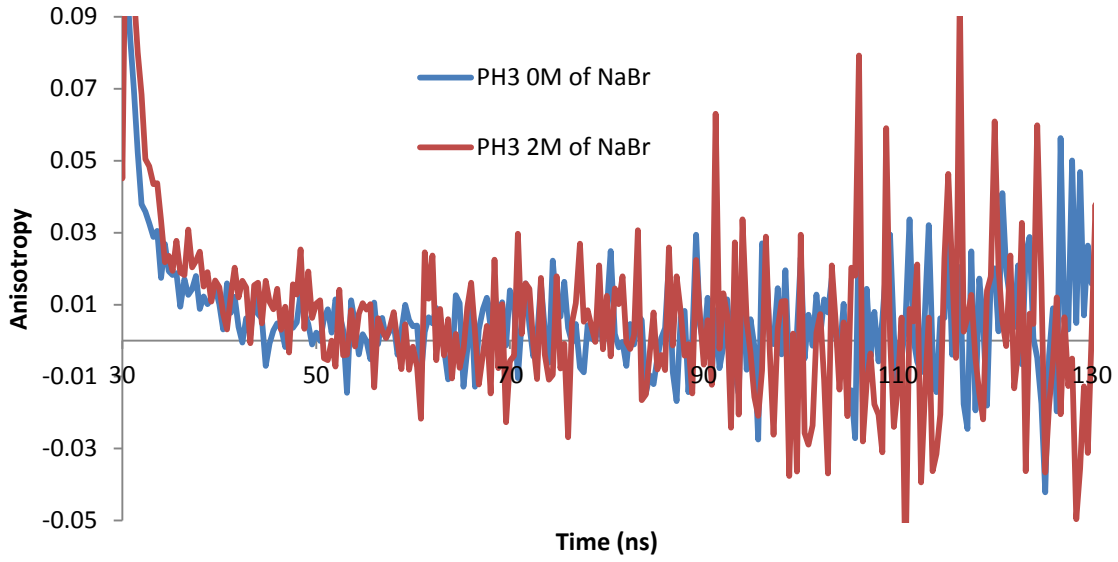

Figure 4.36: Fluorescence time resolved anisotropy data of aqueous ACE-labelled PAA solution (10^{-2} wt%) in the absence of sodium bromide (blue line) and at the sodium bromide concentration of 2 M at pH 3(λ_{ex} = 295 nm and λ_{em} = 340 nm).

In addition to the pH 3 acidic conditions cases, the anisotropy decay of the ACE-PAA at pH 6 has also been investigated. Again, the results of the cases of the free of salt and 2 M NaBr concentrations are plotted and are shown on Figure 4.37. From the figure it can be observed that the anisotropy decays rapidly to zero in the absence of NaBr in comparison to the 2M NaBr concentration case. In the presence of the salt the decay is much slower. This could be attributed to the possible interaction occurring between the Na^+ cations and the COO^- groups of the PAA polymer. This interaction led to the collapse of the polyelectrolyte chain and hence the reduced ACE-PAA polymer chain motion and therefore the slow anisotropy decay.

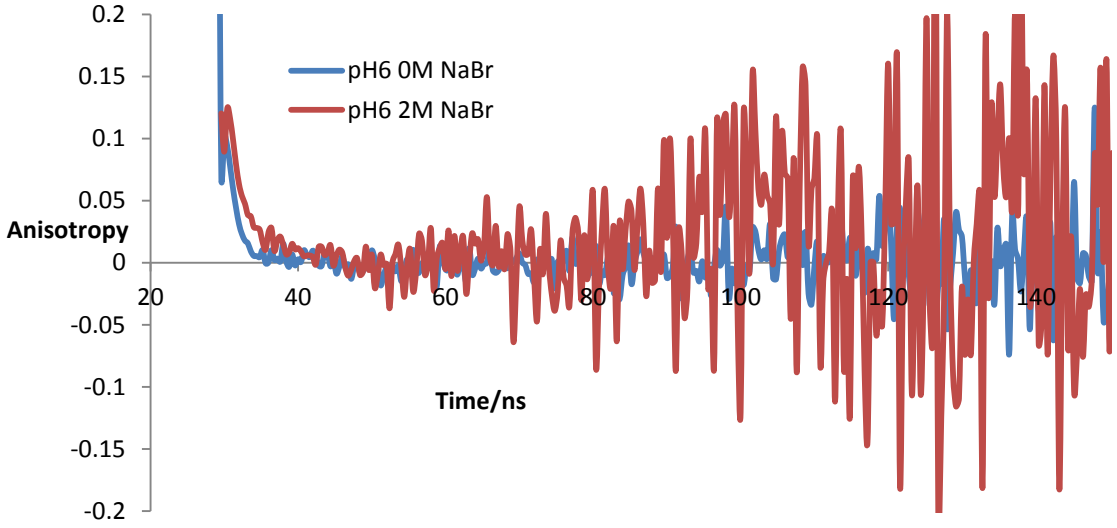

Figure 4.37: Fluorescence time resolved anisotropy data of aqueous ACE-labelled PAA solution (10^{-2} wt%) in the absence of sodium bromide (blue line) and at the sodium bromide concentration of 2 M at pH 6(λ_{ex} = 295 nm and λ_{em} = 340 nm).

The correlation time τ_c (in nanoseconds), derived from mathematical analysis, of the anisotropy decays of the ACE-PAA was best fit with a single exponential function. Figure 4.38 presents three curves (for pH 3, pH6 and pH 11) of the correlation time against the concentration of NaBr. As seen on the figure there is a slight increase in the correlation time upon the initial addition of the NaBr salt at pH 6 and pH 11 but no further changes are observed in the τ_c as the salt concentration increased. This indicates that the polymer underwent a conformational collapse upon the initial addition of a small amount of the NaBr salt in pH6 and 11 level..

On the other hand, a noticeable increase was recorded at pH 3 at higher NaBr concentration, in particular at 1 and 2 M concentrations. Overall, the increment in correlation time values over the entire concentration range at pH 3 is higher than those at pH 6 and pH 11, and also in agreement with the energy transfer (ET) experiment.

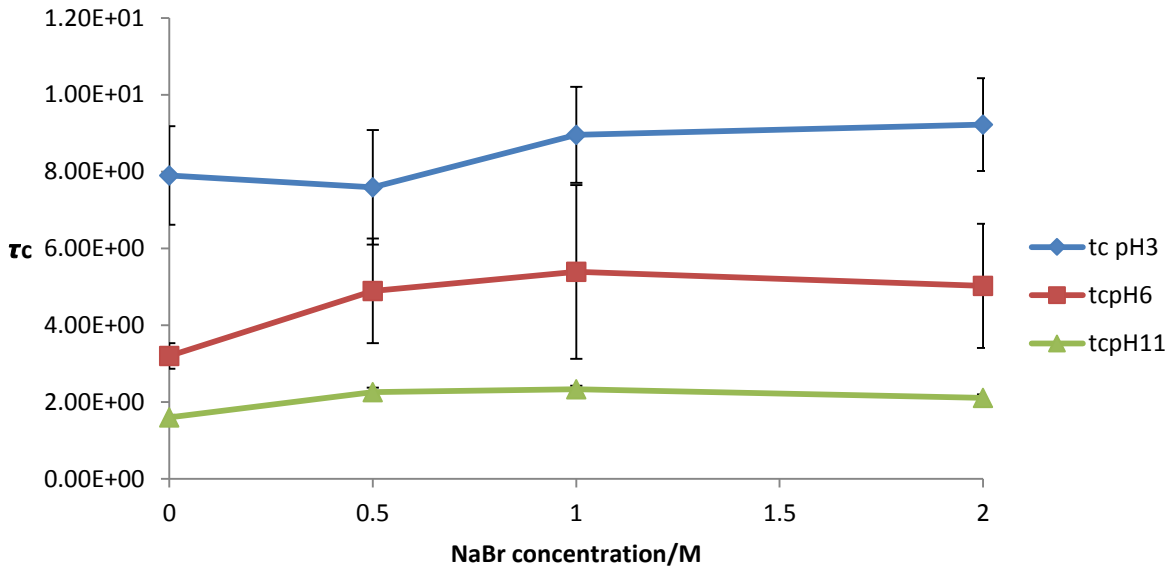

Figure 4.38: A plot of correlation time against NaBr concentration for ACE labelled PAA samples in aqueous solution at three different pH values when excited at 290 nm and observed at 340 nm.

4.1.10 Fluorescence steady state spectra of ACE-AMMA labelled PAA in the presence of $CaBr_2$ as a function of pH

Steady state emission spectra of an ACE-AMMA labelled Poly(acrylic acid) PAA samples were measured for a range of $CaBr_2$ concentrations and at a range of pH levels. The results of these samples measurements are presented in the following paragraphs. At pH 3 level (acidic conditions aqueous solution), the measured spectra (Figure 4.39) shows that the emission intensity of the naphthyl label (ACE) as observed at 340 nm was greatly decreased with the increase of the calcium bromide concentration [$CaBr_2$]. The figure also shows the relative emission from the anthryl label (AMMA) centred at 410 nm is also decreased with the increase of the $CaBr_2$ concentration. This pattern of emission spectra implies the presence of a quencher either acting selectively on the donor (ACE) or the entire system. The emission intensity pattern indicates a collapse of the PAA polymer chains that increases with the increase of the $CaBr_2$ concentration. Energy transfer between the two labels is very likely to have occurred as a result of the close proximity of the two labels when the polymer chains collapsed at high salt concentration.

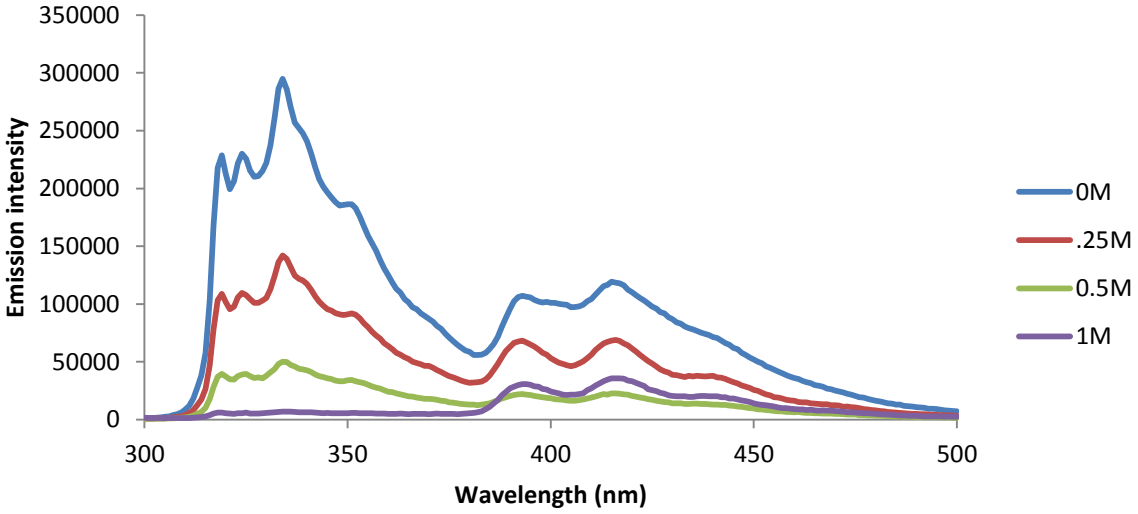

Figure 4.39: Emission scan in a range equal to 300-500 nm at fixed excitation λ_{ex} = 290 nm for ACE-AMMA-PAA sample in aqueous solution at pH 3 and varying $CaBr_2$ concentration

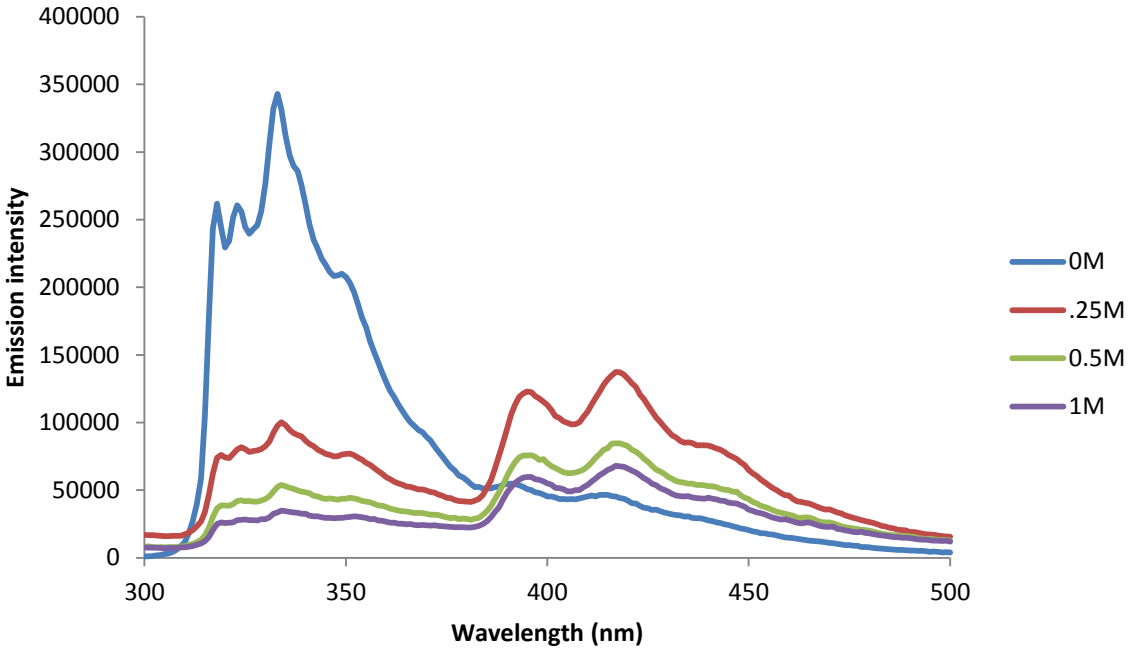

Figure 4.40: Emission scan in a range equal to 300-500 nm at fixed excitation λ_{ex}= 290 nm for ACE-AMMA-PAA sample in aqueous solution at pH 11 and varying $CaBr_2$ concentration

The emission spectra, Figure 4.40, at pH 11 shows an expanded ACE-AMMA-PAA polymer chains conformation in the absence of $CaBr_2$. This is due to the charge repulsion between the carboxylate anions of the PAA polymer. The fluorescence emission from the polymer is largely from the ACE label suggesting that energy transfer is minimal under these conditions (free of $CaBr_2$ and pH 11 solution). Increase of the $CaBr_2$concentration led to a reduction in the naphthyl emission and a corresponding increase in the anthryl fluorescence emission intensity. This is, presumably, due to the complexation of the Ca^{2+} cations with the carboxylate anions which led to the collapse of the polymer chains. Consequently the labels became in close proximity to each other which led to a higher degree of energy transfer in the process.

When the polymer samples, at pH 3 and pH 11, were excited at 370 nm, the AMMA label was also stimulated directly. The emission intensity from the anthryl label decreased as the $CaBr_2$ concentration increased (figure 4.41) in a manner that is similar to the ACE labelled sample. This provided more evidence that the salt has a quenching effect for both labels at low pH levels. In contrast, at high pH the emission intensity increased as the [$CaBr_2$] concentration increases as shown on Figure 4.42. This spectra pattern indicates that the polymer chains underwent a conformation change from a relatively expanded to a

relatively collapsed form at high pH (basic conditions) and no quenching happened for anthryl label.

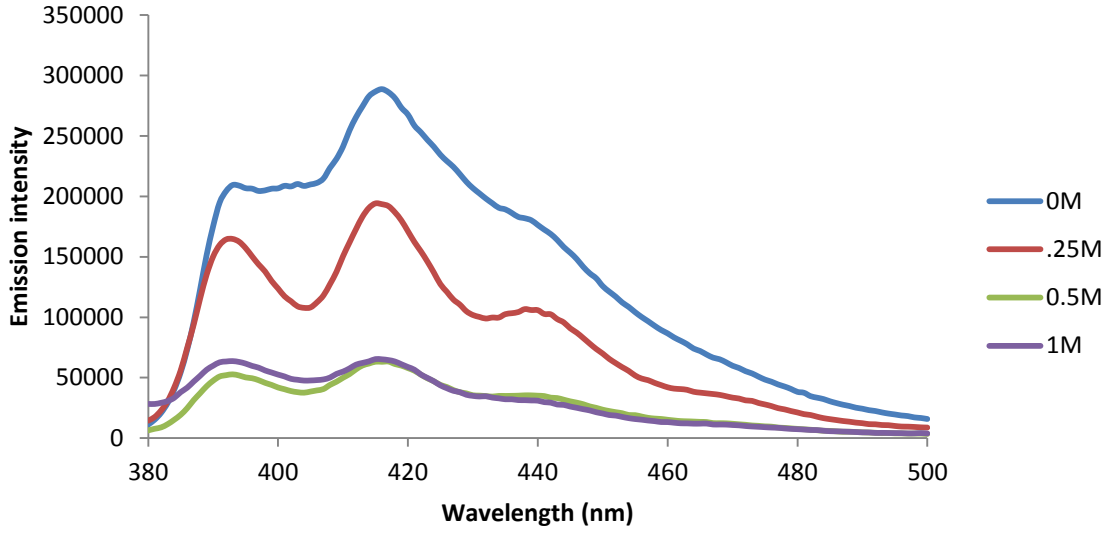

Figure 4.41: Example steady state emission spectra for an ACE-AMMA labelled PAA sample as a function of $CaBr_2$ concentration when excited at 370 nm at pH 3.

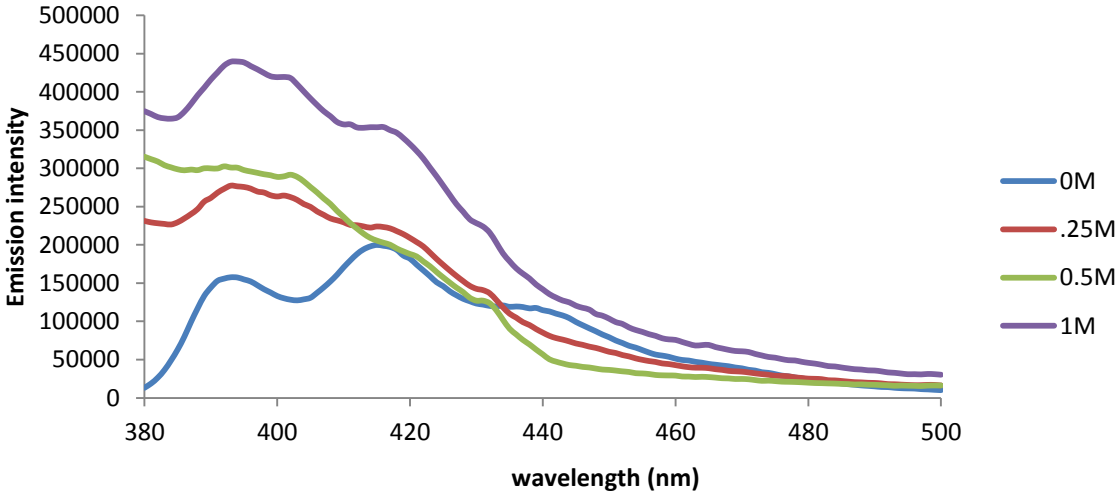

Figure 4.42: Example steady state emission spectra for an ACE-AMMA labelled PAA sample as a function of $CaBr_2$ concentration when excited at 370 nm at pH 11.

The energy transfer efficiency in doubly labelled poly (acrylic acid) as a function of the $CaBr_2$ concentration at three different values of pH was recorded and shown on Figure 4.43. The figure shows a general increase in the I_A/I_D ratio as the concentration of Ca^+ cations increased, irrespective of the pH level. This is consistent with a collapsed polymer chain conformation.

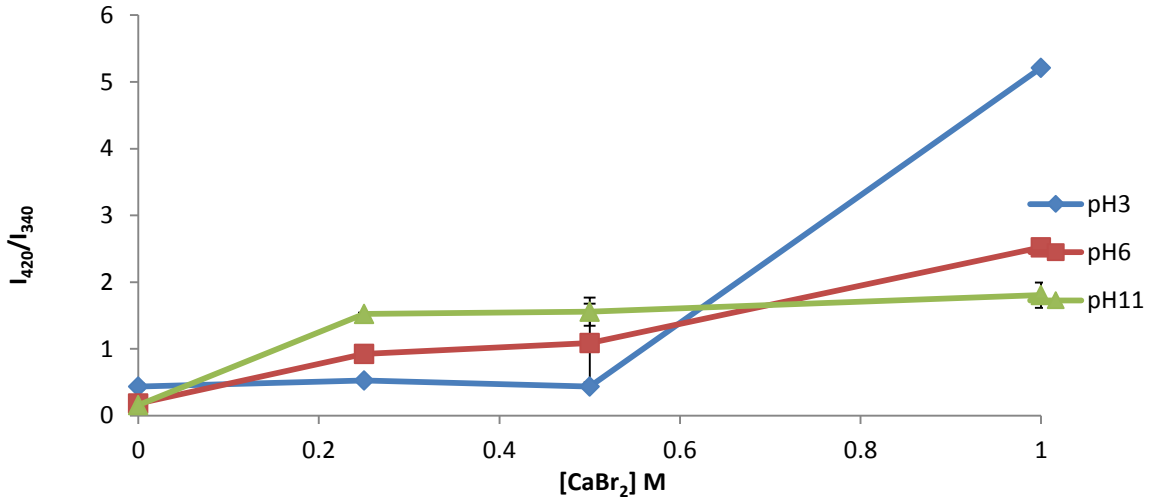

Figure 4.43: Fluorescence emission intensity ratio, I_A/I_D, of 10^{-2} wt % ACE-AMMA-labelled PAA as a function of $CaBr_2$ concentration at different pH values (λ_{ex} = 290 nm)

For low concentration of $CaBr_2$and in particular below 0.5 M the I_A/I_D graph at pH 3 shows no dependence on the $CaBr_2$ concentration. Above 0.5M concentration the ratio rises up and reaches a maximum at ~5.2 at 1M concentration. This indicates large energy transfer efficiency in the partially coiled form of the polymer chain. This high energy transfer suggests that the anthryl label got more close to the naphthyl label when the concentration of the Ca^{2+} cations increased to 1 M.

For pH 6, the I_A/I_D ratio increased as the $CaBr_2$ concentration was increased, indicating some energy transfer in the relatively coiled form of the PAA chain. Whereas at pH 11 and at low concentration of the $CaBr_2$ salt, the graph shows a noticeable increase of the ratio as the concentration increased. However there is no significant change in the ratio value at higher concentrations of $CaBr_2$ (more than ~0.25M). At pH 11 and salt concentrations in the range of 0.025 M to ~0.5 M, the I_A/I_D ratio is slightly greater than the ratio for pH 6. This is unlike the trend of the ratio for the polymer system in the absence of any salt where the ratio slightly decreases as the pH level increases. This indicated that the polymer underwent a conformational transition from an expanded polyelectrolyte chain to a

collapsed form at pH 6 and pH 11 as the concentration of $CaBr_2$ is increased. This is presumably due to complexation of the COO^- groups with the Ca^{2+} cations which lead to the chain aggregation.

4.1.11 Fluorescence excited state lifetimes of singly and doubly labelled PAA in the presence of $CaBr_2$ as a function of pH

For the sample considered in this section (ACE labelled PAA sample as a function of [$CaBr_2$] at various pH values) the best fit to the measured data was achieved using triple exponential fit (Equation 3.5). This data model gave χ^2 statistical values close to unity and a random distribution of residuals with small standard deviation as shown on Figure 4.44 for pH 3 level. The average lifetime was subsequently calculated from equation 3.3, and the results are plotted as a function of the calcium bromide concentration on Figure 4.45.

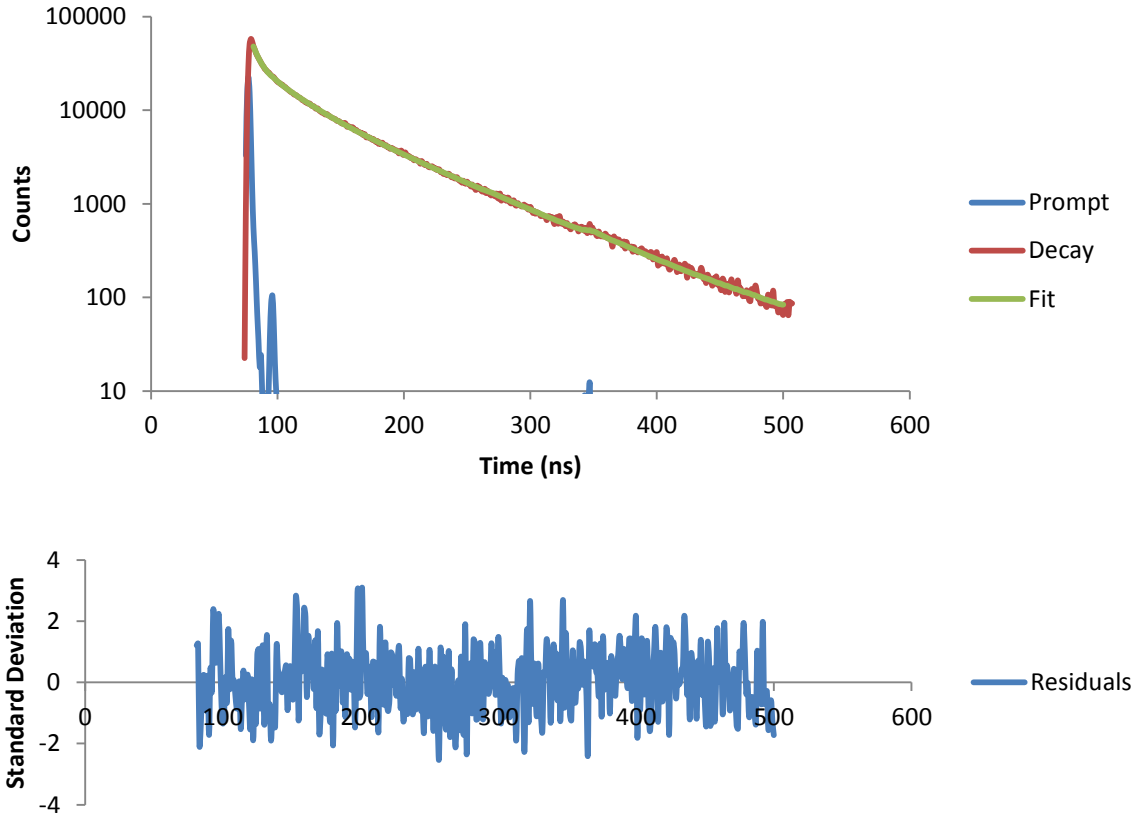

Figure 4.44: A fluorescence decay with corresponding mathematical fit (green) and a plot of the resulting residuals for ACE-PAA in aqueous solution of pH 3 with 0.025 M of $CaBr_2$

The average fluorescence lifetime of the ACE-PAA polymer sample decreased with the increase of the calcium bromide [$CaBr_2$] concentration for all pH values, in particular, in the absence of the bromide calcium salt the fluorescence average lifetime is the highest for each particular pH value. The same pattern of decrease is followed by the relative lifetime values as pH values changed from low to high. The ACE label was quenched by the added $CaBr_2$. This quenching was more pronounced in the $CaBr_2$ salt sample than the PAA-ACE with $CaCl_2$ Sample. At high $CaBr_2$concentrations (1 M) and for all tested pH values (pH 3, 6 and 11), the average lifetime value reached approximately the same value. This is a clear indication that the addition of the calcium bromide to the ACE-PAA system sample increased the quenching of the label and thus decreasing the lifetime. This decrease in the fluorescence average lifetime is an indication of a collapsed conformation was adopted by the polymer ACE-PAA chains.

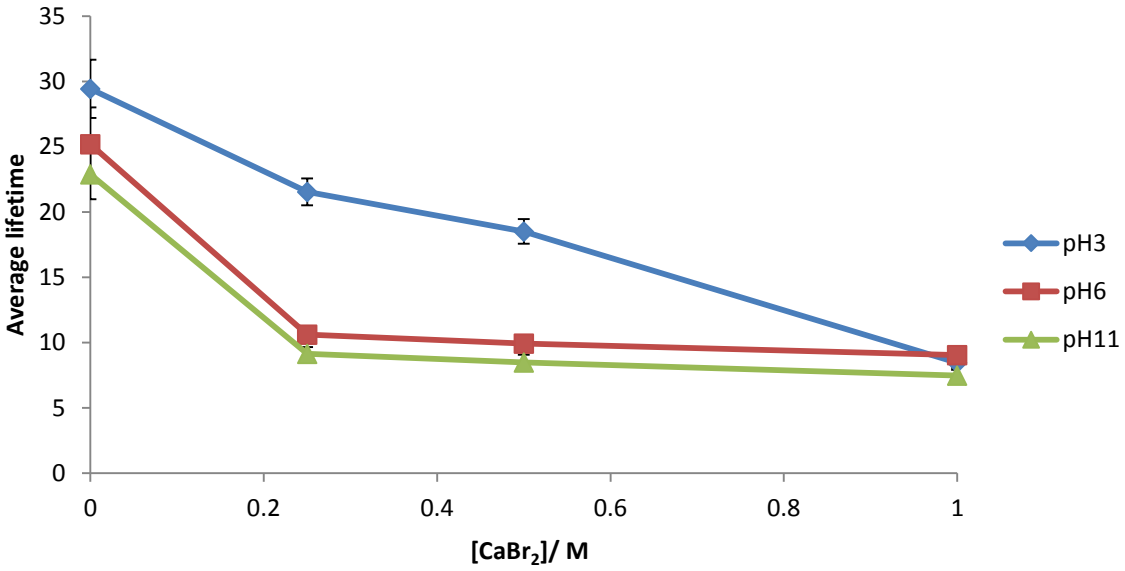

Figure 4.45: A plot of the average lifetime values obtained for ACE-PAA in aqueous solution at three different pH values with increasing $CaBr_2$ concentration when excited at 290 nm and observed at 340 nm.

Again the use of triple exponential functions (Equation 3.5) to model the fluorescence decays of the ACE-AMMA PAA sample was the best fit to the measured data. The χ^2 statistical values are close to unity with small standard deviation and small residual values as shown on Figure 4.46.

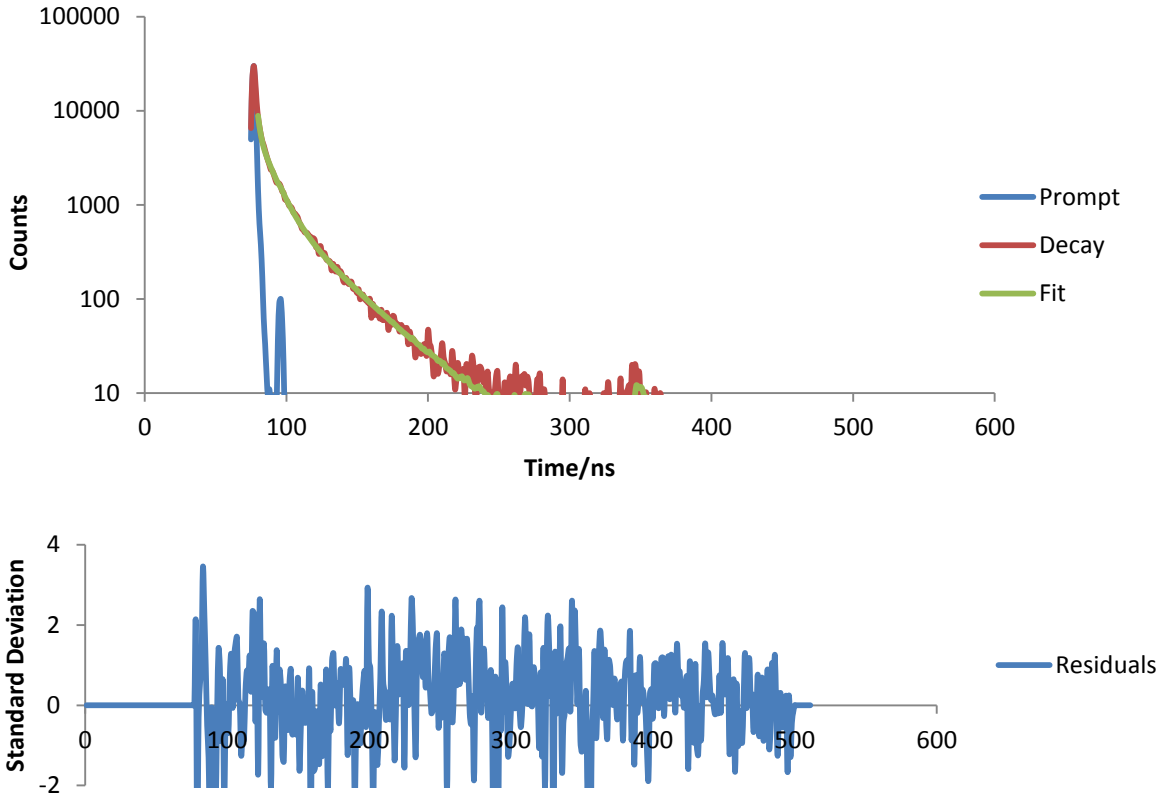

Figure 4.46: A fluorescence decay with corresponding mathematical fit (green) and a plot of the resulting residuals for ACE-AMMA-PAA in aqueous solution of pH 11 with 1 M of $CaBr_2$

The decrease in the lifetime of the ACE label in ACE-AMMA-PAA sample in the presence of salt became substantial compared to that in PAA-ACE system. As it can be observed from Figure 4.47, the curves at pH 3, 6 and 11 displayed the opposite pattern of that obtained from the I_A/I_D ratio against [$CaBr_2$]shown on Figure 4.43. This is consistent with an increased quenching as the polymer adopted a collapsed conformation. The shape of the curve at pH 11 as seen on Figure 4.47 could be attributed to the fact that the polyelectrolyte chains underwent a conformational transition change as the concentration the $CaBr_2$ salt increased from 0 M to 1 M. This transition went from a relatively expanded chain

conformation at the absence of salt, long average lifetime with value of ~21 ns, to a partially collapsed form at high concentration 1M. The average lifetime at which is ~ 4.6 ns (quenched). The quenching is probably due to the collapse of the polymer chains which is caused by the increase of Ca^{+} cations concentration in addition to an energy transfer to the acceptor label. The same lifetime average pattern is also observed at pH 6, however with a slightly higher average lifetime values.

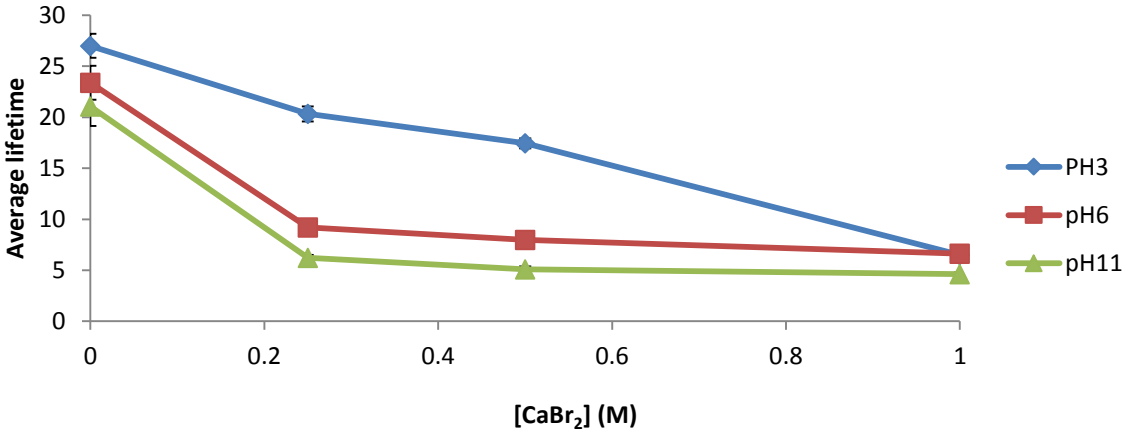

Figure 4.47: A plot of the average lifetime values obtained for ACE-AMMA-PAA in aqueous solution at three different pH values with increasing $CaBr_2$ concentration when excited at 290 nm and observed at 340 nm.

The data collected at pH 3 does show an increase in distance between labels (at 0.25 M and 0.5|) which is consistent with a slight expansion of the polymer chain (figure 4.48). The distance then notably decrease as the concentration increases to 1 M, indicating a further coiling in the chain compared to that in the absence of salt. This observation is a further support to what have been resulted from the fluorescence intensity ratio of donor and acceptor labels.

At pH value of 6 there is a steady decrease in the distance between the ACE and AMMA across the entire concentration range of $CaBr_2$, suggesting increase in the coiling chain as the salt amount is increase. This observation is in agreement with the energy transfer experiment.

At pH11, there is a substantial decrease in the distance between the donor and acceptor labels upon initial addition of calcium bromide but then no further change in the label distance as the salt concentration increases more. This observation is also in agreement with the ET experiment.

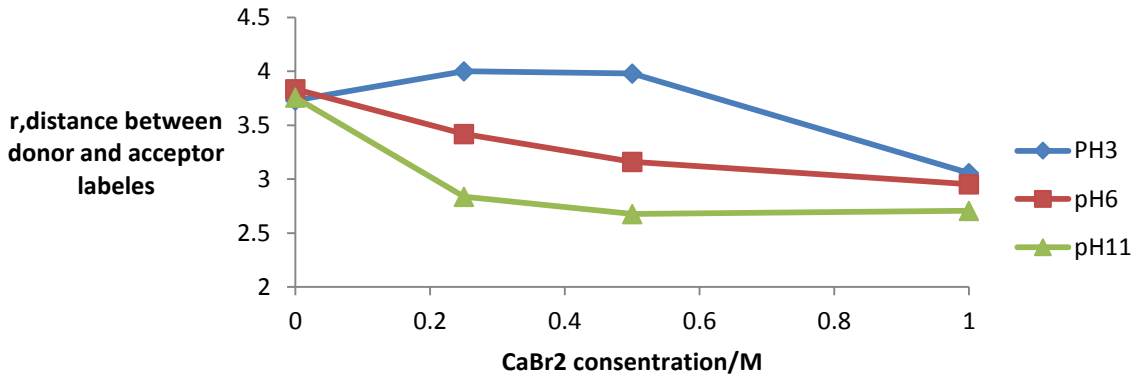

Figure 4.48: Plot of the value r, the distance between ACE (donor) and AMMA (acceptor) labels, as calculated by equation 3.7 for single and double -PAA across a range of pH values and $CaBr_2$ concentrations.

4.1.12 Fluorescence time-resolved anisotropy measurements (TRAMS) of ACE-PAA in the presence of $CaBr_2$ as a function of pH

In this section TRAMS measurements of the ACE-PAA polymer are considered. In order to study the polymer dynamics, measurements were conducted on the ACE labelled-PAA polymer samples with a range of $CaBr_2$ concentration and at various pH values. Figure 4.49 compares the fluorescence anisotropy decays of ACE-labelled-PAA in water ($CaBr_2$ free aqueous solution) and in the presence of calcium bromide 1 M concentration at pH 3 (acidic condition). The figure shows that the anisotropy decayed rapidly to zero in the absence of $CaBr_2$. Conversely, the anisotropy decayed more slowly in the presence of the salt. This behaviour indicates the formation of a more collapsed PAA polymer chains in the presence of the $CaBr_2$ salt and hence the long anisotropy decay.

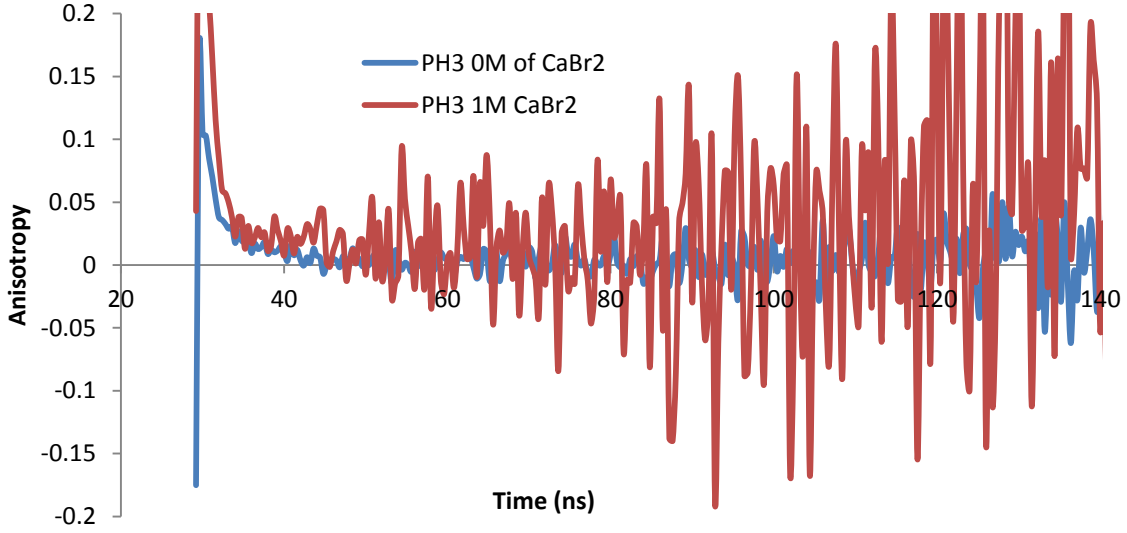

Figure 4.49: Fluorescence time resolved anisotropy data of aqueous ACE-labelled PAA solution (10^{-2} wt %) in the absence of calcium bromide (blue line) and at the calcium bromide concentration of 1 M at pH 3 (λ_{ex} = 295 nm and λ_{em} = 340 nm).

For high level of pH values (basic conditions with pH 11) it can be seen from Figure 4.50 that the anisotropy quickly dropped to zero in the absence of the $CaBr_2$ salt. The presence of the salt lowered the anisotropy decay (longer time of decay to zero value), this is presumably due to the interaction occurring between Ca^{2+} cations and the two COO^- groups of PAA polymer chains. This interaction led to the collapse of the polyelectrolyte chain, which in turn led to the motion reduction of the ACE-PAA chain and therefore the slow anisotropy decay.

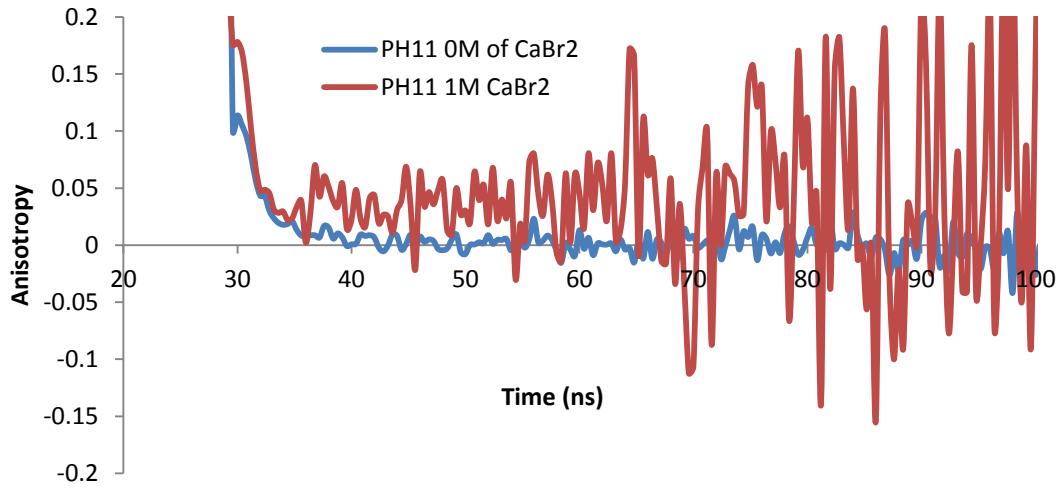

Figure 4.50: Fluorescence time resolved anisotropy data of aqueous ACE-labelled PAA solution (10^{-2} wt%) in the absence of calcium chloride (blue line) and at the calcium bromide concentration of 1 M at pH 11 (λ_{ex} = 295 nm and λ_{em} = 340 nm).

Irrespective of solution condition, single exponential fit was found to be the best model to fit the TRAMS measured data of the ACE- PAA sample. The residuals of the data fit, as can be seen on Figure 4.51, are randomly distributed around zero with χ^2 values close unity which provides statistical confidence in the quality of the data fit model. Figure 4.52 shows the resultant correlation time data plotted as a function of $CaBr_2$ concentration for several pH values.

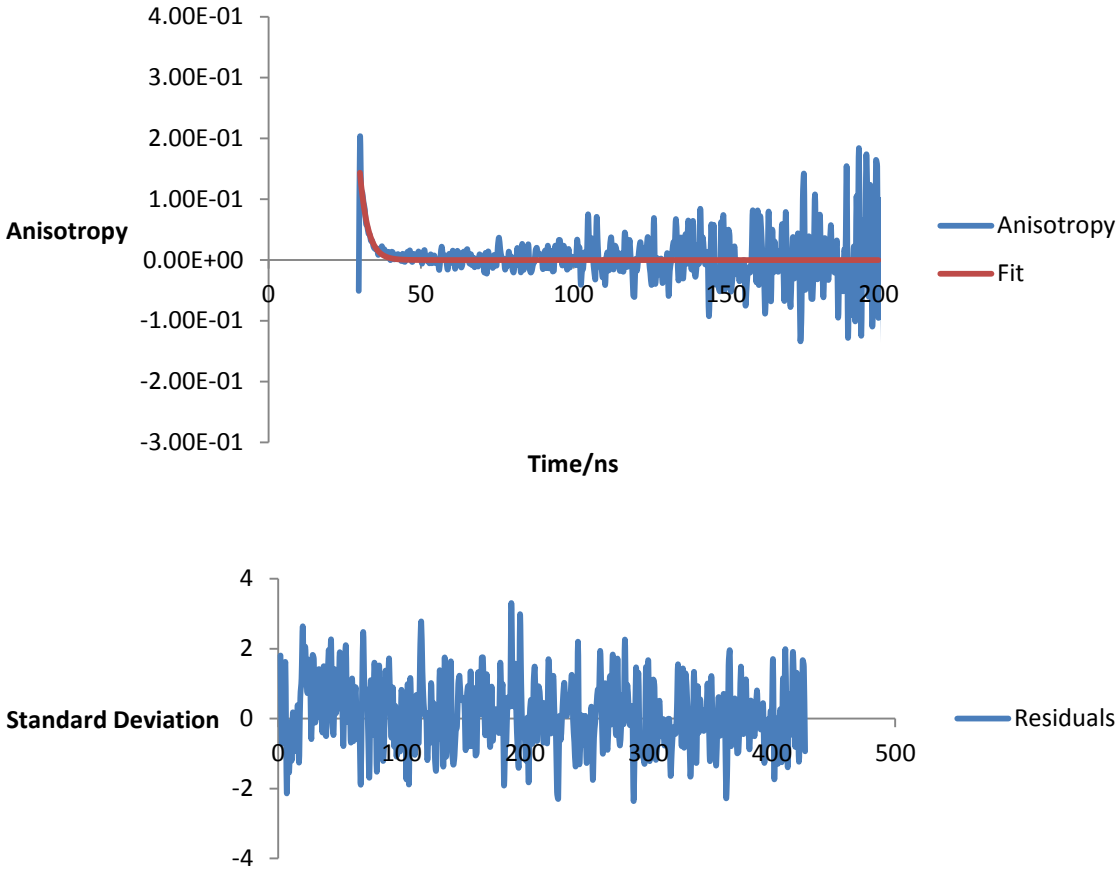

Figure 4.51 Decay of anisotropy, r(t), for ACE-PAA in aqueous solution of pH 3 with 0.25 M of $CaBr_2$, and the associated single-exponential fit with the distribution of residuals. (λex =295nm and λem=350nm).

Figure 4.52 shows a general increase in the correlation time τ_c values at all pH values as the $CaBr_2$ concentration increased. This pattern suggests that mobility of the label is reduced and it is consistent with the collapse of the polymer chains and the increased energy transfer between the labels as previously discussed. The effect is more pronounced at higher pH values suggesting that complexion between the Ca^{2+} and carboxylate anions is more efficient.

It is worth noting that at pH 11 the cross correlation time τ_c increased from 1.6 to ~19.6 ns by increasing Ca^{2+} concentration in the $CaBr_2$ sample as shown on Figure 4.52. In the sample of $CaCl_2$, discussed previously, the τ_c increased from 1.6 to ~26.7 ns at pH 11 as the Ca^{2+} concentration increased (Figure 4.24). This indicates that the Br^- anions have less effect on the PAA aggregation compared to the case for Cl^- anions.

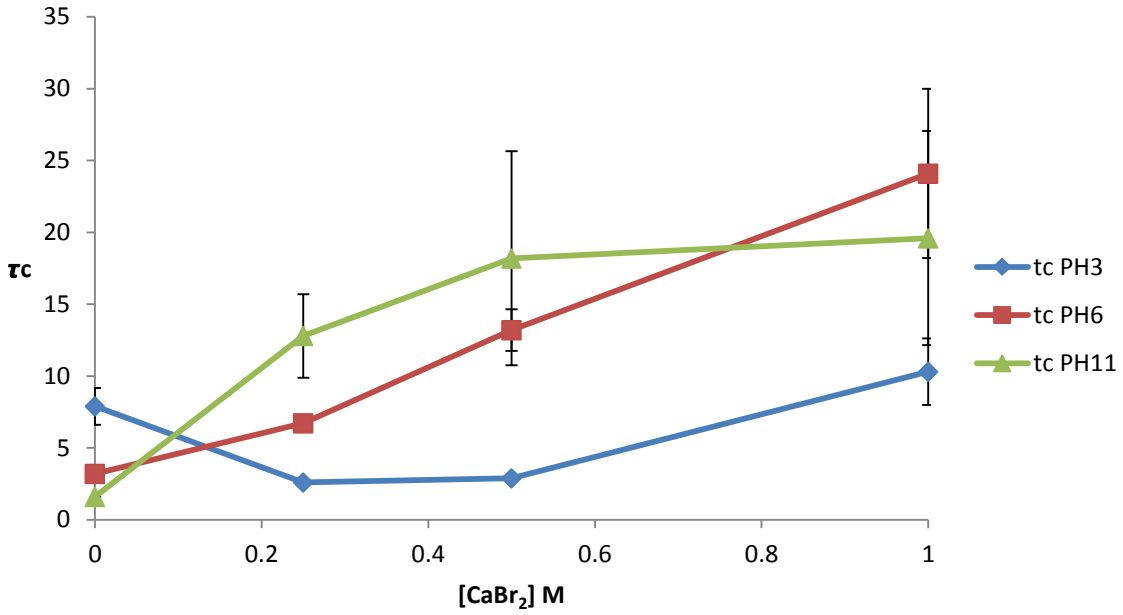

Figure 4.52: A plot of correlation time against $CaBr_2$ concentration for three ACE labelled PAA samples in aqueous solution at three different pH values when excited at 290 nm and observed at 340 nm.

In summary, the experiments of fluorescence steady state and energy transfer showed that by adding sodium chloride to the PAA polymer in acidic media, it leads to a conformation change from collapsed chain to expanded form. Using TRAMS and measuring the distance between labels showed that the polymer only expanded with the initial addition of sodium chloride and recoils at higher salt concentration. The fluorescence technique further demonstrated that in basic media, the unfolded ionic polymer interacted with the cation of the salt causing polymer chain aggregation. The aggregation generated by a complex of Na^+ ions with COO^- ions was noticeably more efficient at pH 6 than at pH 11 conditions.

Coiling was promoted at all pH values with the addition of calcium chloride. However, the interaction between the carboxyl group and the cation caused aggregation which was more pronounced at pH 11 compared to sodium chloride where aggregation was more pronounced at pH 6. By comparing the coiling effect of the PAA polymer by NaCl and NaBr, the TRAMS measurements showed that the increase in anion size in acidic media promoted the PAA polymer aggregation, whilst in basic media the decrease in anion size lead to a promotion of PAA polymer aggregation. However, the interaction of polymer

conformation showed that a decrease of anion size increased the coiling of the chain in both acidic and basic conditions.

4.1.13 A comparative summary

4.1.13.1 The effect of Ionic Strength and type of ion (cations) on the poly (acrylic acid) Conformation

The impact of cations and the concentration of salt on the PAA polymer conformation is found to be different and depends on the type of the salt present in the solution. Moreover**,** the influence of the cations in the solution is different and may also depends on the monovalent and divalent cations. It is expected that divalent ions (such as Ca^{2+}) will have a higher attractive interaction with deprotonated carboxylate groups due to the higher charge. For the purpose of comparisons the TRAMS technique is used to compare the effects of these salts on the PAA coiled polyelectrolyte chains.

4.1.13.2 Fluorescence time-resolved anisotropy measurements (TRAMS) of ACE-PAA in the presence of NaCl and $CaCl_2$ at acidic and basic condition

TRAMS data from Figures 4.53 and Figure 4.54 shows that the poly(acrylic acid) displays an increased coiling upon increasing the ionic strength in the $CaCl_2$ case, whereas in the NaCl case, the cations induced an unfolding effect on the polymer chains except at 2M with low pH value. TRAMS data from Figure 4.55 and Figure 4.56 shows that the poly (acrylic acid) displays more coiling upon the addition of $CaCl_2$ than NaCl in basic media.

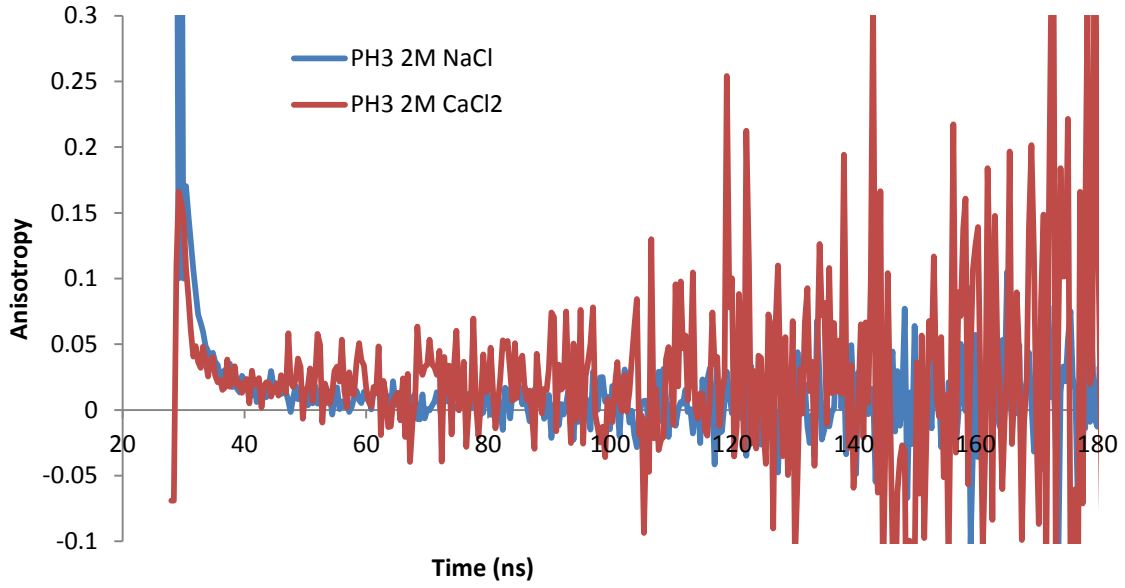

Figure 4.53: Fluorescence time resolved anisotropy data of PAA a function of salt concentration (at pH 3).

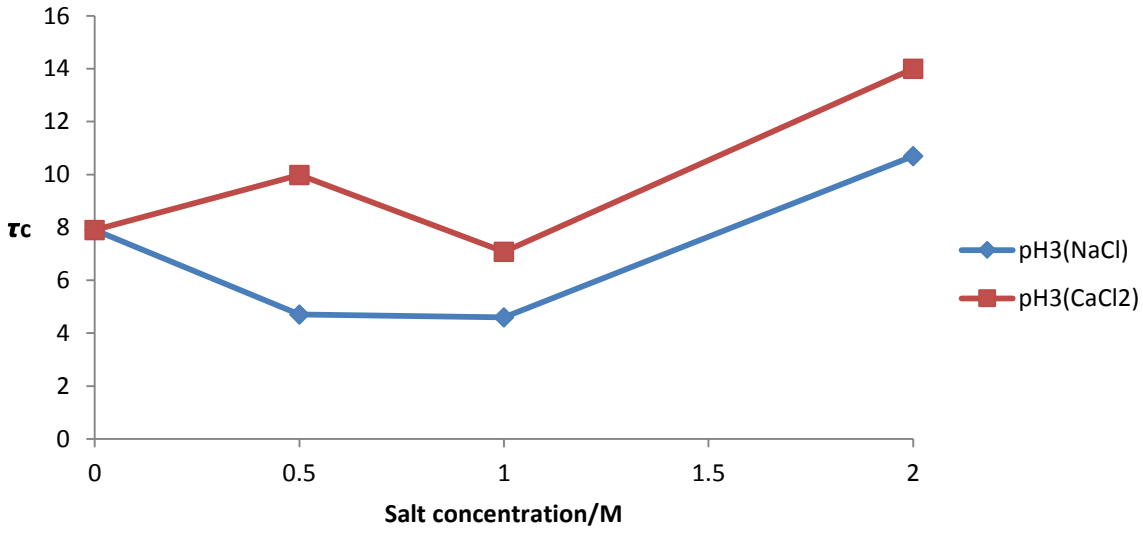

Figure 4.54: Correlation times of PAA as a function of salt concentration (at pH 3).

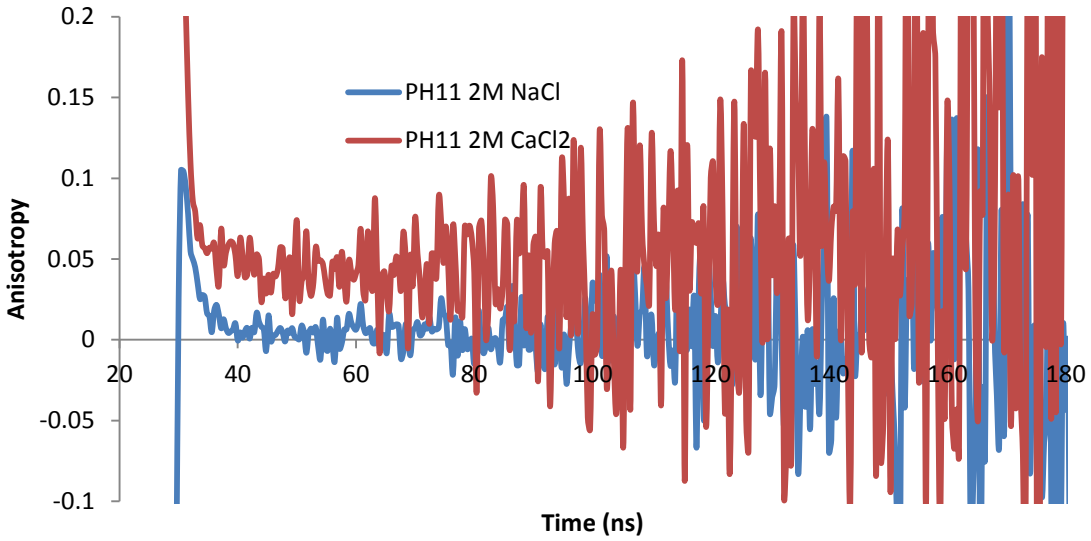

Figure 4.55: Fluorescence time resolved anisotropy data of PAA a function of salt concentration (at pH 3).

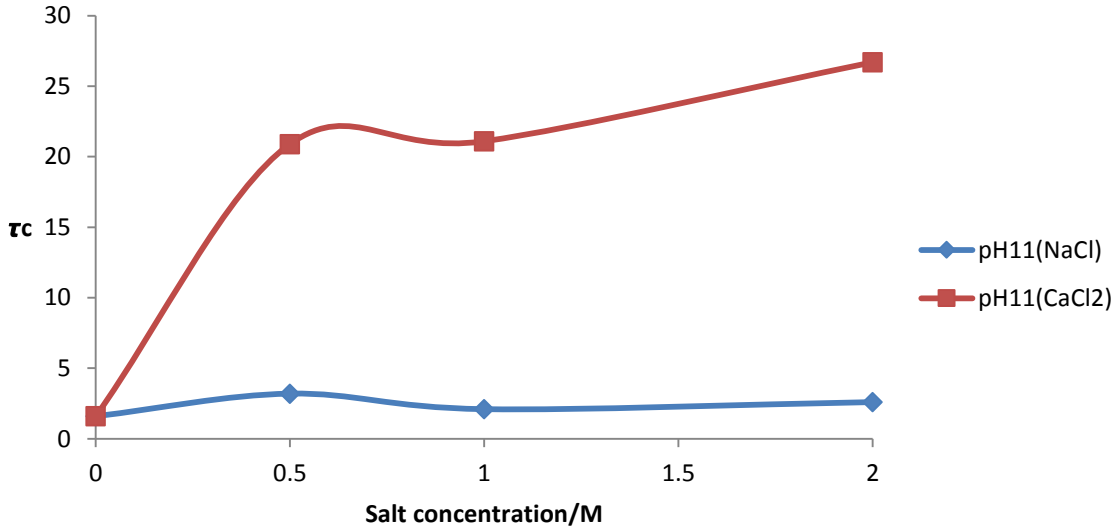

Figure 4.56: Correlation times of PAA as a function of salt concentration (at pH 11).

4.1.13.3 The effect of Ionic Strength and type of ions (anions) on the poly (acrylic acid) Conformation

The experiment results showed that the monovalent and divalent anions salts have different effects. In particular, the effect of the monovalents sodium bromide and sodium chloride anions on the conformation behaviour of the PAA is different from that of the divalents calcium bromide and calcium chloride anions on the PAA. TRAMS technique results have been chosen for this comparative analysis.

4.1.13.4 Fluorescence time-resolved anisotropy measurements (TRAMS) of ACE-PAA in the presence of NaCl and NaBr at acidic and basic condition

TRAMS data from Figure 4.57 and Figure 4.58 shows that the conformation behaviour of the poly (acrylic acid) depends on ionic strength and the anion size in acidic media. pAA displays increased coiling upon increasing the anion size (NaBr > NaCl), except at high ionic strength of NaCl where it induces more collapse chain than in case of NaBr.

TRAMS data from Figure 4.59 and Figure 4.60 shows, although, poly (acrylic acid) displayed a more coiling chain at high pH in the presence of sodium chloride than in case of sodium bromide, there is unexpected expansion of the chain at 1M of NaCl

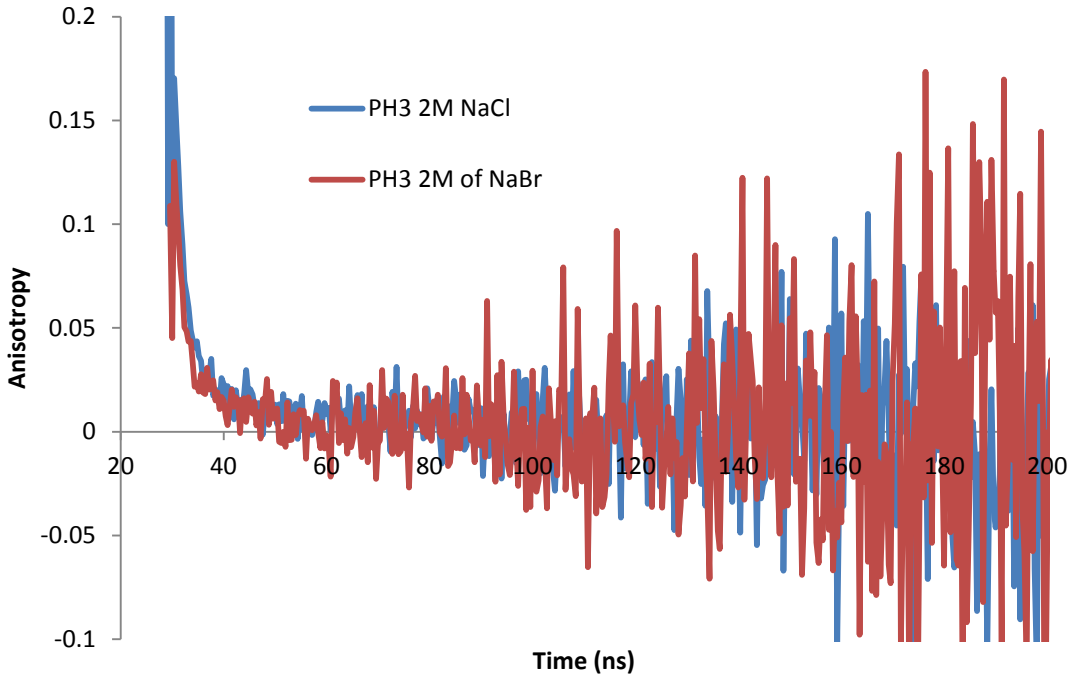

Figure 4.57: Fluorescence time resolved anisotropy data of PAA as a function of salt concentration (at pH 3).

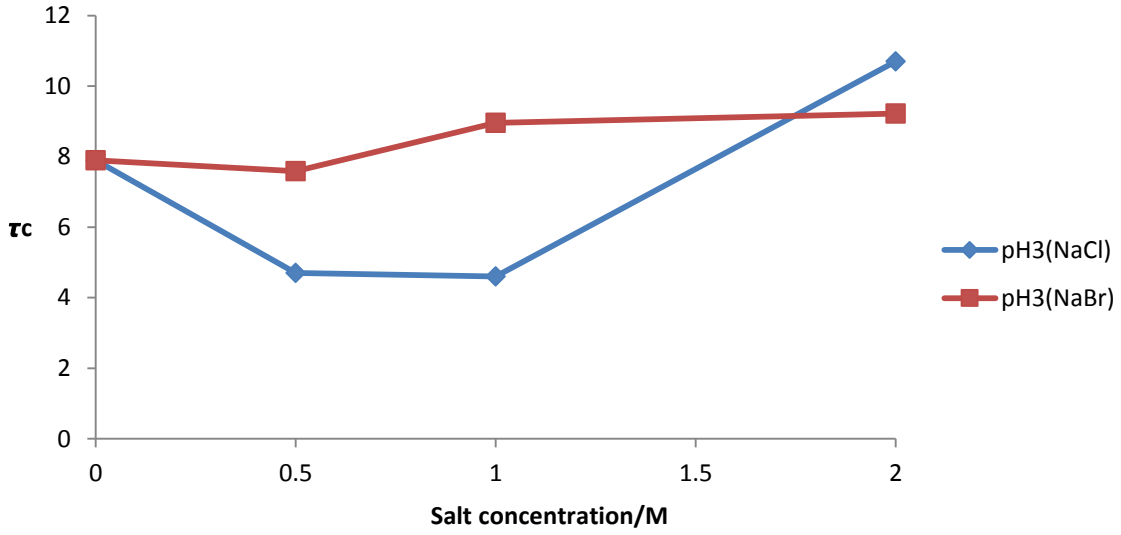

Figure 4.58: Correlation times of PAA as a function of salt concentration (at pH 3).

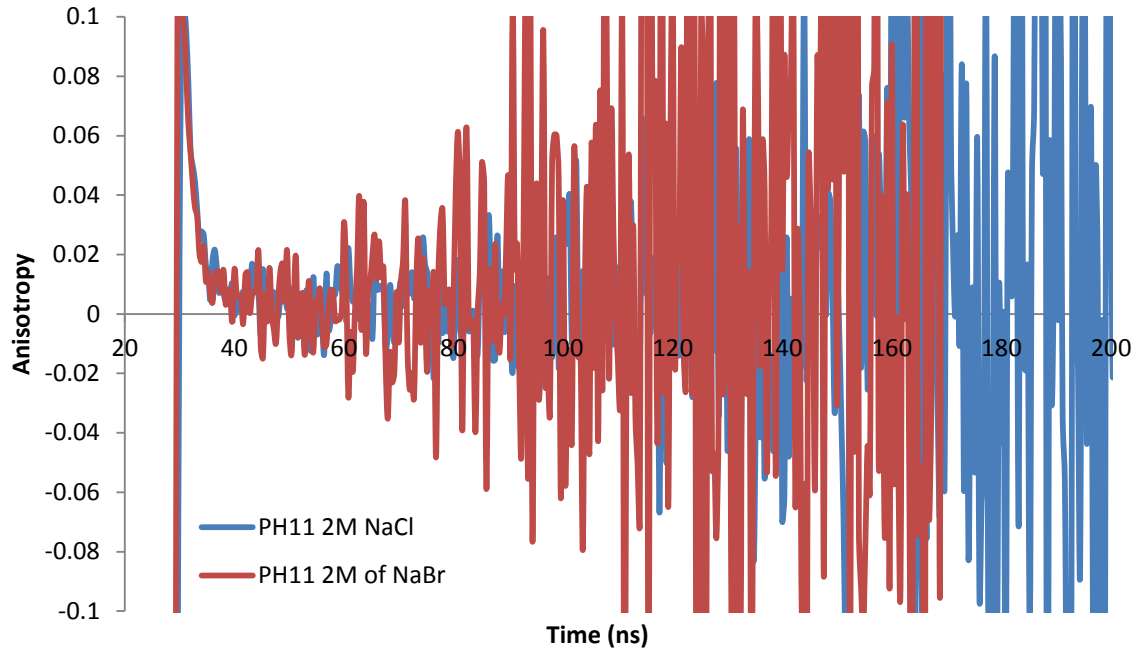

Figure 4.59: Fluorescence time resolved anisotropy data of PAA a function of salt concentration (at pH 11).

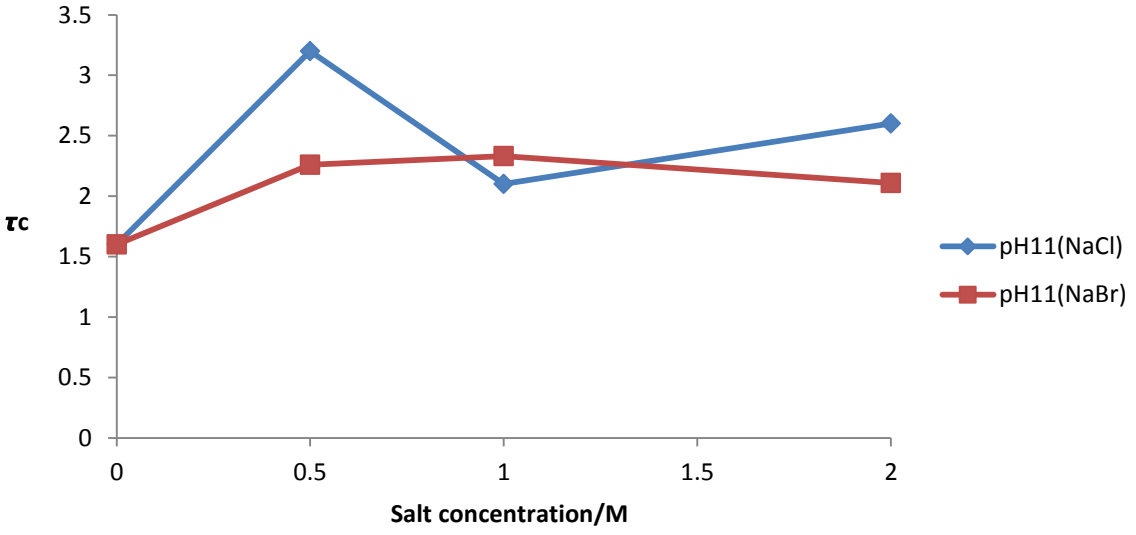

Figure 4.60: Correlation times of PAA as a function of salt concentration (at pH 11).

4.1.13.5 Fluorescence time-resolved anisotropy measurements (TRAMS) of ACE-PAA in the presence of $CaCl_2$ and $CaBr_2$ at acidic and basic condition

TRAMS data from these Figures 4.61 to 4.64 shows the poly (acrylic acid) displays an increased coiling upon increasing the ionic strength and decreasing the anion size ($CaCl_2$> $CaBr_2$). This effect of coiling is more pronounced at acidic condition than at the basic condition.

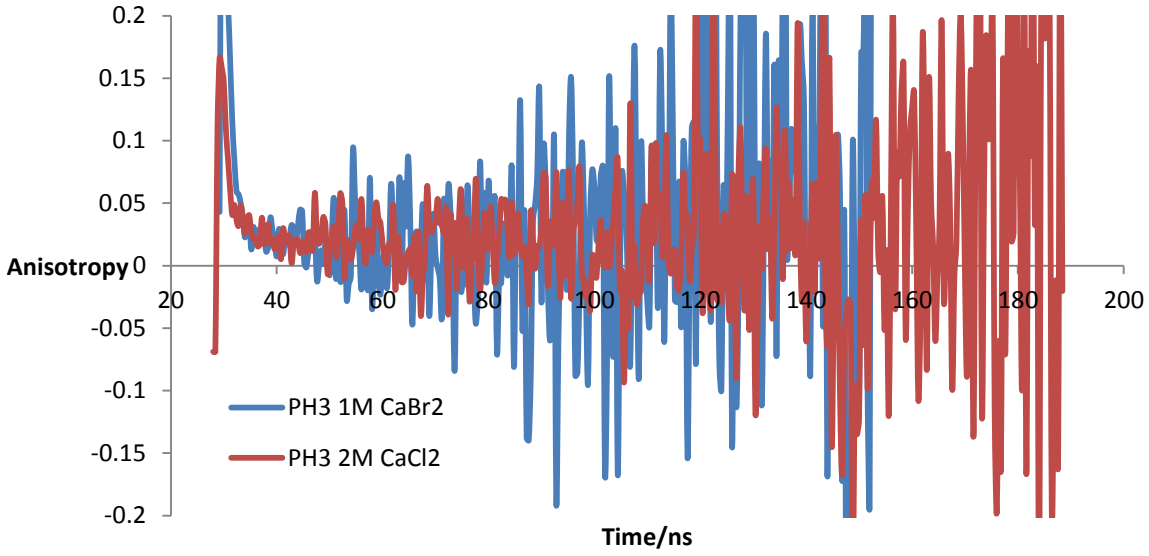

Figure 4.61: Fluorescence time resolved anisotropy data of PAA a function of salt concentration (at pH 3).

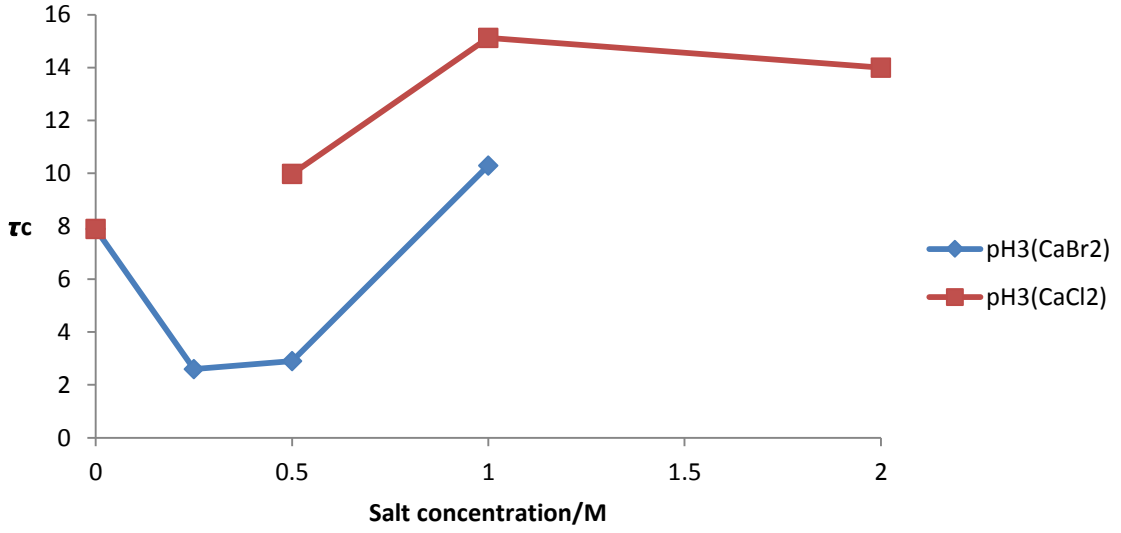

Figure 4.62: Correlation times of PAA as a function of salt concentration (at pH 3).

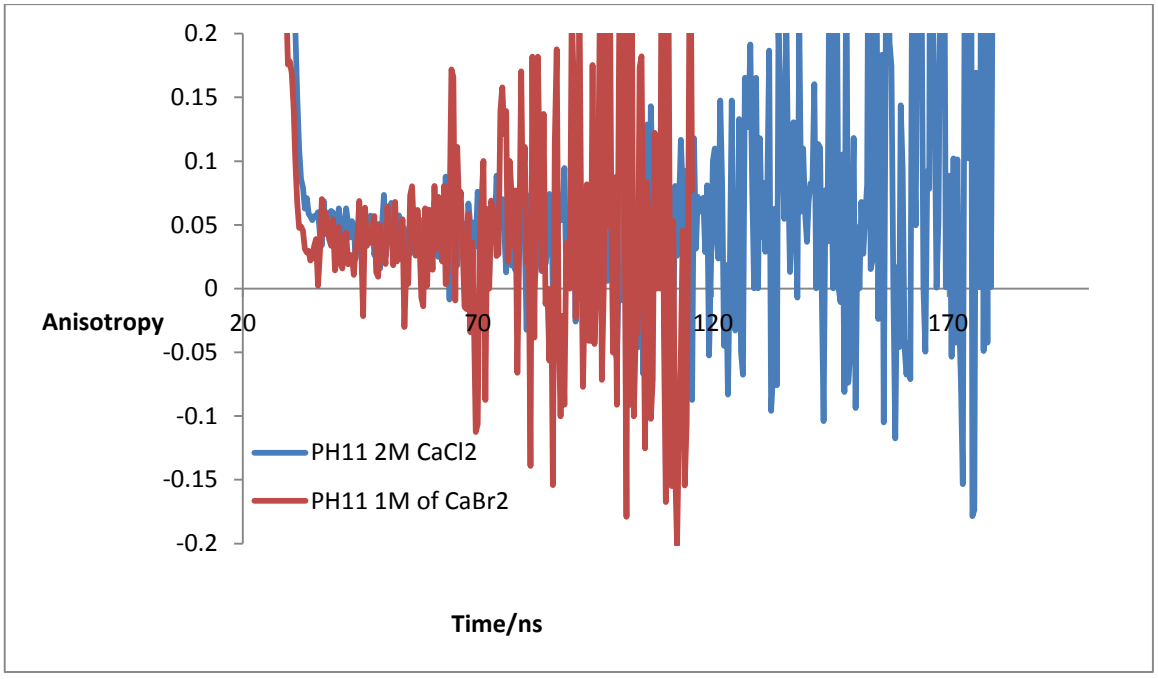

Figure 4.63: Fluorescence time resolved anisotropy data of PAA a function of ionic strength (at pH 11).

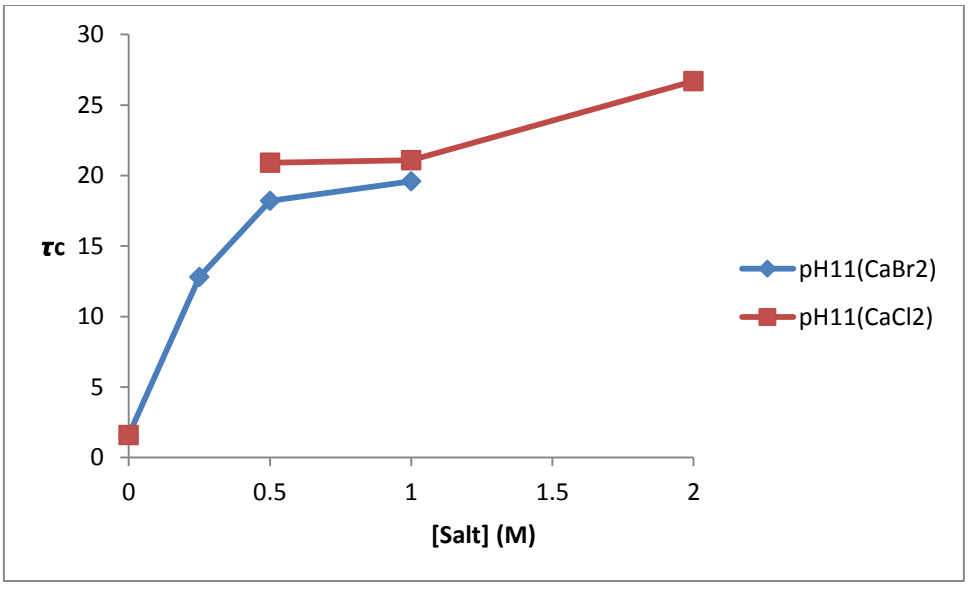

Figure 4.64: Correlation times of PAA as a function of salt concentration (at pH 11)

4.2 Fluorescence investigation of Poly (dimethylamino) ethyl methacrylate (PDMEAMA) in the presence of various salts

Depending on the type of salt used, the effect of ionic strength on Poly (dimethylamino) ethyl methacrylate conformation is found to differ. Furthermore, the size of the anions used has an influence on the polymer conformation in solution. It is expected large anions, such as Br^{1-} would have a higher attractive interaction with deprotonated amine groups. Fluorescence techniques is used to compare the effects of different salts on the coiled polymer chain. It resulted that the influence of monovalent salts differed to divalent salts with the same anions, for example sodium bromide and calcium bromide, on the conformational behaviour of PDMAEA.

4.2.1 Fluorescence steady state spectra of ACE- AMMA labelled PDMEAMA in the presence of NaCl as a function of pH

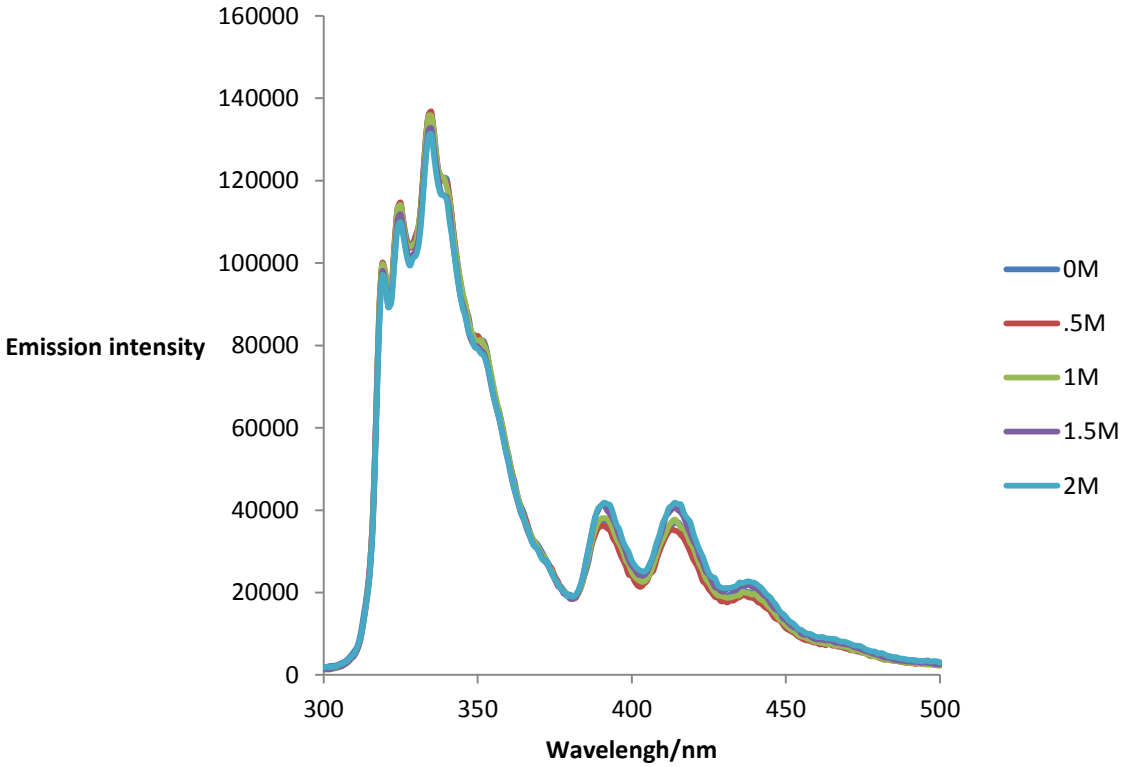

Figure 4.65 Emission scan in a range equal to 300-500 nm at fixed excitation λ_{ex}= 290 nm for ACE-AMMA- PDMEAMA sample in aqueous solution at pH3 and varying NaCI concentrations.

Figure 4.65 shows the emission spectra for an ACE-AMMA labelled PDMEAMA sample at pH3. There is slight increase in the emission intensity of the AMMA label seen at around 420 nm, consistent with a slight decrease in the emission intensity of the ACE label shown at 340 nm as [NaCl] is increased. This would seem to indicate that the polymer is coiling slightly, given further energy transfer from the donor to the acceptor.

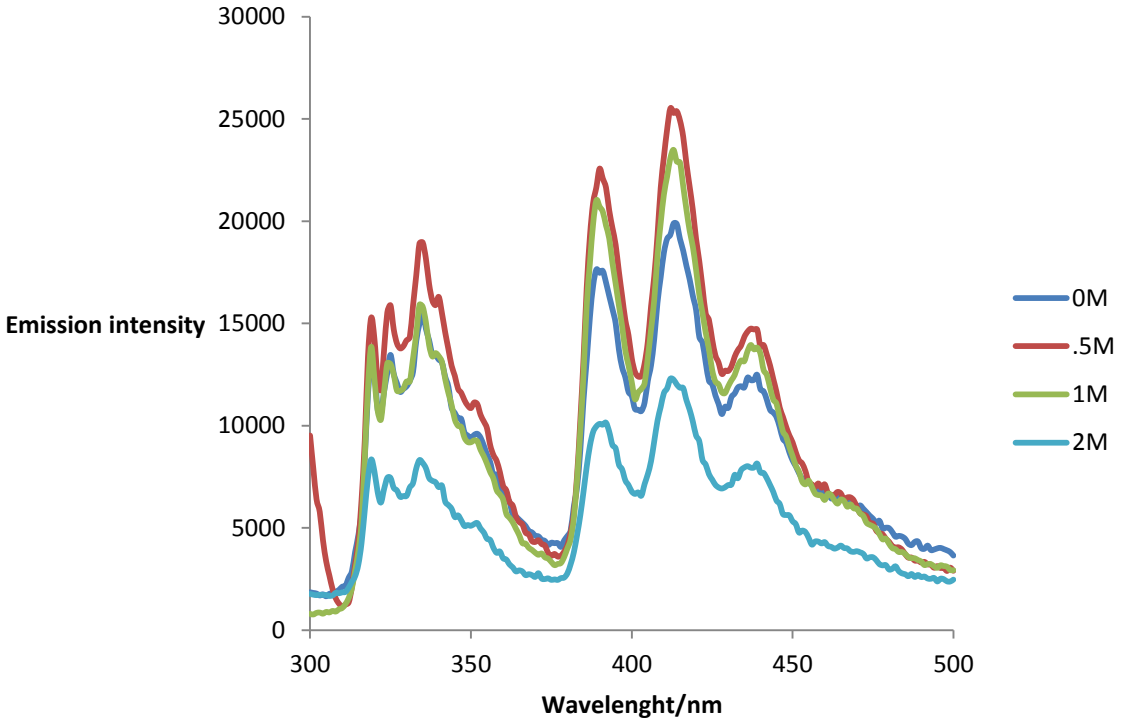

Figure 4.66 Emission scan in a range equal to 300-500 nm at fixed excitation λ_{ex}= 290 nm for ACE-AMMA- PDMEAMA sample in aqueous solution at pH11and varying NaCI concentrations

At pH11, however, (see figure 4.66) there is a very slight increase in the ACE emission at 0.5 M salt, consistent with an increase in the AMMA emission.

This observation suggests that the addition of sodium chloride to a coiled polyelectrolyte leads to a slight opening of the coiled polymer, hence, the donor and the acceptor become further from the amine group which then leads to an enhancement in fluorescence intensity for both labels. On the other hand, emissions from labels start to drop at 1 M and 2 M NaCl, which suggests that at high concentrations of salt the polymer again coils as the solution becomes unstable.

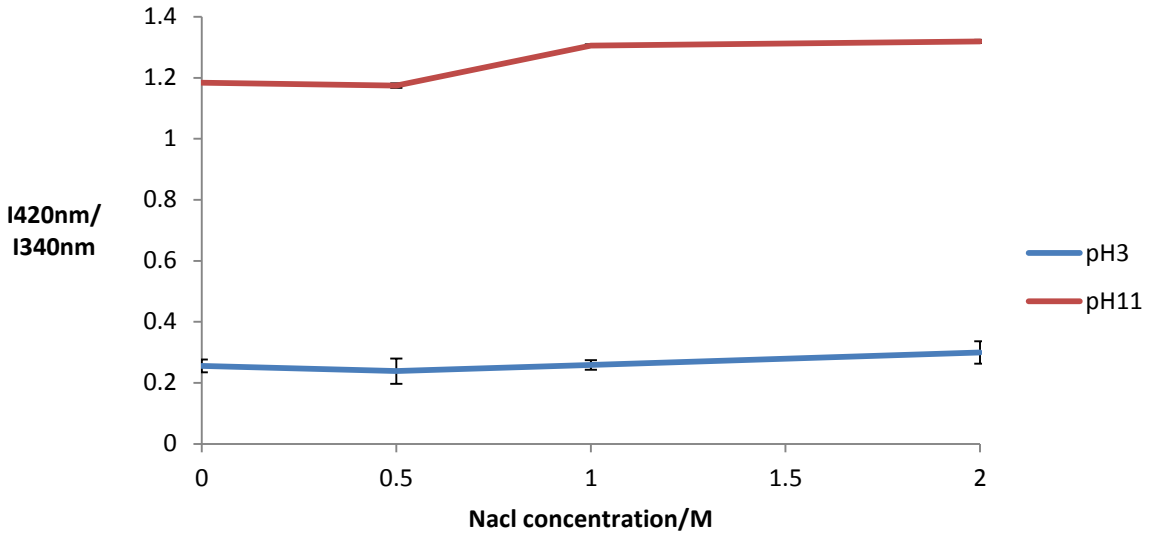

Figure 4.67 Fluorescence emission intensity ratio, I_A/I_D of 10-2 wt % ACE-AMMA-labelled PDMEAMA as a function of NaCl concentration at pH3 and PH11 (λ_{ex} = 290nm)

Figure 4.67 shows the energy transfer efficiency as a function of the sodium chloride concentration at pH 3 and pH11 respectively.

It can be seen from figure 4.67 that I420/ I340 at high pH slightly decreases at the initial concentration of salt, indicating that the polymer chain is opened slightly. This ratio value rises again at 1 M and 2 M indicating that the polymer starts to coil again and the energy transfer between the ACE and AMMA labels increases compared to the emission ratio of the system in the absence of NaCl. This ratio increases very slightly as the NaCl concentration increases at low pH which suggests that the polymer chain collapses when Cl^{1-} ions are added. Possibly, the cation amine groups of PDMAEMA with its expanded chain interact with the anion of salt resulting in coiling of the chain, which means there is a decrease in the separation distance between the donor and acceptor and hence an increase in the I_A/I_D ratio.

4.2.2 Fluorescence excited state lifetimes of singly and doubly labelled PDMAEMA in the presence of NaCl as a function of pH

The fluorescence decays from ACE labelled PDMAEMA at high and low pH values in which sodium chloride concentrations were increased showing a good statistical fit to a triple exponential analysis using equation 3.5 (see figure 4.69 as a selective sample). The

subsequent lifetime values were obtained using equation 3.3. This lifetime data was then plotted in figure 4.68 as a comparison.

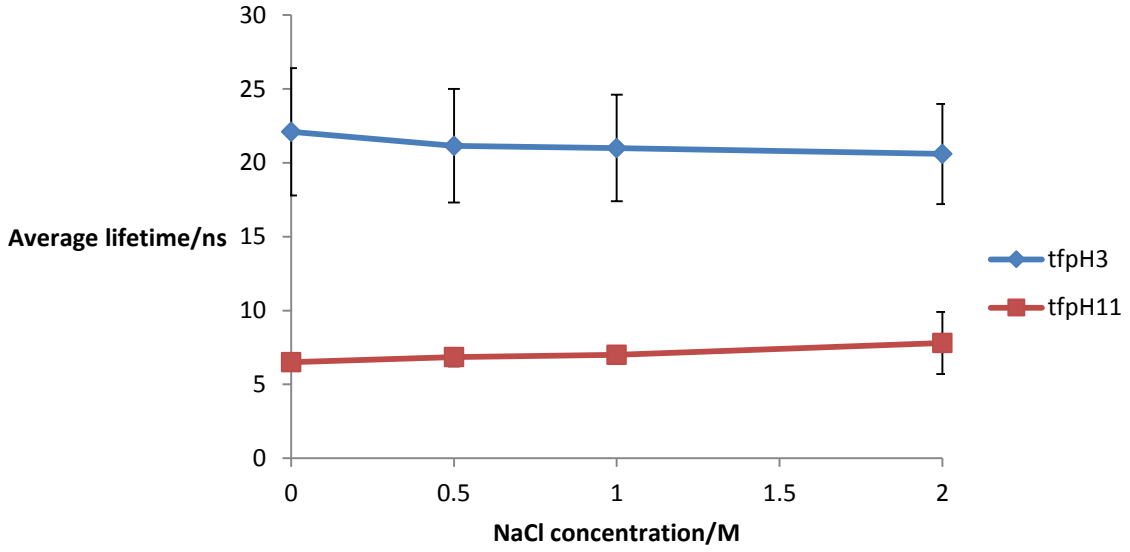

Figure 4.68 A plot of the average lifetime values obtained for ACE-PDMAEMA in aqueous solution at two different pH values with increasing NaCl concentrations when excited at 290 nm and observed at 340 nm.

It can be seen that initially adding sodium chloride (0.5 and 1 M) to the ACE-PDMAEMA solution at PH11 causes the lifetime values to increase slightly, indicating that the coiled polymer starts to expand slightly which is consistent with observations from steady state experiments. At an even higher concentration of salt (2 M) the life time value surprisingly increased even more.

On the other hand, at a low pH there was a slight decrease in the average lifetime value upon the addition of NaCl to the system indicating a slight increase in fluorescence quenching of the label. The most likely cause of this is that charge screening by the chlorine induces a collapse in the macromolecule chain, increasing the contact between the label and the polymer

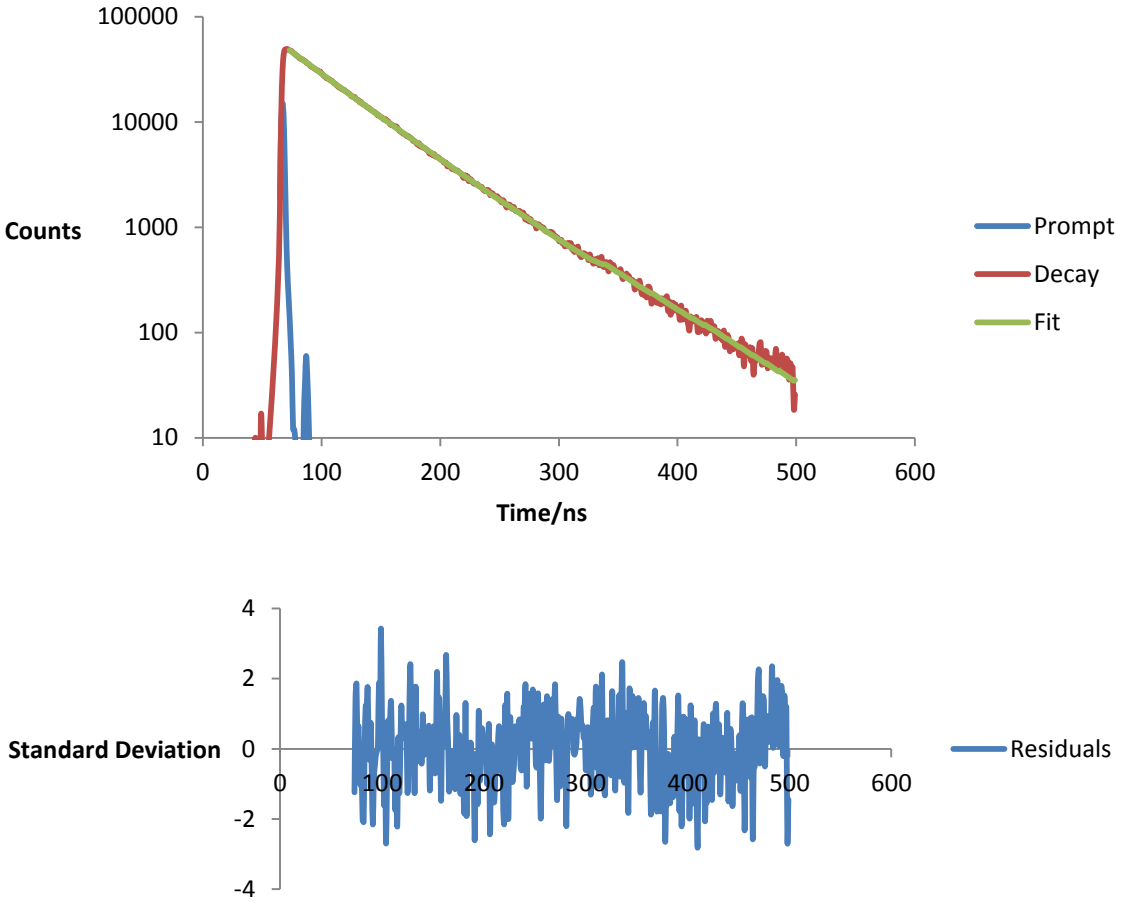

Figure 4.69 Fluorescence decay with corresponding mathematical fit (shown in green) and a plot of the resulting residuals for ACE-PDMAEMA in aqueous solution at pH 3 with 0.5 M NaCl

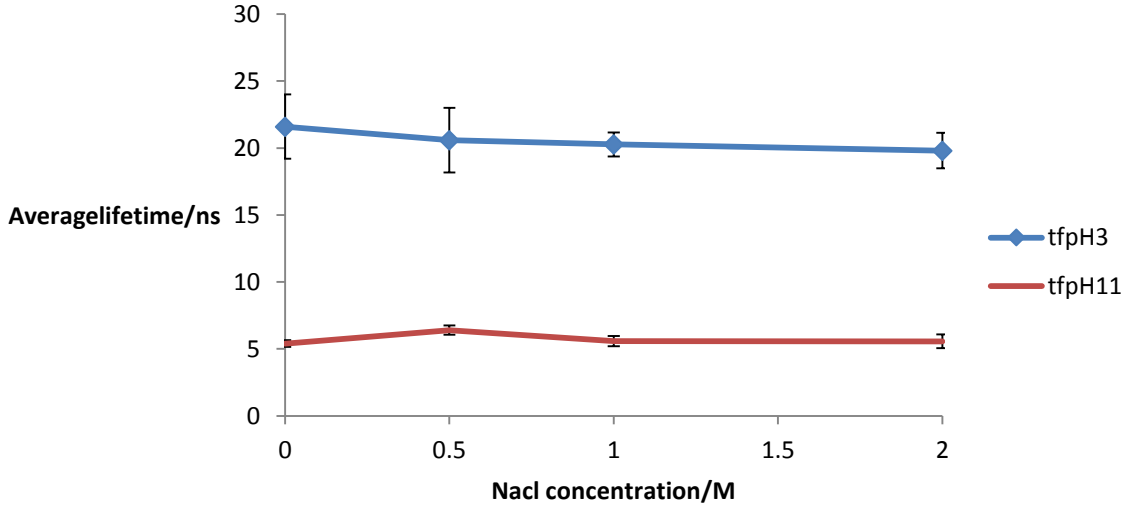

Figure 4.70 A plot of the average lifetime values obtained for ACE-AMMA-PDMAEMA in aqueous solution at two different pH values with increasing NaCl concentrations when excited at 290 nm and observed at 340 nm.

The lifetime data for ACE-AMMA-PDMAEMA at low pH and NaCI concentrations (see figure 4.70) shows that there is a slight drop in the lifetime values compared to those obtained for the macromolecule system in the absence of salt and to those obtained for the single labelled system. This indicates that there was energy transfer from the donor to the acceptor as well as quenching to the label by the amine group of the polymer coil by charge screening. This is in agreement with the steady state experiment.

At high a pH there is a slight increase in the average lifetime value at the initial concentration of salt. This indicates a reduction of quenching perhaps due to an expansion of the polymer chain occuring, reducing the internal quenching between label and polyelectrolyte segments. This is in agreement with the ET experiment.

Figure 4.71 shows the fluorescence decay curve as a selective sample was fitted to a triple exponential as in equation 3.5 and the average lifetime value from these were used in the above plot (figure 4.70)

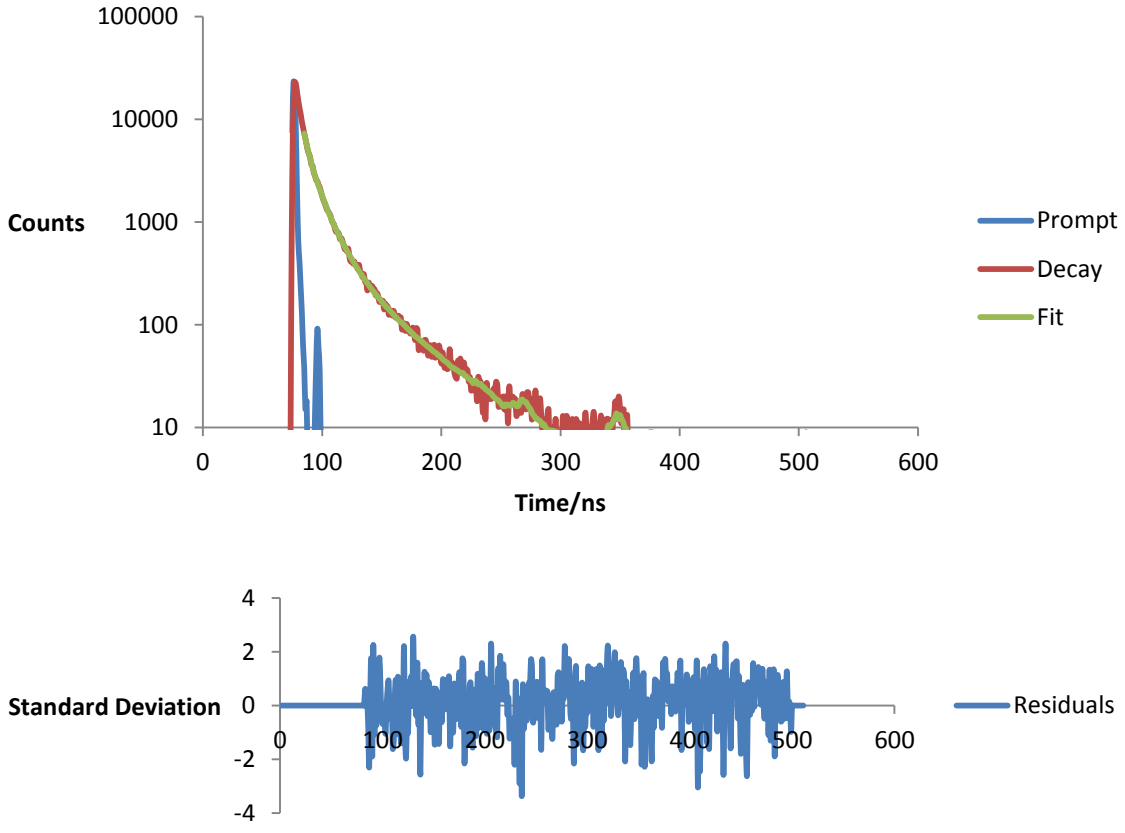

Figure 4.71 Fluorescence decay with corresponding mathematical fit (shown in green) and a plot of the resulting residuals for ACE-AMMA-PDMAEMA in aqueous solution at pH 11 with 2 M NaCl.

The average r value was then estimated for doubly labelled-PDMAEMA as a function of [NaCl] and pH using equations 3.7 and 3.8 respectively. Figure 4.72 shows the calculated distance values (nm) between the ACE and AMMA labels in the double labelled polyelectrolyte system at varying salt concentrations and pH values.

The label distance at pH3 showed a slight decrease as might have been expected given that the polymer was shown to collapse at a lower pH values in the presence of salt.

On the other hand, the distance between the labels showed a significant increase at pH11 when a small amount of salt was added, indicating that the polymer may have adopted a more open chain configuration. The distance value dropped further at higher salt concentrations again suggesting that the polymer adopt a coiled chain at even higher concentrations of salt (2M). This is again in agreement with the steady state experiment.

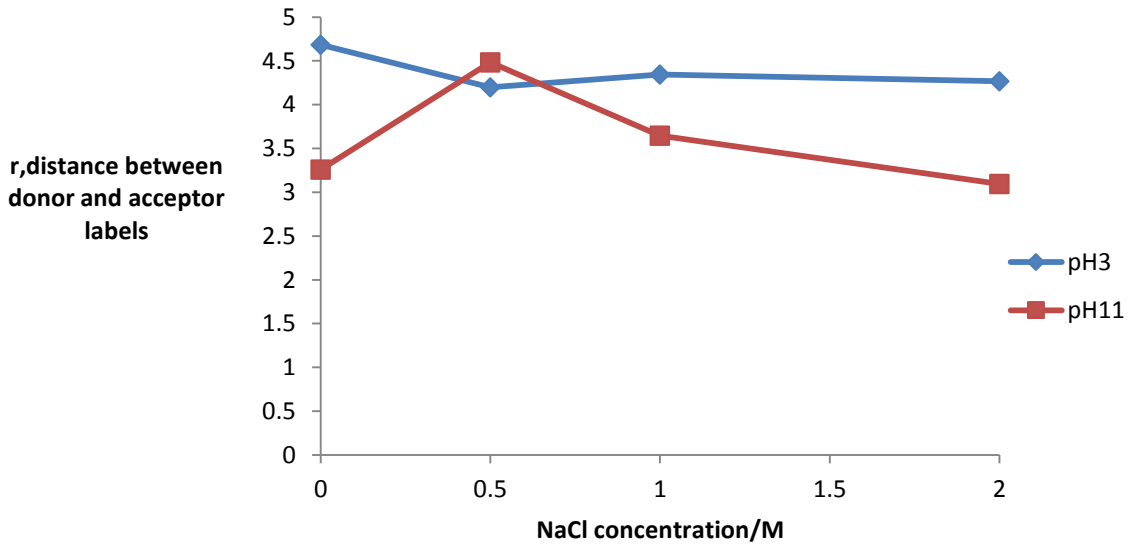

Figure 4.72 A plot of the value r, the distance between the ACE (donor) and AMMA (acceptor) labels, as calculated by equation 3.7 for single and double -PDMAEMA across a range of pH values and NaCl concentrations (M).

4.2.3 Fluorescence time-resolved anisotropy measurements (TRAMS) of ACE-PDMAMA in the presence of NaCl as a function of pH

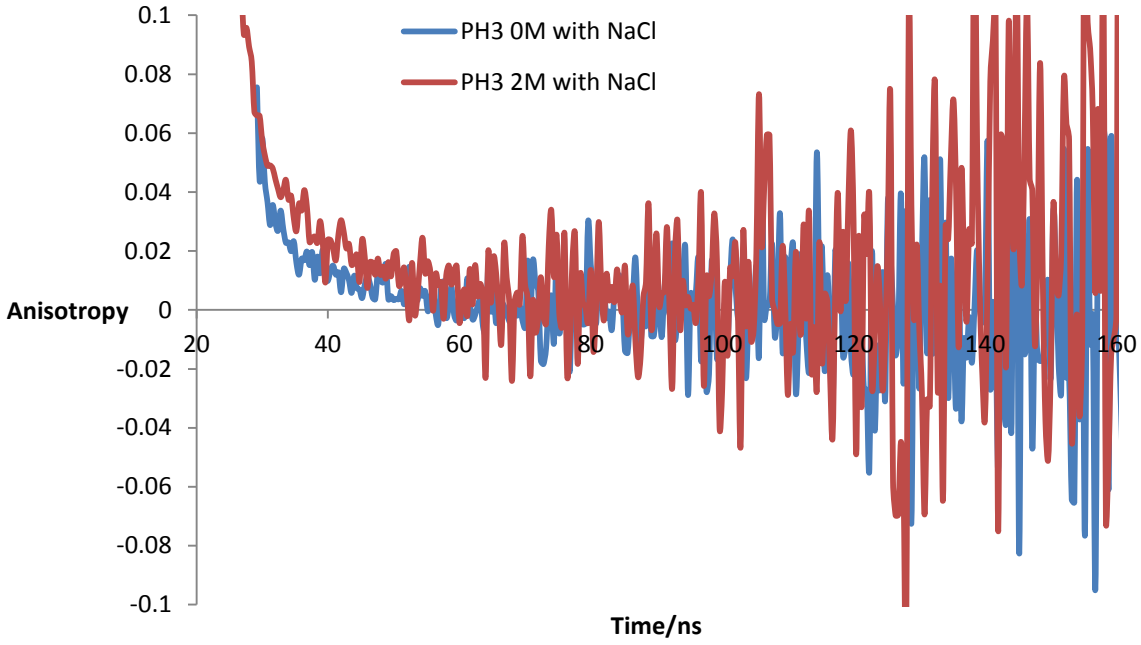

Figure 4.73 Fluorescence time resolved anisotropy data of aqueous ACE-labelled PDMAMA solution (10^{-2} wt%) in the absence of sodium chloride (blue line) and at the sodium chloride concentration of 2M at pH3 (λ_{ex}= 295 nm and λ_{em}= 340 nm).

Figure 4.73 shows the anisotropy decays of ACE- PDMAEMA in the presence and absence of NaCl at pH 3. It was found that the anisotropy decays rapidly to zero in the absence of NaCl. Conversely in the presence of the salt the anisotropy decays slowly to zero. Possibly the interaction which occurs between Cl^- ions and the charged amine group of PDMAEMA leads to the collapse of the polymer chain, which in turn inhibits the motion of the ACE-PDMAEMA chain and, therefore, a slow decay was observed.

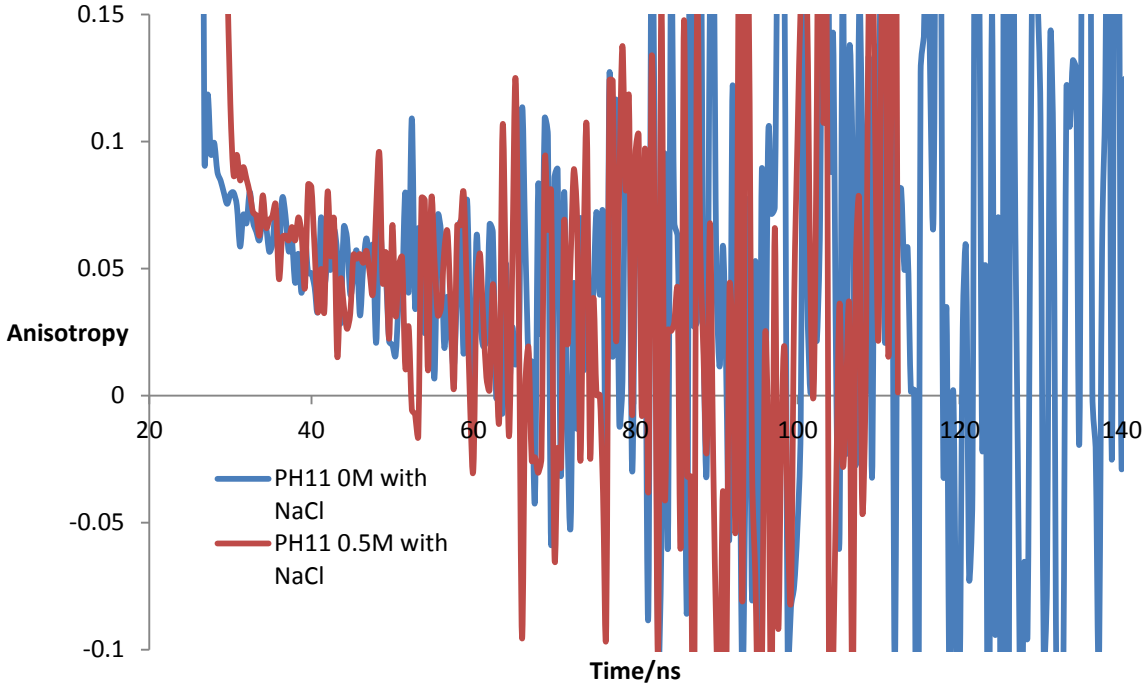

Figure 4.74 Fluorescence time resolved anisotropy data of aqueous ACE-labelled PDMAMA Solution (10^{-2} wt%) in the absence of sodium chloride (blue line) and at the sodium chloride concentration of 0.5M at pH11(λ_{ex}= 295 nm and λ_{em}= 340 nm).

Figure 4.74 a comparison of the fluorescence anisotropy decays of ACE-labelled-PDMAEMA in water in the absence and presence of NaCl at pH11 which shows that the anisotropy in the absence of the salt takes longer to decay to zero than in the presence of NaCl. This photophysical behaviour provides evidence of opening the polymer coil when a small amount of salt is added under basic conditions. Hence, only a short period of anisotropy decay was observed.

It has been reported that the addition of a small amount of NaCl increases the upper critical solution temperature (UCST), similar to polyelectrolyte systems, while the presence of an excess amount of NaCl leads to a decrease in the UCST, attributed to the antipolyelectrolyte effect of polyampholytes [69].

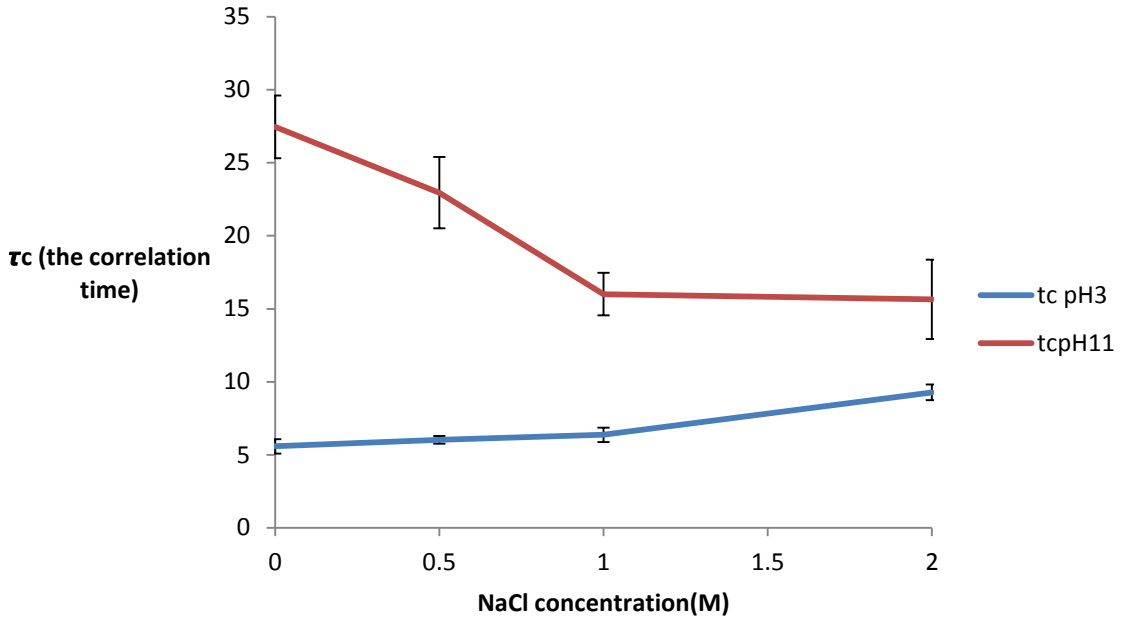

Figure 4.75 A plot of the correlation between time and NaCl concentration for two ACE labelled PDMAEMA samples in aqueous solution at two different pH values when excited at 290nm and observed at 340nm.

The τ_c derived from mathematical analysis of anisotropy decays of ACE-PDMAEMA were best fitted using a single exponential function to determine the correlation time values in nanoseconds. The τ_c data were then plotted in Figure 4.75 as a function of both pH and NaCl content.

There was an increase in the correlation times at pH3 upon the addition of salt to the ACE-PDMAEMA. This could indicate that the segmental motion of the polyelectrolyte is decreased,

given that an increased τ_c indicates a longer time before anisotropy is lost and thus slower segmental motion in the PDMAEMA.

On the other hand, correlation times at pH11 showed a decrease upon addition of 0.5 M and 1 M salt to the system, indicating that the polymer undergoes a conformational expansion. The τ_c value showed no further decrease when increasing amounts of salt were added (2 M) suggesting that the polymer chain may start to recoil.

4.2.4 Fluorescence steady state spectra of ACE- AMMA labelled PDMEAMA in the presence of $CaCl_2$ as a function of pH

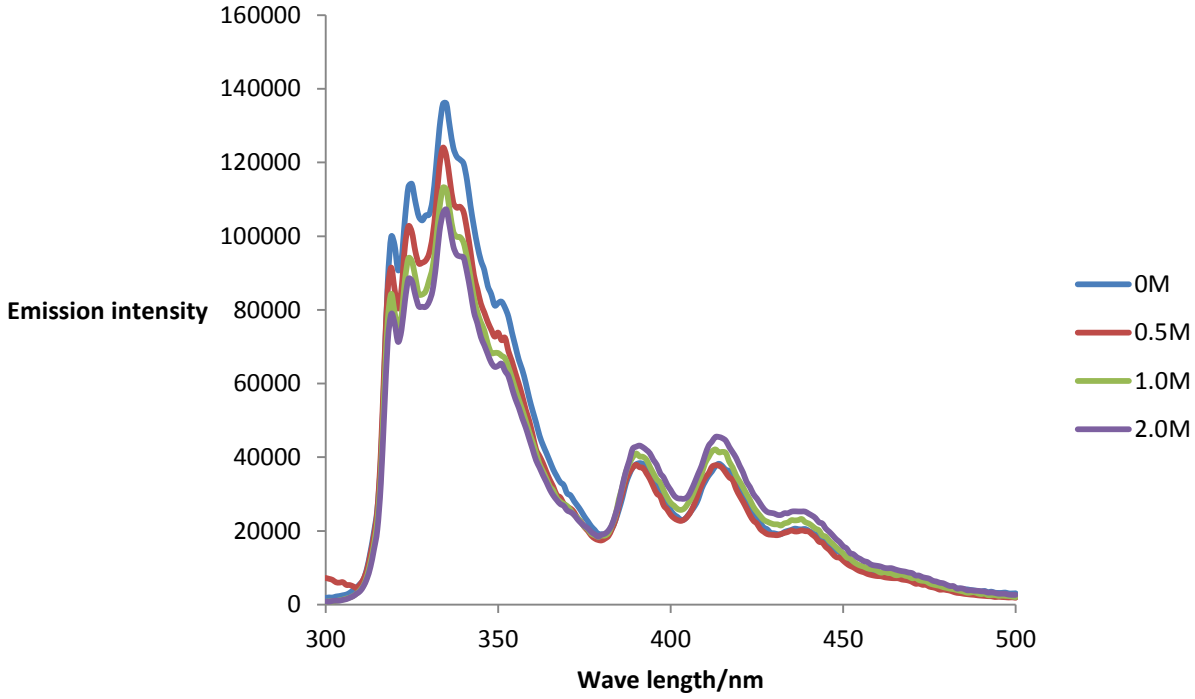

Figure 4.76 Emission scan in a range equal to 300-500 nm at fixed excitation λ_{ex}= 290 nm for ACE-AMMA- PDMEAMA sample in an aqueous solution at pH3 and varying $CaCl_2$ concentrations.

The addition of calcium chloride to a sample of doubly labelled PDMAEMA in aqueous solution at pH 3 showed a decrease in the emission intensity of the donor consistent with an increase in the emission intensity of the acceptor as [$CaCl_2$] was increased (Figure 4.76). This indicates that the salt induces polymer coiling which in turn enhances the energy transfer from donor to the acceptor. The emission intensity changed upon addition of $CaC1_2$ to ACE-AMMA-PDMAEMA and these were bigger than the changes seen upon addition of NaCl to the same polymer as was seen in figure 4.65.

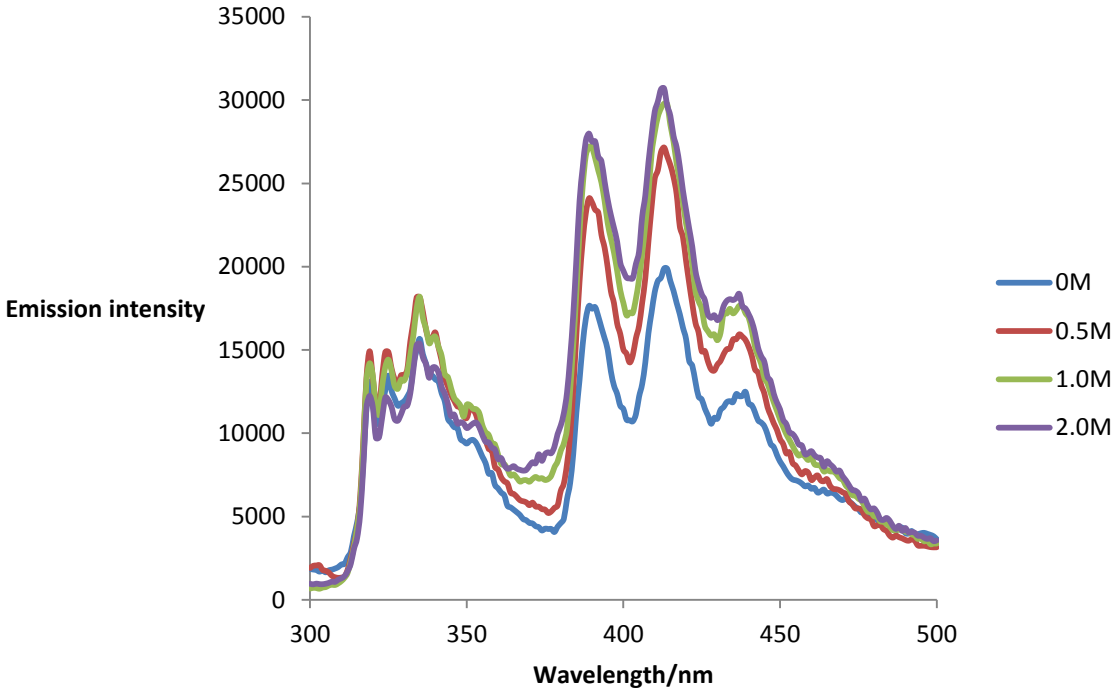

Figure 4.77 Emission scan in a range equal to 300-500 nm at a fixed excitation λex= 290 nm for ACE-AMMA- PDMEAMA samples in aqueous solution at pH11with varying $CaCl_2$ concentrations.

At pH 11 the decrease in the emission intensity of the ACE was consistent with an increase in the emission intensity of the AMMA become more substantial (compared to that at pH 3) upon addition of salt, indicating that there was an increase in energy transfer due to an increase in the degree of coiling of the polyelectrolyte. This further confirmed that increasing the [$CaCl_2$] aided macromolecule contraction.

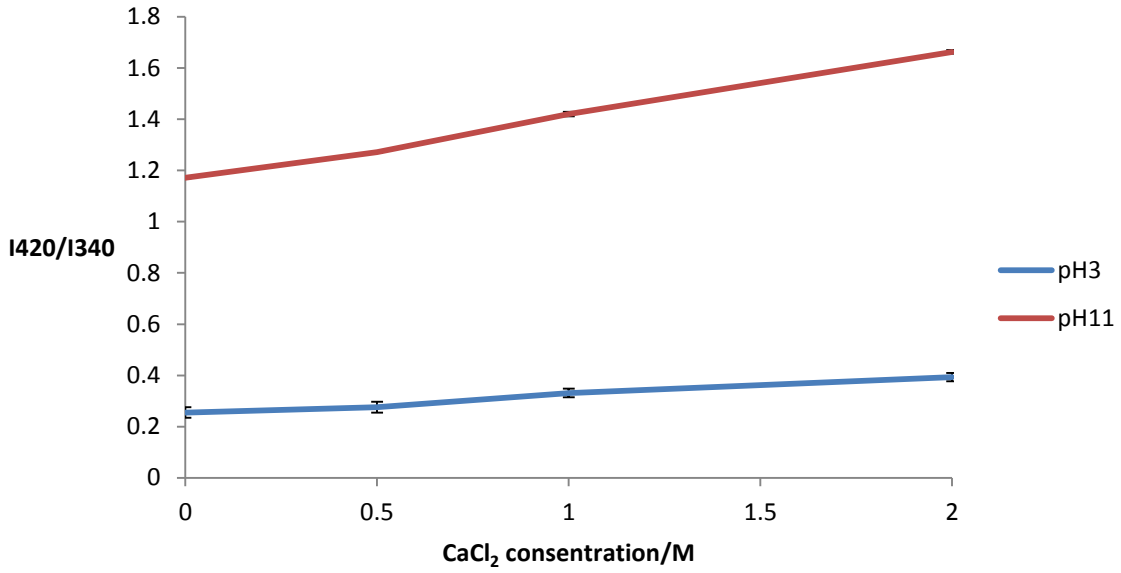

Figure 4.78 The fluorescence emission intensity ratio, IA/ID of 10^{-2} wt % ACE-AMMA-labelled PDMEAMA as a function of $CaCl_2$ concentration at pH3 and pH11 (λ_{ex} = 290nm).

Figure 4.78 shows the fluorescence intensity ratio as a function of the $CaCl_2$ concentration at a low and high pH respectively.

The acceptor to donor ratio slightly increased as the [$CaCl_2$] increased at pH3 which suggests that the macromolecule chain collapses when Cl^- ions are added.

In particular, at 2 M $CaCl_2$ the ratio was at maximum ~0.39 indicating ~39% efficiency of energy transfer in the coiled form of the PDMAEMA chain, since at these extremely concentrated values of Cl^- ions several positively charged amine groups are screened by chlorine .When the transition in conformation occurs at 0.5 and 1 M $CaCl_2$, a noticeable increase in the IA/ID ratio was observed which suggests that a few of the amine groups become neutralised and hence lead to the conversion of the expanded chain to a relatively aggregated form. It can be seen from the curve at pH11 that the fluorescence intensity ratio increases as the $CaCl_2$ concentration increases, this shows that the polymer chain is more coiled in the presence of salt, since the separation distance between the labels becomes shorter.

4.2.5 Fluorescence excited state lifetimes of singly and doubly labelled PDMAEMA in the presence of $CaCl_2$ as a function of pH.

The τ_f data for a single and double labelled PDMAEMA sample in the presence of [$CaC1_2$] at various pH values is also best modelled by a triple exponential as in equation 3.5 which provides an χ^2 value close to unity as well as a small S.D. for the resulting τ_f values. Again these are expressed in figures 4.79 and 4.81 as average lifetime values for simplicity of comparison.

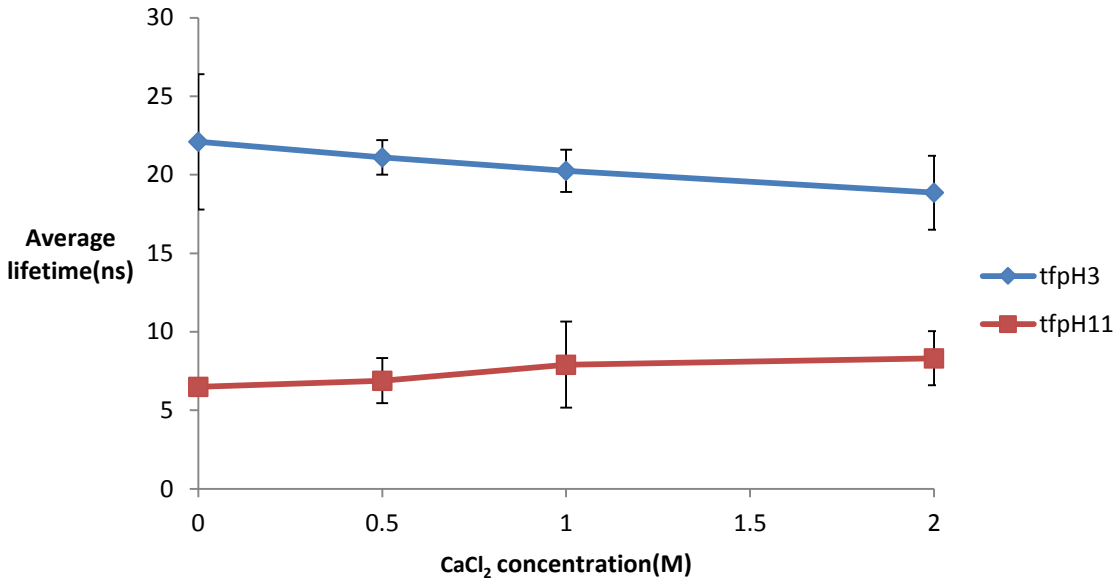

Figure 4.79 A plot of the average lifetime values obtained for ACE-PDMAEMA in aqueous solution at two different pH values with increasing $CaCl_2$ concentration when excited at 290 nm and observed at 340 nm.

Addition of calcium chloride shows an increase in the lifetime value of the ACE label as [$CaCl_2$] was increased at a high pH. This would indicate that the presence of salt in some way shields ACE-PDMAEMA from quenching by the amine groups.

On the other hand, the general effect with increasing the salt concentration at low pH is a decrease in the lifetime indicating a collapse of the polymer chain as the [$CaC1_2$] increases. This suggests that the ionised groups of the expanded polymer become neutralised by Cl^- ions and hence lead to the collapse the polymer, which in turn causes quenching by amine groups.

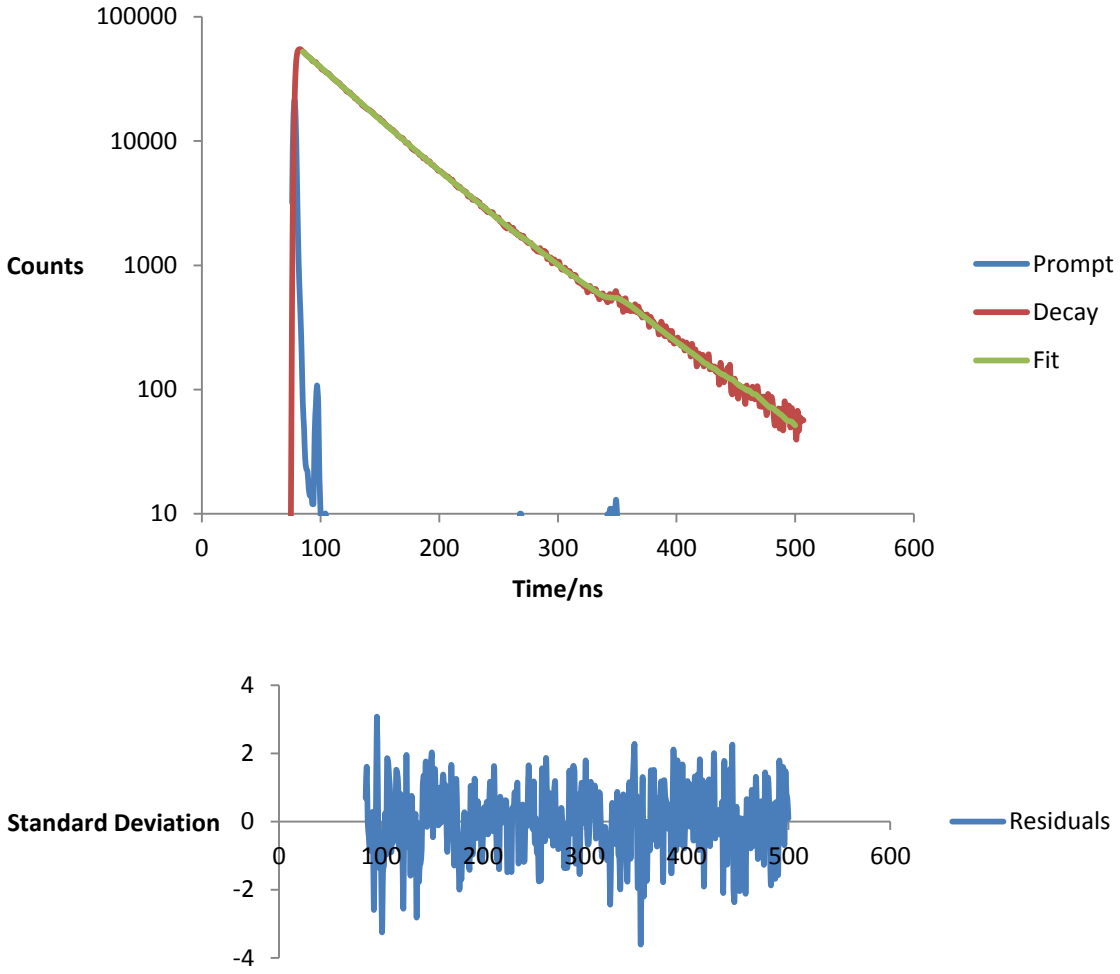

Figure 4.80 Fluorescence decay with corresponding mathematical fit (shown in green) and a plot of the resulting residuals for ACE-PDMAEMA in an aqueous solution at pH3 with 0.5M $CaCl_2$.

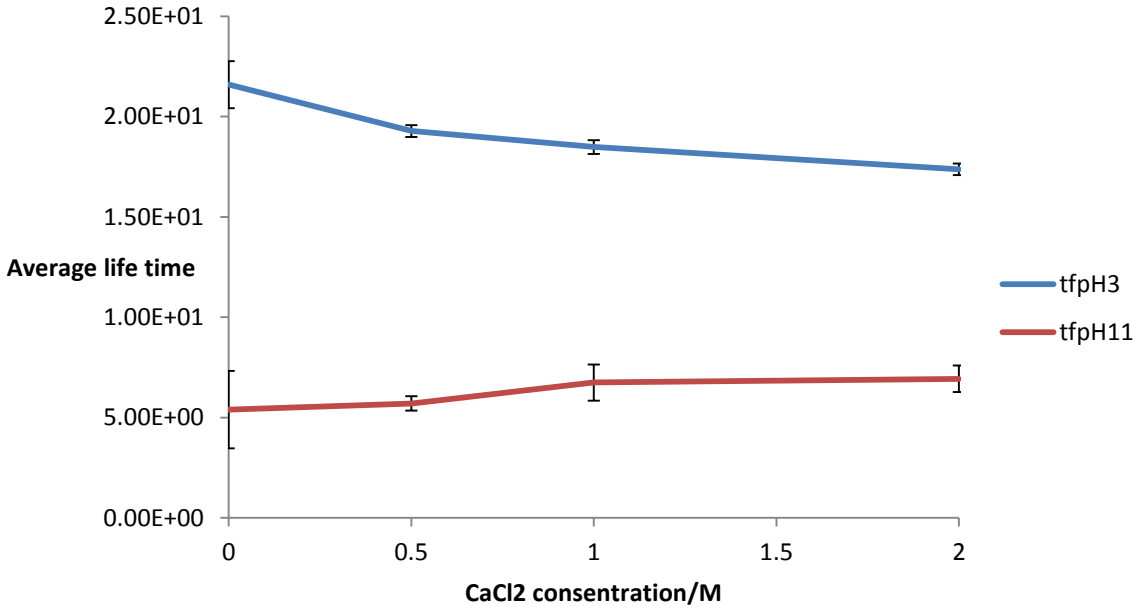

Figure 4.81 A plot of the average lifetime values obtained for ACE-AMMA-PDMAEMA in aqueous solution at two different pH values with increasing $CaCl_2$ concentration when excited at 290 nm and observed at 340 nm.

Figure 4.81 shows the average donor lifetime for ACE-AMMA-PDMAEMA in acidic and basic conditions as a function of the $CaCl_2$ concentration.

As shown in the previous system (single labelled PDMAEMA) there was a decrease in the average lifetime values over the whole range of salt concentrations at low pH and an increase in these values as the salt concentration was increased at high pH levels. However, the rate of decrease and increase in the average lifetime values at pH3 and pH 11 in double labelled PDMAEMA was less than those in single labelled PDMAEMA. These differences could be due to the fact that energy transfer occurs between these two labels. This phenomenon is a result of a collapse of the polyelectrolyte caused by adding $CaCl_2$ in an acidic solution resulting in a more coiled polymer chain formed by adding calcium chloride to the basic medium.

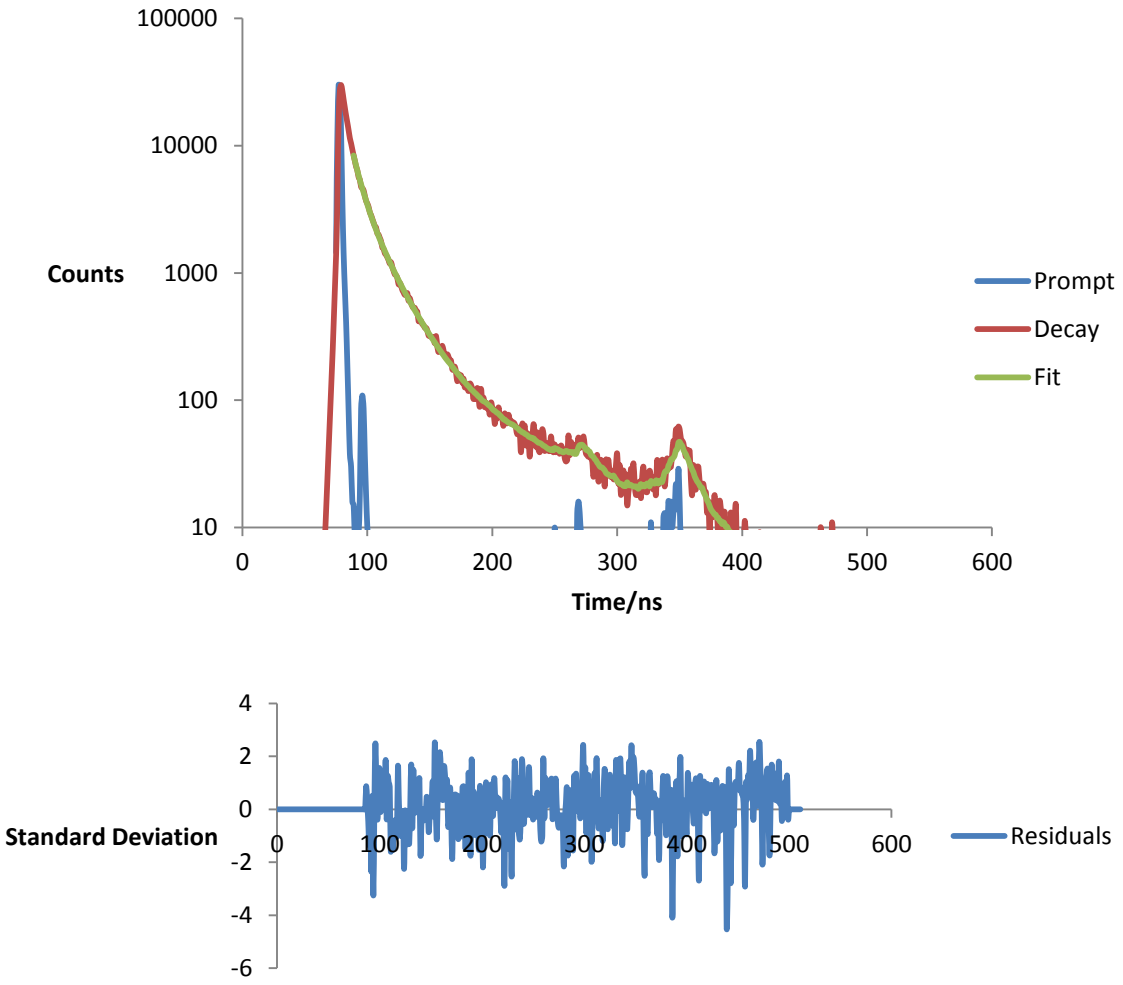

Figure 4.82 Fluorescence decay with corresponding mathematical fit (shown in green) and a plot of the resulting residuals for ACE-AMMA-PDMAEMA in an aqueous solution at pH11 with 2M $CaCl_2$

Figure 4.83 shows the calculated distance values between the ACE and AMMA labels in the double label polyelectrolyte system at varying salt concentrations and pH values.

The label distance at low pH shows a substantial decrease upon addition of small amounts of salt and then no important change in the distance as the salt concentration increases. This indicates that the polymer collapses at acidic media in the presence of salt.

It is worthy to note that at pH 3 the r value between labels is shorter in the presence of $CaCl_2$ than the r value in the presence of NaCl. This indicates that Ca^+ ions have more of an effect on PAA aggregation compared to Na^+ions.

On the other hand at pH 11 the distance between labels displays no important change upon addition of salt which indicates that the polymer still exists in the coiled conformation in the presence of $CaCl_2$.

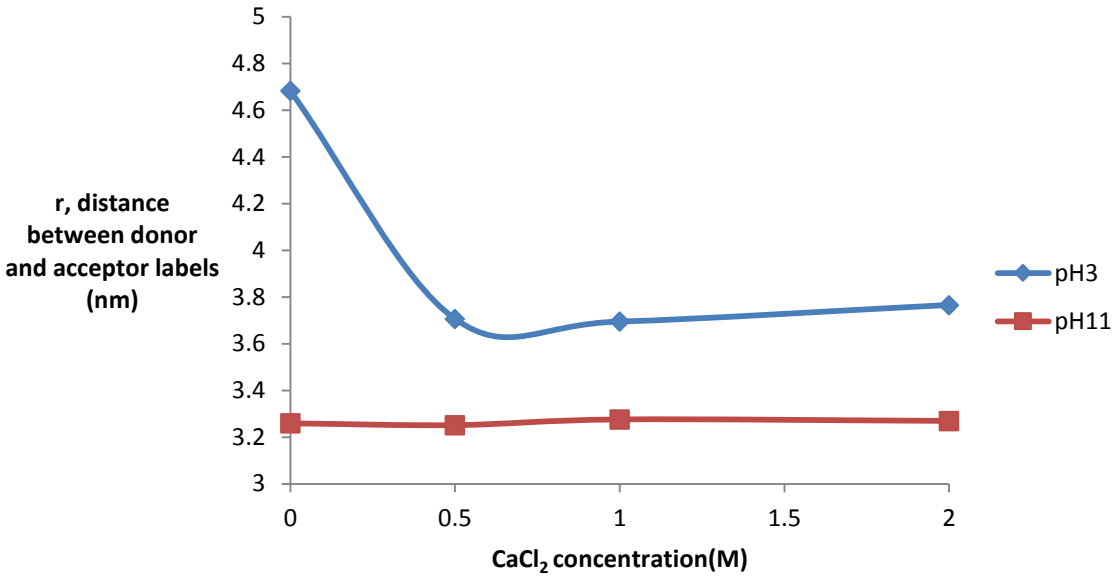

Figure 4.83 A plot of the value r, the distance between ACE (donor) and AMMA (acceptor) labels, as calculated by equation 3.7 for single and double -PDMAEMA across a range of pH values and $CaCl_2$ concentrations.

4.2.6 Fluorescence time-resolved anisotropy measurements (TRAMS) of ACE-PDMAMA in the presence of $CaCl_2$ as a function of pH

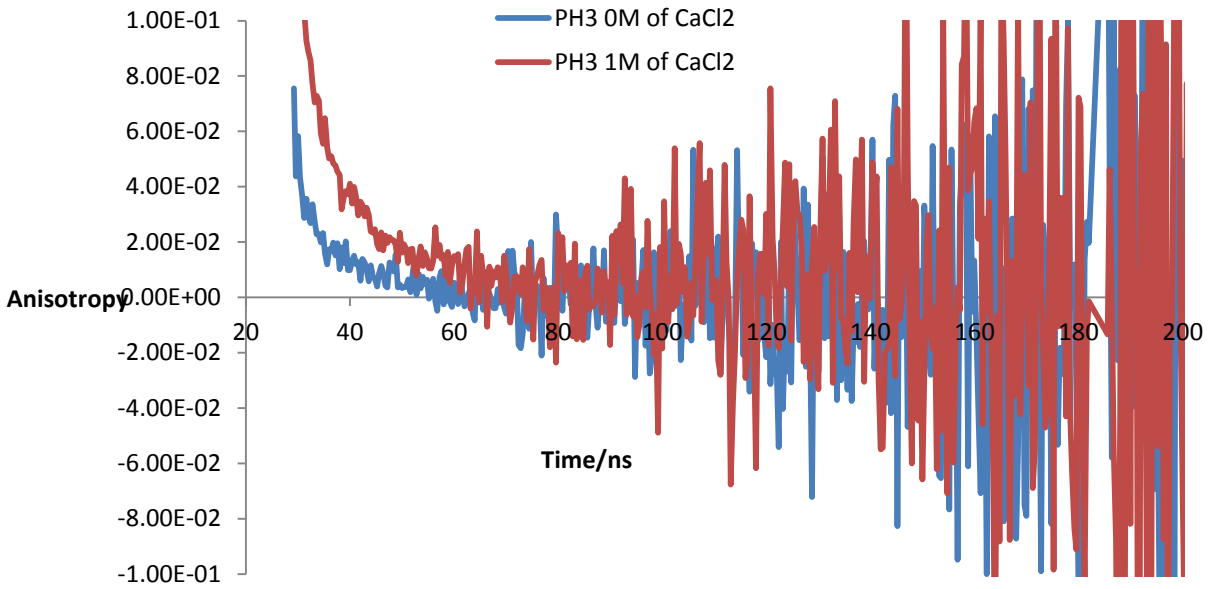

Figure 4.84 Fluorescence time resolved anisotropy data of aqueous ACE-labelled PDMAMA solution (10^{-2} wt%) in the absence of calcium chloride (blue line) and at the calcium chloride concentration of 1 M at pH 3 (λ_{ex}= 295 nm and λ_{em}= 340 nm).

Figure 4.84 matches the anisotropy decays of ACE- PDMAEMA in the presence and absence of $CaCl_2$ at pH 3. It was found that the anisotropy decays rapidly to zero in the absence of $CaCl_2$. When 1 M salt was added the anisotropy decayed slowly to zero. This could be attributed to the neutralisation of amine groups by linking with Cl^- ions which leads to the aggregation of the cationic polymer chain and therefore a slow decay was observed.

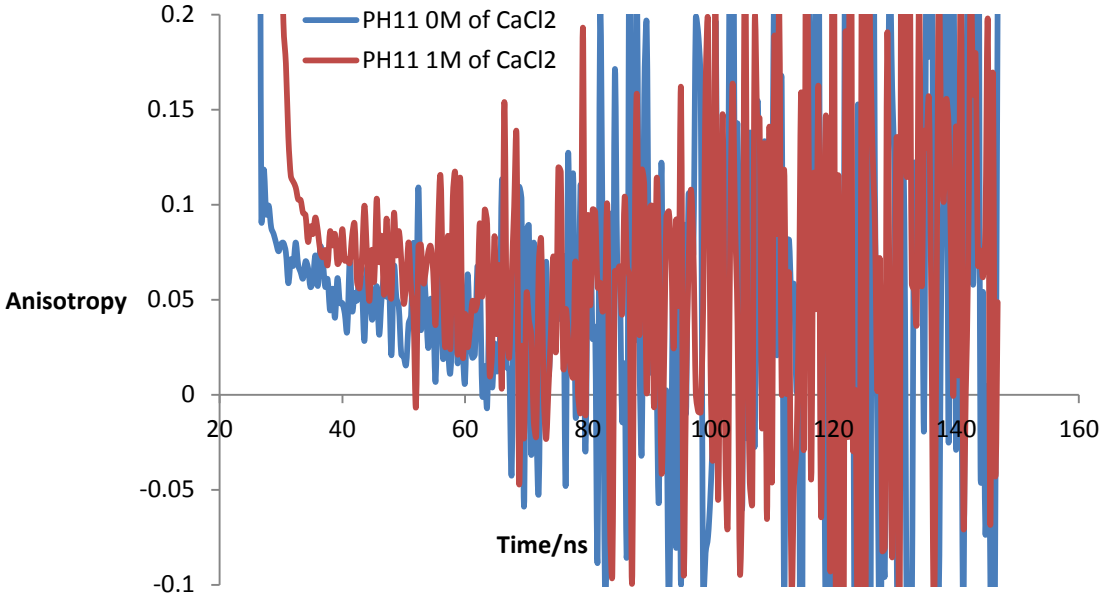

Figure 4.85 Fluorescence time resolved anisotropy data of aqueous ACE-labelled PDMAMA solution (10^{-2} wt%) in the absence of calcium chloride (blue line) and at the calcium chloride concentration of 1M at pH11(λex= 295 nm and λem= 340 nm).

Figure 4.85 compares the fluorescence anisotropy decays of ACE-labelled-PDMAEMA in water in the absence and presence of $CaCl_2$ at pH11, and shows that the anisotropy in the absence of salt decays shorter to zero than in the presence of $CaCl_2$. This photophysical behaviour is in agreement with ET experiment that confirmed there is an increase in coiling in the polymer chain as the concentration of salt was increased and hence a long anisotropy decay was observed.

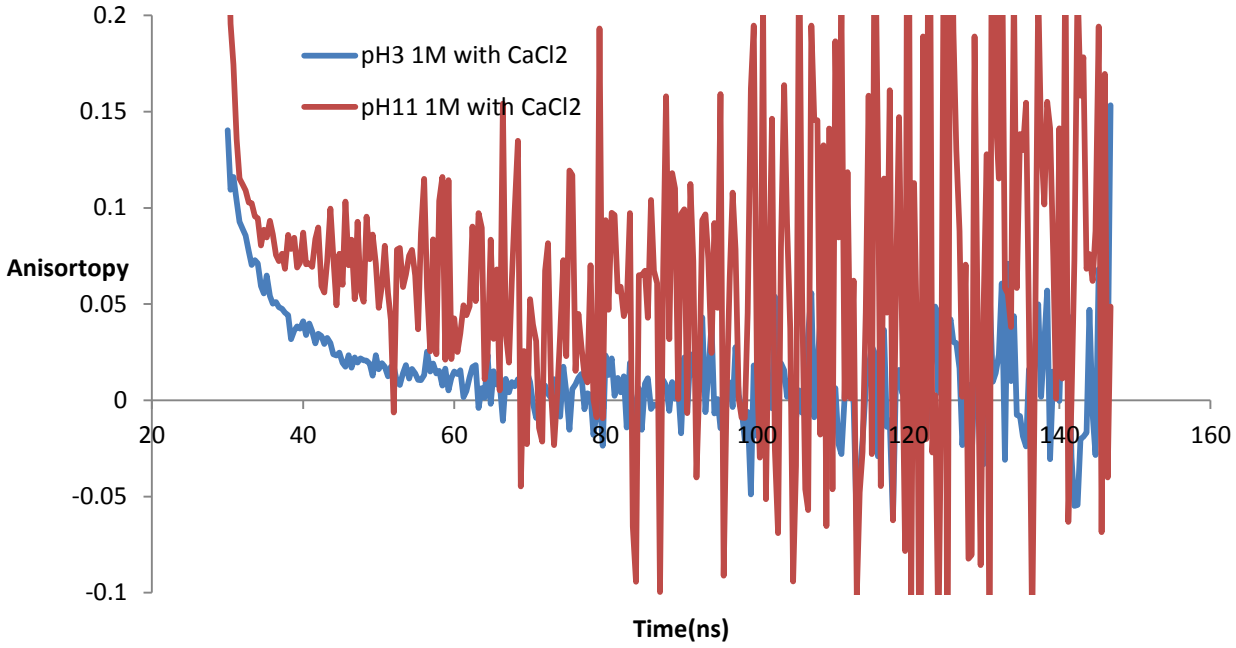

Figure 4.86 Fluorescence time resolved anisotropy data of aqueous ACE-labelled PDMAMA solution (10^{-2} wt%) at the calcium chloride concentration of 1 M at pH 3 (blue line) and at the calcium chloride concentration of 1 M at pH 11(λ_{ex}= 295 nm and λ_{em}= 340 nm).

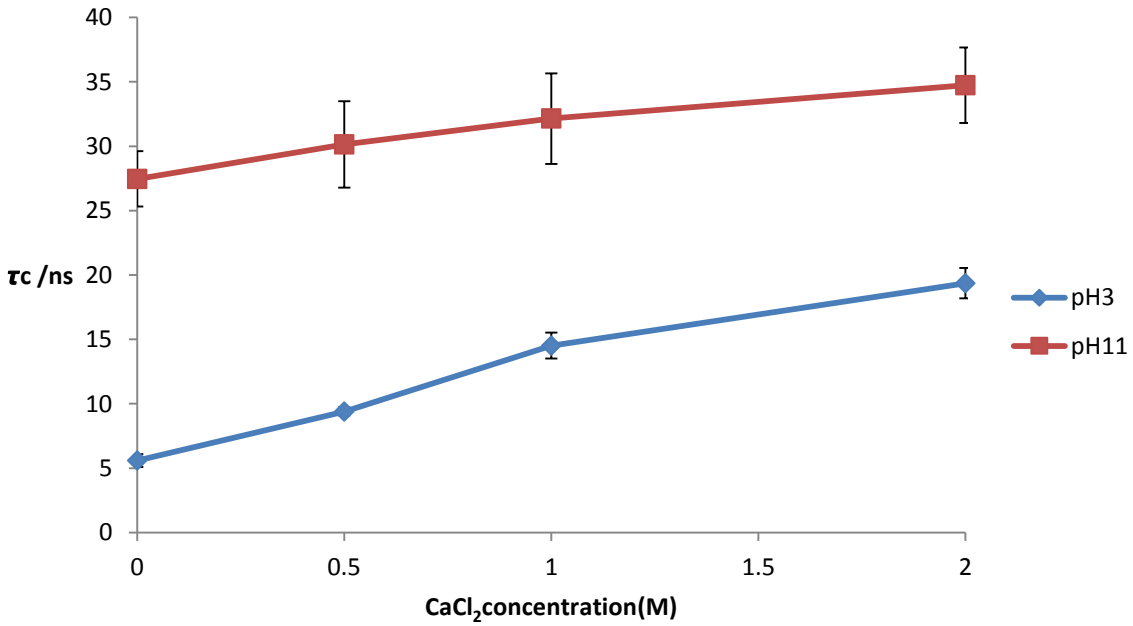

Figure 4.87 A plot of the correlation of time against $CaCl_2$ concentration for two ACE labelled PDMAEMA samples in aqueous solution at two different pH values when excited at 290nm and observed at 340nm.

Figure 4.87 presents the plots of correlation time with respect to the concentration of $CaCl_2$ added to the ACE-PDMAEMA solutions at pH 3 and 11. A marked increase of correlation times (ca.~5.57 to ~ 19.3 ns) with increasing concentration of $CaCl_2$ was recorded at pH 3, whereas a smaller increase was noted at pH 11. However,(as also seen in figure 4.86) over the entire concentration range the increment in τc values at pH 11 is higher than in those at pH 3. The possible effect of Cl^- anions at pH 3 is a shielding effect on the electrostatic repulsions between the cationic amine groups in polyelectrolyte. This may lead to the screening of the electrostatic repulsion in the entire polymer chain. As a result, the collapsed PDMAEMA chains move slower than the expanded form.

4.2.7 Fluorescence steady state spectra of ACE- AMMA labelled PDMEAMA in the presence of NaBr as a function of pH.

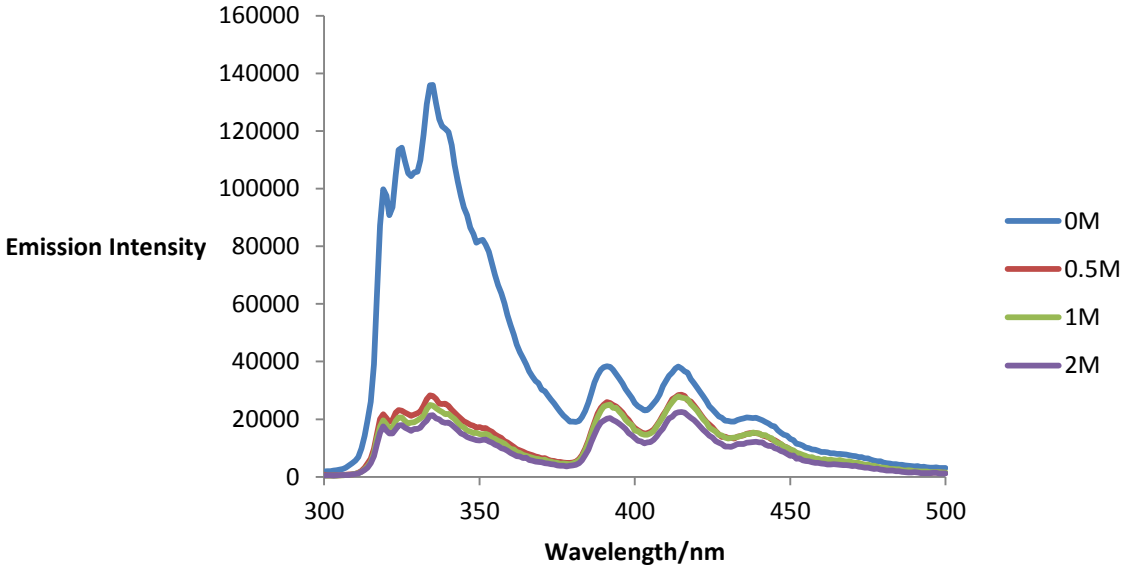

Figure 4.88 Emission scan in a range equal to 300-500 nm at fixed excitation λ_{ex}= 290 nm for ACE-AMMA- PDMEAMA sample in aqueous solution at pH 3 and varying NaBr concentration.

The emission intensity for the fluorescence from the acceptor decreased in going from low to high [NaBr] in a manner similar to that of the ACE labelled sample. This infers that energy is being transferred from the ACE label to the AMMA label because of the collapsing happened by charge screening by Br^- ions, as quenching from the neutralised amine groups of the polymer should affect both labels to the same extent.

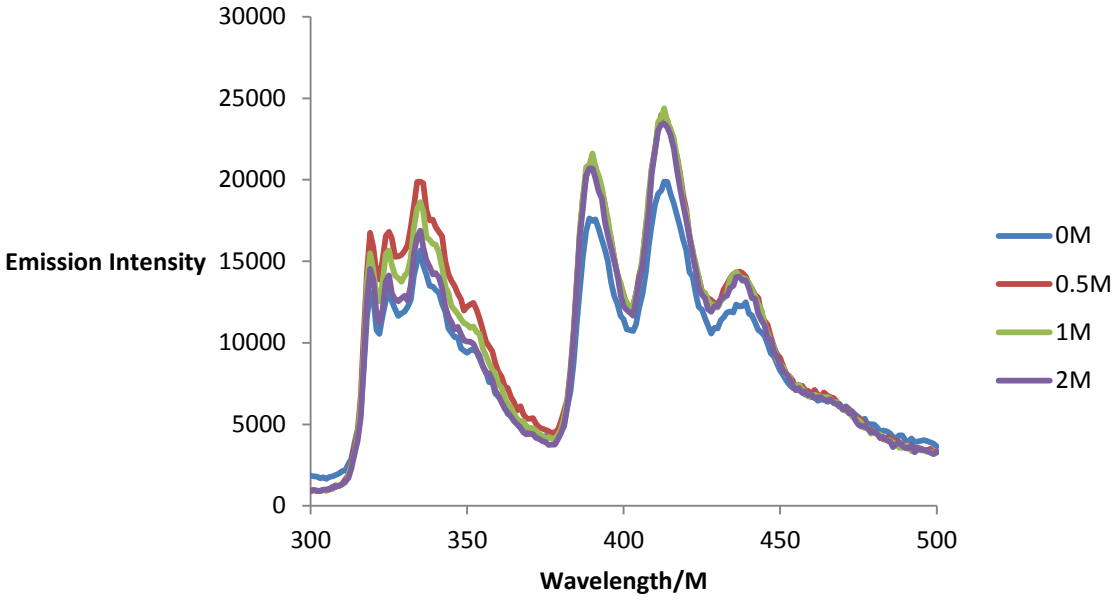

Figure 4.89 Emission scan in a range equal to 300-500 nm at fixed excitation λ_{ex}= 290 nm for ACE-AMMA- PDMEAMA sample in aqueous solution at pH 11and varying NaBr concentrations.

However, at pH 11 (see figure 4.89) there is very slight increase in the ACE emission at the initial concentration of salt, consistent with an increase in the AMMA emission.

This indicates that the addition of a small amount of the salt to a coiled form of the polyelectrolyte leads to a slight opening of the coiled polymer, hence, the donor and the acceptor become far from the amine group which then leads to an enhancement in fluorescence intensity for both of the labels. The emission intensity for the donor then started to drop when a higher amount of salt was added (i.e. at 1 M and 2 M) while it was enhanced for the acceptor to slightly more than was observed in the absence of salt. This signifies that the polymer chain starts to coil again at even higher concentrations of sodium bromide.

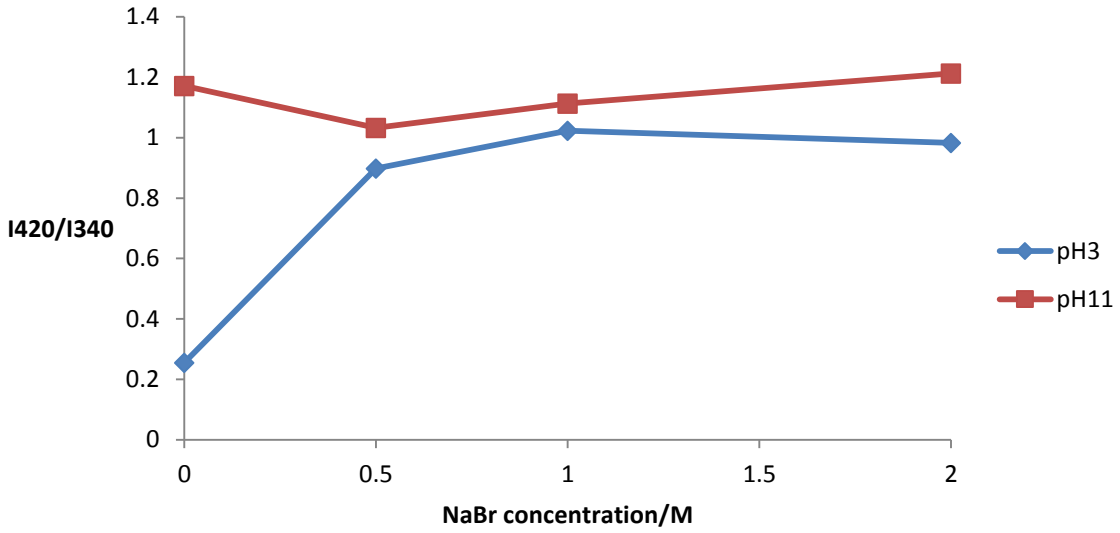

Figure 4.90 Fluorescence emission intensity ratio, IA/ID of 10-2 wt % ACE-AMMA-labelled PDMEAMA as a function of the NaBr concentration at pH3 and pH11 (λex = 290nm).

Figure 4.90 shows the fluorescence intensity ratio as a function of the NaBr at a low and high pH respectively.

That the acceptor to donor ratio slightly increases as the [NaBr] increases at pH 3 suggests that the macromolecule chain collapses when Br-ions are added.

In particular, at 0.5 M NaBr the ratio increases to ~0.89 indicating ~89% efficiency of energy transfer in the coiled form of the polymer chain. This ratio was maximum ~0.98 at 2 M indicating a ~98% efficiency of energy transfer, since at these extremely concentrated values of Br- ions several positively charged amine groups are screened by bromine. It is significant to note that the effect of the larger anion (Br^{-1}) in case of NaBr make the polymer more coiled than the smaller anion (Cl^{-1}) in the case of NaCl (as it showed only ~29% efficiency of energy transfer, figure 4.67).

The effect of increasing ion size on the structure and water content of polyelectrolyte multilayers has been reported in the literature [70]. It was found that the thickness of the multilayers of prepared poly(diallyl dimethyl ammonium chloride) (PDADMAC) using different sodium salts (NaF, NaCl,NaBr) at an ionic strength of 0.25 M increased in the order of F < Cl < Br [71-72].

On the other hand in basic media when the polymer exists in a collapsed form, the addition of a small amount of the salt decreased the I420/ I340 ratio indicating that the polymer chain was opened slightly. This ratio value rose again at 1 M and 2 M indicating that the

polymer started to coil again and the energy transfer between the donor and acceptor labels increase slightly more than that observed in the system in the absence of NaBr.

4.2.8 Fluorescence excited state lifetimes of singly and doubly labelled PDMAEMA in the presence of NaBr as a function of pH

The fluorescence decay from single and double labelled PDMAEMA in basic and acidic conditions and where sodium bromine concentrations were increased show good statistical fits to a triple exponential analysis using equation 3.5 (see figure 4.92, 4.94 as a selective sample). The subsequent lifetime values were obtained using equation 3.3. This lifetime data was then plotted in figure 4.91, 4.93 for comparative purposes.

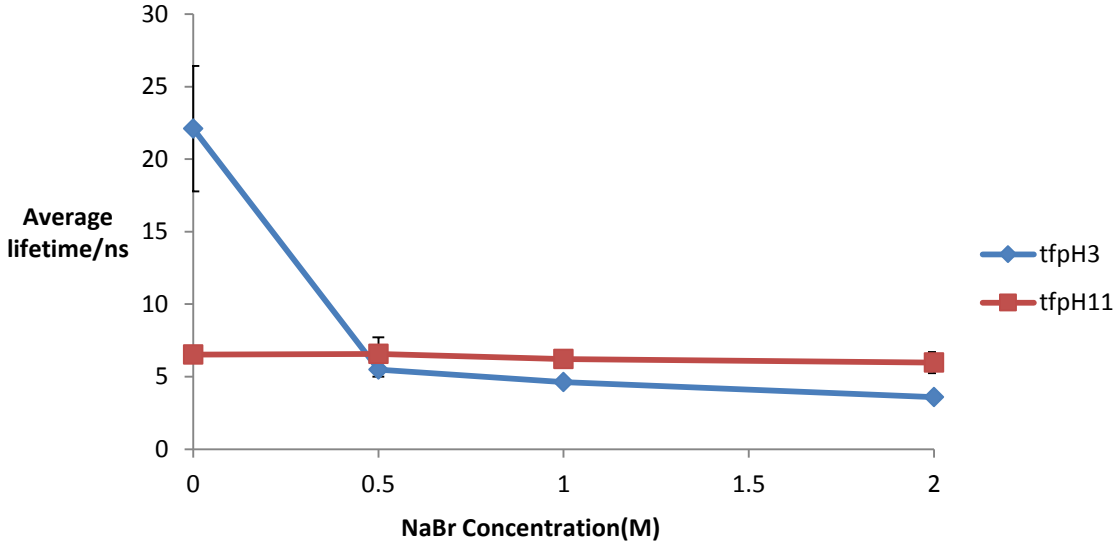

Figure 4.91 A plot of the average lifetime values obtained for ACE-PDMAEMA in aqueous solution at two different pH values with increasing NaBr concentrations when excited at 290 nm and observed at 340 nm.

It can be seen that initially adding sodium bromide (0.5 M) to ACE-PDMAEMA solution at pH 11 caused a minor increase in the lifetime value indicating that the coiled polymer expanded slightly and this is consistent with the observation from steady state experiments. At even higher concentrations of salt (1 M and 2 M) the reading of the life time value give the same value or even less compared to those obtained of the polymer system in the absence of the salt. This suggest that the polymer starts to coil again at

addition of a higher concentrations of salt given that quenching in the lifetime due to the fact that it is closer to the amine group.

On the other hand at a low pH there was a significant decrease in the average lifetime value upon initial addition of NaBr but then there was no change in the τ_f as the salt concentration was increased further, indicating an increase in fluorescence quenching of the label. The most likely cause was charge screening by the bromine induced a collapse in the polymer chain increasing the contact between the label and the polymer.

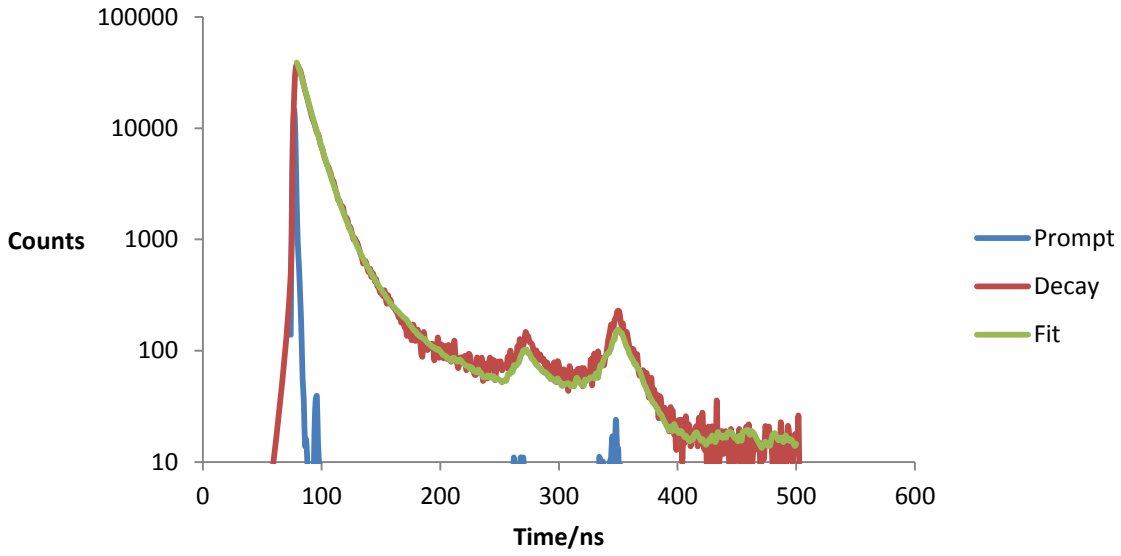

Figure 4.92 Fluorescence decay with corresponding mathematical fit (shown in green) and a plot of the resulting residuals for ACE-PDMAEMA in aqueous solution at pH 3 with 0.5 M NaBr.

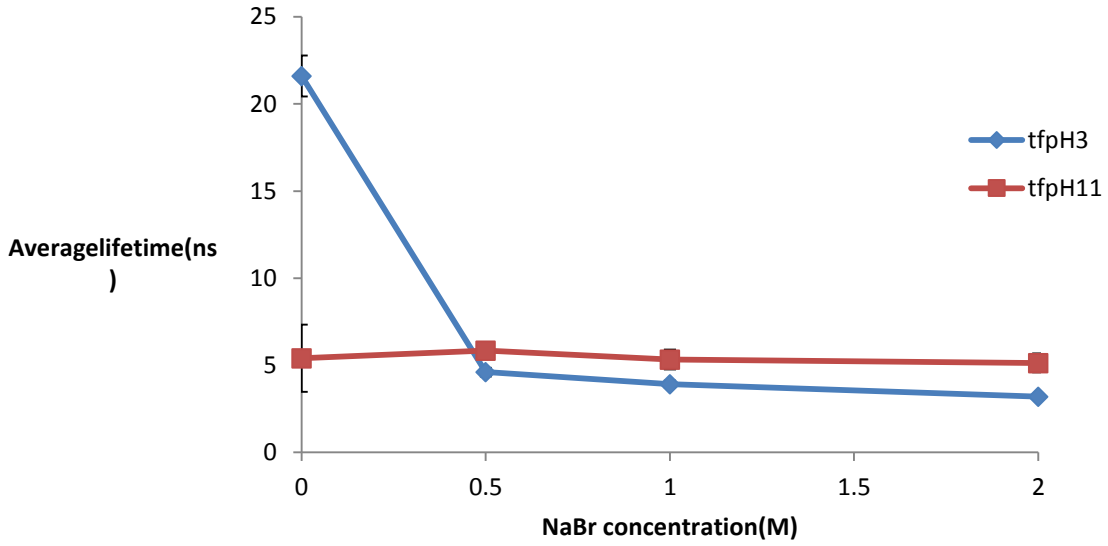

Figure 4.93 A plot of the average lifetime values obtained for ACE-AMMA-PDMAEMA in aqueous solution at two different pH values with increasing NaBr concentration when excited at 290 nm and observed at 340 nm.

The lifetime data for ACE-AMMA-PDMAEMA at low pH and NaBr concentrations (see figure 4.93) shows that there is a substantial drop in the average lifetime values compared to those obtained for the macromolecule system in the absence of salt. In addition those values were slightly less than those obtained for the single labelled system. Presumably, as the polymer coiled due to charge screening, the enhancement of the energy transfer between the donor and acceptor increased as well as the increase of the quenching by the internal group. This is in agreement with the ET experiment.

While at high pH the average lifetime value for the donor was similar to that seen with the single labelled system (in the absence of the acceptor) upon addition of a small concentration of salt. This suggests that the polymer slightly opened and the donor was slightly free from quenching by the acceptor, as well as decreasing in quenching by the amine group. Continuing adding salt made the values decrease more than those observed in the single system which indicates that the macromolecule under these conditions adopted a more coiled form compared to the coiled polymer chain in the absence of the salt.

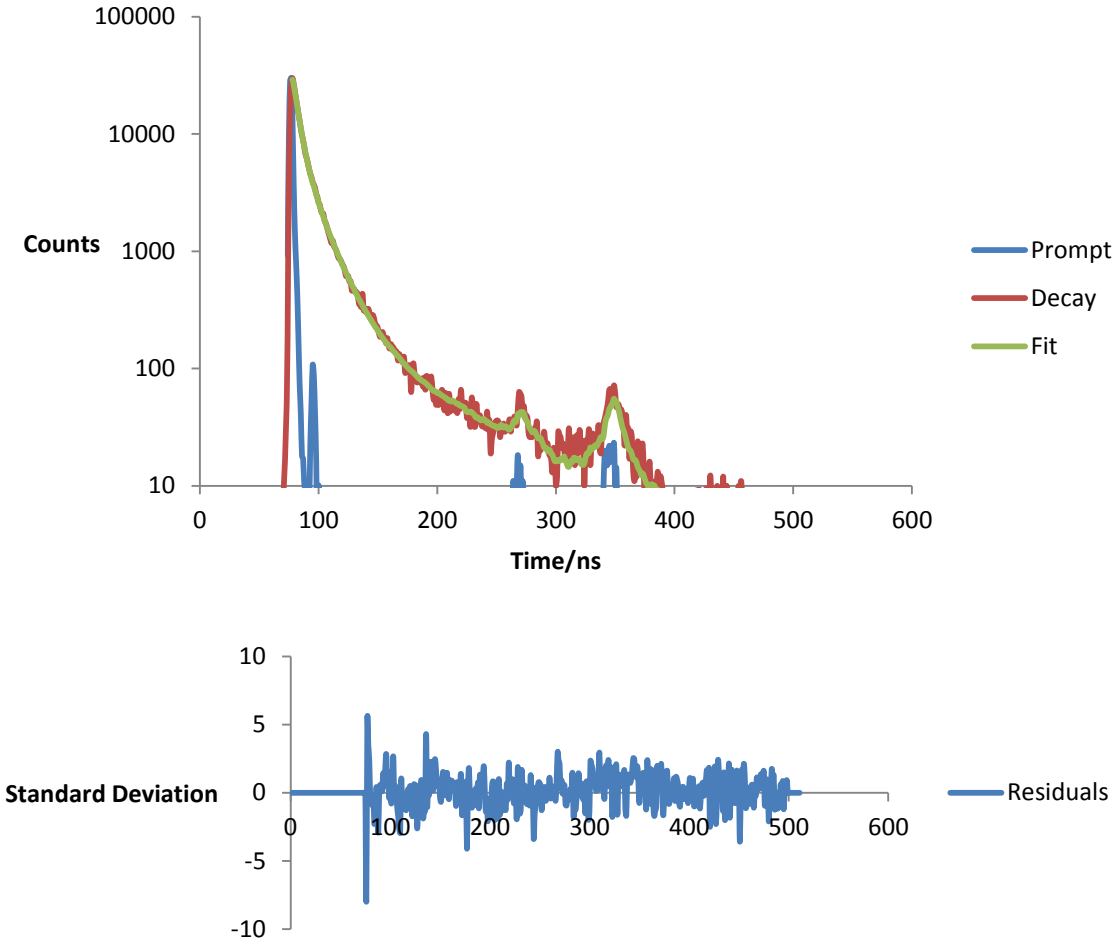

Figure 4.94 Fluorescence decay with corresponding mathematical fit (shown in green) and a plot of the resulting residuals for ACE-AMMA-PDMAEMA in aqueous solution at pH 11 with 2 M NaBr.

The average r value was then estimated for doubly labelled-PDMAEMA as a function of [NaBr] and pH via equation 3.7 and 3.8 respectively. Figure 4.95 demonstrates the calculated distance values between the ACE and AMMA labels in the double label polyelectrolyte system at varying salt concentrations and pH values.

The label distance in acidic media shows a significant decrease as might be expected given that the polymer collapses at pH3 in the presence of salt.

At pH 11 there is an initial increase in the label distance upon addition of small quantities of salt followed by a minor decease at 1 and 2 M in label distance. This observation supports the results that have been demonstrated by previous fluorescence techniques.

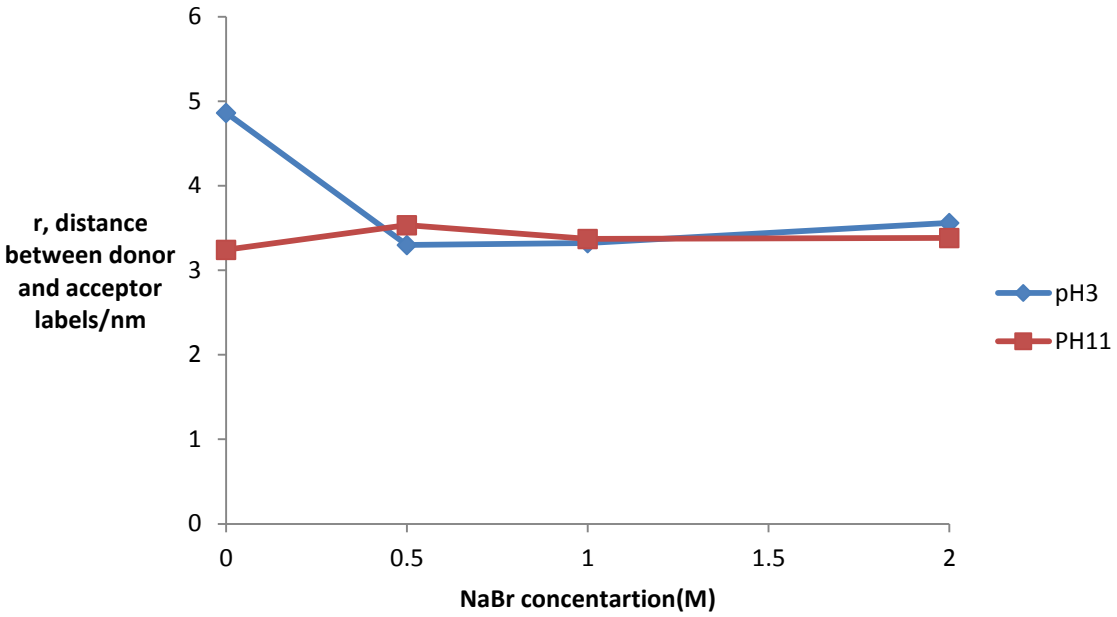

Figure 4.95 A plot of the value r, the distance between ACE (donor) and AMMA (acceptor) labels, as calculated by equation 3.7 for single and double -PDMAEMA across a range of pH values and NaBr concentrations.

4.2.9 Fluorescence time-resolved anisotropy measurements (TRAMS) of ACE-PDMAMA in the presence of NaBr as a function of pH

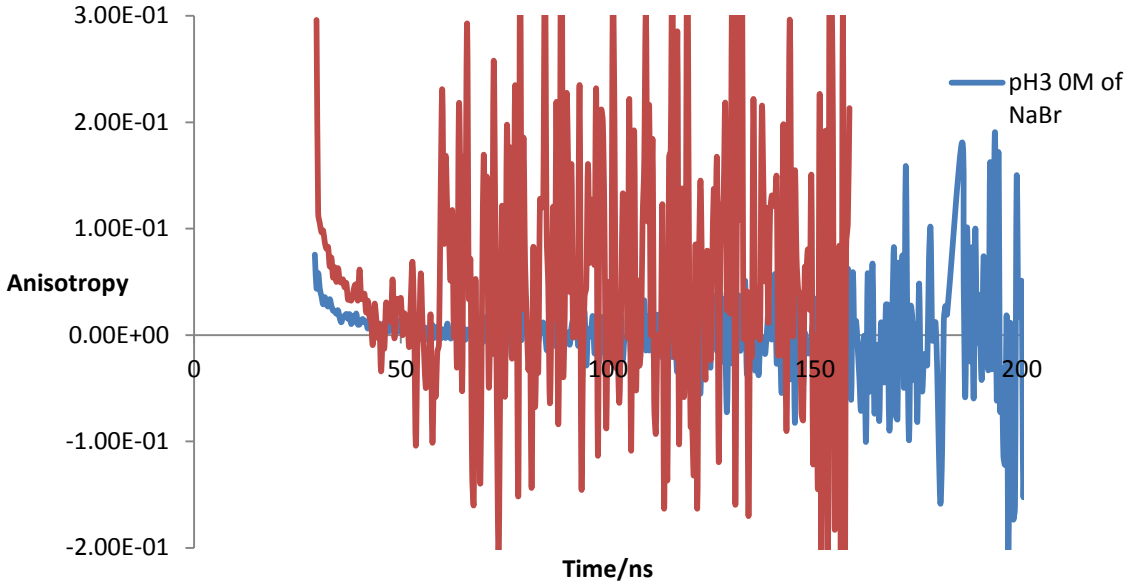

Figure 4.96 Fluorescence time resolved anisotropy data of aqueous ACE-labelled PDMAMA solution (10^{-2} wt%) in the absence of sodium bromide (blue line) and at a sodium bromide concentration of 2M at pH3 (λ_{ex}= 295 nm and λ_{em}= 340 nm).

Figure 4.96 illustrates the fluorescence anisotropy decay of ACE-PMAEMA in water in the absence and presence of sodium bromide. It was found that the anisotropy quickly drops to zero in the absence of sodium bromide while in the presence of salt the anisotropy decays slowly to zero. These results assume that the charge screening by Br- ions leads to the collapse of the macromolecule chain, which would slow down the segmental motion of the fluorescently labelled polymer and hence a long anisotropy decay is observed in the presence of NaBr.

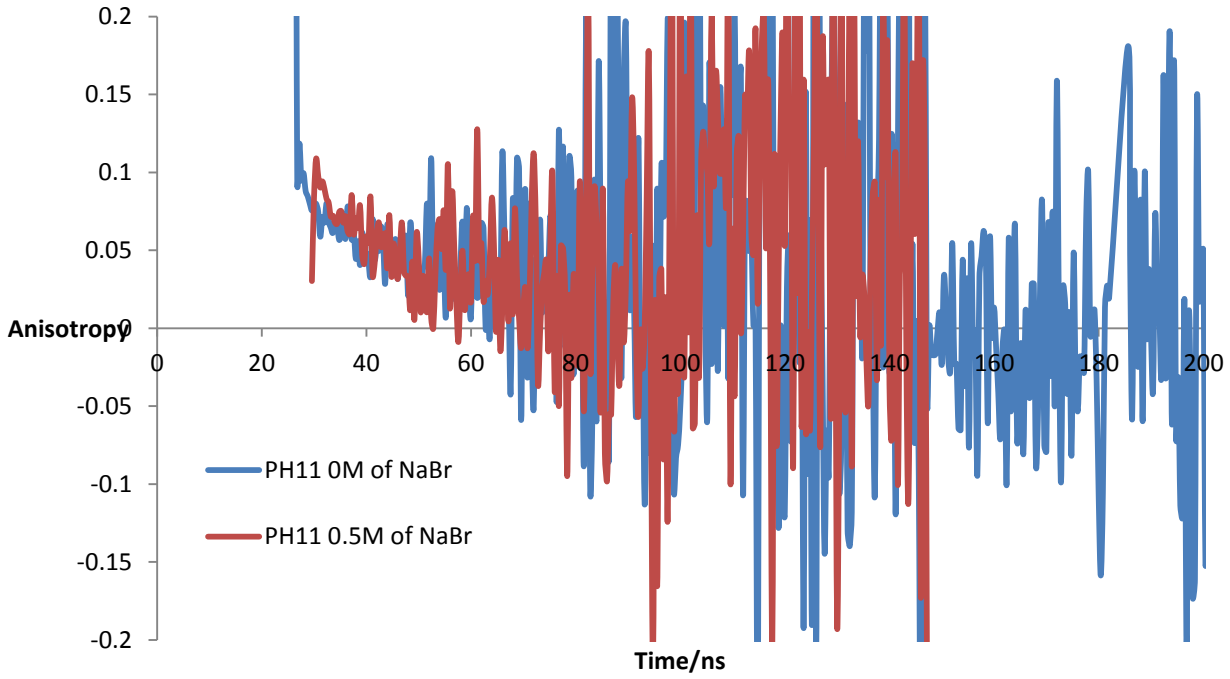

Figure 4.97 Fluorescence time resolved anisotropy data of an aqueous ACE-labelled PDMAMA solution (10^{-2} wt%) in the absence of sodium bromide (blue line) and at the sodium bromide concentration of 0.5M at pH11 (λ_{ex}= 295 nm and λ_{em}= 340 nm).

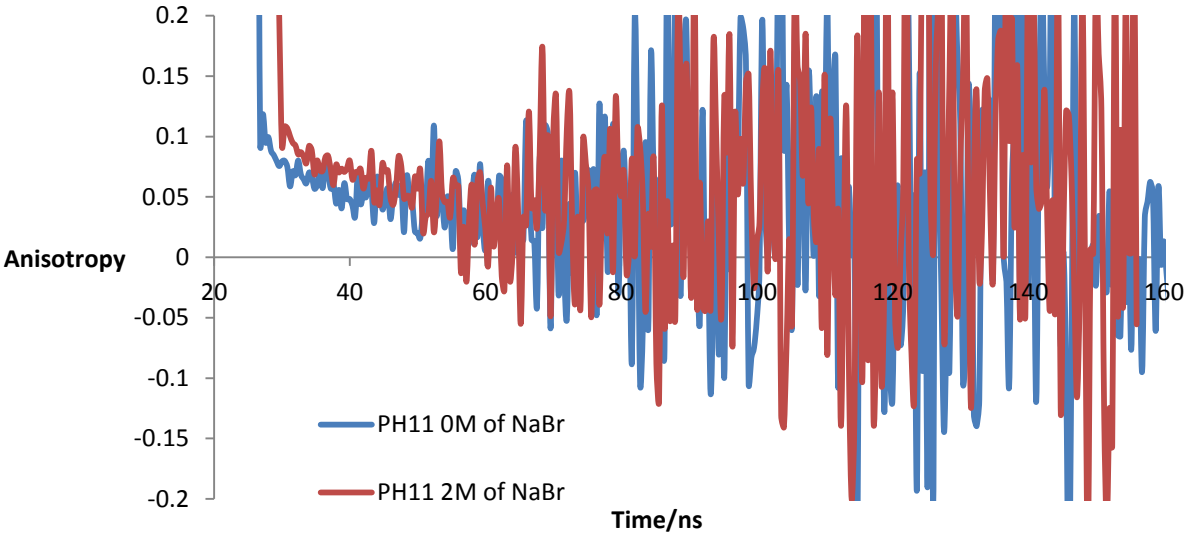

Figure 4.98 Fluorescence time resolved anisotropy data of aqueous ACE-labelled PDMAMA solution (10^{-2} wt%) in the absence of sodium bromide (blue line) and at the sodium bromide concentration of 2 M at pH11(λ_{ex}= 295 nm and λ_{em}= 340 nm).

In addition, the anisotropy decay of poly (acrylic acid) in the presence of sodium bromide at pH 11 (when the polymer chain adopted a coiled form) was found to be salt concentration dependent.

Figures 4.97 and 4.98 compare the anisotropy decays of PDMAEMA in the presence of 0.5 M and in the absence of salt and in the presence of 2 M NaBr and in the absence of salt at pH 11, respectively. It was seen that the anisotropy decayed rapidly to zero when a small amount of salt was added, whereas the anisotropy decayed only slowly to zero at a high concentration of salt compared to the anisotropy decay in the absence of salt. This suggests that the high ionic strength in the presence of 2 M NaBr caused more coiling in the chain and hence a long anisotropy decay was observed. While at low ionic strength less coiling was observed and, consequently, a short anisotropy decay was detected.

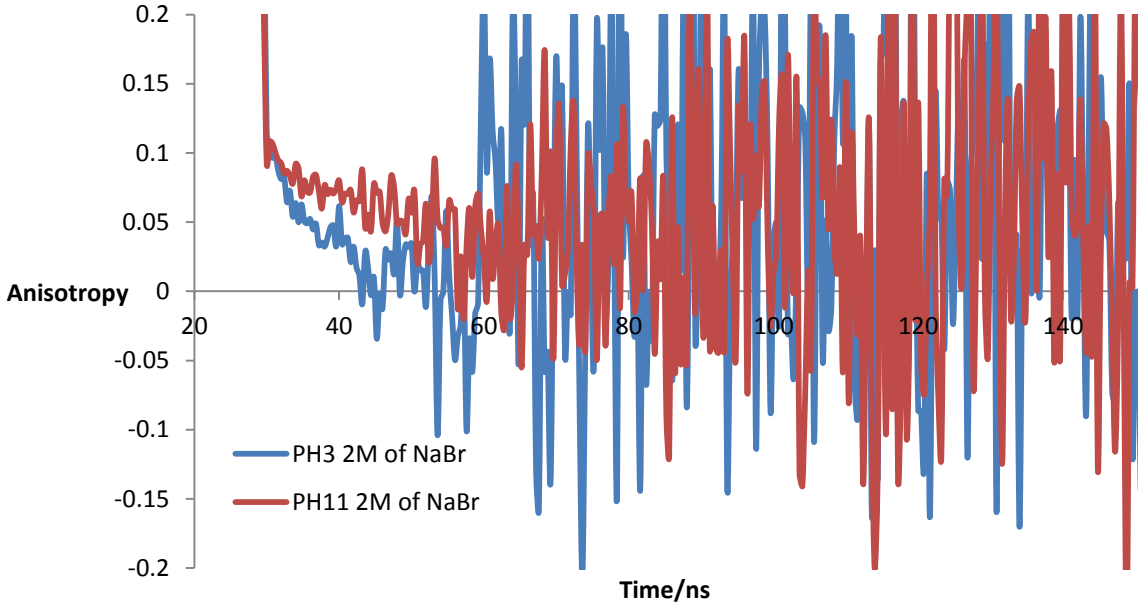

Figure 4.99 Fluorescence time resolved anisotropy data of aqueous ACE-labelled PDMAMA solution (10^{-2} wt%) at the sodium bromide concentration of 2 M at pH 3 (blue line) and at the sodium bromide concentration of 2 M at pH 11 (λ_{ex}= 295 nm and λ_{em}= 340 nm).

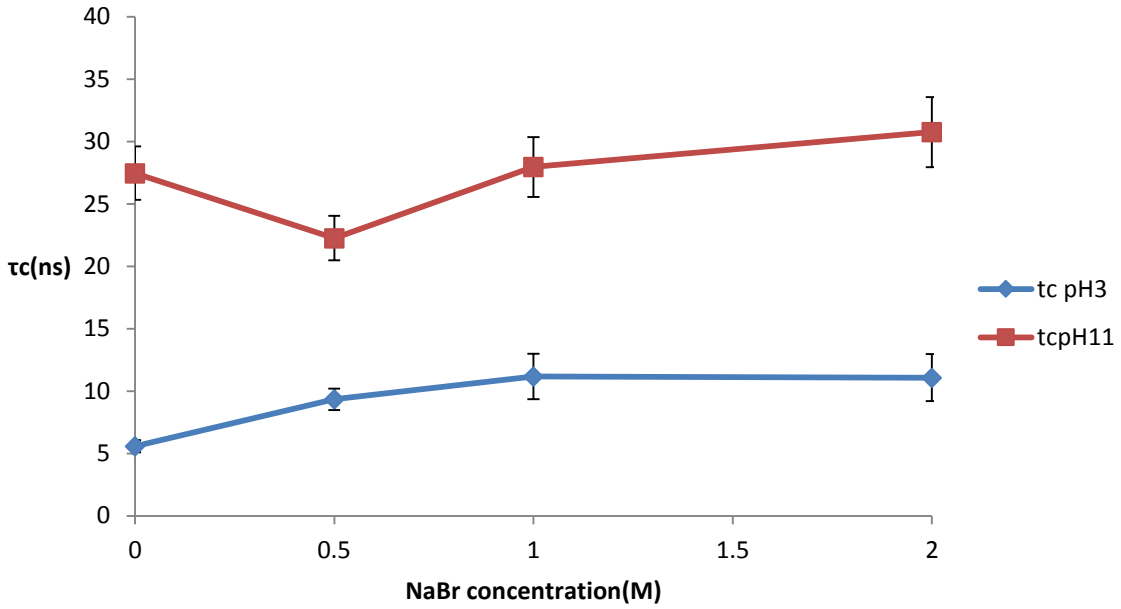

Figure 4.100 A plot of the correlation time against NaBr concentration for two ACE labelled PDMAEMA samples in aqueous solution at two different pH values when excited at 290nm and observed at 340nm.

Figure 4.100 illustrates the correlation times (τ_c) of ACE-labelled-PDMAEM as a function of sodium bromide concentration at two different pH values. A single exponential fit was applied to calculate the correlation time values in nanoseconds.

A general increase in correlation times with increasing concentration of NaBr was recorded at pH 11 and pH 3. However, over the entire concentration range the rate of increment in τc values at pH 11 was more than in those at pH 3 (this was observed using fluorescence anisotropy decay in figure 4.99).

In more detail, at pH 11, when the concentration of added salt was low (0.5 M), a decrease in the correlation time was recorded; this signifies that there was a fast segmental motion of the polyelectrolyte compared to the polymer system in the absence of salt. When the NaBr concentration was increased, a noticeable increase in the τ_c was recorded, indicating that the polymer chain adopted a more coiled configuration because of the high ionic strength effect . In contrast, in acidic media, the correlation time values showed that the addition of salt caused the collapse of the PDMAEMA chain. This could be attributed to the neutralisation of the deprotonated amine groups by linking with Br- ions which leads to the

aggregation of the cationic polymer chain and hence an increase in the correlation time values.

4.2.10 Fluorescence steady state spectra of ACE-AMMA labelled PDMEAMA in the presence of $CaBr_2$ as a function of pH

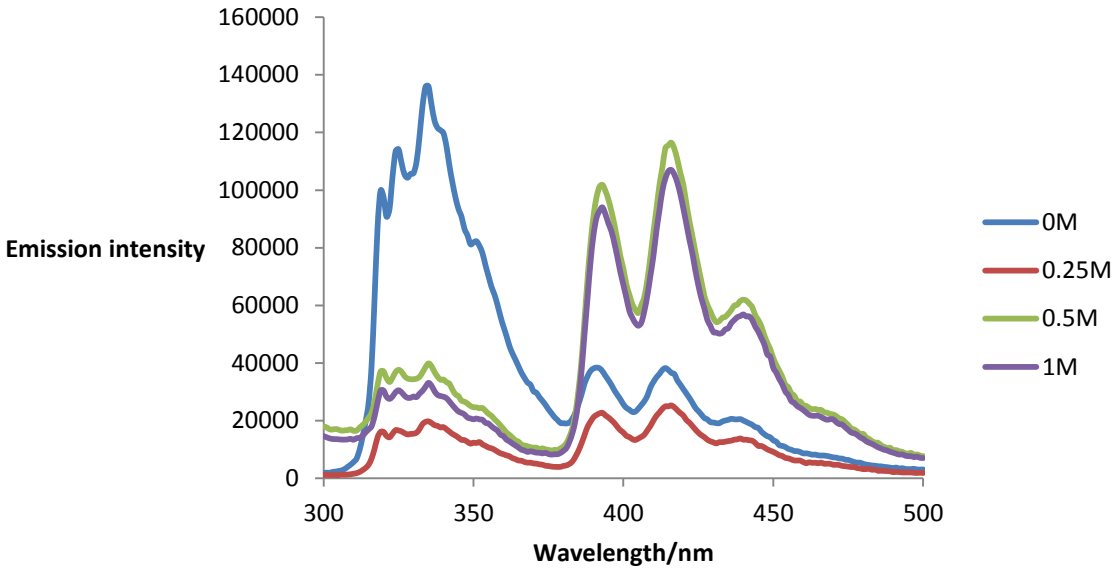

Figure 4.101 Emission scan in a range equal to 300-500 nm at fixed excitation λ_{ex}= 290 nm for ACE-AMMA- PDMEAMA samples in aqueous solution at pH 3 and varying $CaBr_2$ concentrations.

The addition of calcium chloride to a sample of ACE-AMMA PDMAEMA in aqueous solution in acidic media showed an initial decrease in the emission intensity for both donor and acceptor labels (figure 4.101). At higher salt concentrations, the emission intensity of the donor label then decreased along with a corresponding substantial increase in the emission intensity of the acceptor label. This suggests that adding salt induces polymer coiling while the internal quenching effect of both labels at higher salt concentrations (as was seen at low salt concentrations) shielded the acceptor label from internal quenching.

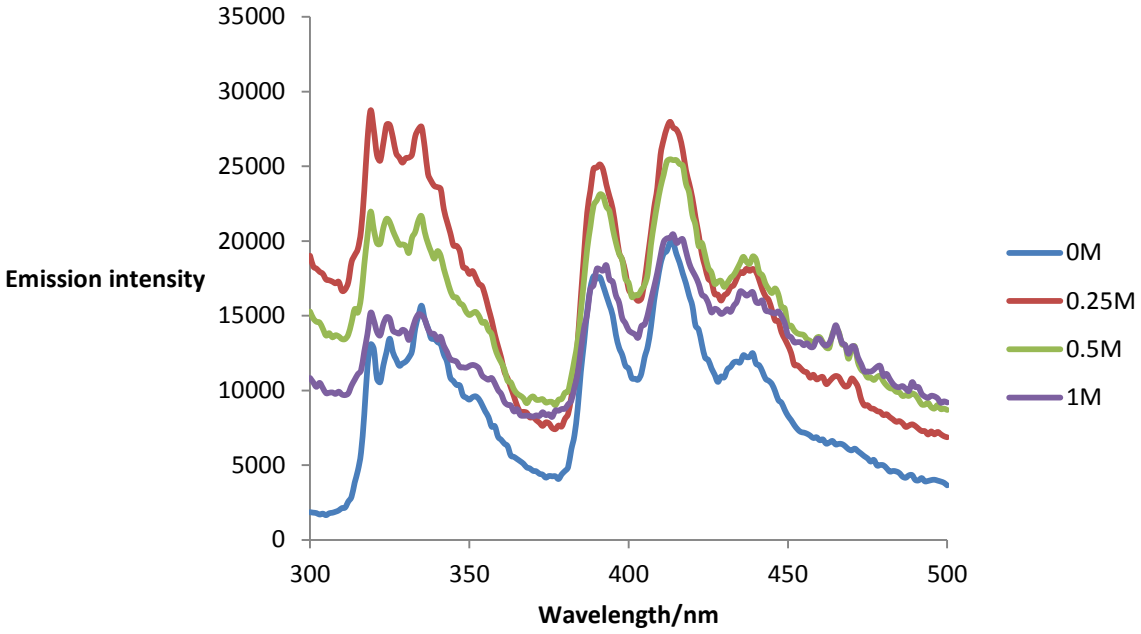

Figure 4.102 Emission scan in a range equal to 300-500 nm at fixed excitation λ_{ex}= 290 nm for ACE-AMMA- PDMEAMA sample in aqueous solution at pH 11and varying $CaBr_2$ concentrations

At pH 11, on the other hand, (figure 4.102) a substantial increase in the polymer emission intensity was seen across the entire wavelength range upon addition of 0.25 and 0.5 M of $CaBr_2$. Further increasing salt concentrations (1 M) showed a decrease in the intensity of both labels (returning to a similar intensity as was seen for the polymer in the absence of salt). This observation suggests that at low concentrations of salt, the polymer adopted a more open configuration and hence an enhancement in the emission intensity for both labels. While at a higher concentration of salt, the polyelectrolyte switched from a partially expanded form to a coiled form which led to a quenching of the emission intensity of both labels.

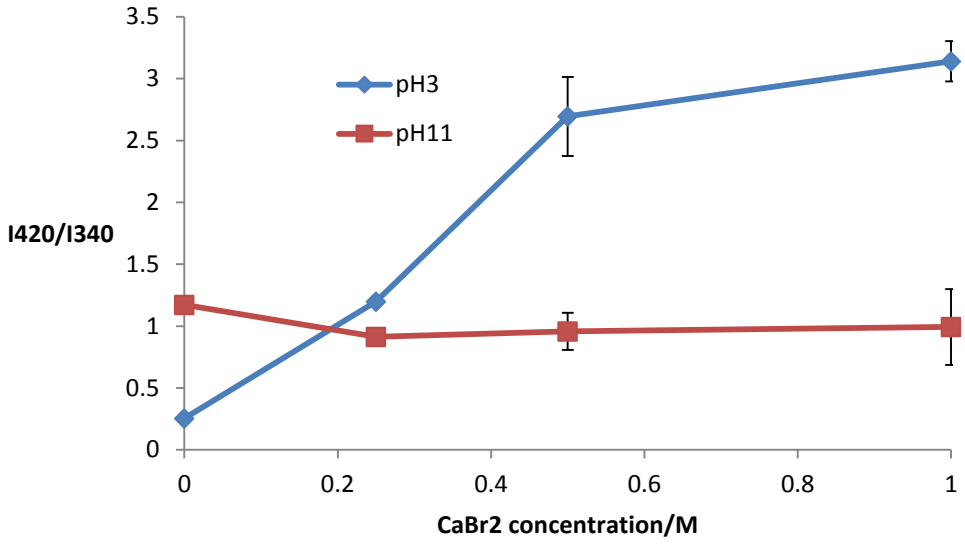

Figure 4.103 Fluorescence emission intensity ratio, I_A/I_D of 10^{-2} wt % ACE-AMMA-labelled PDMEAMA as a function of $CaBr_2$concentration at pH3 and PH11 (λ_{ex} = 290nm).

Figure 4.103 demonstrates the energy transfer efficiency in ACE-AMMA-PDMAEMA as a function of the calcium bromide concentration at low and high pHs.

It can be observed that the IA/ID ratio increased as the CaBr2 concentration increased at pH 3, suggesting that the AMMA label gets close to the ACE label when Br^- ions are added.

When the concentration of salt was high (0.5 M and 1 M), the fluorescence intensity ratio reached the extreme ~3, indicating a large efficiency of energy transfer in the coiled form of the polyelectrolyte chain. At these concentrated levels of calcium bromide, positively charged amine groups are linked by Br- ions and thus chain aggregation occurs. When the transition in conformation occurs at 0.25 M $CaBr_2$, a marked increase in the acceptor to donor ratio is seen, suggesting that in the presence of a sufficient concentration of Br- ions there is crosslinking of the amine groups and this leads to the conversion of the expanded form to the aggregated form.

On the other hand, the curve at pH11 demonstrated that the fluorescence intensity ratio decreased when a low concentration of $CaBr_2$ was added, this suggest that the polymer chain switches to an expanded form in the initial amount of salt, since the separation distance between labels becomes longer. While, when the highest concentration of the salt was added, a minor increase in the IA/ID ratio was observed, suggesting that the

macromolecule conformation is coiled since the separation distance between labels become shorter.

4.2.11 Fluorescence excited state lifetimes of singly and doubly labelled PDMAEMA in the presence of $CaBr_2$ as a function of pH

The lifetime data for single and double labelled PDMAEMA samples in the presence of increasing concentrations of calcium bromide at two pH values is also best modelled by a triple exponential as in equation 3.5 which shows only small standard deviations for the resulting lifetime values as well as an χ^2 value close to unity (see figures 4.105, 4.107 as selective examples). Once again these are shown in figure 4.104 and 4.106 as average lifetime values for simplicity of comparison.

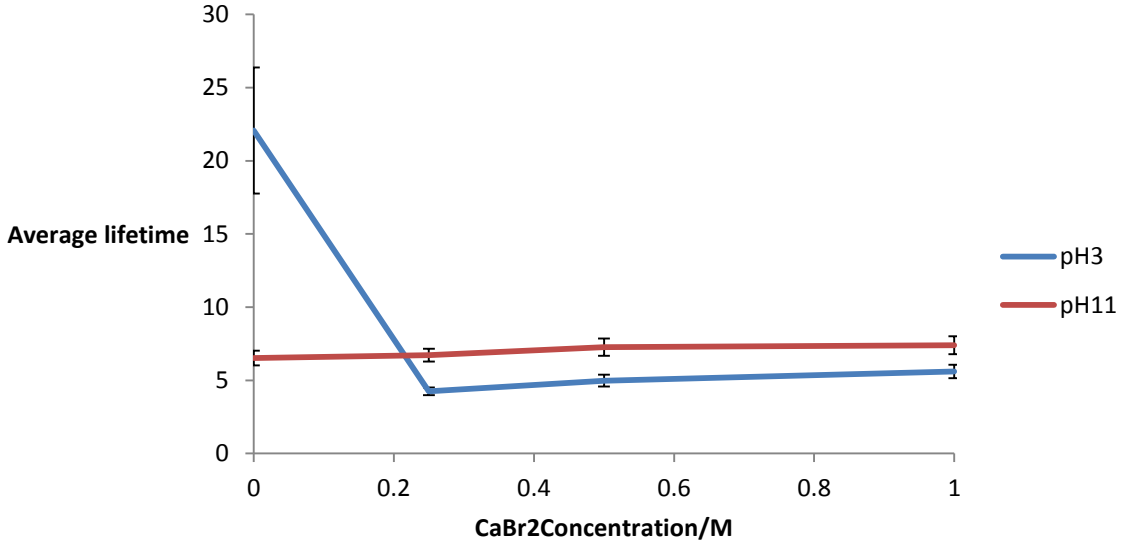

Figure 4.104 A plot of the average lifetime values obtained for ACE-PDMAEMA in aqueous solution at two different pH values with increasing $CaBr_2$ concentration when excited at 290 nm and observed at 340 nm.

It can be seen that, at low pH there is a large decrease in the average lifetime value upon initial addition of $CaBr_2$ indicating that the calcium bromide is having an important effect on PDMAEMA conformation and that increasing the salt concentration does not substantially increase this effect. Presumably screening of the charge on the polyelectrolyte collapses the chain and hence quenching by amine group occurs.

On the other hand, the addition of calcium bromide to the ACE-PDMAEMA solution at pH 11 causes a small increase in the lifetime value which indicates a reduction of

quenching due to the expansion of the polyelectrolyte chain, reducing the internal quenching between the label and the polymer backbone.

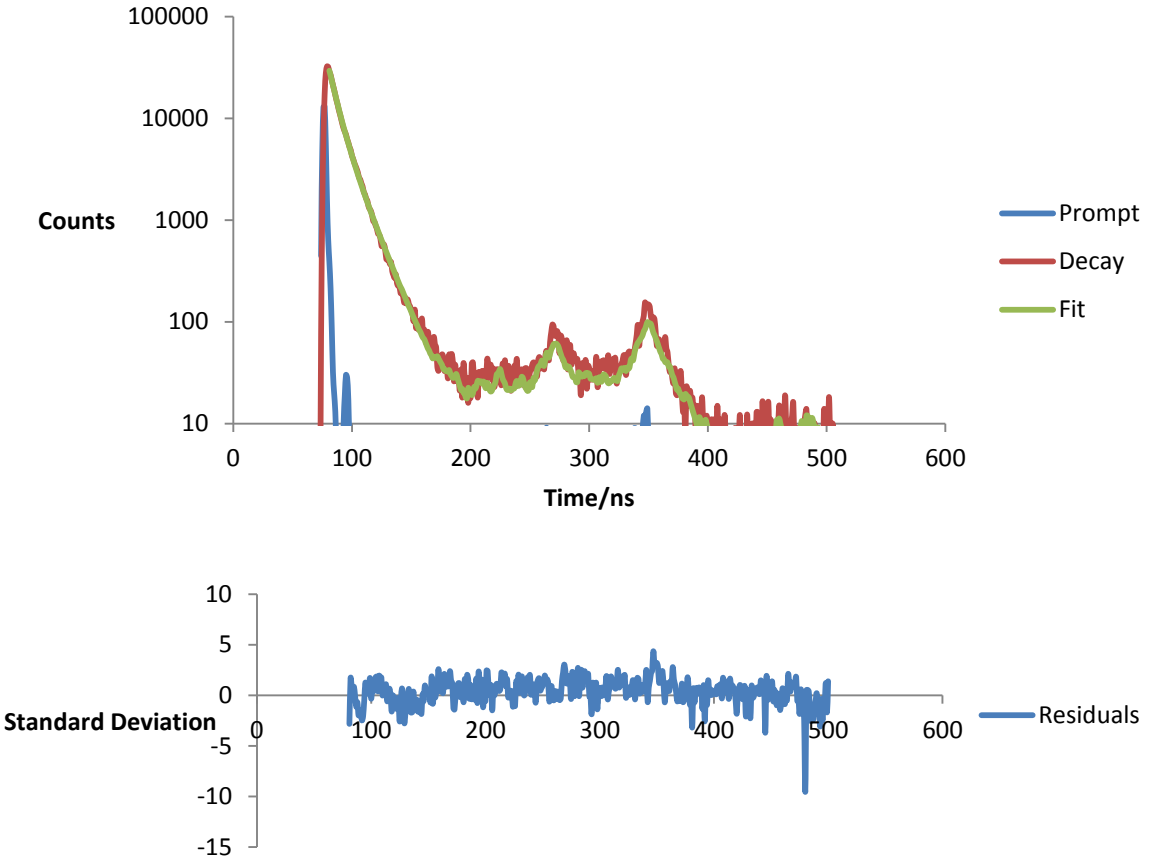

Figure 4.105 Fluorescence decay with corresponding mathematical fit (shown in green) and a plot of the resulting residuals for ACE-PDMAEMA in aqueous solution at pH 3 with 0.25M $CaBr_2$

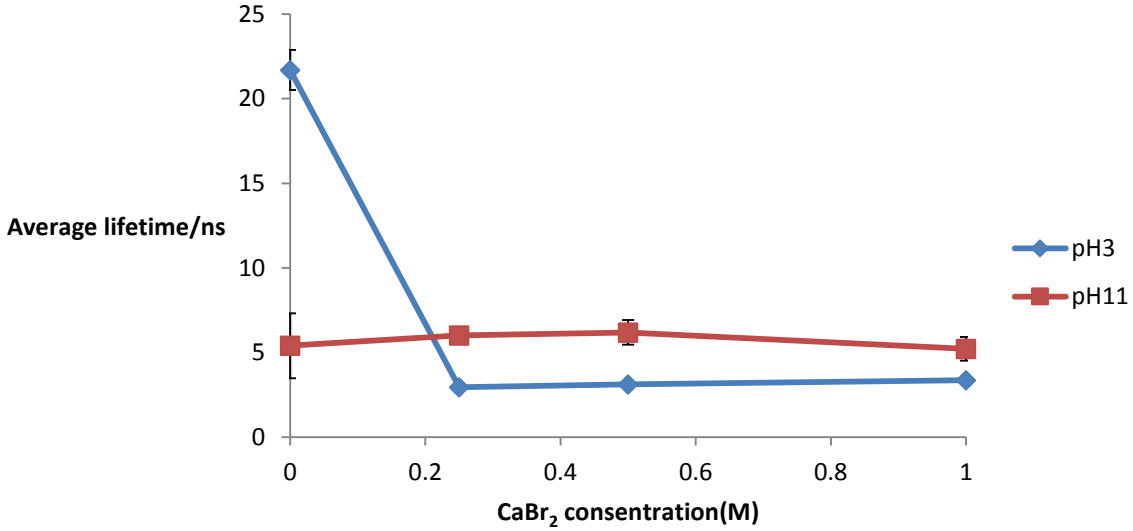

Figure 4.106 A plot of the average lifetime values obtained for ACE-AMMA-PDMAEMA in aqueous solution at two different pH values with increasing $CaBr_2$ concentration when excited at 290 nm and observed at 340 nm.

As it can be observed from figure 4.106, the curve at pH 3 displays the opposite pattern obtained from the intensity of the acceptor to the donor ratio against [$CaBr_2$], see Figure 4.103. This is consistent with the process in the quenching as the collapsed conformation is adopted. In addition, the shape of the curve at pH 3 could be attributed to the fact that a conformational transition occurs in the macromolecule chain when the initial amount of salt was added (0.25 M). This transition goes from an expanded chain in the absence of salt (long average lifetime value is recorded ~22 ns) to a collapsed form at all given concentrations of salt. The average lifetime value was quenched to ~ 3.35 ns perhaps due to the interaction of Br- ions with the deprotonated amine groups which in turn lead to a collapse of the chain and hence quench the fluorescence intensity of the donor by the internal group in addition to energy transfer to the acceptor group.

Upon addition of salt at 0.25 and 0.5 M in basic media the average lifetime value for the donor was similar to that seen with the single labelled system. This assumes that the polymer starts to open slightly and hence increases the distance between the donor and the acceptor labels. At a higher concentration of salt (1 M) the average lifetime value decreases more than that observed in the single system which indicates that the transfer in energy from donor to acceptor occurs due to collapsing of the polymer chain.

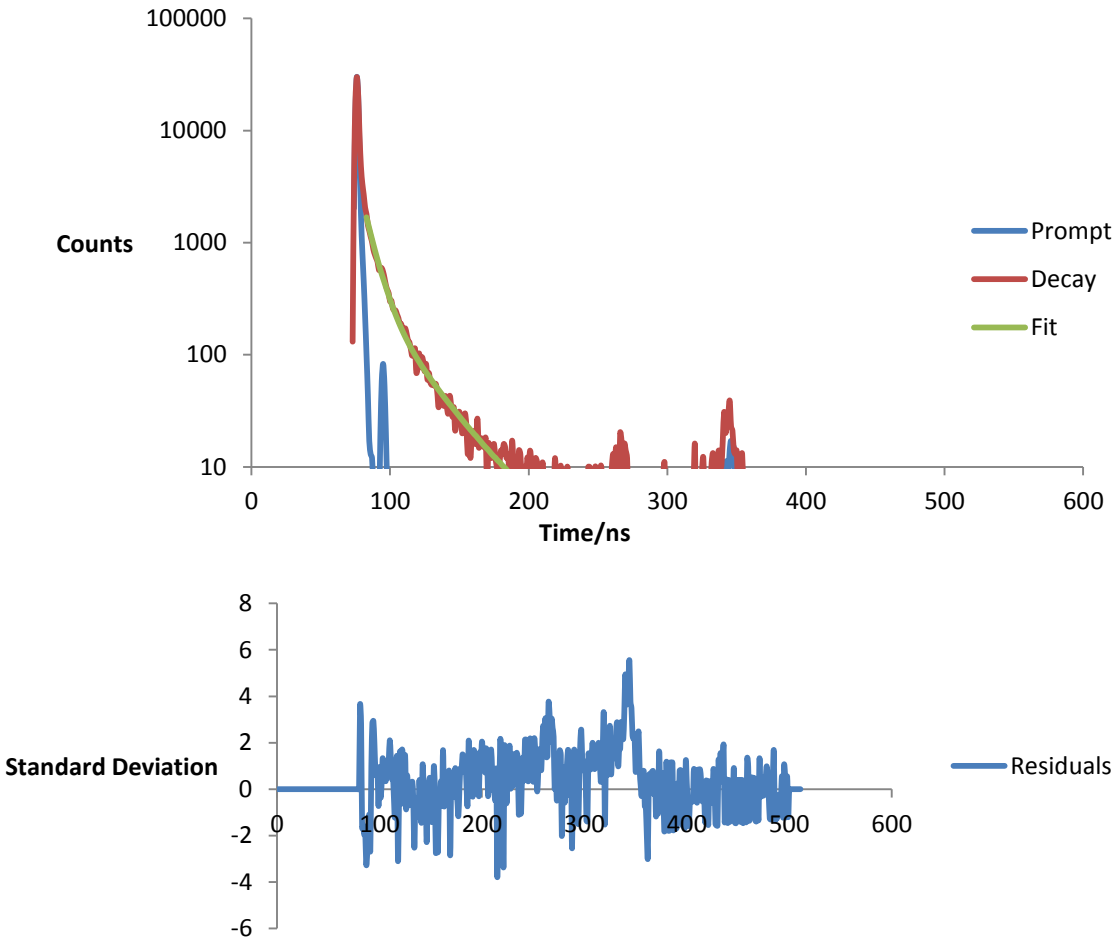

Figure 4.107 Fluorescence decay with corresponding mathematical fit (shown in green) and a plot of the resulting residuals for ACE-AMMA-PDMAEMA in aqueous solution at pH11 with 1 M $CaBr_2$

The average r value was then calculated for doubly labelled-PDMAEMA as a function of [$CaBr_2$] and pH via equation 3.7 and 3.8 respectively (figure 4.108).

The distance, r, seen for pH3 is lower upon addition of small amounts of calcium bromide and then does not change with further salt addition.

The r values obtained for pH 11 show an initial increase with addition of salt up to 0.5 M. This then decreases with increasing $CaBr_2$ concentration.This is further evidence of what was seen previously in which the addition of small amounts of salt causes the coiled polymer chain to open and then coil again under a higher salt concentrations.

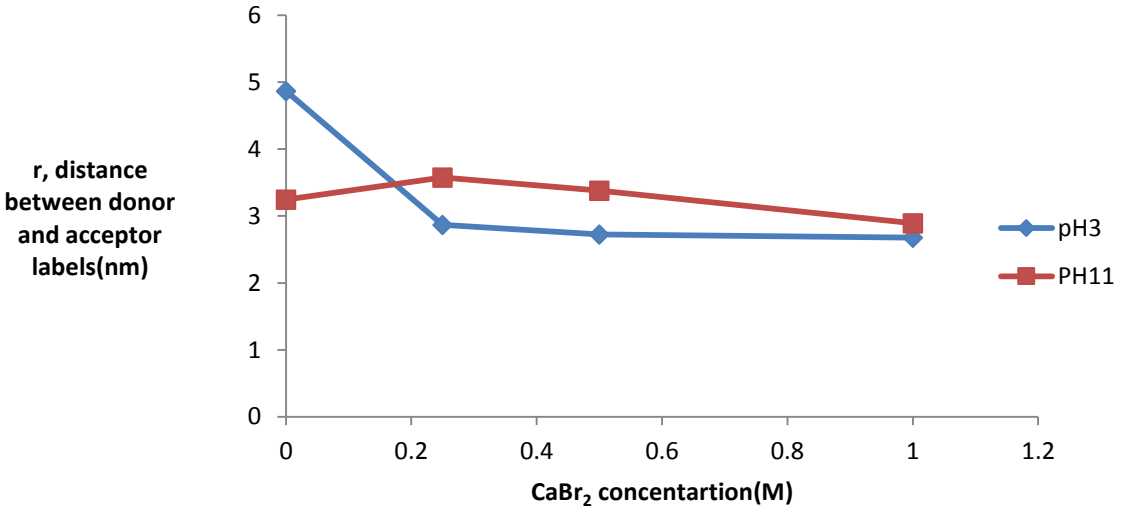

Figure 4.108 A plot of the value r, the distance between ACE (donor) and AMMA (acceptor) labels, as calculated by equation 3.7 for single and double -PDMAEMA across a range of pH values and $CaBr_2$ concentrations.

4.2.12 Fluorescence time-resolved anisotropy measurements (TRAMS) of ACE-PDMAMA in the presence of $CaBr_2$ as a function of pH

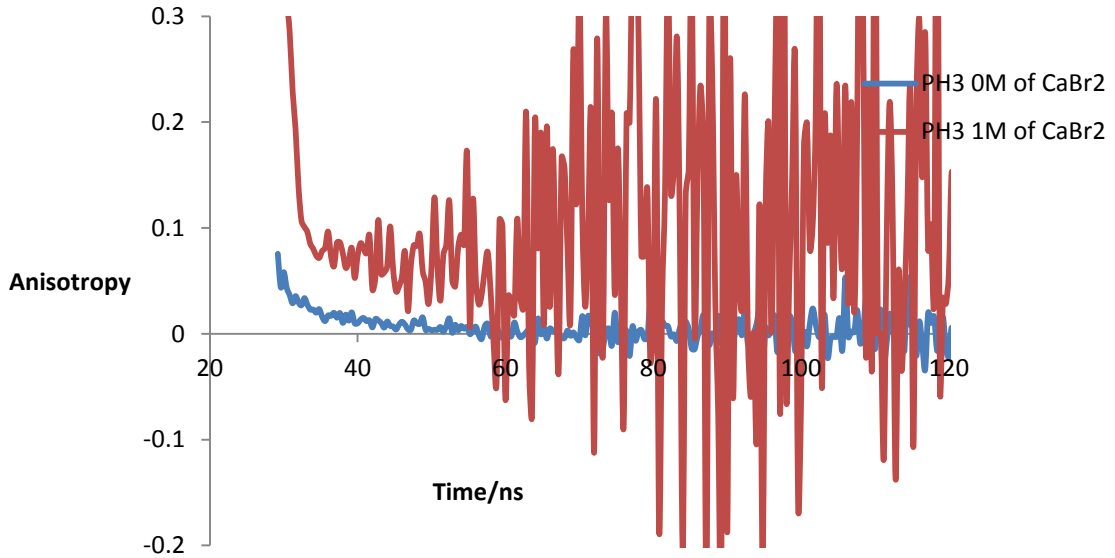

Figure 4.109 Fluorescence time resolved anisotropy data of aqueous ACE-labelled PDMAMA solution (10^{-2} wt%) in the absence of calcium bromide (blue line) and at the calcium bromide concentration of 1 M at pH 3(λ_{ex}= 295 nm and λ_{em}= 340 nm).

Figure 4.109 shows the fluorescence anisotropy decay of ACE-PMAEMA in aqueous solution in the absence and presence of calcium bromide. As it can be seen, a long duration anisotropy decay is given at 1 M salt compared to 0M which indicates that the mobility of the polymer is restricted when the PDMAEMA chain is coiled in the presence of 1 M of $CaBr_2$. The observation suggests that the lowering in the anisotropy for high salt concentrations results from the collapse of the polyelectrolyte chain. This could be attributed to the decrease of the electrostatic repulsion between the ionized amine groups because of the Br- ions since screening of the positively charged PDMAEMA chain by bromine anion cause a transition of the open form to the coiled conformation, hence a long anisotropy decay was observed.

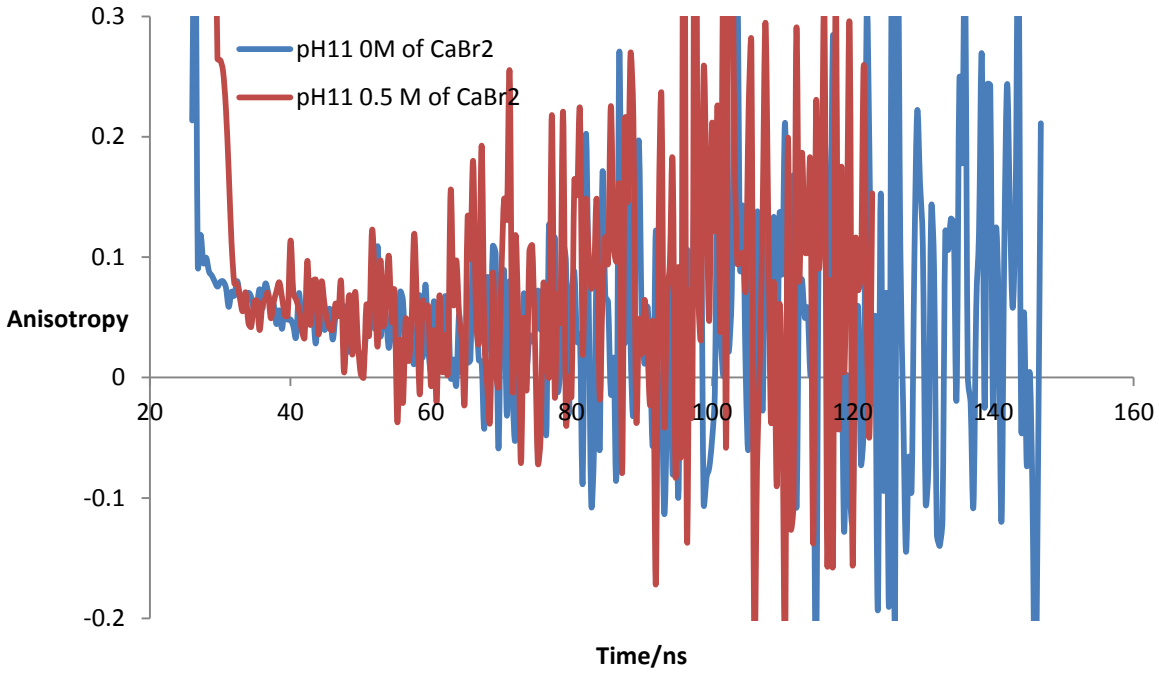

Figure 4.110 Fluorescence time resolved anisotropy data of aqueous ACE-labelled PDMAMA Solution (10^{-2} wt%) in the absence of calcium bromide (blue line) and at the calcium bromide concentration of 0.5M at pH 11(λ_{ex}= 295 nm and λ_{em}= 340 nm).

Conversely, the addition of [$CaBr_2$] on ACE-labelled PDMAEMA at pH 11 (when the polymer chain adopted a coiled conformation) shows a transition from a coiled form to an open chain form. Selective decays are shown in Figure 4.110. It was found that, a short duration anisotropy decay is given at 0.5 M compared to that in the absence of salt which

indicates that the mobility of the macromolecule becomes faster when the polymer chain is opened as a salt is added.

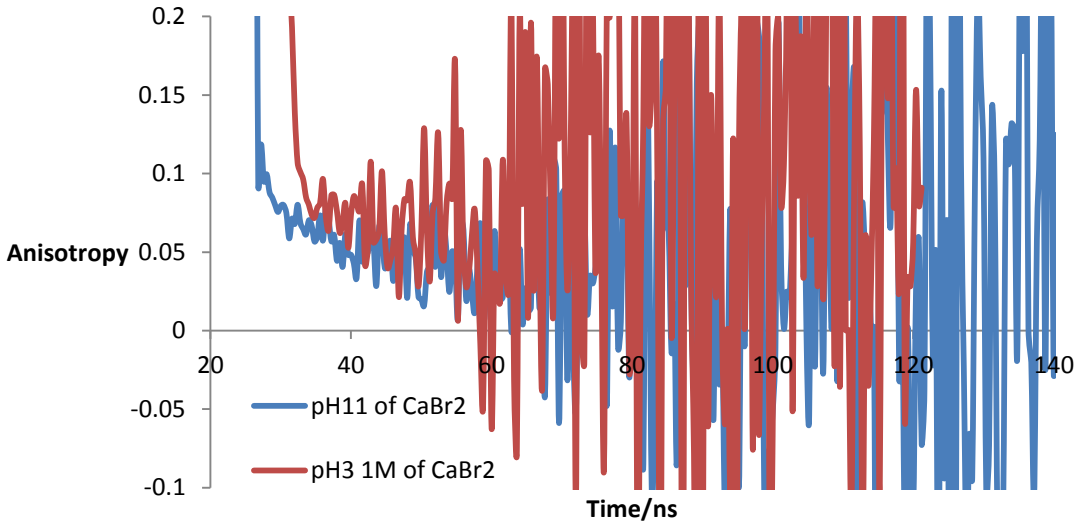

Figure 4.111 Fluorescence time resolved anisotropy data of aqueous ACE-labelled PDMAMA Solution (10^{-2} wt%) at the calcium bromide concentration of 0 M at pH 11 (blue line) and at the calcium bromide concentration of 1M at pH3(λ_{ex}= 295 nm and λ_{em}= 340 nm).

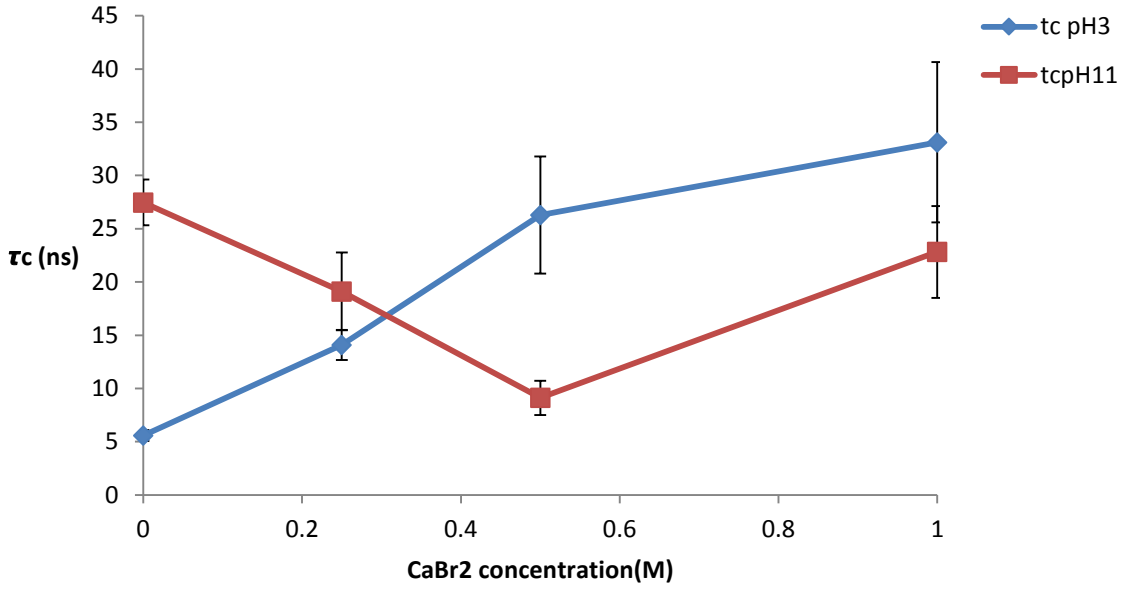

Figure 4.112 A plot of correlation time against $CaBr_2$ concentration for two ACE labelled PDMAEMA samples in aqueous solution at two different pH values when excited at 290nm and observed at 340nm.

Figure 4.112 represents the plots of rotational correlation time with respect to the concentration of $CaBr_2$ added to the ACE- PDMAEM solutions at pH 3 and 11. A marked decrease of correlation time was recorded at pH 11 when 0.25 and 0.5 M of $CaBr_2$ were added, indicating that the polymer chain undergoes a conformation transition from a collapsed form to a swollen open structure at these salt concentrations. In 1 M calcium bromide, the τ_c value increased suggesting that the polymer chain adopt a coiled form at a high salt concentration.

Whereas, a substantial increase in the correlation time values was recorded as the salt concentration was increased at a low pH the polymer chain may have adopted a more coiled formation than was seen in basic media (see figure 4.111) due to the possible effect of Br- anions at pH 3 in shielding the electrostatic repulsions between the cationic amine groups in polyelectrolytes. This may have led to the screening of the electrostatic repulsion in the entire PDMAEMA chain. As a result, the collapsed polymer chains move slower than the expanded form. It is worthy to note that the τ_c increased from 5.57 to ~19.36 ns at pH 3 when the Cl^{-1} concentration was increased in the case of $CaCl_2$ (Figure 4.87), while τc increased from 5.57 to ~33.11 ns by increasing the Br^{-1} concentration in the case of $CaBr_2$ (Figure 4.112). This indicates that the large ions had more effect on PDMAEMA aggregation compared to small ions.

In summary, the steady state and lifetime measurements showed aggregation of the polymer chain due to complex formation of the salt anion with the cationic amine group, when adding the sodium chloride and sodium bromide to the cationic PDMAEMA in acidic media. With larger anions (i.e NaBr > NaCl) aggregation was more pronounced. When in basic media the polymer chains adopted a coiled form; the initial addition NaCl and NaBr induced an expansion of the chains and then at higher concentrations of the salts the structure became coiled again. Using TRAMS measurement, NaCl compared to NaBr induced a slightly more pronounced enhancement of recoiling.

For the cationic PDMAEMA chain, more coiling was induced by the addition of divalent salts such as calcium bromide compared to the monovalent salt, such as sodium bromide. However using time resolved anisotropy measurements for uncharged polymer in basic media, sodium bromide had a greater effect on coiling than calcium bromide.

4.2.13 A comparative summary

4.2.13.1 The effect of Ionic Strength and the type of ion (anions) on the Poly (dimethylamino) ethyl methacrylate (PDMEAMA) conformation

The effect of salt concentration on polymer conformation was found to differ depending on the type of salt used. Moreover**,** the influence of anions on polymer conformation in solution seemed to be dependent on the size of the anions used. It is expected that large ions (such as Br^{1-}) will have a higher attractive interaction with deprotonated amine groups due to their large size. The effects of different salts on the coiled polymer chain were also compared using the TRAMS technique.

4.2.13.2 Fluorescence time-resolved anisotropy measurements (TRAMS) of ACE-PDMAEM A in the presence of NaCl and NaBr at acidic and basic condition

TRAMS data from figures 4.113 and 4.114 showed that PDMAEM displayed increased coiling upon increasing the ionic strength and increasing the anion size in acidic media (NaBr > NaCl). Whereas, TRAMS data from figures 4.115 and 4.116 showed that both salts initially induced unfolding of the polymer chains and then folding of the polymer chain at higher concentrations of NaBr.

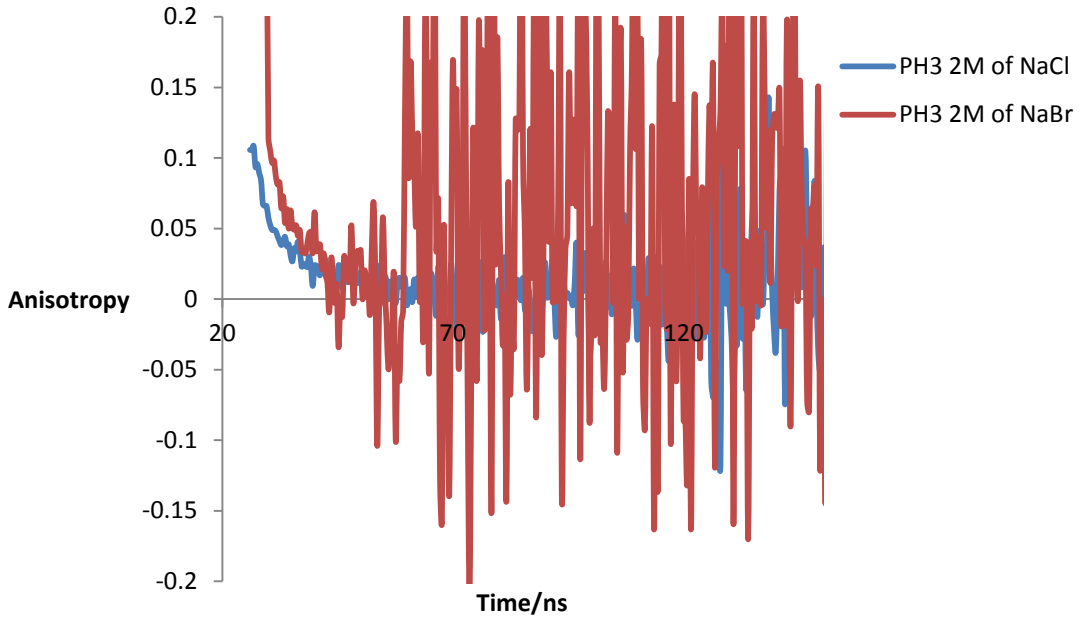

Figure 4.113 . Fluorescence time resolved anisotropy data of PDMAEM as a function of salt concentration (at pH 3).

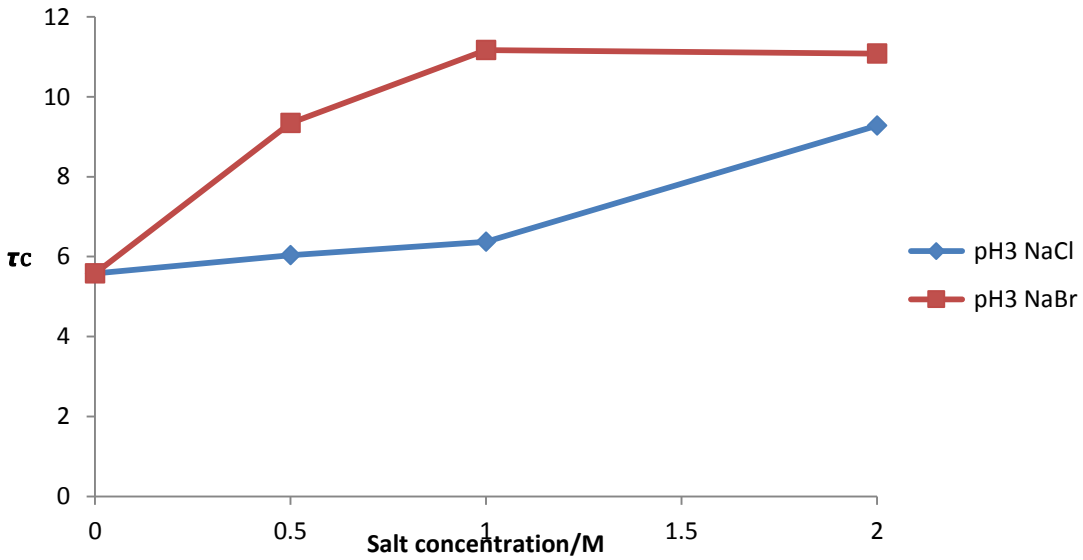

Figure 4.114. Correlation times of PDMAEM as a function of salt concentration (at pH 3).

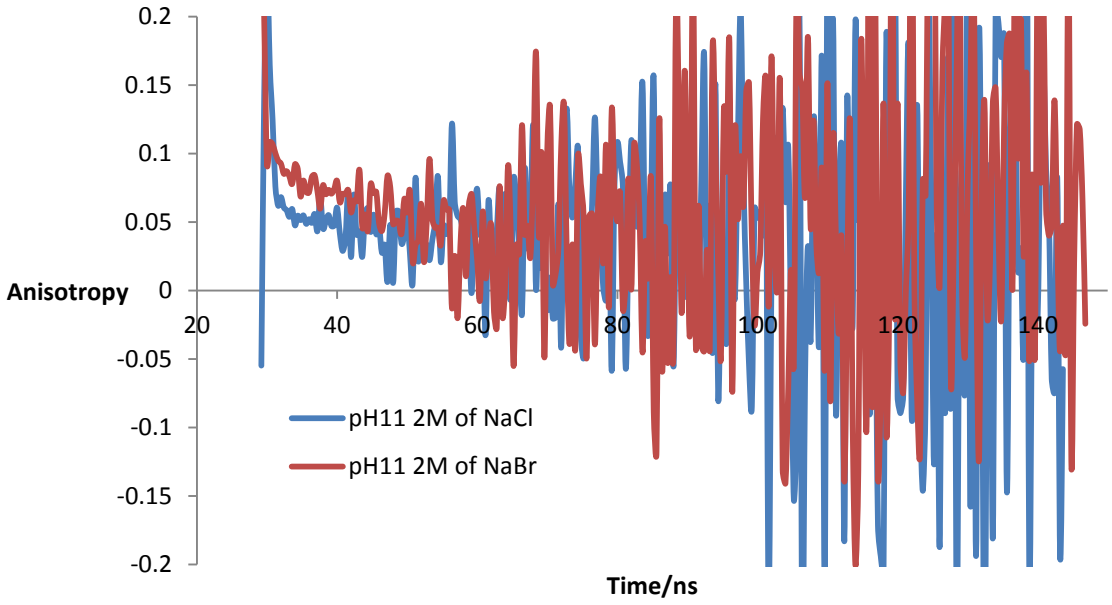

Figure 4.115. Fluorescence time resolved anisotropy data of PDMAEM as a function of salt concentration (at pH 3).

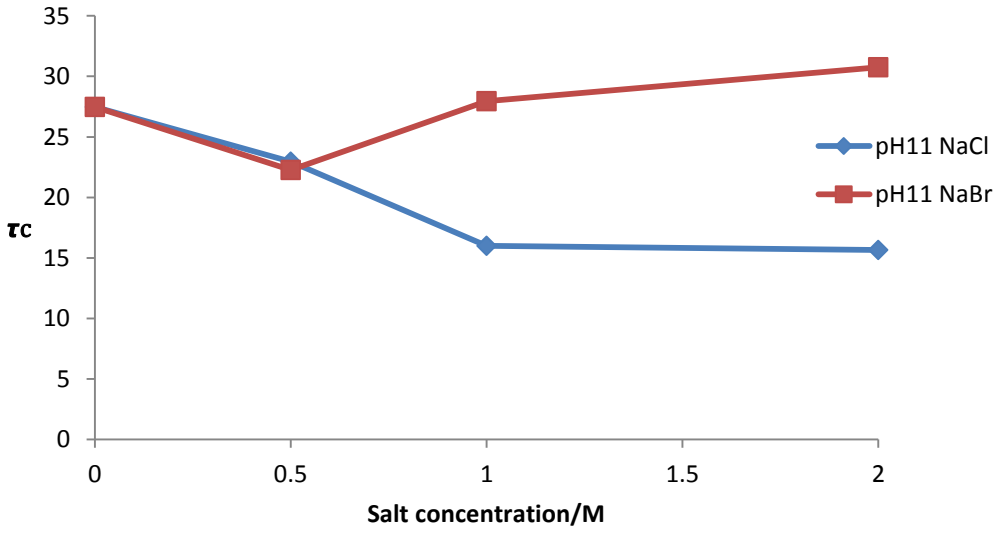

Figure 4.116. Correlation times of PDMAEM as a function of salt concetration (at pH 11).

4.2.13.3 Fluorescence time-resolved anisotropy measurements (TRAMS) of ACE-PDMAEM A in the presence of $CaCl_2$ and $CaBr_2$ at acidic and basic conditions.

TRAMS data from these figures 4.117 and 4.118 showed that PDMEAMA displayed increased coiling upon increasing ionic strength and increasing anion size in acidic media ($CaBr_2$> $CaCl_2$).

Whereas, TRAMS data in figures 4.119 and 4.120 showed that PDMEAMA displayed increased coiling upon addition of $CaCl_2$ while $CaBr_2$ induced unfolding of the polymer chain except at a high concentration (1 M) in basic media.

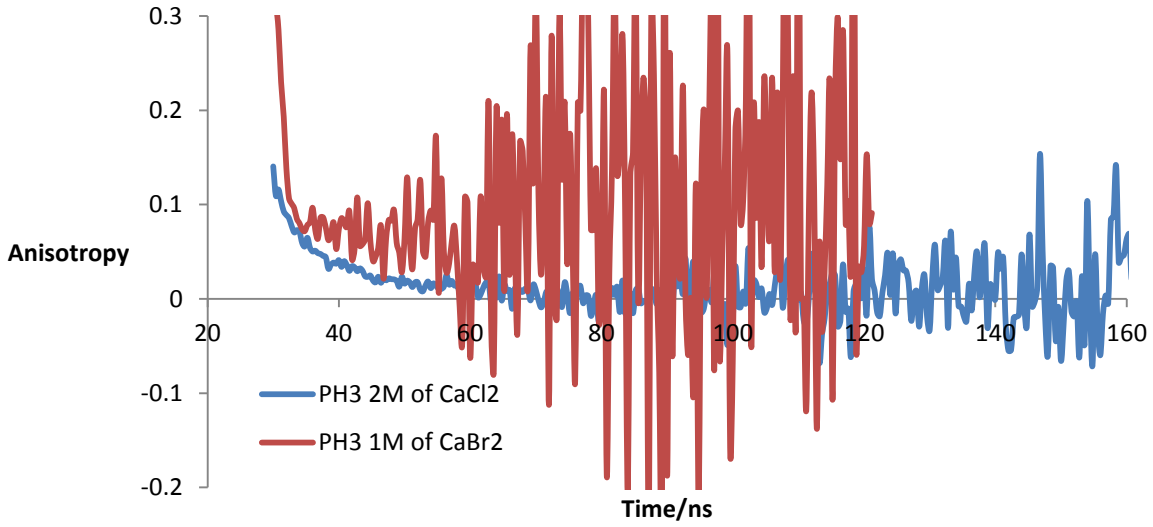

Figure 4.117. Fluorescence time resolved anisotropy data of PDMAEM as a function of salt concentration (at pH 3).

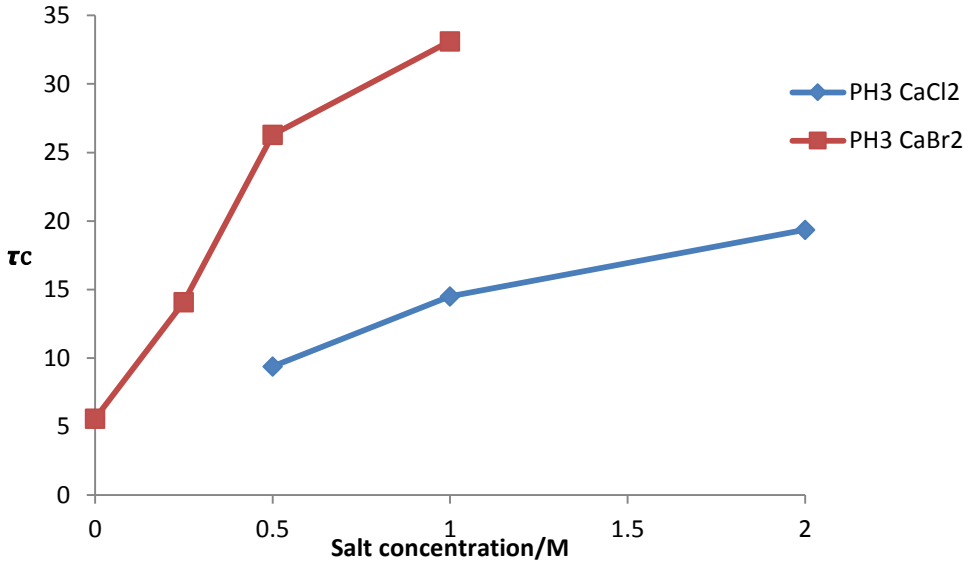

Figure 4.118. Correlation times of PDMAEM as a function of salt concentration (at pH 3).

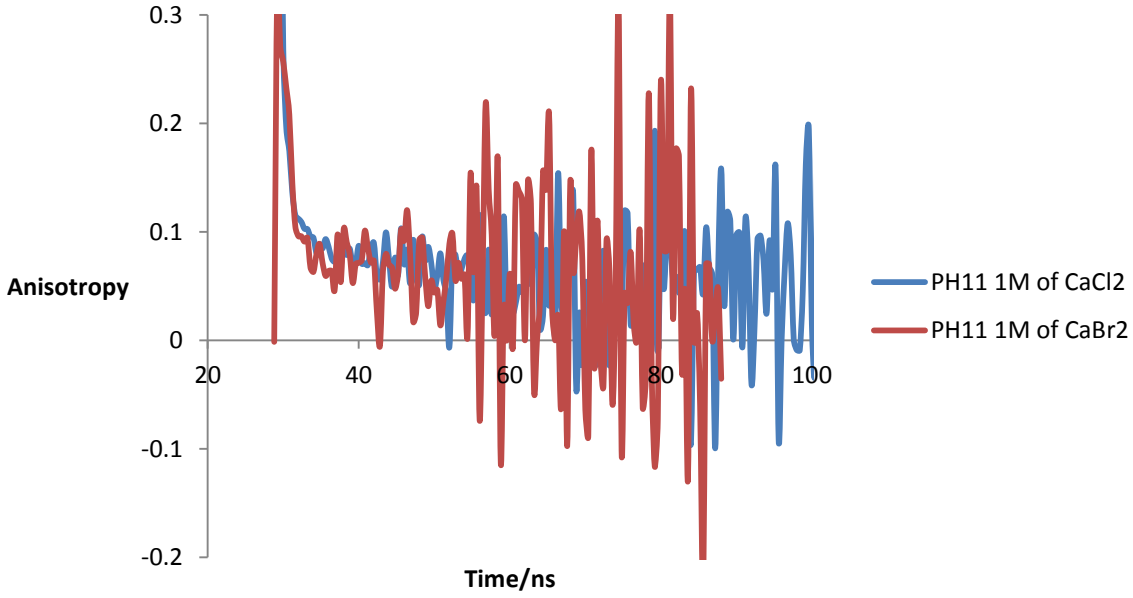

Figure 4.119. Fluorescence time resolved anisotropy data of PDMAEM a function of salt concentration (at pH 11).

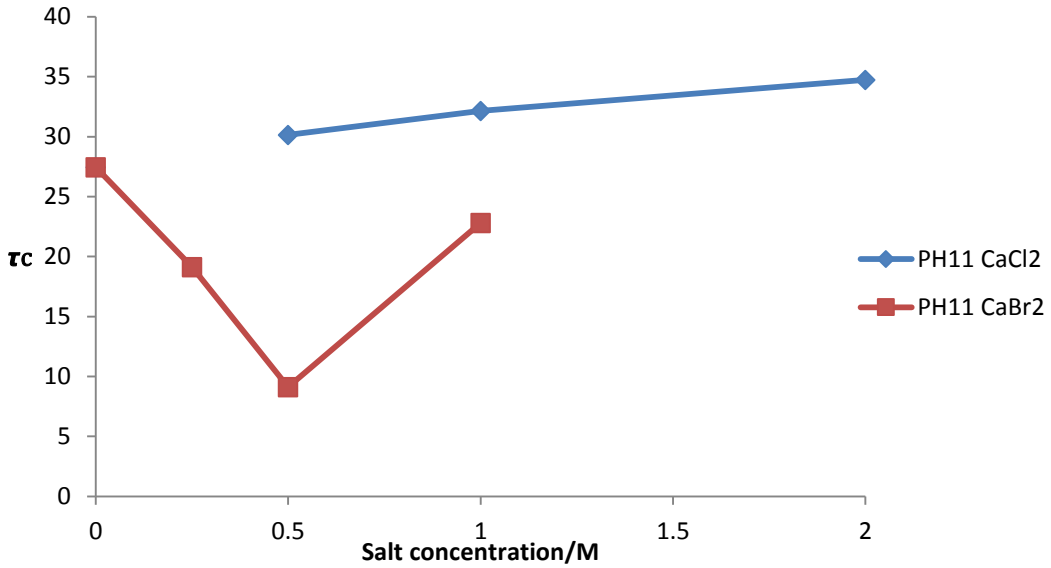

Figure 4.120. Correlation times of PDMAEM as a function of salt concentration (at pH 11).

4.2.13.4 The effect of Ionic Strength and type of ion (cations) on the Poly (dimethylamino) ethyl methacrylate (PDMEAMA) conformation

It was found that the influence of monovalent salt was different to divalent salt (with similar in anions, such as sodium bromide and calcium bromide) on the conformational behaviour of PDMAEMA as was illustrated with the TRAMS technique.

4.2.13.5 Fluorescence time-resolved anisotropy measurements (TRAMS) of ACE-PDMAEMA in the presence of NaBr and $CaBr_2$ at acidic and basic conditions

TRAMS data from figures 4.121 and 4.122 showed that PDMEAMA displayed increased coiling upon increasing ionic strength, this effect on coiling was more pronounced in the case of the divalent ($CaBr_2$) salt than the monovalent salt (NaBr) in acidic conditions.

On the other hand, TRAMS data as shown in figures 4.123 and 4.124 showed that PDMEAMA demonstrated increased coiling upon addition of NaBr while $CaBr_2$ induced unfolding of the polymer chain except at high concentrations (1 M) of salt at a high pH

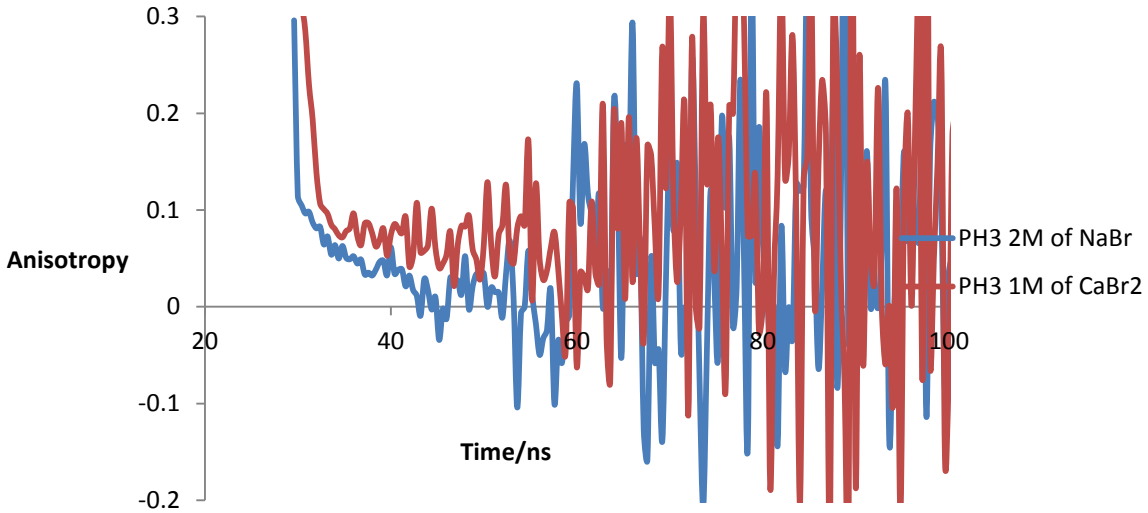

Figure 4.121. Fluorescence time resolved anisotropy data of PDMAEMA as a function of salt concentration (at pH 3).

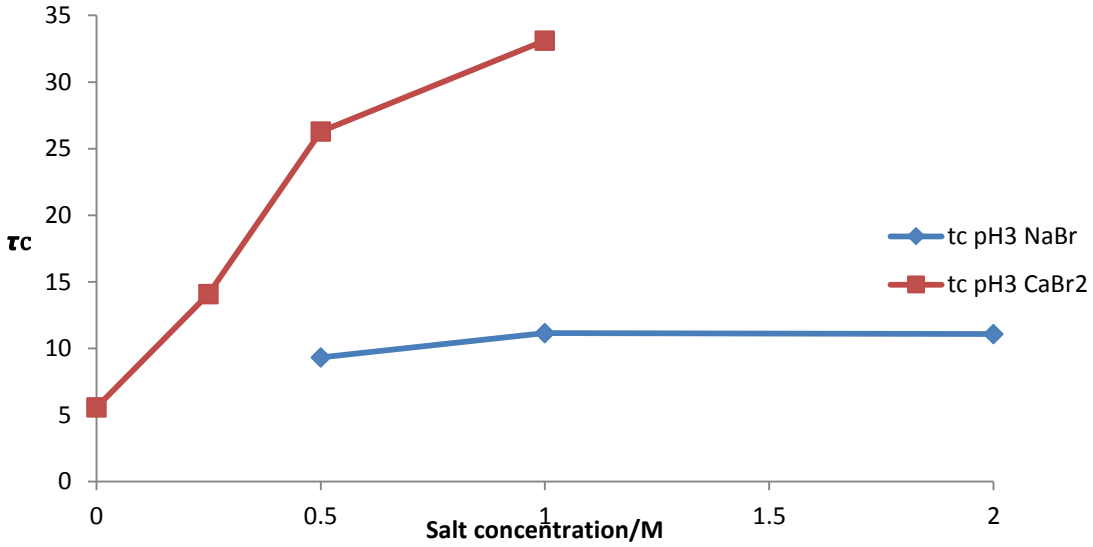

Figure 4.122. Correlation times of PDMAEMA as a function of salt concentration (at pH 3).

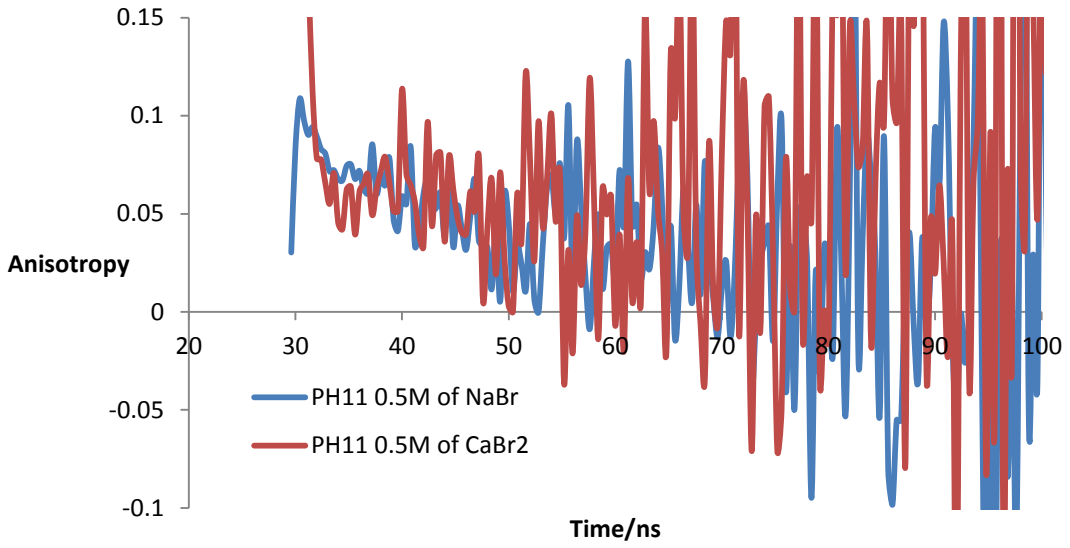

Figure 4.123. Fluorescence time resolved anisotropy data of PDMAEMA as a function of salt concentration (at pH 11).

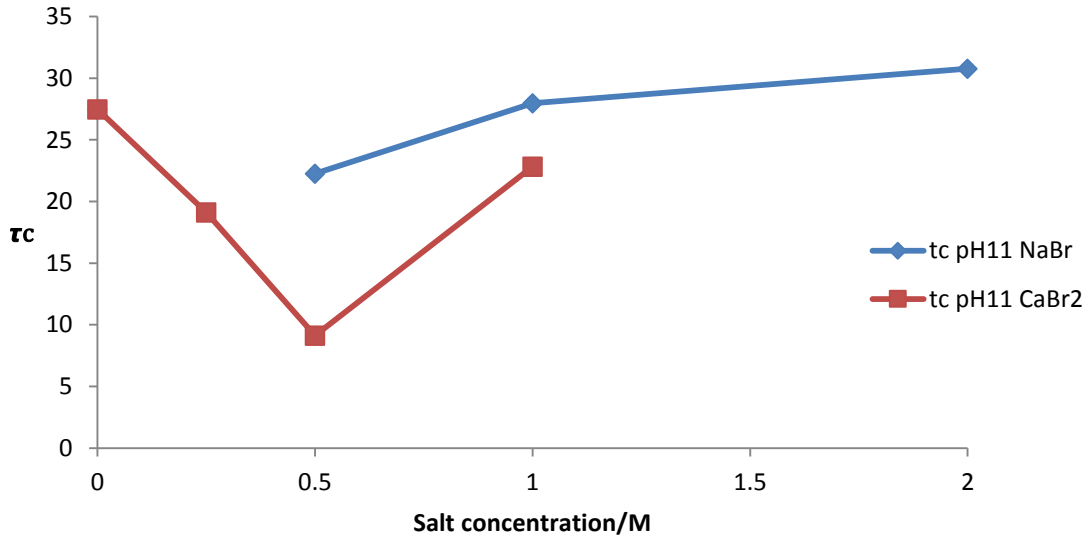

Figure 4.124. Correlation times of PDMAEMA as a function of salt concentration (at pH 11).

Chapter 5 The use of fluorescence spectoscropy to study the molecular interactions between [poly(dimethylaminoethyl) methacrylate] and poly(acrylic acid) with oppositely charged surfactant micelles in aqueous solutions

In this chapter, fluorescence spectroscopic techniques, such as steady state, excited state lifetime and time resolved anisotropy, are used to explore and gain information on the interaction between polyelectrolytes and oppositely charged surfactants at the molecular level. Recently, Polyelectrolyte-surfactant complexes received considerable attention from the scientific community and practitioners. The strong mutual interactions between the components of such polyelectrolyte raised fundamental and interesting questions, on the behaviour of charged particles, for the scientific community to investigate. From practitioners' perspectives, these systems have unique material properties which made them interesting materials for practical applications. The application of the Polyelectrolytes surfactant complexes includes the adjustment of rheological properties and the enhancements of personal care products mildness and solubilisation of hydrophobic materials. The use of these materials for the formation of metal nanoparticles and the fabrication of novel shapes memory networks also has been recently proposed by recent investigations [73].

The study of such interactions also are important in stimulating the accumulation of unwanted biomacromolecules, for example in water purification processes. As far as the current work is concerned, the effects of varying the amount of surfactant (at surfactant concentration levels higher than the CMC of the surfactant) on complex formation will be monitored through the use of fluorescence spectroscopy. The pH of the solution also will be varied in order to estimate the effect upon complex processes such as the interaction between PAA with cationic surfactant micelles (Hexadecyltrimethylammonium chloride) and the interaction between PDMAEMA with anionic surfactant micelles (Sodium hexadecyl sulphate).These interactions are considered in this research study and the results are detailed in the following sections.

5.1 Fluorescence investigation of poly(acrylic acid) in the presence of oppositely charged surfactant micelles (Hexadecyltrimethylammonium chloride).

5.1.1 Fluorescence steady state spectra of ACE- AMMA labelled PAA in the presence of Hexadecyltrimethylammonium chloride as a function of pH

The effects of complex formation, with surfactant micelles, on the conformation of PAA, were investigated through the use of intra-molecular energy transfer. To investigate these effects a sample of 10^{-2} wt% concentration of ACE-AMMA labelled PAA is used. Several experiments have been conducted on the sample with different surfactant concentration levels. Data has been collected from samples with three different pH levels (pH 3, pH 6 and pH 11) and different surfactant concentration (10 mM, 5 mM and 2 mM). These concentration levels are higher than the critical micelles concentration (1.27 mM as reported in the literature [49].

Figure 5.1 shows the energy transfer efficiency IA/ID in the doubly labelled poly (acrylic acid) PAA as a function of the CTAC surfactant micelles concentration at the three different pH levels. For pH3, a noticeable decrease in the IA/ID ratio is observed upon the initial addition of the micelles to the PAA polymer solution. After this initial decrease and at higher concentrations, the graph shows no further significant decrease in the IA/ID ratio. This behaviour suggests that the anthryl label gets relatively far apart from the naphthyl label when the cationic micelles are added. This process can be explained as a flow: at low level of pH, pH 3, a majority of the carboxylic acid groups are protonated and hence the PAA polymer is uncharged. Therefore the hydrophobic forces, of the PAA/cationic micelles system, dominate the polymer/micelles interaction at low pH,. In thi low pH level the micelles bind in a non-cooperative way with the PAA polymer which might be enough to separate apart the two labels. This observation have been reported in the literature, it was found that the addition of cationic surfactants to NP labelled PAA polymer solution of pH 3 leads to a decrease in the IE/IM ratio. It was suggested that this decrease was due to the hydrophobic interaction between the detergent molecule and the naphthalene group.

This interaction causes a separation of the NP molecules in the naphthalene aggregates, leading to a loss in emission of excimer and an increase in emission of monomer [49].

For pH 6, the figure shows an initial increase in the intensity ratio when the cationic micelles added to the solution. For an initial concentration of 2 mM the ratio intensity rose to a level close to that of the final value of the pH 3 case. No important change in this value at higher concentration is observed. The initial intensity ratio for pH 11 case is slightly greater than that of the pH 6. Further increase in the surfactant concentration lead to a decrease in the intensity and at high concentrations the ration reached the final value of the pH 3 case. This samples measurement shows that the intensity ratio increased with the increase of the pH values consistently. This indicates that the polymer undergoes a conformational transition from an expanded polymer chain to a collapsed form at pH 6 and pH11. This is attributed to the COO^- groups being linked by the oppositely charged head group of the micelles and hence leading to polymer chain aggregation.

Researchers have found that the addition of oppositely charged surfactants to Poly(methacrylic acid) brushes at neutral pH leads to a drop in the hydrodynamic radius. This drop is mainly due to the cooperative binding driven by electrostatic interactions between the PAA and the micelles [73].

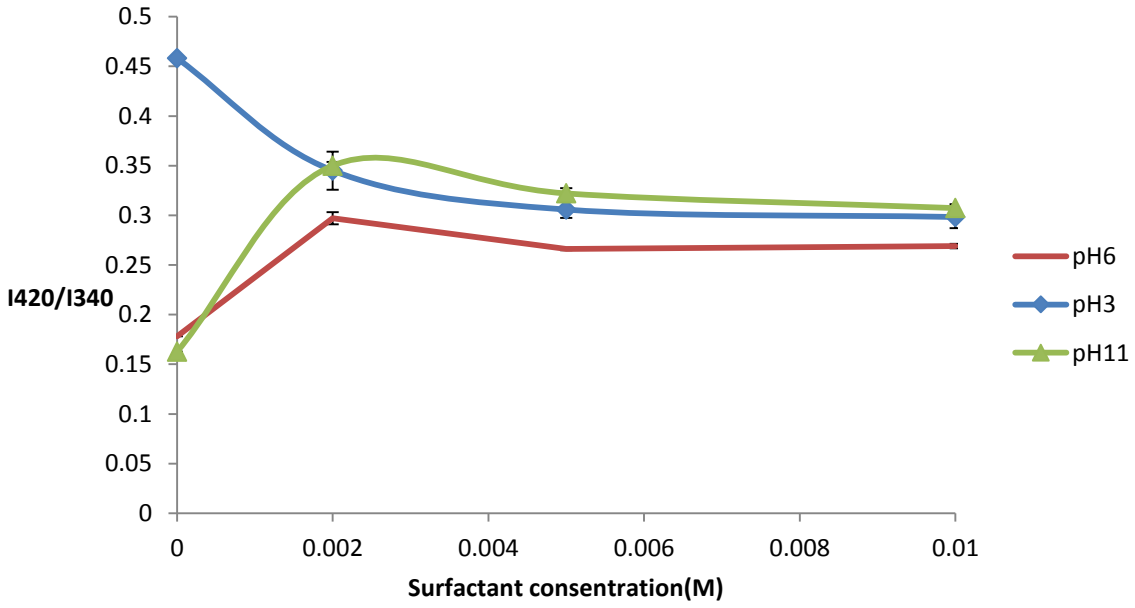

Figure 5.1: Fluorescence emission intensity ratio, IA/ID of 10^{-2} wt % ACE-AMMA-labelled PAA as a function of Hexadecyltrimethylammonium chloride concentration at different pH values (λex = 290nm)

5.1.2 Fluorescence excited state lifetimes of an aqueous solution of ACE-AMMA PAA in the presence of Hexadecyltrimethylammonium chloride as a function of pH

Fluorescence decay measurements was performed on a doubly labelled poly(acrylic acid) sample. The emission from the donor label was measured under different pH values and various surfactant micelles concentrations. Similar to the lifetime analysis conducted in this research study, the fluorescence decays was best modelled with a triple exponential function as in equation 3.5 and represented with an average lifetime as in equation 3.3. The resultant average lifetime values of the donor (ACE) label are plotted as a function of both CTAC micelles and pH values in Figure 5.2.

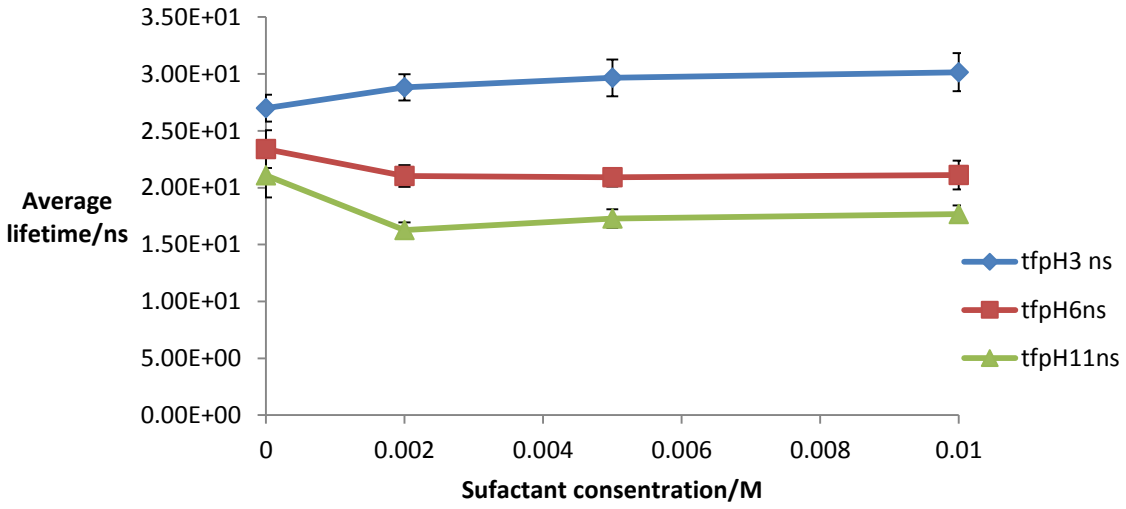

Figure 5.2: Plot of the average lifetime values obtained for ACE-AMMA-PAA in aqueous solution at three different pH values with increasing CTAC concentration when excited at 290 nm and observed at 340 nm.

Examination of Figure 5.2 for pH 3 level shows that the addition of CTAC micelles to the system resulted in a slight increase in the lifetime of the ACE label compared to that of the free surfactant ACE-AMMA- PAA sample (0 mM). This is clear evidence in which that the hydrophobic forces dominate the polymer-surfactant micelles interactions at low pH values. The addition of the surfactant micelles resulted in a more hydrophobic environment, which is increased by this interaction.

At higher pH values, pH 6 and pH 11, an initial decrease in the average lifetime of the decay can be observed from the figure. Further increase in the surfactant concentration did not result in any important change in the average lifetime decay value, even at the higher concentrations of surfactant micelles. This is consistent with a PAA polymer adopting a coiling conformation. The aggregation process is assumed to be due to electrostatic attraction between the PAA and the surfactant micelles. This coiled adopted conformation allowed the energy transfer from the donor label to the acceptor, this is different to what is seen with ACE-AMMA-PAA in solution alone (0 mM) indicating the CTAC micelles clearly have had an effect.

Figures 5.3 and 5.4 shows the results of the triple exponential model data fit. The results show that this model best fit the fluorescence decays data as it gave random distribution of residuals close to zero and χ^2 values close to unity.

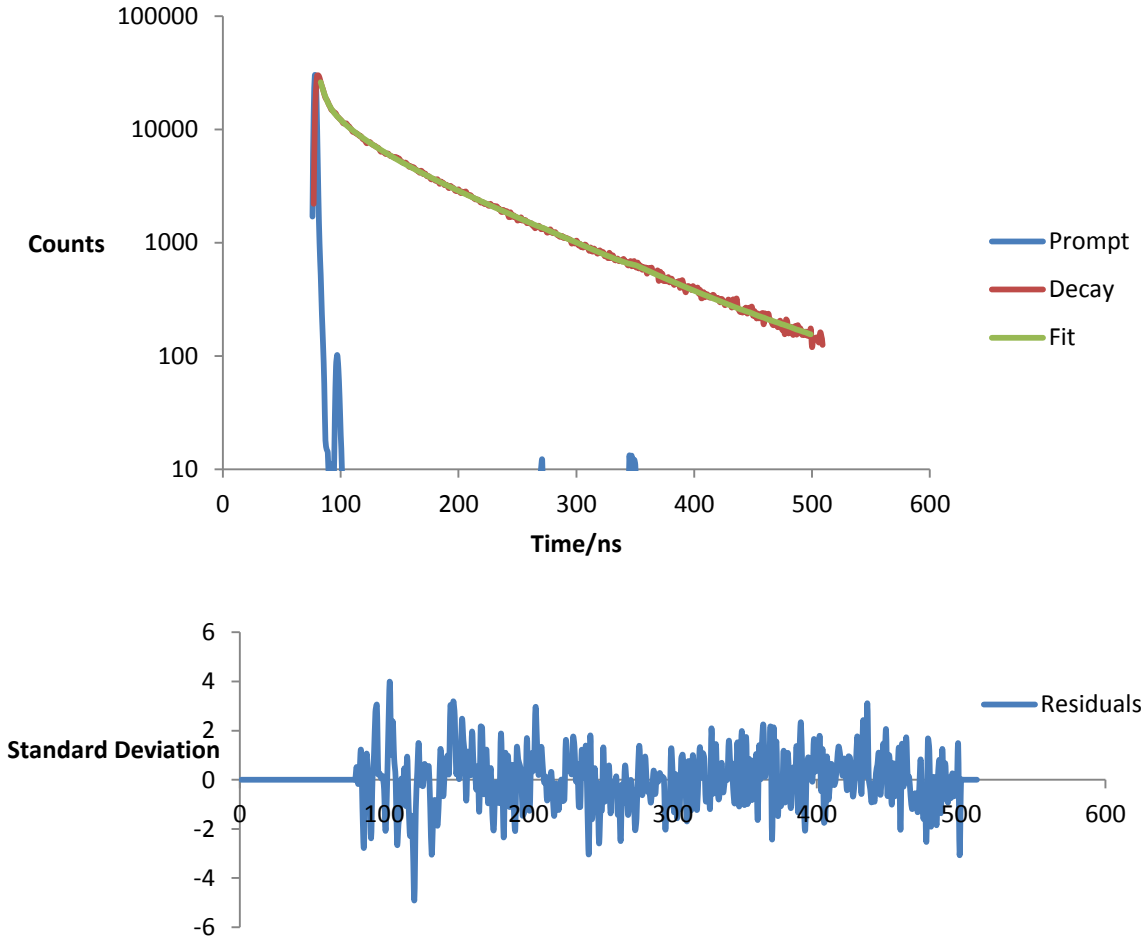

Figure 5.3: Fluorescence decay with corresponding mathematical fit (shown in green) and a plot of the resulting residuals for ACE-AMMA PAA in aqueous solution of pH 3 with 0.002 M of CTAC micelles

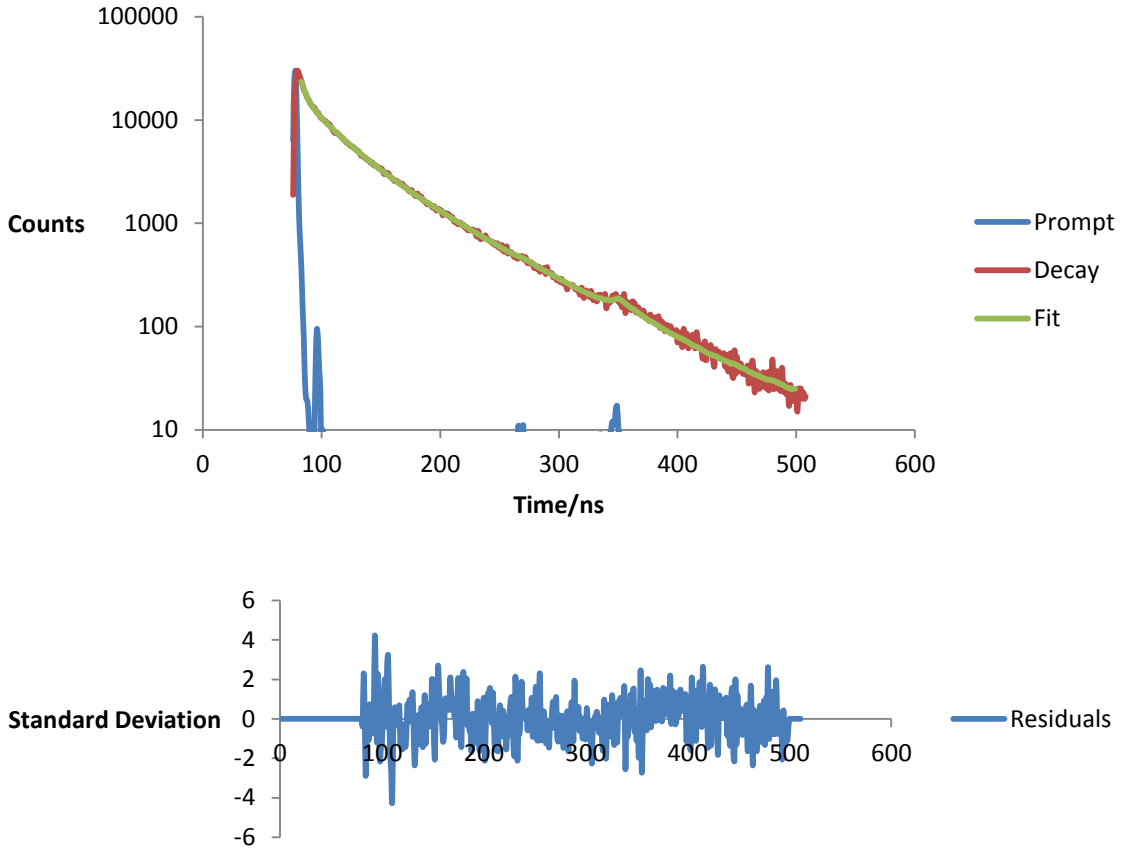

Figure 5.4: Fluorescence decay with corresponding mathematical fit (shown in green) and a plot of the resulting residuals for ACE-AMMA PAA in aqueous solution of pH 11 with 0.01M of CTAC micelles

5.1.3 Fluorescence time-resolved anisotropy measurements (TRAMS) of ACE-PAA in the presence of Hexadecyltrimethylammonium chloride as a function of pH

TRAMS measurement was conducted on an ACE labelled-PAA polymer sample with an increasing hexadecyltrimethylammonium chloride micelles (CTAC) concentration. In order to study the polymer dynamics with varying pH environment, three different values of pH was investigated.

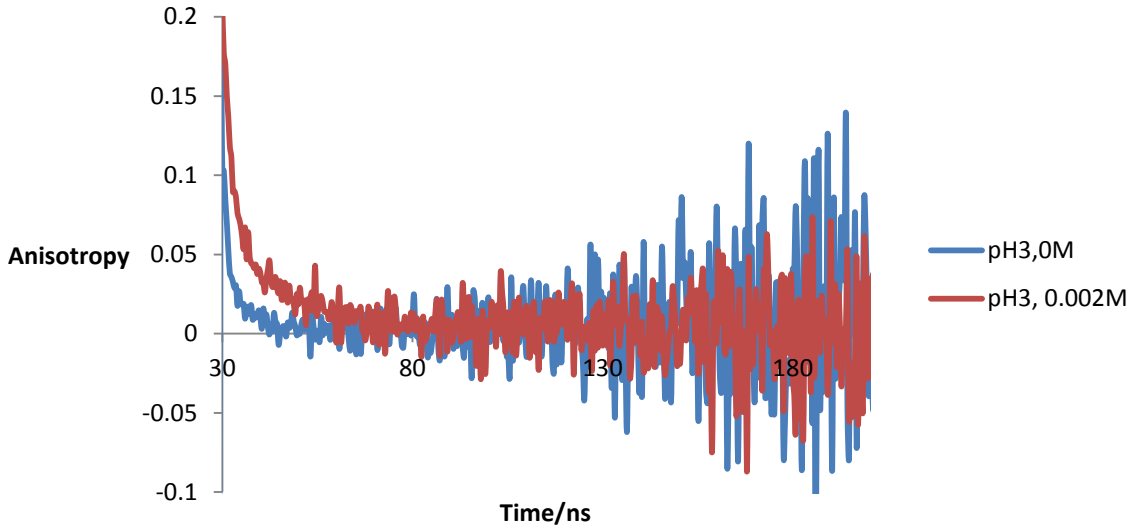

Figure 5.5: Fluorescence time resolved anisotropy data of aqueous ACE-labelled PAA solution(10^{-2} wt%) in the absence of CTAC micelles (blue line) and at the CTAC micelles concentration of 0.00 2M at pH3(λex= 295 nm and λem= 340 nm).

Figure 5.5 displays the fluorescence anisotropy decays of the singly-labelled-PAA polymer in water (blue colour) and in 0.002 M concentration CTAC micelles (red colour) solutions.. It can be observed from the figure, in the absence of micelles the anisotropy quickly drops to zero. In the presence of CTAC micelles the anisotropy slowly decays to zero. It is assumed that the PAA polymer chains are solubilised into the CTAC micellar cores, since the polymer is in a hydrophobic state at low pH, which would slow down the segmental motion of the polymer chains, hence the observed long anisotropy decay in the presence of the 0.002 M concentration of CTAC micelles. It is reported in the literature [46] that the hydrogen bonding plays a dominant role in the interactions at low pHs, such as in the reaction of PAA with poly(acrylamido-2- methylpropane sulfate) in NaCl and tetramethylammonium chloride.

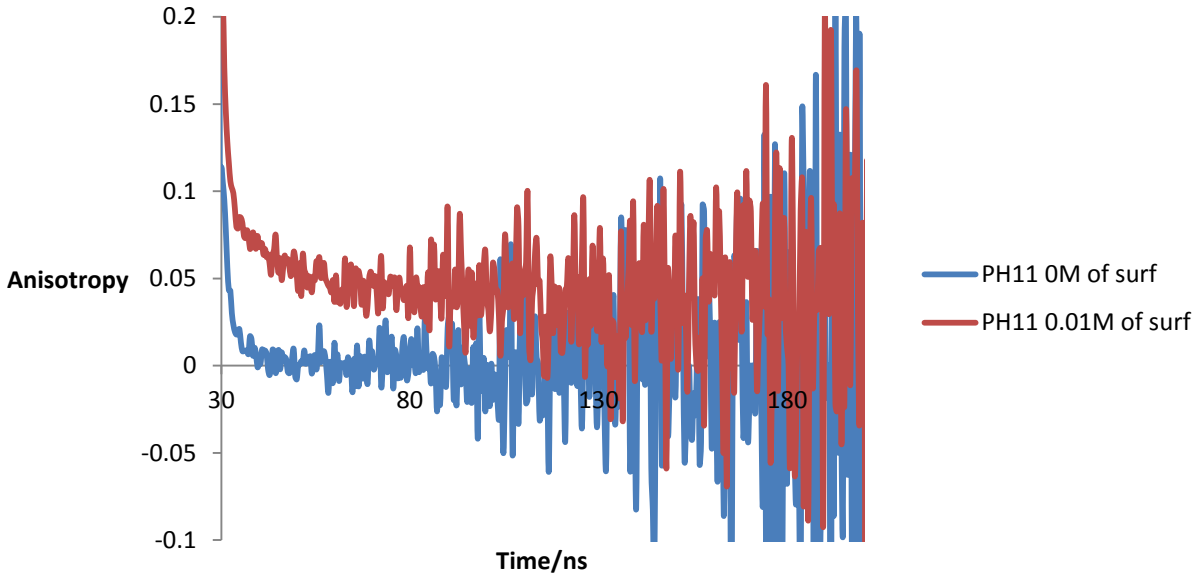

Figure 5.6: Fluorescence time resolved anisotropy data of aqueous ACE-labelled PAA solution (10^{-2} wt%) in the absence of CTAC micelles (blue line) and at the CTAC micelles concentration of 0.01M at pH11(λex= 295 nm and λem= 340 nm).

Figure 5.6 contrasts the fluorescence anisotropy decays of the singly-labelled-PAA in water and in the presence of Hexadecyltrimethylammonium chloride micelles at pH 11. The graph clearly shows the anisotropy quickly drops to zero in the absence of micelles. In the presence of the CTAC micelles, the anisotropy slowly decays to zero. This result can be attributed to the interaction that occurs between the charged micellar surfaces and the charged COO^- groups of the PAA polymer. This interaction screens out the carboxylate groups charge and hence leads to the collapse of the PAA chains. This collapse inhibits the motion of the polymer chain and hence the observed slow anisotropy decay.

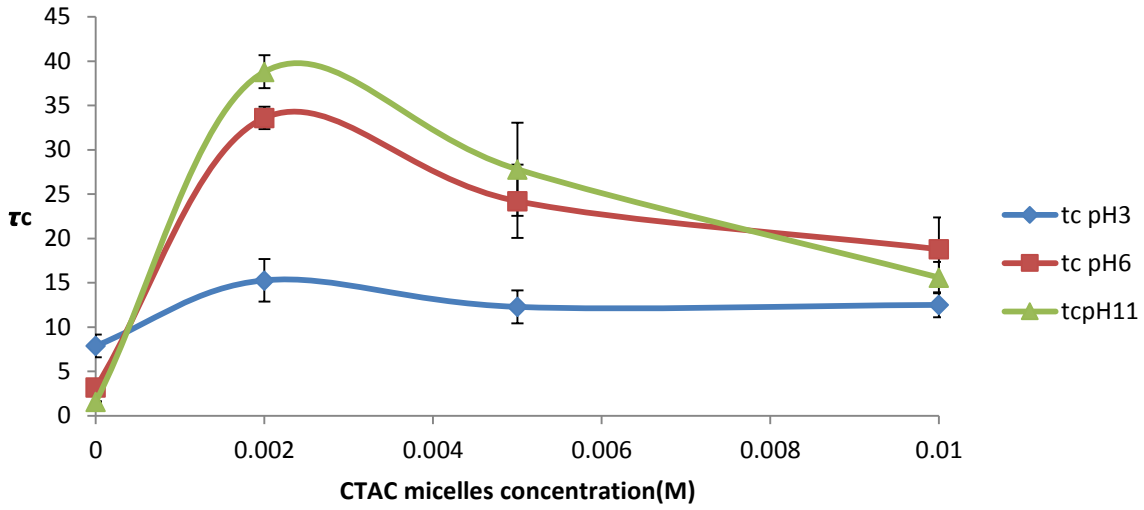

Figure 5.7 A plot of the correlation time against CTAC micelles concentration for three ACE labelled PAA samples in aqueous solution at three different pH values when excited at 290nm and observed at 340nm.

The TRAMS data for complexes between ACE-PAA and surfactant micelles was analysed using a double exponential fit for the anisotropy decay in this situation which means that the ACE label is dispersed in two different microenvironments.

The resultant correlation time data are plotted as a function of CTAC concentration at three pH values in figure 5.7.

Generally, pH 3 seemed to show the lowest tc or in other words, the least compact system with the lowest viscosity.

Initial addition of micelles in small amounts showed a substantial increase in the correlation time for pH6 and pH 11 whereas, for pH 3, a slight increase was recorded, indicating that a decrease in the polymer segmental motion correlated with an increase in the microviscosity of the complex. With increasing concentrations of CTAC the correlation time then decreased at high pH, perhaps indicating that the precipitation of the complex occurs at a higher concentration of micelles due to a charge neutralization of the polymer and to the hydrophobic nature of the bound surfactant micelles which adopt a form in which their ionic headgroups are effectively removed from the solution [74]

5.2 Fluorescence investigation of poly(dimethylamino)ethyl methacrylate (PDMEAMA) in the presence of oppositely charged surfactant micelles (sodium hexadecyl sulphate).

5.2.1 Fluorescence steady state spectra of ACE-AMMA labelled PDMAEMA in the presence of sodium hexadecyl sulphate as a function of pH

Intramolecular energy transfer was used to investigate the polymer/surfactant micelles system. In this study a solution of 10^{-2} wt% of ACE-AMMA labelled PDMEAEMA was exposed to varying pH values and concentrations of detergent upper of CMC (0.55 mM as reported in the literature [75], (i.e 10mM, 5mM and 2mM) (see figure 151).

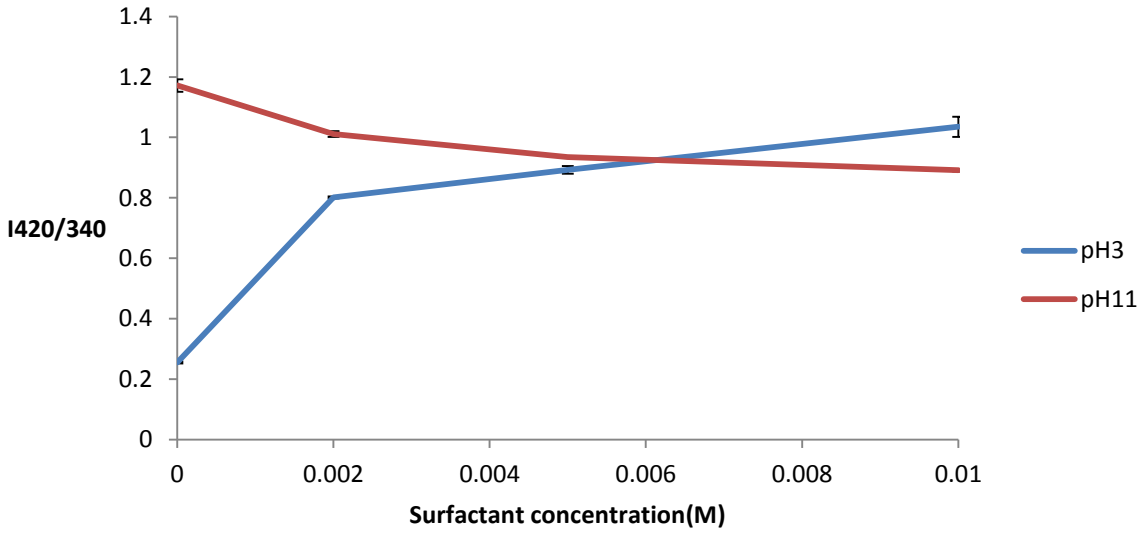

Figure 5.8 The fluorescence emission intensity ratio, I_A/I_D of 10^{-2} wt % ACE-AMMA-labelled PDMAEMA as a function of sodium hexadecyl sulphate concentration at different pH values (λ_{ex} = 290nm)

The anthryl to naphthyl emission ratio for the AMMA-ACE labelled PDMAEMA system with increasing amounts of anionic surfactant micelles, sodium hexadecyl sulphate (SHS) micelles was calculated and plotted in Figure 5.8. The PDMAEMA polymer is extended because the amine groups on the PDMAEMA are fully protonated at low pH (pH 3) and the intra chain electrostatic repulsions lead to macromolecule expansion. Addition of

SHS micelles has the effect of screening the electrostatic repulsion, therefore allowing larger numbers of chains to aggregate and causing a significant increase in the ratio which indicates that the distance between the acceptor and donor labels is reduced. Upon further increases in the anionic surfactant micelle concentration the ratio begins to gradual increase as the SHS reaches 10 mM.

At pH11, where the polyelectrolyte would be expected to be in an aggregated form, since the amino groups on PDMAEMA are deprotonated, addition of SHS micelles to the polybase causes a drop in the emission ratio which could indicate an expansion of the polymer. It was reported that the addition of anionic surfactant micelles, Sodium Dodecyl Sulfate to the PDMAEMA at which pH 9.1 leads to a significant perturbed in the polymer shape as it becomes structured around the surfactant micelles [74]Also it showed that Poly(N-isopropylacrylamide exhibited LCST (a lower critical solution temperature) in water above which it precipitated upon heating since attached anionic surfactant aggregates create an electrostatic barrier that resist polymer collapse and aggregation [75].

5.2.2 Fluorescence excited state lifetimes of an aqueous solution of ACE AMMAPDMAEMA in the presence of sodium hexadecyl sulphate as a function of pH

Average donor lifetimes for ACE-PDMAEMA and ACE-AMMA-PDMAEMA as a function of anionic surfactant micelles of Sodium hexadecyl sulphate concentration at two different pH values are plotted in Figure 5.9 and Figure 5.10. Generally, all average lifetime values increase over the whole SHS micelles concentration. Additionally, the rate of increase in $<\tau_f>$ values in ACE-AMMA-PDMAEMA is less than in those in ACE-PDMAEMA polymer at both pH values. However, the shape of the plots at pH 3 can also be attributed to the conformational transition occurring in the PDMAEMA chain when SHS micelles are added. Such a transition goes from an open coil at low pH, which in turn leads to enhanced lifetime values (as the ACE becomes further from the internal quenching), to a coiled

shape, when longer lifetime values are displayed (perhaps, due to the micelles in some way shielded the label from quenching by both aqueous medium and amine groups).

Whereas, at pH11, the shape of the plots can be attributed to the conformational transition occurring in the polymer chain when surfactant micelles are added. Such a transition goes from coiled at high pH, which in turn leads to a quenching of the lifetime values (as the ACE is nearer to the source of the internal quenching), to an open coil shape (where the donor is free from the quenching effect of the amine groups) and thus, longer lifetime values are observed.

Exclusively, it can be noted from Figure 5.9, that over the whole range of SHS micelle concentrations, the $< \tau_f >$ values are shorter for donor in ACE-AMMA-PDMAEMA than those for ACE-PDMAEMA. This big difference in average lifetime values (compared to that in figure 5.10) could be attributed to the maximum energy transfer which occurs from the donor to the acceptor. This *ET* is a result of a collapsed polyelectrolyte, formed by adding the anionic surfactant micelles to acidic media.

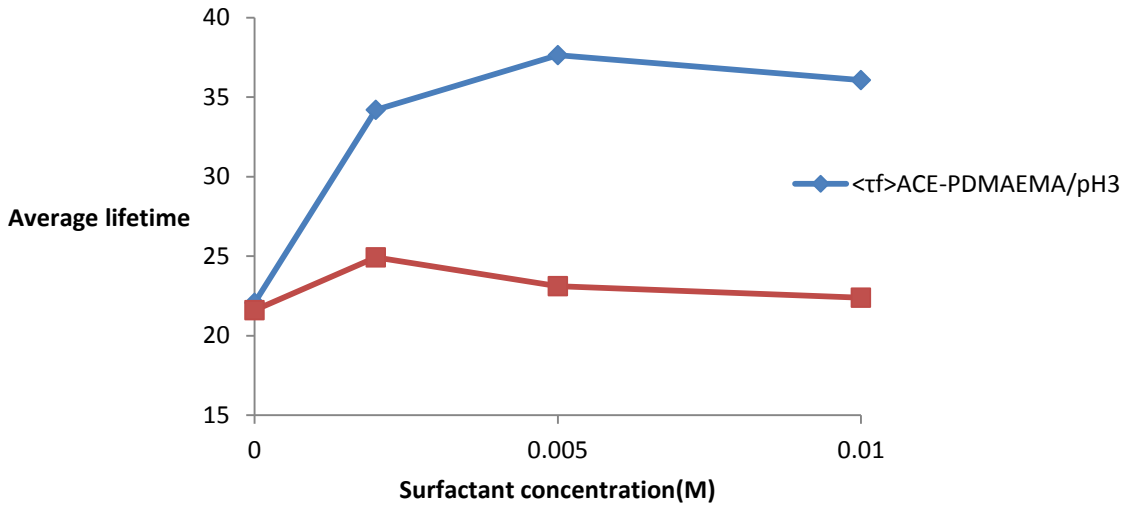

Figure 5.9 Average donor lifetime for ACE- PDMAEMA and ACE-AMMA- PDMAEMA (10^{-2} wt %) as a function of Sodium hexadecyl sulphate concentration at pH 3 (λex = 295 nm and λem = 340 nm).

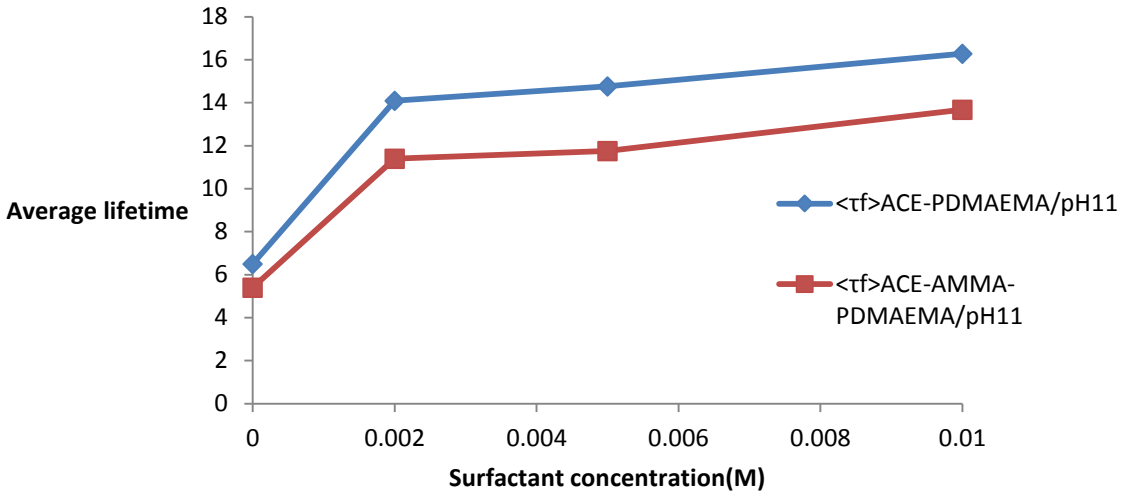

Figure 5.10 Average donor lifetime for ACE- PDMAEMA and ACE-AMMA- PDMAEMA (10^{-2} wt %) as a function of Sodium hexadecyl sulphate concentration at pH 11 (λex = 295 nm and λem = 340 nm).

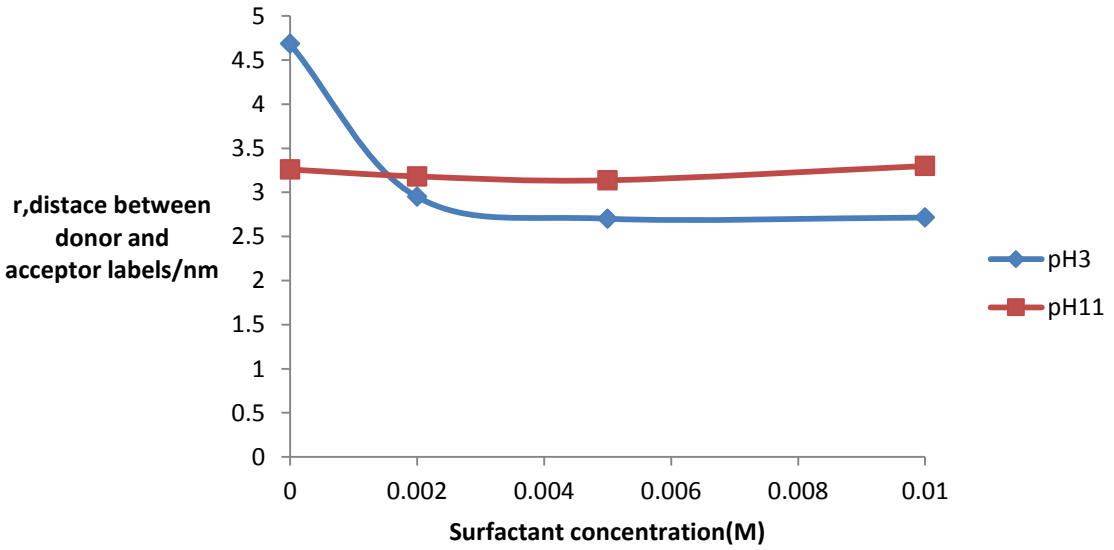

Figure 5.11 A plot of the value r, the distance between ACE (donor) and AMMA (acceptor) labels, as calculated by equation 3.7 for single and double -PDMAEMA at low and high pH and Sodium hexadecyl sulphate concentrations.

The average r value was then calculated for doubly labelled-PDMAEMA as a function of [SHS] and pH via equation 3.7 and 3.8 respectively (figure 5.11).

A very slight increase in the distance between donor and acceptor at pH 11 was recorded, when 0.01 M of Surfactant micelles was added. This is supported by the

expansion of the polymer chain under such conditions which had been shown by ET and life time experiments.

The label distance at pH 3 decreased at 0.002 M of the anionic surfactant micelles and then there was no significant change in this distance when more of the micelles were added. This suggests that the addition of SHS micelles to the PDMAEMA polymer causes the chains to unfold as a consequence of charged screening by the oppositely charged head group of micelles.

5.2.3 Fluorescence time-resolved anisotropy measurements (TRAMS) of ACE-PDMAEMA in the presence of (Sodium hexadecyl sulphate) as a function of pH

In this section the work was intended to assess the applicability of TRAMS to monitor the dynamics of fluorescently labelled PDMAEMA and its interaction with SHS micelles.

The anisotropy decay of 10^{-2} wt% ACE-PDMAEMA in acidic medium quickly reaches zero in the absence of micelles, reflecting the freedom of the donor molecule motion in solution. However, by adding surfactant micelles to the labelled- PDMAEMA system, the anisotropy value takes a longer time to decay to zero, as is shown in Figure 5.12**.** This behaviour can be explained as follows:

Since the polymer chain is expanded at low pH (due to the electrostatic repulsion) it interact strongly with the oppositely charged surfactant micelles, leading to the limit of the segmental motion of the polyelectrolyte chain and as a result a long anisotropy decay is generated.

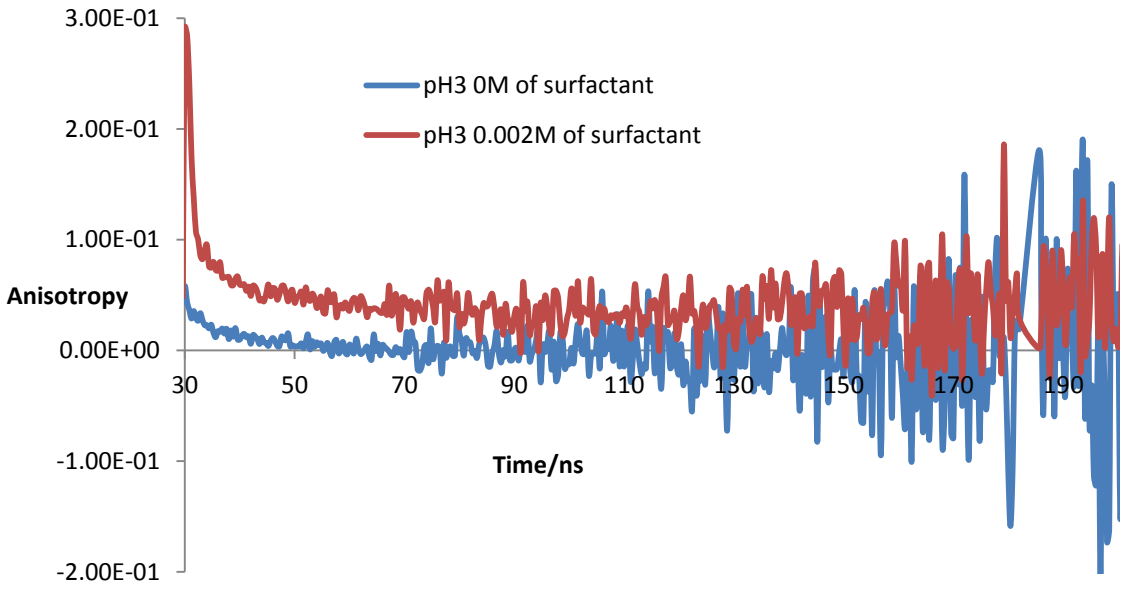

Figure 5.12 Fluorescence time resolved anisotropy data of aqueous ACE-labelled PDMAEMA solution (10^{-2} wt%) in the absence of SHS micelles (blue line) and at the SHS micelles concentration of 0.002 M at pH3 (λex= 295 nm and λem= 340 nm).

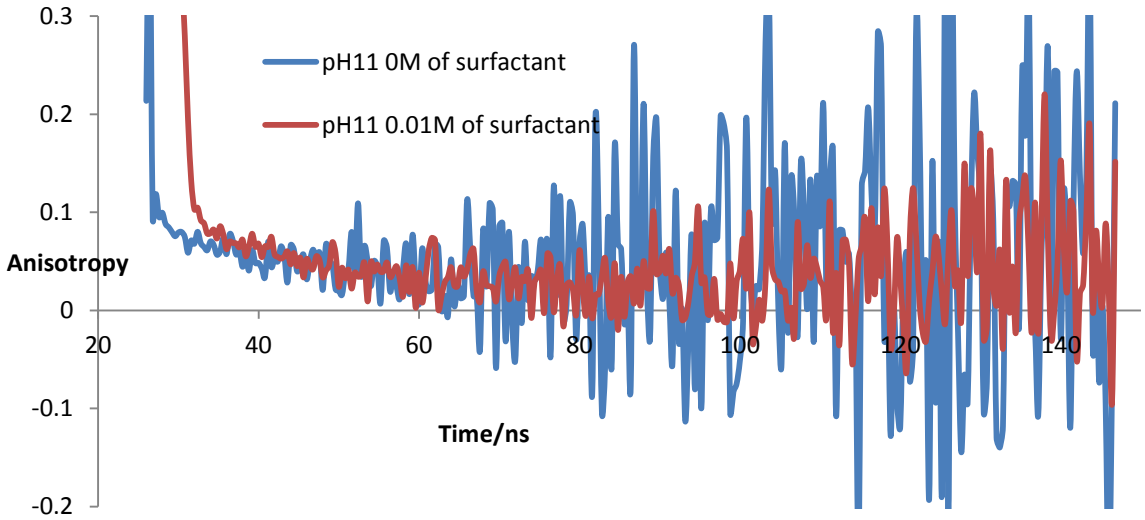

Figure 5.13 Fluorescence time resolved anisotropy data of aqueous ACE-labelled PDMAEMA solution (10^{-2} wt%) in the absence of SHS micelles (blue line) and at the SHS micelles concentration of 0.01M at pH11 (λex= 295 nm and λem= 340 nm).

Figure 5.13 compares the fluorescence anisotropy decay of ACE-labelled-PAA in water in the absence and presence of the sodium hexadecyl sulphate micelles at pH 11(basic conditions) and shows that in the absence of surfactant micelles the anisotropy decay is longer than that observed when the SHS micelles were added. This photophysical evidence indicates an unfolding effect of the coiled chain which is caused by the addition of the anionic surfactant micelles, hence, a short anisotropy decay is generated.

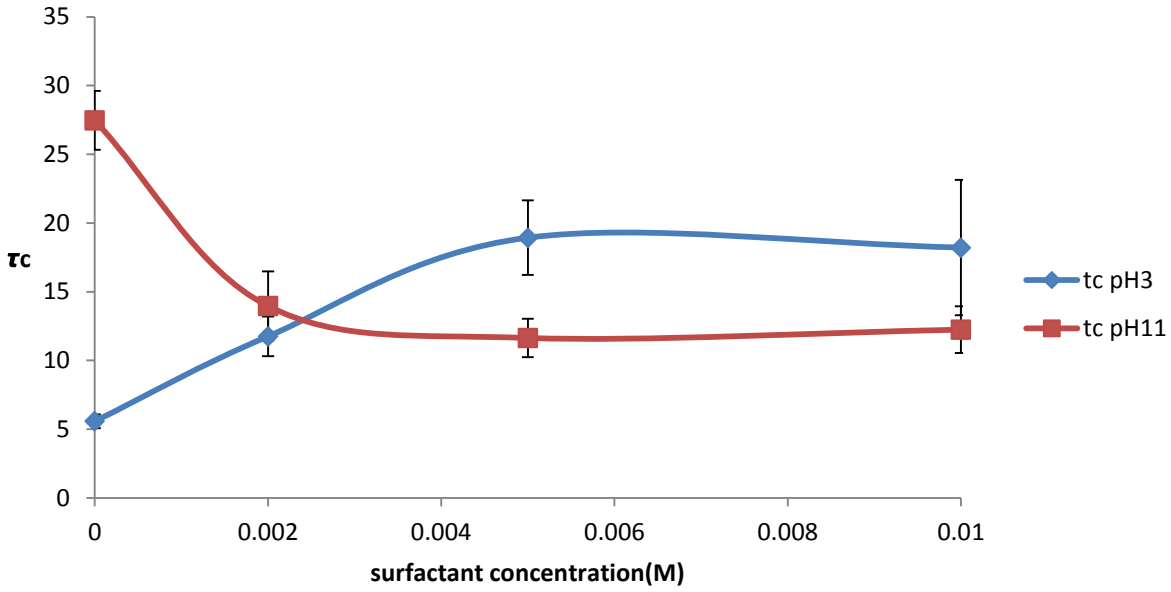

Figure 5.14 A plot of correlation time against SHS micelles concentration for three ACE labelled PDMAEMA samples in aqueous solution at three different pH values when excited at 290nm and observed at 340nm.

The TRAMS data for complexes between ACE-PDMAEMA and the oppositely charged surfactant micelles was analysed using a double exponential fit to analyse the anisotropy decays in this situation, which means that the ACE label is dispersed in two different microenvironments.

Figure 5.14 shows the plots of *rotational correlation time* with respect to the concentration of sodium hexadecyl sulphate micelles added to the ACE-PDMAEM solution at pH 3 and pH 11. A distinct decrease of the correlation time was recorded after the initial addition of the anionic surfactant micelles (SHS) in basic conditions (pH 11) indicating that the polymer chain underwent a conformation transition from a coiled chain to an opened

swollen form. No changed in the τc value was recorded upon further addition of SHS micelles.

However, there was a marked increase in the correlation time values as the micelles concentration was increased from 0.002 M to 0.005 M in the acidic solution (pH 3) and then no change when this concentration was increased to 0.01 M. which suggests that the cationic polymer chain has a more open structure at low pH (due to the electrostatic repulsions between the cationic amine groups) allowing it to bind more strongly with the oppositely charged micelles and form a collapsed chain which, in turn, causes a decrease in the segmental motion of the polyelectrolyte and thus give a high τc value. This observation was previously reported in the literature for the aggregation of a hydrophilic-hydrophobic diblock copolymer consisting of poly(2-(dimethylamino ethyl methacrylate) (PDMAEMA) and poly(methyl methacrylate) (PMMA) in aqueous solution which was investigated by small-angle neutron scattering. It was found that at higher surfactant concentrations using sodium dodecyl sulphate that a severe structural reorganization occurred as the poly acids became solubilised into the SDS micellar cores and the poly base chains interacted with the surfactant micelles, resulting in a "pearl-necklace" structure [76].

In summary, Fluorescence techniques are powerful tools that are able to reveal the conformational behaviour of poly acrylic acid interacting with cationic micelles, such as CTAC micelles, and poly dimethylaminoethylmethacrylate interacting with anionic micelles, such as SHS micelles. These techniques include energy transfer experiments, lifetime and time resolved anisotropy measurements.

A combination of these energy transfer experiments and lifetime measurements revealed that at low pH, ACE-AMMA-PAA/CTAC micelles interaction is dominated by the hydrophobic forces whilst in basic media the electrostatic interaction might dominate in the doubly labelled PAA/surfactant micelles complex.

Time resolved anisotropy measurements showed that in acidic conditions when the CTAC micelles were added the PAA chain moved slower. The hydrogen bonds that are assumed to have a dominant role in interaction for acidic conditions may restrict the polymer chain motion. However, this powerful technique revealed a possibility of precipitation for the PAA micelles complexes at high concentrations of surfactant micelles.

The energy transfer experiment and excited state lifetime experiments showed that at low pH, when SHS micelles are added to the PDMAEMA polymer it undergoes a conformational transition from an expanded to a collapsed state. However in basic media with surfactant micelles, the PDMAEMA chains switch from collapsed to an open structure conformation. Thus a decrease in the IA/ID was recorded and an enhancement in the lifetime is observed due to micelles protecting the donor from internal quenching in aqueous solution.

The correlation time of ACE-PDMAMA, increased as the amount of surfactant micelles (SHS) suggesting that the polyelectrolyte chains interact strongly with oppositely charged micelles changing the structure from a more expanded form at low pH to a collapsed form. However, the correlation time decreased as the initial amount of detergent in basic media was increased which suggests that the polymer chain motion became faster as it expanded.

Chapter 6 **Conclusions**

PAA in an aqueous acidic solution appears to form a collapsed structure as supported by an apparent decrease in energy transfer with increasing pH and an increase in the AMMA label emission intensity relative to the ACE label emission and a decrease in the ACE label lifetime above pH4. The TRAMS measurements reveal that PAA has two transition regions. As the pH is increased from 3 to 4 there is a decrease of correlation time value. Upon reaching pH 4, the τ_c value plateaus till pH 6 from which the τ_c value continues to decrease again. This double decrease implies that there may be two stages to the coiling of the polymer system. The first up to pH 3, due to the hydrophobic interactions between carboxylic units, and then a second shorter change between pH 7 and 8, as a result of repulsive interactions between carboxylate anions that dominate. The stability of correlation time between pH 4 and 6 (which is equal to pKa of PAA ~4.5) could be attributed to an aggregation in the chain, in which hydrogen bonding between carboxylic groups and any remaining carboxylate ions enhances the rigidity of the PAA chain.

The distance between the labels is bigger than that over which NRET occurs from pH11 and even at low pH the labels are not predominantly close - showing that PAA exhibits only partial coiling.

PDMAEMA in aqueous solution showed an increase in the intensity of fluorescence and lifetime with decreasing pH which implied that there was an expansion of the polymer chain as the donor label become distant from the internal quencher (amine group).
PDMAEMA in aqueous solution also showed an increase in the amount of energy transfer between donor and acceptor labels with increasing pH. This collapse of the polyelectrolyte backbone is supported by TRAMs studies which show a decrease in segmental mobility at the same pH range.

Fluorescence steady state and energy transfer experiments showed that addition of sodium chloride to the PAA polymer led to a switch from the collapsed chain conformation to an expanded form in acidic media - whereas the distance between labels using TRAMS measurements showed that the polymer expanded only with the initial addition of NaCl and

it then coiled again at higher concentrations of salt. In basic media the fluorescence technique demonstrated that the unfolded ionic polymer interacted with the cationic ion of salt leading to polymer chain aggregation. Noticeably the aggregation generated by a complex of Na^+ ions with COO^- ions was more efficient in pH 6 than at pH 11.

Addition of calcium chloride promoted coiling at all pH values. However, the aggregation caused by the interaction between the carboxyl group and the cation of calcium was more pronounced at pH 11 in contrast to sodium chloride where the aggregation of the polymer chain was more pronounced at pH 6.

In comparing the effect of NaCl and NaBr on coiling of the PAA polymer, TRAMS measurements showed that the anion size in acidic media promoted PAA polymer aggregation as the anion size became larger, whereas in basic media the anion size promoted PAA polymer aggregation as the anion size become smaller. On the other hand, the effect of anion size (i.e. $CaCl_2$ versus $CaBr_2$) on the polymer conformation showed that the coiling of the chain increased as the anion size of the salt decreased in both acidic and basic conditions.

Steady state and lifetime measurements showed that addition of salts to the PAA polymer chain formation experiments promoted the quenching phenomena and, interestingly, the sodium cation in its self was found to be a quencher for both donor and acceptor labels whereas the calcium cation quenched only the donor label.

Steady state and lifetime measurements showed that the addition of sodium chloride and sodium bromide to cationic PDMAEMA in acidic media led to the aggregation of the polymer chain as due to complexing of the anion of salt with the cationic amine group. The aggregation was more pronounced with the larger anion (i.e. NaBr > NaCl). In basic media, where the polymer chain adopted a coiled form, both NaCl and NaBr induced an expansion of the chains after initial addition of the cations and then the macromolecule recoiled again at higher concentration of both salts. However, NaCl appeared to show a slightly more pronounced enhancement of recoiling compared to NaBr as demonstrated by TRAMS measurement.

The addition of a divalent salt such as calcium bromide seemed to induce more coiling for the cationic PDMAEMA chain compared to the monovalent salt (such as sodium bromide). However, NaBr had a greater effect on coiling than was seen for $CaBr_2$ when the polymer

was uncharged in basic media as was demonstrated by the time resolved anisotropy measurements.

Fluorescence techniques such as energy transfer experiments, lifetime and time resolved anisotropy measurements are powerful tools to reveal the conformational behaviour of poly (acrylic acid) (PAA) it interacts with cationic micelles such as CTAC micelles and poly (dimethylamino) ethyl methacrylate) (PDMAEMA)interacting with anionic micelles such as SHS micelles.

A combination of these with energy transfer experiments and lifetime measurements revealed that the hydrophobic forces dominated the ACE-AMMA-PAA/CTAC micelles interaction at low pH while electrostatic attraction might predominate in the doubly labelled PAA /surfactant micelles complex in basic media.

TRAMS measurements showed that the PAA chain moved slower when the CTAC micelles were added in acidic conditions as the hydrogen bond which was assumed to have a dominant role in the interaction in these conditions, might restrict the polymer chain motion. On the other hand, this powerful technique revealed a possibility of precipitation for the PAA-micelles complexes at high concentrations of surfactant micelles.

ET experiment and excited state lifetime experiments showed that the PDMAEMA polymer undergoes a conformational transition from an expanded state to a collapsed form when SHS micelles are added at low pH, therefore the intensity ratio of donor and acceptor and the average lifetime was increased. Whereas, PDMAEMA chains switch from collapsed conformation to an open structure as the surfactant micelles were added in basic media and thus a decrease in the IA/ID was recorded and an enhancement in the lifetime was observed as the micelles in some way protected the donor from internal quenching in aqueous solution.

The correlation time (τ_c) of ACE-PDMAMA increased as the amount of surfactant micelles (SHS) increased at low pH which this suggests that the polyelectrolyte chains interact strongly with the oppositely charged micelles from a more expanded form at low pH to a collapsed structure. On the other hand, the correlation time decreased as the initial amount of detergent in basic media was increased, suggesting that polymer chain motion become faster as it was expanded.

Chapter 7 **Future work.**

It would be interesting to study the effect of the addition of the surfactant to a polymer that was already bound to inorganic counter ions, e.g. chloride (sodium), as this study would suggest that an ion exchange process would take place (i.e. positively charged ions would be displaced by surfactant anions (cations) as shown by van den Berg and Staverman , and by Vanlerberghe et al [77].

It would also be interesting to study the effect of ionic strength (in addition to tpH) on the conformational behaviour of the labelled polymer/micelles complex, as the effect of pH may have an important role in the growth and aggregation of the chains [49].

It would be useful to studying the interaction between polymers and the concentration of surfactant near or equal to the critical micelle concentration CMC and more fully characterize the CMC for surfactants in pure aqueous solution as the formation of free micelles in bulk solution, as the capacity of placing induced micelles on the polymer chain is saturated at these concentrations.

It could also be worthwhile to extend this work and examine the interactions of polyelectrolytes and surfactants of the same charge, as it seems to present only very weak interactions, which might be assigned to the solubilisation of the hydrophilic heads on the surfactant in the domains formed by the charged groups of the polymers.

The effect of the chain length of surfactants could be important as the polymer chain adopts a more compact conformation, which would then make the macromolecule more hydrophobic - the more hydrophobic the surfactant, the stronger the polymer surfactant interaction would be.

Chapter 8 **References:**

1. Crescenzi, V., Some recent studies of polyelectrolyte solutions, in Fortschritte der Hochpolymeren-Forschung. 1968, Springer Berlin Heidelberg. p. 358-386.
2. Li, K., et al., Conformational transition of poly (acrylic acid) detected by microcantilever sensing. Chinese Physics Letters, 2007. 24(6): p. 1502-1504.
3. Sarkar, D. and P. Somasundaran, Conformational dynamics of poly(acrylic acid). A study using surface plasmon resonance spectroscopy. Langmuir, 2004. 20(11): p. 4657-4664.
4. Authors, et al., Binding methyl orange and hydrophobic fluorescent probes by poly(2-dimethylaminoethyl methacrylate) and copolymers of 2-dimethylaminoethyl methacrylate and N-vinyl-2-pyrrolidone: pH dependence of the binding and fluorescence intensity. Journal of Polymer Science Part A: Polymer Chemistry, 1989. 27(1): p. 1-13.
5. Samsonova, O., et al., Low Molecular Weight pDMAEMA-block-pHEMA Block-Copolymers Synthesized via RAFT-Polymerization: Potential Non-Viral Gene Delivery Agents? Polymers, 2011. 3(2): p. 693-718.
6. Přádný, Martin, and Stanislav Ševčík. "Precursors of hydrophilic polymers, 3. The potentiometric behaviour of isotactic and atactic poly (2- dimethylaminoethyl methacrylate) in water/ethanol solutions." Die Makromolekulare Chemie 186.1 (1985): 111-121
7. Gupta, S., et al., Synthesis and characterization of stimuli-sensitive micro- and nanohydrogels based on photocrosslinkable poly(dimethylaminoethyl methacrylate). Journal of Polymer Science Part A: Polymer Chemistry, 2007. 45(4): p. 669-679.
8. van de Wetering, P., et al., A mechanistic study of the hydrolytic stability of poly(2-(dimethylamino)ethyl methacrylate). Macromolecules, 1998. 31(23): p. 8063-8068.
9. Swanson, Linda. "Optical Properties of Polyelectrolytes." Photochemistry and Photophysics of Polymeric Materials (2010): 41.

10. Pradny, M., S. Sevcik, and S. Dragan, Kinetics of quaterrnization reactions of polymeric amines. Collection of Czechoslovak Chemical Communications, 1989. 54(3): p. 663-672.
11. Plamper, Felix A., et al. "Star-shaped poly [2-(dimethylamino) ethyl methacrylate] and its derivatives: toward new properties and applications." Polimery 59.1 (2014): 66-73.
12. Mori, Hideharu, et al. "Synthesis of highly branched cationic polyelectrolytes via self-condensing atom transfer radical copolymerization with 2-(diethylamino) ethyl methacrylate." Macromolecules 37.6 (2004): 2054-2066
13. Swift, Thomas, et al. "The pH-responsive behaviour of poly (acrylic acid) in aqueous solution is dependent on molar mass." Soft matter 12.9 (2016): 2542-2549.
14. Swanson, L., Photochemistry and photophysics of polymer materials, in optical properties of polyelectrolytes, N.S. ALLEN, Editor, John Wiley: Hoboken.
15. Leyte, J. C., and M. Mandel. "Potentiometric behavior of polymethacrylic acid." Journal of Polymer Science Part A: General Papers 2.4 (1964): 1879-1891.
16. Anghel, Dan F., et al. "Fluorescent dyes as model 'hydrophobic modifiers' of polyelectrolytes: a study of poly (acrylic acid) s labelled with pyrenyl and naphthyl groups." Polymer 39.14 (1998): 3035-3044.
17. Bolto, Brian A. "Soluble polymers in water purification." Progress in Polymer Science 20.6 (1995): 987-1041.
18. Oliveira, Pedro C., et al. "Poly (dimethylaminoethyl methacrylate) grafted natural rubber from seeded emulsion polymerization." Polymer 46.4 (2005): 1105-1111.
19. Zhang, X., Xia, J., & Matyjaszewski, K. (1998). Controlled/"living" radical polymerization of 2-(dimethylamino) ethyl methacrylate. Macromolecules, 31(15), 5167-5169
20. Cho, S.H., et al., Temperature-induced phase transition of poly(N,N-dimethylaminoethyl methacrylate-co-acrylamide). Journal of Polymer Science Part B: Polymer Physics, 1997. 35(4): p. 595-598.
21. Hui, H., F. Xiao-dong, and C. Zhong-lin, Thermo- and pH-sensitive dendrimer derivatives with a shell of poly(N,N-dimethylaminoethyl methacrylate) and study of their controlled drug release behavior. Polymer, 2005. 46(22): p. 9514-9522.

22. Edgar, K.J., et al., Advances in cellulose ester performance and application. Progress in Polymer Science, 2001. 26(9): p. 1605-1688.
23. Kuila, D., et al., Polyacrylic acid (Poly-A) as a chelant and dispersant. Journal of Applied Polymer Science, 1999. 73(7): p. 1097-1115.
24. Kozuka, H., T. Hosokawa, and T. Takagishi, Binding of butyl orange by poly(2-dimethylaminoethyl methacrylate) and copolymers of 2-dimethylaminoethyl methacrylate and N-vinyl-2-pyrrolidone: Peculiar temperature dependence of the binding. Journal of Polymer Science Part A: Polymer Chemistry, 1989. 27(2): p. 555-563.
25. Huang, X.J., Y. Xiao, and M.D. Lang, Synthesis of star-shaped PCL-based copolymers via one-pot ATRP and their self-assembly behavior in aqueous solution. Macromolecular Research, 2012. 20(6): p. 597-604.
26. Anghel, D.F., et al., Fluorescent dyes as model 'hydrophobic modifiers' of polyelectrolytes: a study of poly(acrylic acid)s labelled with pyrenyl and naphthyl groups. Polymer, 1998. 39(14): p. 3035-3044.
27. Soutar, I. and L. Swanson, Luminescence studies of polyelectrolyte behaviour in solution.3. time-resolved fluorescence anisotropy measurements of the conformational behaviour of poly(methacrlylic acid) in dilute aqueous solution. Macromolecules, 1994. 27(15): p. 4304-4311.
28. Soutar, I., et al., Synchrotron-generated time-resolved fluorescence anisotropy studies of the semental relaxition poly(acrylic acid) and poly(methacrylic acid) in dilute methanolic solutions. Macromolecules, 1992. 25(17): p. 4399-4405.
29. Swift, T., L. Swanson, and S. Rimmer, Poly(acrylic acid) interpolymer complexation: use of a fluorescence time resolved anisotropy as a poly(acrylamide) probe. Rsc Advances, 2014. 4(101): p. 57991-57995.
30. Swanson, L., Photochemistry and Photophysics of Polymer Materials. NS Allen, Ed, 2010: p. 41-92.
31. De Silva, A. Prasanna, et al. "Signaling recognition events with fluorescent sensors and switches." Chemical Reviews 97.5 (1997): 1515-1566.
32. J.R. Ebdon, B.J.H., D.M. Lucas, I. Soutar, L. Swanson, A.R. Lane, Luminescence studies of hydrophobically modified, water-soluble polymers. I. Fluorescence anisotropy and spectroscopic investigations of the conformational behaviour of

copolymers of acrylic acid and styrene or methyl methacrylate. 1995, 73(11): 1982-1994.

33. Ruiz-Perez, L., et al., Conformation of poly(methacrylic acid) chains in dilute aqueous solution. Macromolecules, 2008. 41(6): p. 2203-2211.
34. Zinsli, P.E., Inhomogeneous interior of aerosol of microemulsions probed by fluorescence and polarisation decay. Journal of Physical Chemistry, 1979. 83(25): p. 3223-3231.
35. Chen, M., et al., Amphiphilic acenaphthylene-maleic acid light-harvesting alternating copolymers: Reversible addition - Fragmentation chain transfer synthesis and fluorescence. Macromolecules, 2005. 38(8): p. 3475-3481.
36. Balzani, V., Supramolecular photochemistry. Tetrahedron, 1992. 48(48): p. 10443-10514.
37. Lakowicz, J.R., Principles of Fluorescence Spectroscopy. 1999.
38. Jones, G. and M.A. Rahman, Fluorescence properties of coumarin laser-dyes in aqueous po;ymer media - chromophore isolation in poly(methaacrylic acid) hypercoils. Journal of Physical Chemistry, 1994. 98(49): p. 13028-13037.
39. D. Phillips, E., Polymer photophysics, luminescence, energy migration and molecular motion in synthetic polymers, D. Phillips, Ed., Chapman and Hall, New York, 1985, 437 pp. Chapman and Hall, New York, 1985.
40. Pereira, R.V. and M.H. Gehlen, Spectroscopy of auramine fluorescent probes free and bound to poly(methacrylic acid). Journal of Physical Chemistry B, 2006. 110(13): p. 6537-6542.
41. Stramel, RrD, et al. "Photophysical properties of pyrene covalently bound to photoelectrolytes." The Journal of Physical Chemistry 92.10 (1988): 2934-2938.
42. Soutar, I., et al., Luminescence techniques and characterization of the morphology of polymer latices - 2. Fluorescence lifetime, phosphorescence and fluorescence anisotropy studies. Journal of Colloid and Interface Science, 2006. 303(1): p. 205-213.
43. Delaire, J.A., M.A.J. Rodgers, and S.E. Webber, Quenching of fluorescence in water- soluble polymers of methacrylic acid and vinyl diphenylanthracene. Journal of Physical Chemistry, 1984. 88(25): p. 6219-6227.

44. Neumann, M.G., C.C. Schmitt, and E.T. Iamazaki, A fluorescence study of the interactions between sodium alginate and surfactants. Carbohydrate Research, 2003. 338(10): p. 1109-1113.
45. Hoffman, A.S. and P.S. Stayton, Bioconjugates of smart polymers and proteins: Synthesis and applications. Macromolecular Symposia, 2004. 207: p. 139-151.
46. Yoshida, K. and P.L. Dubin, Complex formation between polyacrylic acid and cationic/nonionic mixed micelles: effect of pH on electrostatic interaction and hydrogen bonding. Colloids and Surfaces a-Physicochemical and Engineering Aspects, 1999. 147(1-2): p. 161-167.
47. Lee, M.S. and J.C. Kim, Effects of Surfactants on Phase Transition of Poly(N-isopropylacrylamide) and Poly(N-isopropylacrylamide-co-dimethylaminoethylmethacrylate). Journal of Dispersion Science and Technology, 2012. 33(1-3): p. 272-277.
48. Taktak, F., et al., A Novel Triple-Responsive Hydrogels Based on 2 (Dimethylamino) Ethyl Methacrylate by Copolymerization With 2-(N-morpholino) Ethyl Methacrylate. Journal of Macromolecular Science Part a-Pure and Applied Chemistry, 2015. 52(1): p. 39-46.
49. Schillen, K., et al., Association of naphthalene-labeled poly(acrylic acid) and interaction with cationic surfactants. Fluorescence studies. Langmuir, 2000. 16(26): p. 10528-10539.
50. Gao, G.Z., W.Z. Xu, and J.F. Kadla, Reversible ph-responsive hydrogels of softwood kraft lignin and poly(2- dimethylamino)ethyl methacrylate-based polymers. Journal of Wood Chemistry and Technology, 2015. 35(1): p. 73-90.
51. Chee, C.K., et al., Fluorescence investigations of the thermally induced conformational transition of poly(N-isopropylacrylamide). Polymer, 2001. 42(12): p. 5079-5087.
52. Huh, G., et al., Synthesis of a Photo-Patternable Cross-linked Epoxy System Containing Photodegradable Carbonate Units for Deep UV Lithography. Journal of Applied Polymer Science, 2009. 114(4): p. 2093-2100.
53. Hao, J.K., et al., Interchain Hydrogen-Bonding-Induced Association of Poly(acrylic acid)-graft-poly(ethylene oxide) in Water. Macromolecules, 2010. 43(4): p. 2002-2008.

54. Tsukida, N., et al., Effect of neutralization of poly(acrylic acid) on the structure of water examined by Raman spectroscopy. Journal of Physical Chemistry B, 1997. 101(34): p. 6676-6679.
55. Benegas, J.C., F.M.J. Cleven, and M. van den Hoop, Potentiometric titration of poly(acrylic acid) in mixed counterion systems: Chemical binding of Cd ions. Analytica Chimica Acta, 1998. 369(1-2): p. 109-114.
56. Soutar, I., et al., Fluorescence studies of the dynamic behavior of poly(dimethylacrylamide) and its complex with poly(methacrylic acid) in dilute solution. Macromolecules, 1996. 29(3): p. 918-924.
57. Winnik, M.A., et al., Synthesis and characterization of pyrene-labeled poly(ethylenimine). Macromolecules, 1998. 31(20): p. 6855-6864.
58. Tchaikovskaya, O.N., et al., Fluorescence investigations of phenol phototransformation in aqueous solutions. Journal of Fluorescence, 2000. 10(4): p. 403-408.
59. Chee, C.K., et al., Manipulating the thermoresponsive behavior of poly(N-isopropylacrylamide). 1. On the conformational behavior of a series of N-isopropylacrylamide - Styrene statistical copolymers. Macromolecules, 2001. 34(21): p. 7544-7549.
60. Bradbury, R.B., N.C. Hancox, and H.H. Hatt, The reaction between acetone and ammonia- the formation of pyrimidine compounds analogous to the aldoxans of spath. Journal of the Chemical Society, 1947(OCT): p. 1394-1399.
61. Gijsman, P. and M. Gitton, Hindered amine stabilisers as long-term heat stabilisers for polypropylene. Polymer Degradation and Stability, 1999. 66(3): p. 365-371.
62. Pickett, J.E. and J.E. Moore, Photostability of UV screeners in polymers and coatings, in Polymer Durability: Degradation, Stabilization, and Lifetime Prediction, R.L. Clough, N.C. Billingham, and K.T. Gillen, Editors. 1996, Amer Chemical Soc: Washington. p. 287-301.
63. Volponi, J.E., L.H.I. Mei, and D.D. Rosa, The use of differential photocalorimetry to measure the oxidation induction time of isotatic polypropylene. Polymer Testing, 2004. 23(4): p. 461-465.

64. Carlsson, D. J., T. Suprunchuk, and D. M. Wiles. "Photo- oxidation of polypropylene films. VI. Possible UV- stabilization mechanisms." Journal of Applied Polymer Science 16.3 (1972): 615-626.
65. Schweins, R., J. Hollmann, and K. Huber, Dilute solution behaviour of sodium polyacrylate chains in aqueous NaCl solutions. Polymer, 2003. 44(23): p. 7131-7141.
66. Bonapasta, A.A., F. Buda, and P. Colombet, Interaction between Ca ions and poly(acrylic acid) chains in macro-defect-free cements: A theoretical study. Chemistry of Materials, 2001. 13(1): p. 64-70.
67. Schweins, R. and K. Huber, Collapse of sodium polyacrylate chains in calcium salt solutions. European Physical Journal E, 2001. 5(1): p. 117-126.
68. Dreher, W. Reid, William L. Jarrett, and Marek W. Urban. "Stable nonspherical fluorine-containing colloidal dispersions: synthesis and film formation." Macromolecules 38.6 (2005): 2205-2212.
69. Ravi, P., S. Dai, and K.C. Tam, Synthesis and self-assembly of 60 fullerene containing sulfobetaine polymer in aqueous solution. Journal of Physical Chemistry B, 2005. 109(48): p. 22791-22798.
70. Dodoo, S., et al., Effect of ionic strength and type of ions on the structure of water swollen polyelectrolyte multilayers. Physical Chemistry Chemical Physics, 2011. 13(21): p. 10318-10325.
71. Salomaki, M., T. Laiho, and J. Kankare, Counteranion-controlled properties of polyelectrolyte multilayers. Macromolecules, 2004. 37(25): p. 9585-9590.
72. Salomaki, M., et al., The Hofmeister anion effect and the growth of polyelectrolyte multilayers. Langmuir, 2004. 20(9): p. 3679-3683.
73. Konradi, R. and J. Ruhe, Binding of oppositely charged surfactants to poly(methacrylic acid) brushes. Macromolecules, 2005. 38(14): p. 6140-6151.
74. Wesley, R.D., et al., Structure of polymer/surfactant complexes formed by poly(2-(dimethylamino)ethyl methacrylate) and sodium dodecyl sulfate. Langmuir, 2002. 18(15): p. 5704-5707.
75. Schild, H.G. and D.A. Tirrell, Interaction of poly(N-isopropylacrlamide) with sodium normal-alkyl sulfates in aqueus solution. Langmuir, 1991. 7(4): p. 665-671.

76. Wesley, R.D., et al., Structure of a hydrophilic-hydrophobic block copolymer and its interactions with salt and an anionic surfactant. Langmuir, 2005. 21(11): p. 4856-4861.
77. GODDARD, E.D., Polymer- surfactant interaction part2. polymer and surfactant of opposite charge. 1985. 19: p. 301-329.

Jun19
Ameerah Theqah Sample ref. AMMA in CDCl3

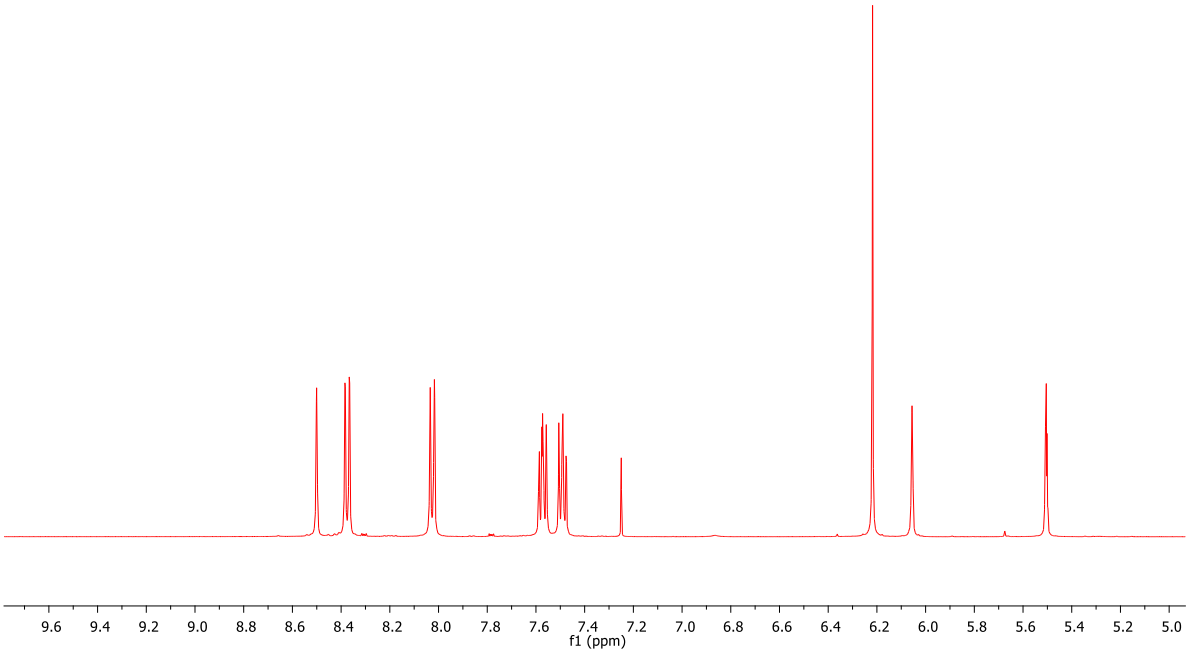

Jun19
Ameerah Theqah Sample ref. Unlabelled PAA in D2O with water suppression

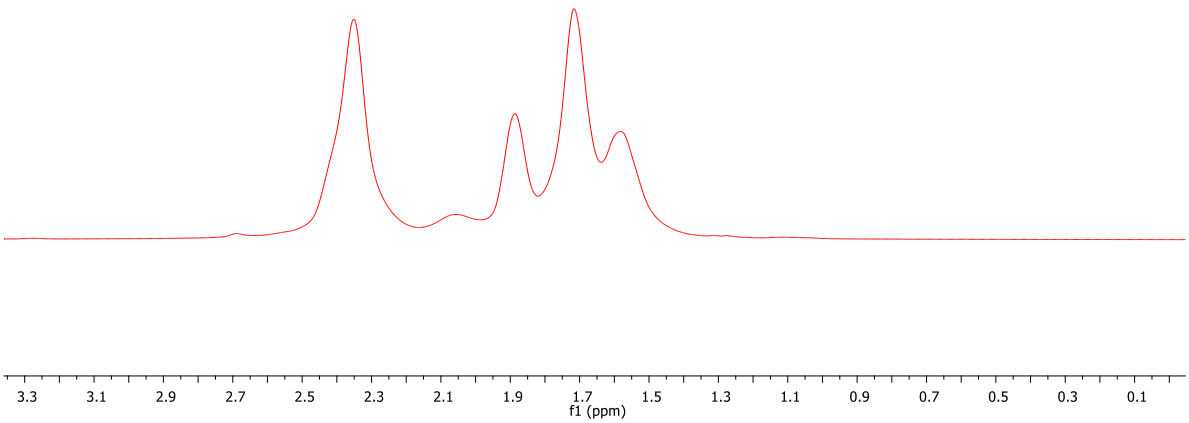

Jun19
Ameerah Theqah Sample ref. ACE-PAA in D2O with water suppression

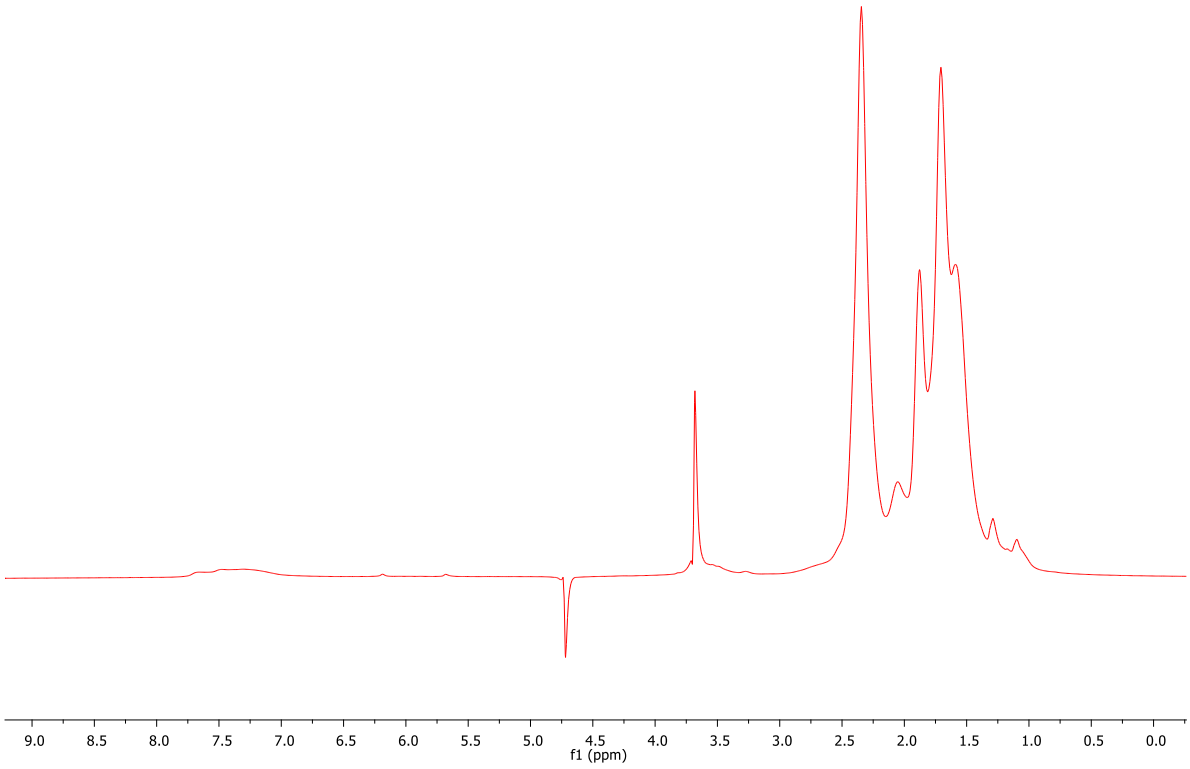

Jun19
Ameerah Theqah Sample ref. d-PAA in D2O with water suppression

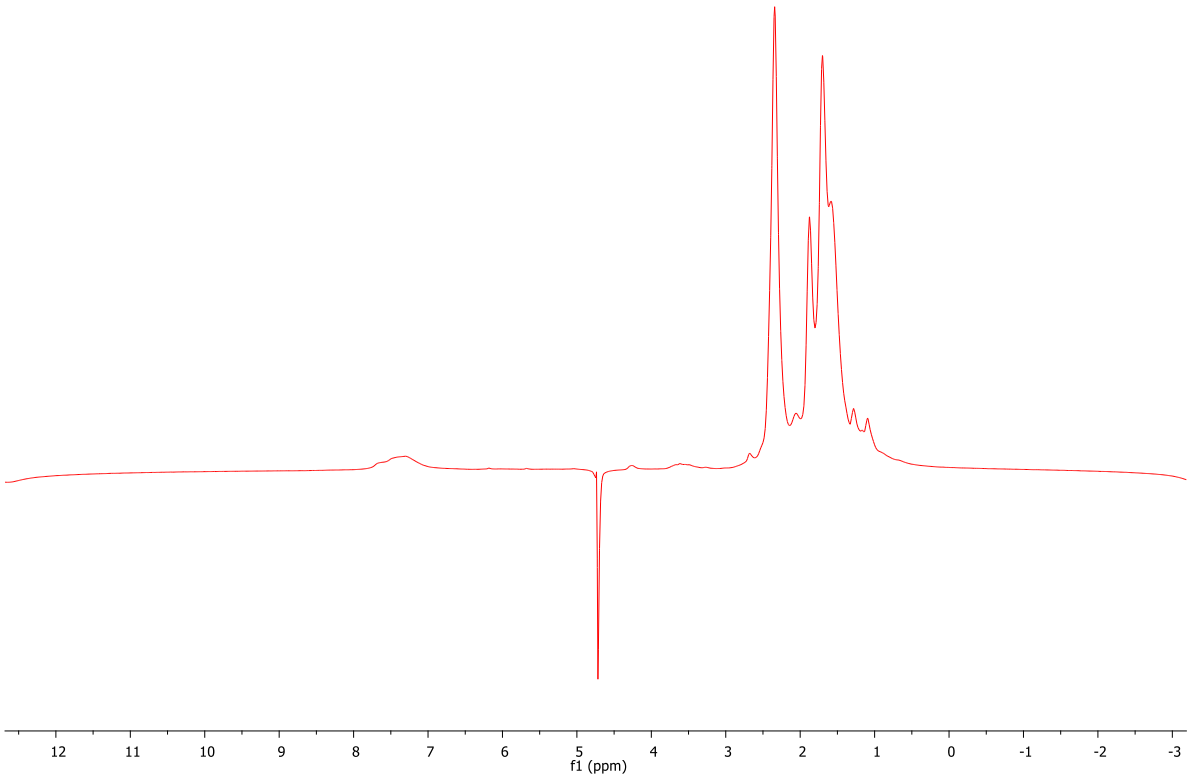

Jun02
Ameerah Theqah Sample ref. Unlabelled- PDMAEMA in D2O with presaturation

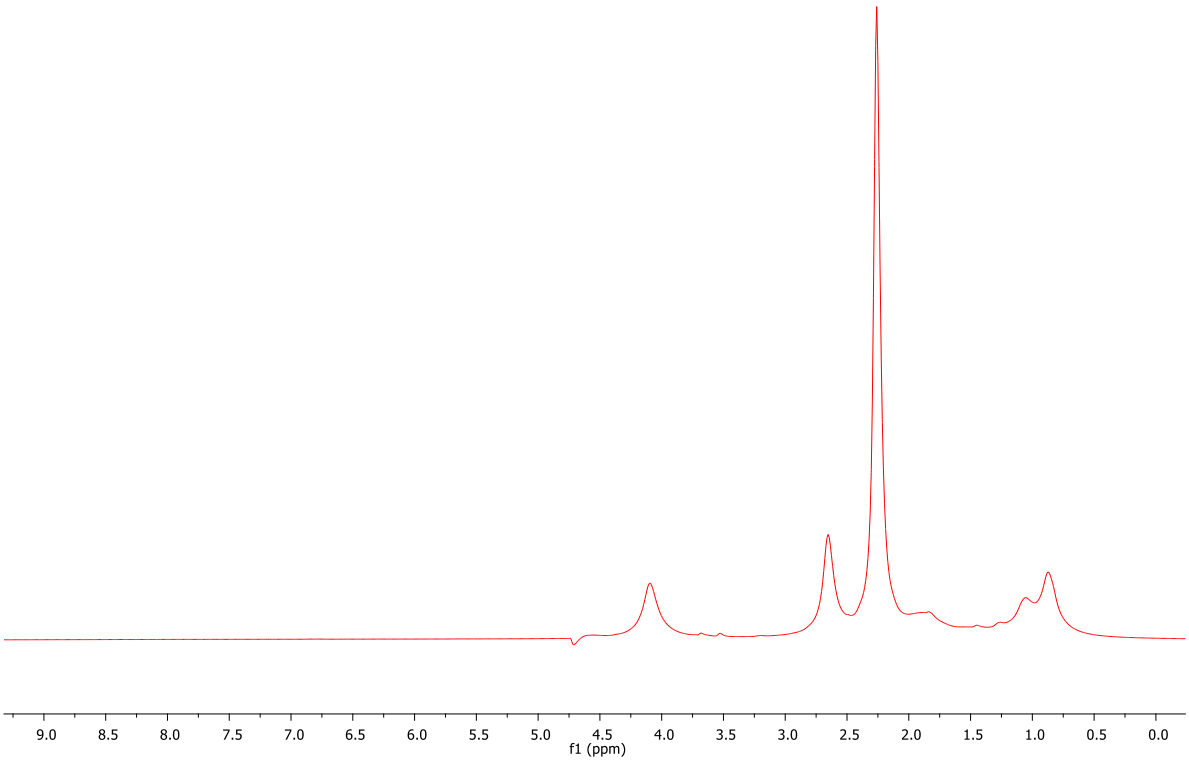

Jun02
Ameerah Theqah Sample ref. ACE-PDMAEMA in D2O with presaturation

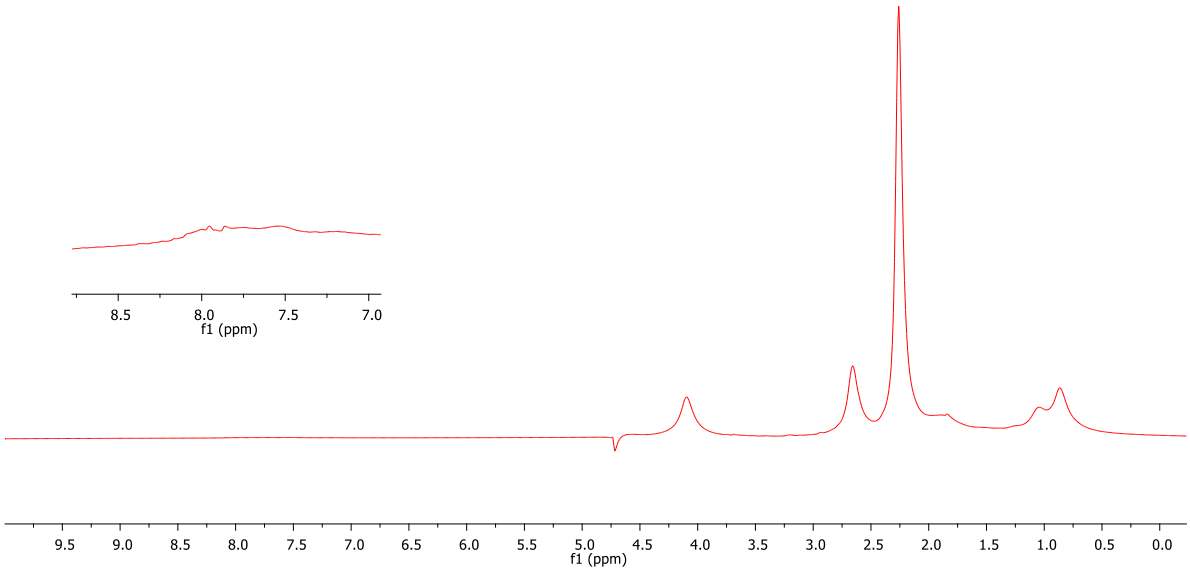

Jun02
Ameerah Theqah Sample ref.d-PDMAEMA in D2O with presaturation